Immobilisation and Application of Bifunctional Iminophosphorane Organocatalysts

A thesis submitted in partial fulfilment of the requirement for the degree of Doctor of Philosophy (DPhil)

Anna Magdalena Goldys

Magdalen College University of Oxford Michaelmas 2014

Supervisor: Prof. Darren J. Dixon

Table of Contents

Declarations and copyright

I declare that thesis has been written by me, that it is the record of work carried out by me and that it has not been submitted in any previous application for a higher degree at this or any other university or institute of learning. Any work done in collaboration with a research colleague has been fully acknowledged and referenced within the text. All compounds in the experimental chapter were synthesised and characterised by myself unless otherwise stated.

I was admitted as a probationary research student in October 2011 and as a candidate for the degree of Doctor of Philosophy in October 2012; the higher study for which this is a record was carried out in the University of Oxford between 2011 and 2014.

Anna M. Goldys

Date Signature of candidate:

In submitting this thesis to the University of Oxford, I understand that I am giving permission for it to be made available for use in accordance with the regulations of the University Library for the time being in force, subject to any copyright vested in the work not being affected thereby. I also understand that the title and the abstract will be published, and that a copy of the work may be made and supplied to any *bona fide* library or research worker, that this thesis will be electronically accessible for personal or research use, and that the library has the right to migrate this thesis into new electronic forms as required to ensure continued access to the thesis. I have obtained any third-party copyright permissions that may be required in order to allow such access and migration.

Abstract

Immobilisation and Application of Bifunctional Iminophosphorane Organocatalysts
Anna M. Goldys Magdalen College D. Phil. Michaelmas 2014

Bifunctional iminophosphoranes, containing a triaryl-substituted iminophosphorane and bis(3,5-trifluoromethyl)phenyl thiourea on a single enantiomer scaffold are novel asymmetric superbase organocatalysts reported by the Dixon group in 2014. This thesis describes our efforts to expand their scope and utility in a variety of challenging chemical transformations.

Chapter 2 describes the development and application of immobilised bifunctional iminophosphorane organocatalysts. We have successfully immobilised bifunctional iminophosphoranes on a cross-linked polystyrene support and applied this sold-supported catalyst to three challenging asymmetric reactions; namely the nitro-Mannich reaction of phosphinoyl ketimines and the conjugate addition of alkylmalonates and *N*,*N*-dimethyl *β*-keto amides to nitrostyrene. Very good yields, enantio- and diasteroselectivities were obtained in all cases. We have also demonstrated their use in a range of conjugate additions of cyclic 1,3-dicarbonyl compounds to nitroalkenes, which suffered from very slow reaction rates under tertiary amine-based bifunctional catalysis. In all cases, the immobilised bifunctional iminophosphoranes performed very well in comparison to their homogeneous counterparts. We have also demonstrated catalyst recycling over 10 cycles and application in a continuous flow system with a productivity of 7.20 $mmol_{product}\ h^{-1}\ g_{catalyst}^{-1}$.

Chapter 3 describes the application of homogeneous bifunctional iminophosphorane organocatalysts to the ring-opening polymerisation (ROP) of cyclic esters. We have demonstrated the performance of bifunctional iminophosphorane organocatalysts in the ROP of L-lactide (LA), *δ*-valerolactone (VL) and *ε*-caprolactone (CL). The polymerisation of LA and VL proceeded rapidly and was well controlled, while only short lengths (< 100 DP) of poly(CL) could be prepared in a controlled fashion due to hypothesised competing initiation from the catalyst. We have shown that the polymerisation of LA using our catalyst may be considered a living polymerisation. Di-block co-polymers could also be successfully prepared via sequential monomer addition or through the use of macroinitiators. We then investigated the roles of the iminophosphorane and the thiourea component of the catalyst.

Acknowledgements

Przede wszystkim, dla moich rodziców.

First of all I must thank Prof. Darren Dixon for supporting me in coming to Oxford and giving me the opportunity to work in this group. I'm very grateful to have been given the chance to work on such a productive project.

To all the members of the Dixon group, past and present – you've been so, so important to me for these past three years. Thank you so much for being your very unique selves.

More specifically, thank you to Daniel, Bal, Adam, Alistair, Kayli, Iacovos and Allegra for giving up their own time to proofread this thesis. Thanks to Alistair (most of all) as well as Daniel for invaluable chemistry chats and support, I hope I didn't bother you too much. And thanks to Marta, who was first on the immobilisation project, for all the help at the beginning and also more recently with the paper.

I am very grateful for the generous assistance of the NMR and mass spectrometry staff, in particular Prof. Tim Claridge and Colin Sparrow. And last but not least, thank you to Bryony Core and members of the Mountford group for their help with using the GPC.

Finally, I would like to acknowledge the Clarendon Fund, Magdalen College and the Vice-Chancellor's Fund for their financial support over the course of my DPhil.

Abbreviations

°C	degrees Celsius
Å	Ångström
Ac	acetyl
AcOH	acetic acid
AIBN	2,2′-azobis(2-methylpropionitrile)
aq	aqueous
app	apparent
Ar	aryl
atm	atmosphere
BEMP	2-*tert*-butylimino-2-diethylamino-1,3-dimethylperhydro-1,3,2-diazaphosphorine
BINOL	1,1´-binaphtalene-2,2´-diol
Bn	benzyl
Boc	*tert*-butoxycarbonyl
b.p.	boiling point
br	broad
brsm	based on recovered starting material
n-Bu	*n*-butyl
Cbz	carboxybenzyl
conc	concentration
conv	conversion
COSY	correlation spectroscopy
cp	cyclopentadienyl
cy	cyclohexyl
d	doublet
DBU	1,8-diazabicyclo[5.4.0]undec-7-ene
DCE	1,2-dichloroethane
DCM	dichloromethane
dd	doublet of doublets
DEPT	distortionless enhancement by polarisation transfer
DIBAL	diisobutylaluminium hydride
DIPEA	*N*,*N*-diisopropylethylamine
DMAP	4-dimethylaminopyridine
DMF	dimethylformamide
DMP	Dess-Martin periodinane
DMSO	dimethyl sulfoxide
dq	doublet of quartets
d.r.	diastereoisomeric ratio
dt	doublet of triplets
e.e.	enantiomeric excess
EI	electron impact
equiv	equivalents
ES	electrospray ionisation
Et	ethyl
EDG	electron donating group
EWG	electron withdrawing group
Et_2O	diethyl ether
EtOAc	ethyl acetate
FCC	flash column chromatography
FI	field ionisation
g	gram
GPC	gel permeation chromatography
h	hour(s)
HOMO	highest occupied molecular orbital
HMBC	heteronuclear multiple-bond correlation experiment
HPLC	high pressure liquid chromatography
HRMS	high resolution mass spectrometry
HSQC	heteronuclear single-quantum coherence experiment
Hz	Hertz
IR	infrared
IUPAC	International Union of Pure and Applied Chemistry
IPA	*iso*-propyl alcohol
J	coupling constant
KHMDS	potassium bis(trimethylsilyl)amide
LDA	lithium diisopropylamide
LUMO	lowest unoccupied molecular orbital
[M]	metal complex
M	molar concentration

m	multiplet
MALDI-ToF	matrix-assisted laser desorbtion ionisation-time of flight
Me	methyl
MeOH	methanol
mg	milligram
MHz	mega Hertz
min	minute(s)
mL	millilitre
µL	microlitre
mmol	millimole
mM	millimolar
MO	molecular orbital
mol	mole
MOM	methoxymethyl
m.p.	melting point
MS	low resolution mass spectrometry
Ms	methanesulfonyl
m/z	mass to charge ratio
NMR	nuclear magnetic resonance
NMO	4-methylmorpholine *N*-oxide
Ns	*para*-nitrobenzenesulfonyl
nOe	nuclear Overhauser effect
Nu	nucleophile
o	ortho
OH	hydroxy
OTf	trifluoromethanesulfonate
p	*para*
PDI	polydispersity index
PE	petroleum ether b.p. 30-40 °C
PEG	polyethylene glycol
PG	protecting group
Ph	phenyl
PMB	*para*-methoxybenzyl
PMP	*para*-methoxyphenyl
ppm	parts per million
Pr	propyl
PS	polystyrene
q	quartet
quint	quintet
R	generic substituent
rac	racemic
R_f	retention factor
r.r.	regioisomeric ratio
r.t.	retention time
rt	room temperature
s	singlet
sxt	sextet
t	triplet
TBAF	tetrabutylammonium fluoride
TBAI	tetrabutylammonium iodide
TBAB	tetrabutylammonium bromide
TBS	*tert*-butyldimethylsilyl
t-Bu	*tert*-butyl
temp	temperature
t/*tert*	tertiary
Tf	triflate
TFA	trifluoroacetic acid
THF	tetrahydrofuran
TLC	thin layer chromatography
TMS	trimethylsilyl
TMSOTf	trimethylsilyl trifluoromethanesulfonate
t_R	retention time (HPLC)
Ts	*para*-toluenesulfonyl
TS	transition state
p-TsCl	*para*-toluenesulfonyl chloride
p-TsOH	*para*-toluenesulfonic acid
UV	ultraviolet

Chapter 1: General Introduction

1.1 General aims

This thesis concerns the applications of bifunctional iminophosphorane organocatalysts, the development of which was reported recently by the Dixon group.[1] Its primary goal is to expand the scope and utility of these novel catalysts by investigating their use in previously unexplored areas for this catalyst class.

Catalyst immobilisation holds great potential for increasing the usefulness of organocatalysts with the prospect of benefits such as easy workup, catalyst recycling and applications in continuous flow systems. We therefore aim to investigate the development and application of immobilised variants of bifunctional iminophosphorane organocatalysts.

We aim to extend the catalyst scope by investigating novel reactions and methodologies. In particular, as a unique feature of this class of catalysts is their strong basicity, we aim to explore the reactions of substrates which have previously been poorly accessible due to the low reactivity of tertiary amine-based bifunctional organocatalysts or known to only proceed under superbase catalysis.

1.2 Asymmetric bifunctional organocatalysis

In the 1960's and 70's the mechanisms of enzymatic catalysis, such as the discovery of the "catalytic triad" of chymotrypsin and its proposed mode of action,[2] began to come to light. This era also saw the advent of asymmetric catalysis (as opposed to chiral pool synthesis or the use of auxiliaries) as the preferred method of accessing enantioenriched molecules.[3] Motivated by the appeal and efficiency of chiral catalysts and inspired by nature, researchers began to look to naturally occurring chiral organic molecules as possible agents for enantioselective synthesis. Since these very early days of organocatalysis, bifunctional modes of activation were an area of active study.[4] The term "bifunctional organocatalysis" refers to catalytic systems exhibiting two simultaneous modes of activation. This introduction will focus on the simultaneous activation of a nucleophile and an

electrophile by the Brønsted base and hydrogen bond (H-bond) donor moieties, respectively, of a chiral catalyst.

An important pioneer of this approach was Wynberg, who demonstrated that enantioselectivity could be induced by cinchona alkaloids and their derivatives in the Michael addition of thiols,[5] selenols[6] and carbon-centered pronucleophiles such as β-keto esters[7] to α,β-unsaturated ketones. Wynberg and Hiemstra undertook a detailed and comprehensive study of the Michael addition of thiophenols to cyclohexanones in order to elucidate the mechanism of catalysis by the cinchona alkaloids.[8] The most striking result from this study was the loss of catalytic activity and enantioselectivity in the Michael addition upon acylation of the C-9 hydroxyl group of quinine (Table 1).

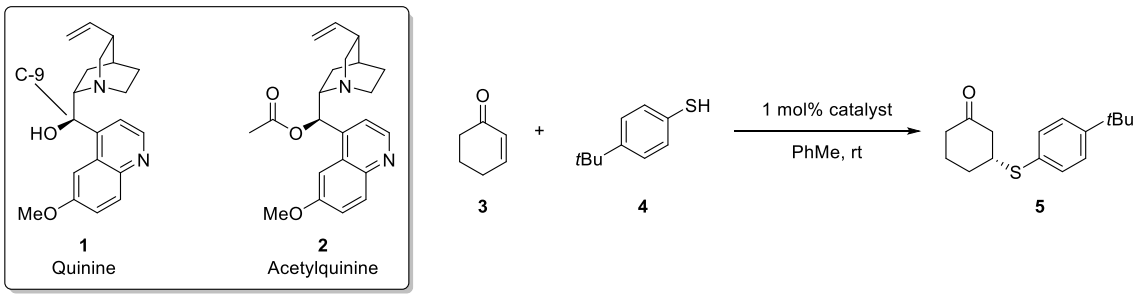

Catalyst	Equiv. thiophenol	k_{obs} (kg^2 mol^{-2} s^{-1})	e.e. (%)
Quinine	2.0	1.02	41
Acetylquinine	2.8	0.0039	10

Table 1. *Dependence of reaction rate and enantiomeric excess (e.e.) of* ***5*** *on catalyst structure in the Michael addition of thiophenol to cyclohexanone.*

From this and other results, Wynberg and Hiemstra proposed a model of dual activation where the quinuclidine moiety of the catalyst deprotonates the thiophenol, forming a tight ion pair. A hydrogen bond between the C-9 hydroxyl group and the oxygen of the cyclohexanone activates the enone to nucleophilic attack, as well as stabilising the incipient negative charge of the enolate-like transition state (Figure 1). The two activated reagents are held in close proximity *via* their interactions with the catalyst and spatially arranged to ensure their stereoselective union. Thus quinine acts as a bifunctional catalyst for this Michael addition.

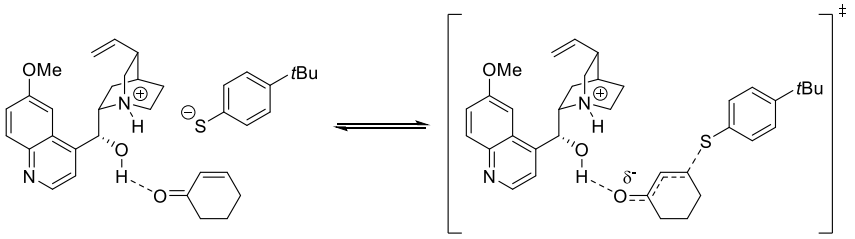

Figure 1. *Activation of cyclohexanone and thiophenol by quinine leading to the transition state for the Michael addition.*

A more directly biologically-inspired approach to asymmetric organocatalysis is to try to mimic enzymatic catalysis by using small peptides as organocatalysts. This was the methodology investigated by Inoue in the 1970's and 80's. After initially studying the catalytic activity of linear polypeptides,[9,10] Inoue and co-workers undertook the study of more conformationally rigid cyclic dipeptides as catalysts in the asymmetric synthesis of cyanohydrins. All peptides studied contained histidine, with the view that the imidazole would act as a basic catalyst in the reaction. At a 7 mol% loading, the use of a cyclic dipeptide of L-alanine and L-histidine gave a 9.9% e.e.at 50% conversion in the addition of hydrogen cyanide to benzaldehyde,[11] however, swapping the L-alanine fragment for L-phenylalanine (**6**) resulted in an impressive 90% e.e. at 40% conversion with 2 mol% catalyst loading.[12] This work was then taken up by Lipton, in search of a peptide catalyst for the Strecker reaction. The cyclic peptide of L-histidine and L-phenylalanine developed by Inoue (**6**) was found not to be a useful catalyst for the Strecker reaction, which was presumed by Lipton and co-workers to be due to slow proton transfer by the imidazole. Lipton and co-workers therefore replaced the imidazole with a strongly basic guanidine (**7**), creating the first successful asymmetric catalyst for the Strecker reaction (Scheme 1).[13]

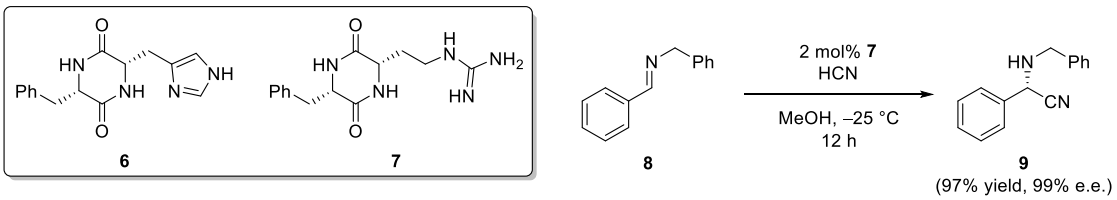

Scheme 1. *Strecker reaction catalysed by Lipton's dipeptide organocatalyst **7**.*

A major advance in the field of bifunctional organocatalysis came with the development of (thio)urea catalysis by Schreiner and co-workers.[14] Urea derivatives are a uniquely useful class of compounds due to their strong H-bond donating ability combined with the fact that they can form bidentate

hydrogen bonds (Figure 2).[15] The superior effectiveness of bidentate, compared to monodentate, hydrogen bonding for H-bond donor organocatalysis was demonstrated in 1985 by Hine and co-workers using 1,8-biphenylenediol in a nucleophilic epoxide opening.[16] Building on this work, in 2002 Schreiner and co-workers identified thioureas to be potent Lewis-acidic organocatalysts as well as being convenient to prepare and use.[17] In their seminal work, the *bis*-trifluoromethyl thiourea **10** was identified as the optimal catalyst for the Diels-Alder reaction of cyclopentadiene and methyl vinyl ketone.[18] The important feature of this thiourea are the strongly electron-withdrawing trifluoromethyl groups at the 3 and 5 positions, which increase the acidity of the N-H's. Their placement at the *meta* position allows for a weak H-bonding interaction between the *ortho* protons and the thiourea sulfur atom, which increases the rigidity of the compound. This is important because of the large entropic contribution to the strength of the complexation of thioureas to carbonyl compounds.

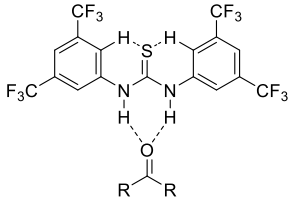

Figure 2. *Thiourea **10** forming a bidentate hydrogen bond to a ketone. H-bonding interactions between the* ortho *protons and the sulfur atom are also shown.*

The first asymmetric organocatalyst to make use of the unique hydrogen-bonding properties of ureas and thioureas was Jacobsen's Schiff base organocatalyst for the asymmetric Strecker reaction. In their search for amino acid-containing, urea derived, Schiff base ligands for a metal-catalysed asymmetric Strecker reaction, Jacobsen and co-workers found that a control experiment in the absence of any metal gave the highest product e.e. of 19%. This result was "not unexpected" in the light of the previous work of Lipton, and Jacobsen and co-workers decided to pursue it further. After extensive screening using resin-bound catalysts and combinatorial techniques, an optimal catalyst was identified which gave the benzonitrile of *N*-allyl benzaldimine **11** in 78% yield and 91% e.e.[19] Further adjustments to the catalyst structure identified **12** as a general catalyst for the asymmetric Strecker reaction and an extensive substrate scope was demonstrated (Scheme 2).[20]

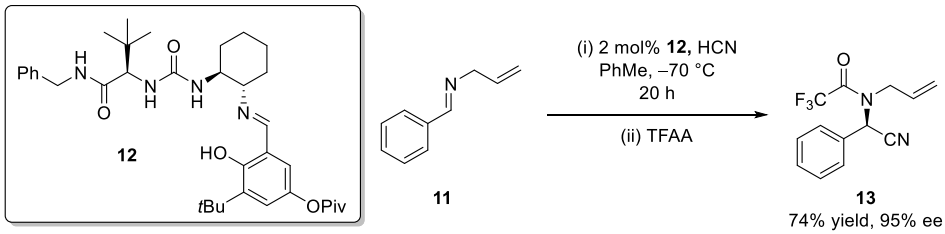

Scheme 2. *Jacobsen's asymmetric Strecker reaction catalyst. TFAA = trifluoroacetic anhydride.*

Experimental and computational studies were then undertaken to explain the mode of action of this catalyst.[21] Kinetic studies indicated reversible complex formation between the catalyst and aldimine, presumably involving a hydrogen bond between one of the acidic catalyst protons and the aldimine nitrogen. Successive deletion of the acidic sites on the catalyst combined with isotope shift experiments showed that hydrogen bonding only between the two urea protons and the aldimine was necessary for catalytic activity. NMR and computational studies suggested that the imine forms hydrogen bonds to both urea N-H's simultaneously, and that the intermolecular interactions in this bridging mode are stronger than the single hydrogen bond which forms with the product amine, providing a plausible justification for catalyst turnover. Interestingly, Jacobsen notes that deletion of the catalyst imine did not suppress catalytic activity, however both of the "imine-deleted" catalysts in this study contained other Brønsted basic moieties in its place – one a secondary amine and the other a hemiaminal – and both retained excellent reactivity and good enantioselectivity. A Brønsted base is necessary to deprotonate the HCN and as the aldimine is doubly hydrogen bonded to the urea, this must apparently be done by the catalyst, if an enantioselective reaction is to ensue. Thus presumably the catalyst acts in a bifunctional fashion, however this is not explicitly discussed by the authors. From this initial work on the Strecker reaction, Jacobsen and co-workers developed a family of structurally related thiourea catalysts which could be used in a range of reactions such as the acylcyanation of imines,[22] the Mannich reaction,[23] the cyanosilylation of ketones[24] and the dynamic kinetic resolution of azalactones,[25] and others.[14]

Another important example of a bifunctional catalyst is that developed by Takemoto (**14**), originally used in the addition of malonates to nitroolefins.[26] It is perhaps the first organocatalyst to be designed explicitly as a bifunctional catalyst. In this initial work, Takemoto and co-workers demonstrated the

importance of both the Brønsted base and H-bond donor components of the catalyst for obtaining good yield and enantioselectivity (Table 2).

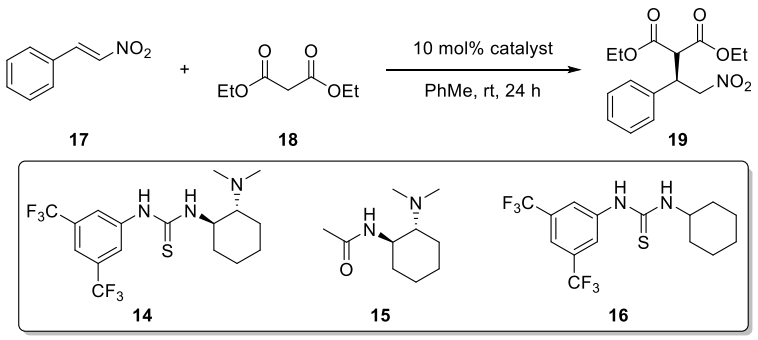

Additive	Yield (%)	e.e. (%)
14	86	93
15	14	35
NEt_3	17	–
NEt_3 + **16**	57	–

Table 2. *Enantioselective addition of malonates to nitroolefins developed by Takemoto and co-workers, and demonstration of the bifunctional nature of the catalyst.*

Two mechanistic proposals have been made regarding the precise nature of the H-bonding interactions that take place in the conjugate addition of malonates to nitroolefins catalysed by **14**. The first was suggested by Takemoto and co-workers and involves the activation of the nitroolefin by H-bonding to both of the thiourea N-H's while the enolate form of the malonate is stabilised by the protonated amine (Figure 3, A).[27] ^{1}H-NMR studies of the association of nitrostyrene with bis(3,5-bis(trifluoromethyl)phenyl)thiourea **10** supported this model of substrate activation. This work was followed by computational studies by Liu and co-workers, describing the reaction mechanism in more detail.[28]

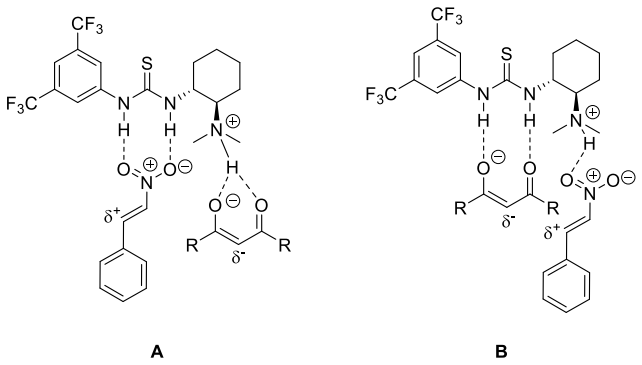

Figure 3. *Two modes of activation proposed for the conjugate addition of 1,3-dicarbonyl compounds to nitroolefins. A – proposed by Takemoto and co-workers, B – proposed by Soós and co-workers. R = OCH_3 in Takemoto's original experimental study, R = CH_3 in the computational studies of Soós and co-workers. This figure only indicates the H-bonding in both models, the relative positions of the reactants are arbitrary and arranged for clarity.*

Further computational studies by Soós and Pápai, as well as showing Takemoto's original mechanistic proposal to be plausible, suggested the possibility of a second reaction pathway.[29] In this pathway, the enolate of the pronucleophile (acetylacetone in this study) is stabilised by H-bonding with both of the thiourea N-H's, while nitrostyrene is associated with the protonated amine of the catalyst (Figure 3, B). Both models correctly predict the observed enantioselectivity and whilst the transition state of Soós's model was calculated to be lower in energy than that of Takemoto's (2.7 kcal mol^{-1} difference in the gas phase, 1.9 kcal mol^{-1} solvated) both pathways were considered to be feasible. Takemoto's catalyst has since been applied to a wide range of asymmetric reactions such as conjugate additions to nitroalkenes,[27] aza-Michael reactions,[30] aldol reactions,[31] Strecker reactions,[32] Mannich reactions[33] and others.[14]

Another important group of bifunctional organocatalysts are the cinchona-based thiourea derivatives,[34] which are formed by derivatising cinchona alkaloids at the C-9 position. This concept was developed independently by the groups of Chen,[35] Soós,[36] Connon[37] and Dixon in 2005.[38] Chen and co-workers found catalyst **20** to be a very active promoter of the Michael addition of thiophenol to imides, however enantioselectivity was very low. Soós applied catalyst **21** to the Michael addition of nitromethane to chalcone, obtaining excellent yield and enantioselectivity, while Connon and Dixon both successfully investigated the conjugate addition of malonates to nitroalkenes. It was found that the configuration at C-9 was important for catalytic activity, with the thiourea derivative of the natural C-9 epimer, **22**, exhibiting no catalytic activity (Table 3).[36,37] This was taken as

evidence for a bifunctional mode of operation, due to the importance of the relative orientation of the thiourea and quinuclidine moieties. Computational studies by Soós and Pápai also supported a bifunctional model of substrate activation, with analogous activation modes to those found for Takemoto's catalyst being identified for the cinchona-derived thioureas.[29] The applications of the cinchona-derived thiourea organocatalysts are very broad and include various aza-,[39] oxy-[40] and sulfa-[41] conjugate additions, aldol reactions,[42,43] Mannich reactions,[44] desymmetrisations[45] and Friedel-Crafts reactions,[46] amongst others.[14,34]

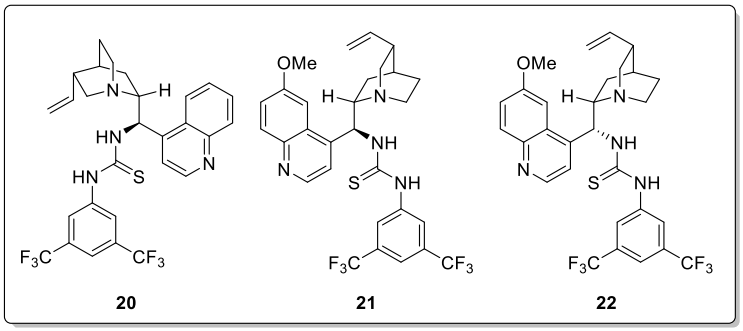

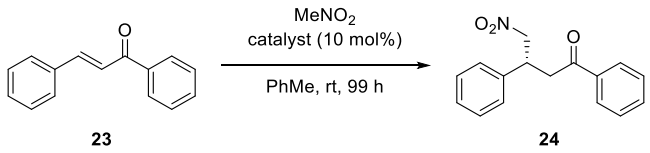

23 24

Catalyst	Yield (%)	e.e. (%)
22	N.R.	-
21	71	95

Table 3. *Cinchona-derived thiourea catalysts and the performance of C-9 epimers in the Michael addition of nitromethane to chalcone.*

The pioneering developments of the early 2000's initiated a wave of prolific catalyst development. Many catalyst structures combining Brønsted bases and H-bond donors, typically tertiary amines and urea derivatives, respectively, have been reported and applied to a wide range of reactions (Figure 4).[34,47,48] Several "privileged" scaffolds can be seen to be repeatedly used in bifunctional catalysis such as the cinchona alkaloids, BINOL and 1,2-diamines. Despite the great achievements of bifunctional Brønsted base/H-bond door organocatalysis, challenges remain, such as the related issues of low reactivity, long reaction times and high catalyst loading, one solution to which will be discussed below.

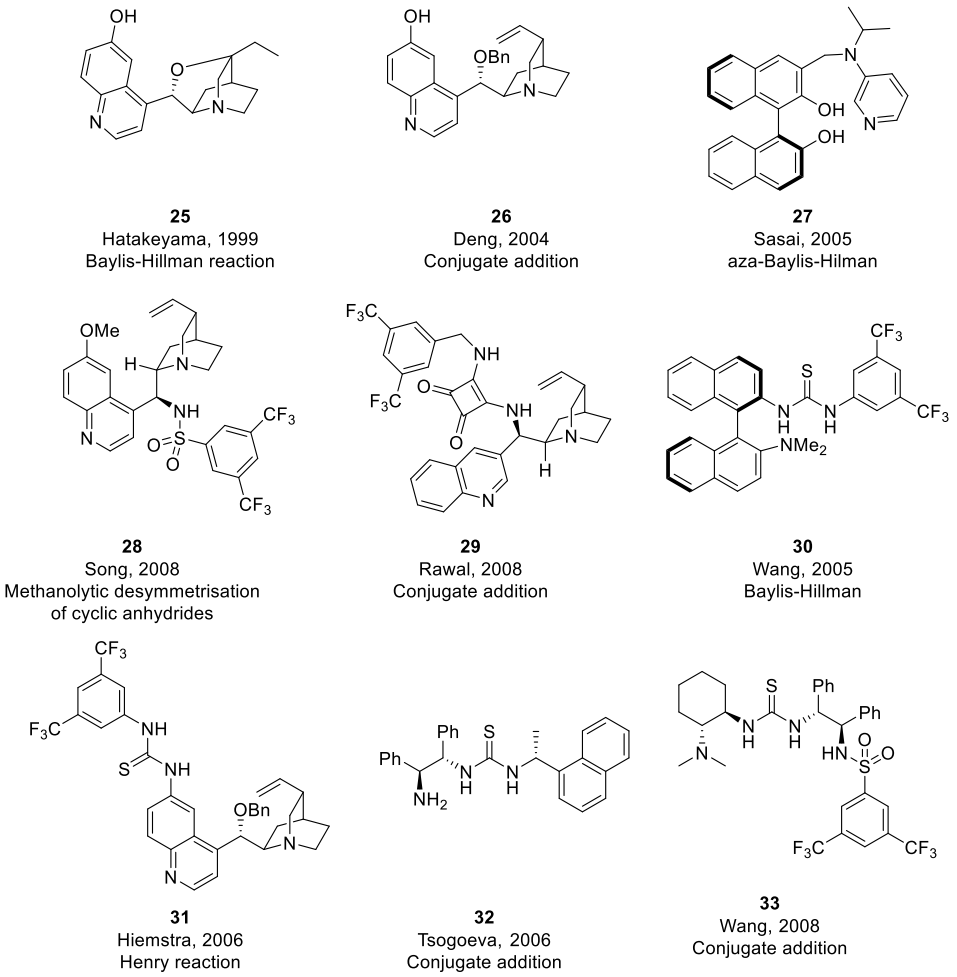

Figure 4. *Representative examples of bifunctional Brønsted base/H-bond donor organocatalysts. Captions state the reaction in which the catalyst was used in its first report.*[49–57]

1.3 Organic superbases in organocatalysis

Although the use of Brønsted base/H-bond donor organocatalysis using amine bases allows chemists to access a broad range of chiral compounds through a wide range of reactions with excellent enantioselectivity, amine bases have quite low pK_a (e.g. 9.80 in DMSO for quinuclidine) and this arguably leads to low reaction rates and a limited substrate scope. For example, the reaction of pyrrolidinone **34** with nitrostyrene catalysed by bifunctional cinchonine-derived organocatalyst **20**, although it is high yielding and highly enantioselective, requires 14 days to reach completion (Scheme 3).[58]

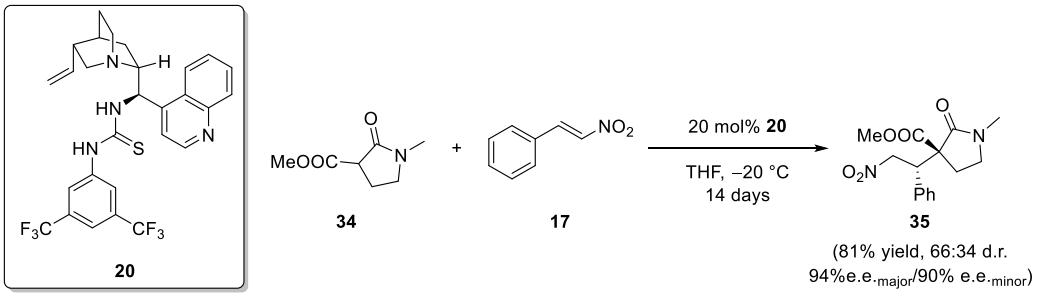

Scheme 3. *Reaction of pyrrolidinone **34** with nitrostyrene catalysed by **20**. Yield, d.r. and e.e. determined from reaction performed by Dr. Pavol Jakubec.*

Considering the issue of substrate scope, a relevant example is the first known example of the nitro-Mannich reaction of ketimines catalysed by an organic base, reported by Terada and co-workers (Scheme 4).[59] In this work, it was found that triethylamine did not promote the reaction and the use of organic superbases, such as 1,1,3,3-tetramethylguanidine (TMG) and Schwesinger's P_1-*t*-Bu base[60] was required for reactivity.

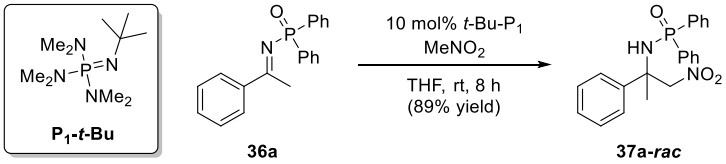

Scheme 4. *Nitro-Mannich reaction of ketimines by Terada and co-workers.*

Thus, if strong organic bases – "superbases" were to be incorporated into bifunctional organocatalysts, one could envisage that this would allow for faster reaction rates, lower catalyst loadings and broader substrate scope through enabling the use of higher pK_a pronucleophiles.

The definition of exactly what constitutes an organic superbase is ambiguous. In Ishakawa's comprehensive text *Superbases for Organic Synthesis*[61] the definition developed by Caubère is adopted:

> *The term "superbases" should only be applied to bases resulting from a mixing of two (or more) bases leading to new basic species possessing inherent new properties. The term "superbase" does not mean a base is thermodynamically and/or kinetically stronger than another, instead it means that a basic reagent is created by combining the characteristics of several different bases.*[62]

A good illustration of this concept is the base 1,8-bis(dimethylamino)naphthalene (DMAN) (Figure 5). Although aromatic amines are weak bases (the pK_a of *N*,*N*-dimethylaniline is only 2.4 in DMSO),[63] combining two such amines on the *peri* position of naphthalene leads to two phenomena

which greatly increases the basicity of DMAN relative to *N,N*-dimethylaniline (pK_a of 7.5 in DMSO).[63] Due to steric hindrance from the adjacent dimethylamine moiety, the nitrogen lone pair is not able to delocalise into the aromatic system, increasing its basicity, and secondly, the two adjacent amines are also able to chelate protons. Note that DMAN is less basic than quinuclidine in DMSO (pK_a of 9.8), however it is still considered a superbase under this definition.

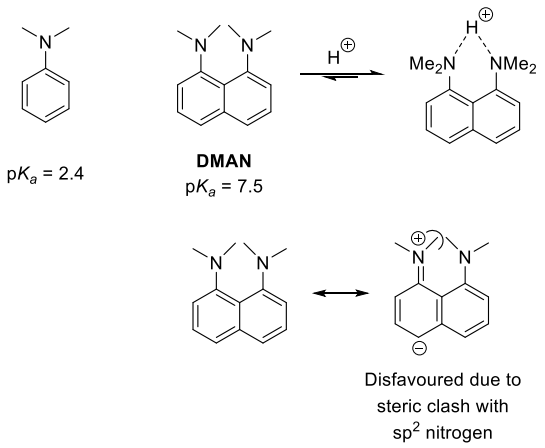

Figure 5. *pK_a of N,N-dimethylaniline and DMAN and properties leading to enhanced basicity of DMAN*

Because we are interested in developing organocatalysts incorporating basic moieties stronger than those traditionally found in bifunctional catalysts (i.e. quinuclidine and other tertiary amines), pK_a values are more important than novel properties leading to enhanced basicity *per se*. When the term "superbase" is used in this text, it is referring to basic moieties with pK_a comparable to, or greater than, that of guanidine (28.5 in DMSO).[63]

Of the organic superbases, guanidines have been perhaps the most commonly used in asymmetric organocatalysis.[64] Guanidines are a particularly interesting superbase functional group due to the fact that protonated guanidines can form dual hydrogen bonds in a similar fashion to a urea moiety. These additional H-bonding interactions enable guanidines to function as bifunctional catalysts, though not all guanidine organocatalysts function in this way.[65] The chiral guanidine-catalysed addition of *α*-fluoro-*β*-ketoesters such as **38** to *N*-alkyl maleimides developed by Tan and co-workers (Scheme 5) is an example of bifunctional catalysis by a guanidine.[66] In this study, Tan and co-workers found that a variety of *α*-fluoro-*β*-ketoesters could be added to a cyclic or acyclic Michael acceptors with excellent yield and enantioselectivity, catalysed by **39**.

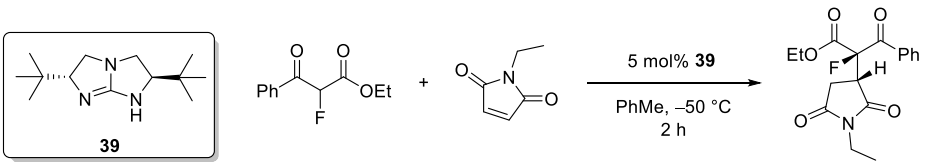

Scheme 5. *Chiral guanidine-catalysed addition of α-fluoro-β-ketoesters to N-alkyl maleimides developed by Tan and co-workers. Representative substrates shown.*

Computational studies were undertaken to elucidate the mechanism of this reaction. The first step in the catalytic cycle is the deprotonation of the *α*-fluoro-*β*-ketoester by **39** and the formation of a hydrogen-bonded complex between the guanidinium cation and the substrate anion. The maleimide then approaches this complex, at which point two complexes may be formed – a "face on" complex where only the enolate is H-bonded to the catalyst (Figure 6, A) and a "side on" complex where the guanidinium forms hydrogen bonds with both reactants (Figure 6, B). Both complexes can lead to a C–C bond-forming transition state, however, the "side on" complex was found to be energetically favourable due to the increased hydrogen bonding stabilisation of charge transfer in the transition state. Therefore it was concluded that **39** functions as a bifunctional organocatalyst.

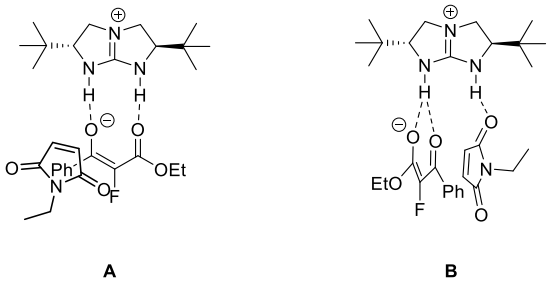

Figure 6. *"Face on" (A) and "Side on" (B) complexes. Complex B only shows the relative position of catalyst ad reactants, not the full extent of hydrogen bonding.*

Another approach to using guanidines as bifunctional catalysts is to attach an additional H-bond donor moiety to the guanidine. This was the approach taken by Ishikawa and co-workers who developed synthetic routes to various chiral guanidines bearing hydroxyl moieties.[67] The first successful application of these compounds to asymmetric methodologies was in the enantioselective Michael addition of glycine imine to acrylate, but in this case, the catalyst is proposed only to activate the nucleophile.[68] However, in further work on the synthesis of chromanes via the intramolecular oxa-Michael reaction, Ishikawa's chiral guanidine catalyst is believed to function in a bifunctional

manner.[69] This is also an instructive example from the point of view of expanding the substrate scope of organocatalytic reactions through the use of strong bases. During studies of the formation of 2,2-disubstituted chromanes *via* the intramolecular oxa-Michael reaction of a phenol tethered to a *β*-substituted, *α,β*-unsaturated ester (Scheme 6) Ishikawa and co-workers found that although dihydrocinchonine may be used to successfully catalyse the formation of a 2-substituted chromane from the analogous system to **42** featuring a *β*-monosubstituted, *α,β*-unsaturated ester,[70] attempts to react the *β*-disubstituted substrate **42** with quinine were unsuccessful. Similarly, the use of triethylamine, even at reflux, did not result in any reaction taking place. The use of 20 mol% of TMG, however, resulted in 75% yield of desired 2,2-disubstituted chromane in 75% yield, proving that a strong organic base is necessary for the cyclisation of this substrate. Extensive optimisation studies showed that guanidines with pendant hydroxyl groups gave the best yield and enantioselectivity, with guanidine **43** chosen as the optimal catalyst. The authors proposed that the hydroxyl group of **43** hydrogen bonds to the ester of **42**, while the exocyclic guanidine nitrogen deprotonates the phenol (Figure 7), thus activating **42** in a bifunctional fashion.

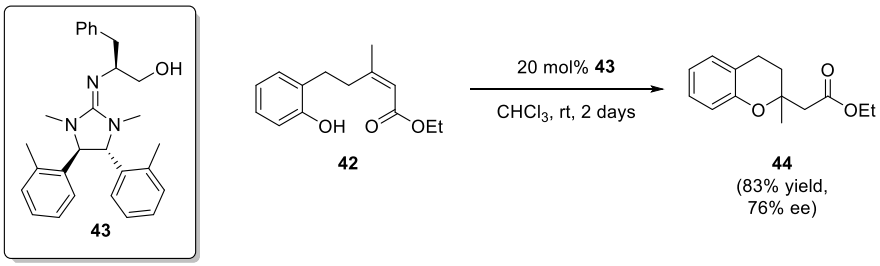

Scheme 6. *Chiral guanidine-catalysed intramolecular oxa-Michael reaction for the synthesis of 2,2-disubstituted chromanes.*

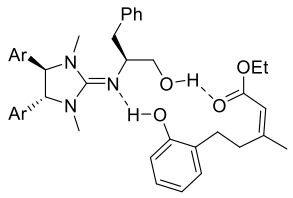

Figure 7. *Depiction of hydrogen bonding in the transition state of the oxa-Michael reaction catalysed by **43**.*

Another important class of superbase organocatalysts are the phosphazenes (or iminophosphoranes). The two terms are often used interchangeably however in this text "phosphazene" typically refers to compounds containing one or more R-N=P(NR_2)$_3$ units while "iminophosphorane" refers to

molecules of the form R-N=PR_3, where R represents an aryl or alkyl group. The use of chiral phosphazenes as organocatalysts was pioneered by the group of Ooi in the late 2000's. Ooi and co-workers reported the preparation of the chiral tetraaminophosphonium salt **45**, which, when treated with potassium *tert*-butoxide, generated phosphazene **46** which was an excellent catalyst for the Henry reaction (Scheme 7, b).[71] The very high basicity of these phosphazene bases was also exploited to activate the challenging dialkyl phosphite nucleophile **49** in the asymmetric hydrophosphonylation of aldehydes (Scheme 7, c).[72] Although thorough mechanistic investigations of reactions involving these catalysts do not appear to have yet been undertaken, the authors propose that in the Henry reaction, apart from deprotonating the nitroalkane, the phosphonium form of the catalyst imparts spatial organisation *via* hydrogen bonding. This class of catalysts has also been used in Mannich-type reactions,[73] conjugate additions[74,75] and the Payne oxidation.[76] Notably, a related supramolecular catalyst can be prepared *via* self-assembly in solution.[77]

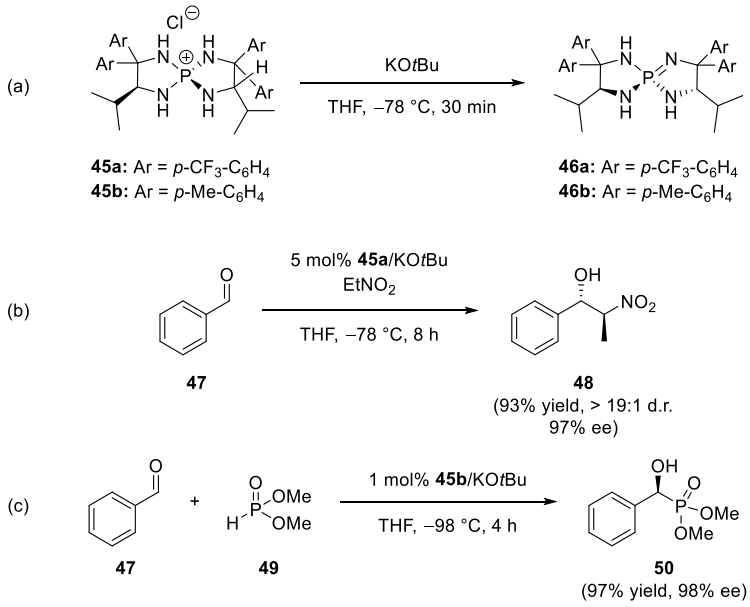

Scheme 7. *Formation of chiral phosphazene organocatalysts from the corresponding phosphonium salts (a) and application to the Henry reaction (b) and the phosphinylation of aldehydes (c).*

A notable recent development in the field of asymmetric superbase organocatalysis is the work of Lambert and co-workers on the use of chiral cyclopropenimines as organocatalysts. Cyclopropenimines are potent bases due to the fact that upon protonation, they form the aromatic cyclopropenium cation and this aromatic stabilisation makes protonation highly favourable. The positive charge is also stabilised by the three amine substituents.[78] Lambert's initial report of

cyclopropenimine organocatalysis[79] closely mirrored but greatly improved on Ishikawa's 2001 report of the chiral guanidine-catalysed Michael addition of glycine-derived imine to acrylate (Table 4).[68] Cyclopropenimine **51** has also been shown to be an excellent catalyst for the Mannich reaction of glycine imines and Boc-protected aldimines.[80] It is postulated by the authors that in both of these reactions, hydrogen bonding between the catalyst N-H and O-H and both of the substrates serves to simultaneously activate both the nucleophile and the electrophile and organise the reaction transition state (Figure 8).

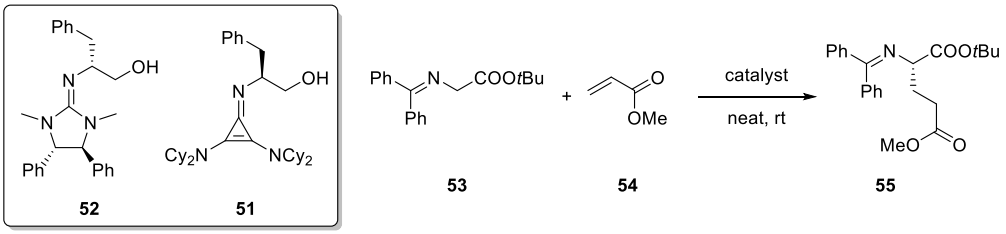

Catalyst	Loading (mol%)	Time	Yield (%)	e.e. (%)
51	10	5 min	99	91
52	20	3 d	98	93

Table 4. *Addition of glycine imine to acrylate catalysed by cyclopropenimine **51** and comparison with guanidine **52**.*

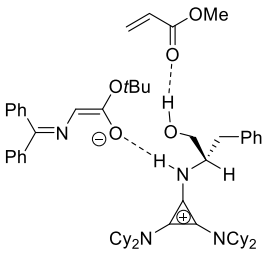

Figure 8. *Activation of glycine imine and acrylate by cyclopropenimine **51**.*

Finally, the contribution of the Dixon group to bifunctional superbase organocatalysis, and the work we hope to build upon in this thesis, is the development of bifunctional iminophosphorane organocatalysts.[1] With the aim of incorporating a potent, modular and tuneable basic moiety into a bifunctional organocatalyst, the formation of iminophosphoranes *via* the Staudinger reaction of triaryl phosphines and chiral azides bearing a H-bond donor motif was investigated. The testing ground for this novel catalyst was to be the nitro-Mannich reaction of phosphinoyl ketimines, which had previously been shown to require a strong organic base for successful catalysis (*vide supra*). Extensive screening of various catalyst scaffolds, H-bond donor groups and phosphines led to the

identification of **56** as the optimal catalyst in terms of reactivity and enantioselectivity in this reaction (Scheme 8). The reaction scope was then demonstrated as well as the use of **56** on a preparative scale.

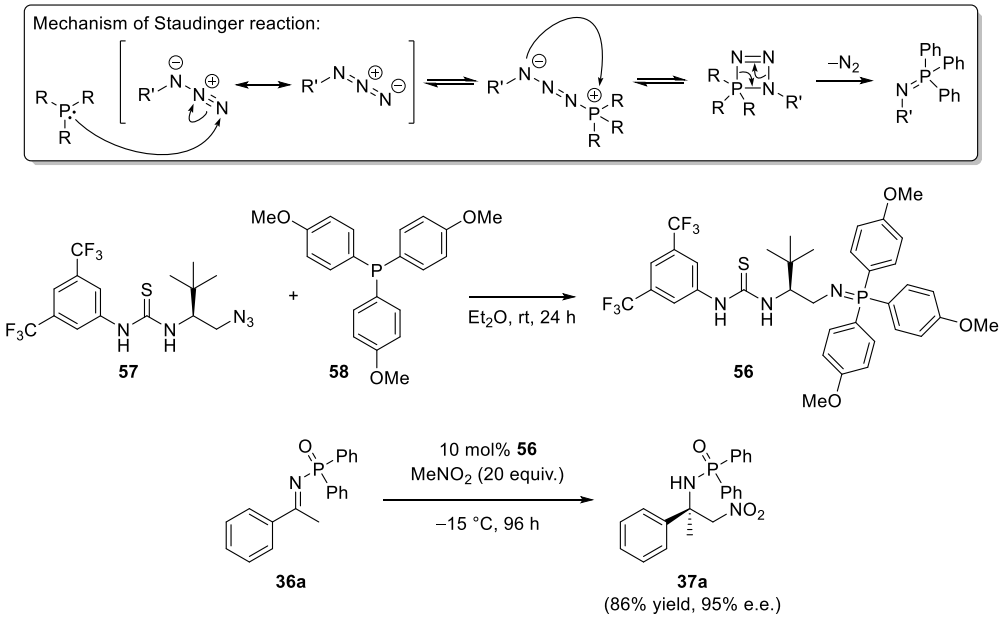

Scheme 8. *Preparation of bifunctional iminophosphorane catalyst **56** via Staudinger reaction and application to the nitro-Mannich reaction of phosphinoyl ketimine **36a**.*

Although phosphazenes such as BEMP and Schwesinger's phosphazene bases[60] have been extensively studied,[81] the properties of alkyl or aryl substituted iminophosphoranes are less well known. In fact, the aforementioned work from the Dixon group was the first to measure the pK_a of this class of compounds (Figure 9). It was found that the nature of the substituents on the phosphine had a large effect on the basicity of the resulting iminophosphorane, with the tris(4-methoxy)phenyl-substituted iminophosphorane **58** being 2.3 units more basic than the phenyl-substituted iminophosphorane **59**.

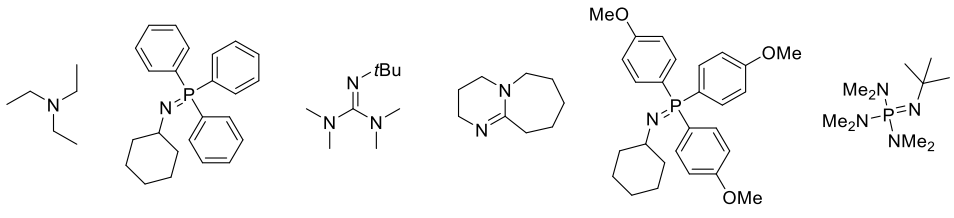

Figure 9. *pK_a of iminophosphoranes compared to other bases, measured in acetonitrile.*[1]

This was also shown to affect the activity of the corresponding bifunctional iminophosphorane organocatalysts in the nitro-Mannich reaction, with catalysts featuring the more strongly basic iminophosphoranes catalysing the nitro-Mannich reaction faster than less basic catalysts (Figure 10). Although the pK_a of the tris(4-chloro)phenyl-substituted iminophosphorane was not measured, it is presumably less basic than the phenyl-substituted iminophosphorane and its observed reactivity is in agreement with this.

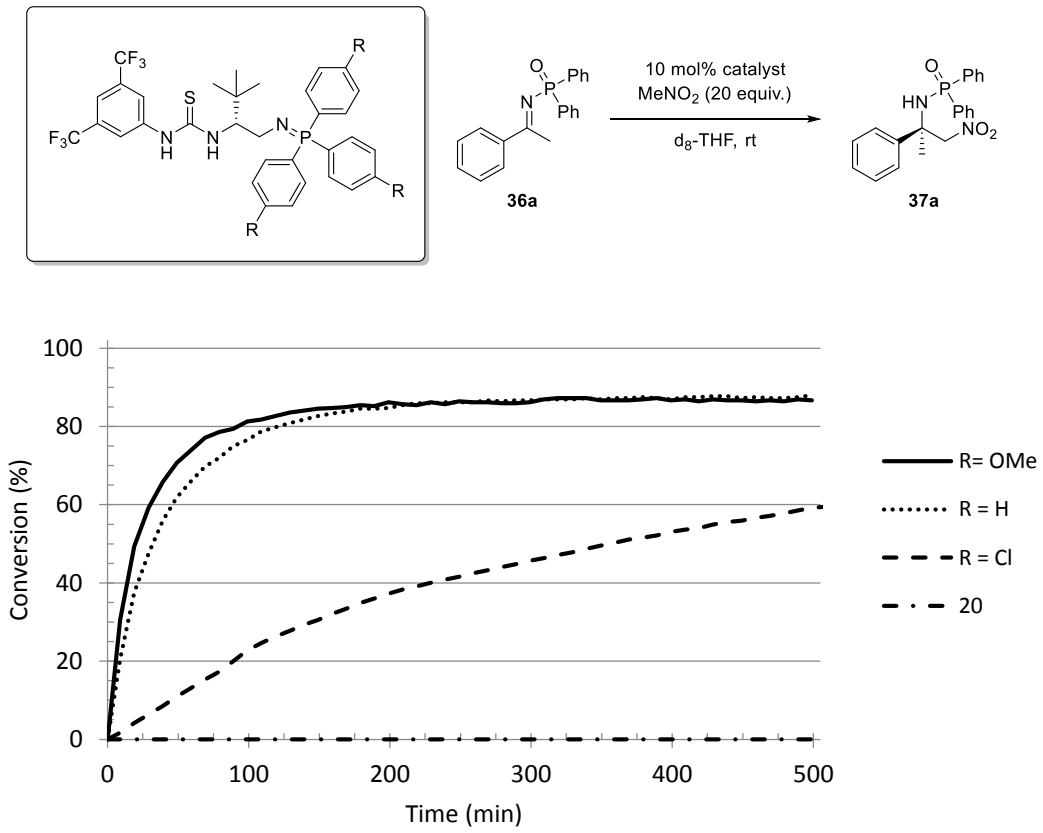

Figure 10. *[1]H-NMR kinetic study showing the performance of bifunctional iminophosphoranes, measured as conversion to **37a** over time, in the nitro-Mannich reaction of **36a**, with different phosphorus substituents (Study carried out by Alistair Farley and Dr. Marta Garcia Núñez).*[1]

References

(1) Núñez, M. G.; Farley, A. J. M.; Dixon, D. J. *J. Am. Chem. Soc.* **2013**, *135*, 16348–16351.
(2) Blow, D. M.; Birktoft, J. J.; Hartley, B. S. *Nature* **1969**, *221*, 337–340.
(3) Scott, J. W.; Valentine Jr., D. *Science (80-.).* **1974**, *184*, 943–952 CR – Copyright © 1974 American Assoc.
(4) Oleinik, L. M.; Litvinenko, N. M. *Russ. Chem. Rev.* **1978**, *47*, 401.
(5) Helder, R.; Arends, R.; Bolt, W.; Hiemstra, H.; Wynberg, H. *Tetrahedron Lett.* **1977**, *18*, 2181–2182.
(6) Pluim, H.; Wynberg, H. *Tetrahedron Lett.* **1979**, *20*, 1251–1254.
(7) Wynberg, H.; Helder, R. *Tetrahedron Lett.* **1975**, *16*, 4057–4060.
(8) Hiemstra, H.; Wynberg, H. *J. Am. Chem. Soc.* **1981**, *103*, 417–430.
(9) Ueyanagi, K.; Inoue, S. *Die Makromol. Chemie* **1978**, *179*, 887–893.
(10) Inoue, S.; Kawano, Y. *Die Makromol. Chemie* **1979**, *180*, 1405–1411.
(11) Oku, J.; Ito, N.; Inoue, S. *Die Makromol. Chemie* **1979**, *180*, 1089–1091.
(12) Oku, J.; Inoue, S. *J. Chem. Soc. Chem. Commun.* **1981**, 229–230.
(13) Iyer, M. S.; Gigstad, K. M.; Namdev, N. D.; Lipton, M. *J. Am. Chem. Soc.* **1996**, *118*, 4910–4911.
(14) Dalko, P. I. (Ed. . *Comprehensive Enantioselective Organocatalysis: Catalysts, Reactions, and Applications*; Dalko, P. I., Ed.; Wiley-VCH, 2013.
(15) Etter, M. C.; Urbanczyk-Lipkowska, Z.; Zia-Ebrahimi, M.; Panunto, T. W. *J. Am. Chem. Soc.* **1990**, *112*, 8415–8426.
(16) Hine, J.; Linden, S. M.; Kanagasabapathy, V. M. *J. Am. Chem. Soc.* **1985**, *107*, 1082–1083.
(17) Schreiner, P. R.; Wittkopp, A. *Org. Lett.* **2002**, *4*, 217–220.
(18) Wittkopp, A.; Schreiner, P. R. *Chem. – Eur. J.* **2003**, *9*, 407–414.
(19) Sigman, M. S.; Jacobsen, E. N. *J. Am. Chem. Soc.* **1998**, *120*, 4901–4902.
(20) Sigman, M. S.; Vachal, P.; Jacobsen, E. N. *Angew. Chem., Int. Ed.* **2000**, *39*, 1279–1281.
(21) Vachal, P.; Jacobsen, E. N. *J. Am. Chem. Soc.* **2002**, *124*, 10012–10014.
(22) Pan, S. C.; Zhou, J.; List, B. *Angew. Chem., Int. Ed.* **2007**, *46*, 612–614.
(23) Wenzel, A. G.; Jacobsen, E. N. *J. Am. Chem. Soc.* **2002**, *124*, 12964–12965.
(24) Fuerst, D. E.; Jacobsen, E. N. *J. Am. Chem. Soc.* **2005**, *127*, 8964–8965.
(25) Berkessel, A.; Mukherjee, S.; Cleemann, F.; Muller, T. N.; Lex, J. *Chem. Commun.* **2005**, 1898–1900.
(26) Okino, T.; Hoashi, Y.; Takemoto, Y. *J. Am. Chem. Soc.* **2003**, *125*, 12672–12673.
(27) Okino, T.; Hoashi, Y.; Furukawa, T.; Xu, X.; Takemoto, Y. *J. Am. Chem. Soc.* **2004**, *127*, 119–125.
(28) Zhu, R.; Zhang, D.; Wu, J.; Liu, C. *Tetrahedron: Asymmetry* **2006**, *17*, 1611–1616.
(29) Hamza, A.; Schubert, G.; Soós, T.; Pápai, I. *J. Am. Chem. Soc.* **2006**, *128*, 13151–13160.
(30) Enders, D.; Göddertz, D. P.; Beceño, C.; Raabe, G. *Adv. Synth. Catal.* **2010**, *352*, 2863–2868.
(31) Zu, L.; Xie, H.; Li, H.; Wang, J.; Jiang, W.; Wang, W. *Adv. Synth. Catal.* **2007**, *349*, 1882–1886.
(32) Enders, D.; Gottfried, K.; Raabe, G. *Adv. Synth. Catal.* **2010**, *352*, 3147–3152.
(33) Yamaoka, Y.; Miyabe, H.; Yasui, Y.; Takemoto, Y. *Synthesis (Stuttg).* **2007**, *2007*, 2571–2575.
(34) Connon, S. J. *Chem. Commun.* **2008**, 2499–2510.
(35) Li, B.-J.; Jiang, L.; Liu, M.; Chen, Y.-C.; Ding, L.-S.; Wu, Y. *Synlett* **2005**, 603–606.
(36) Vakulya, B.; Varga, S.; Csámpai, A.; Soós, T. *Org. Lett.* **2005**, *7*, 1967–1969.
(37) McCooey, S. H.; Connon, S. J. *Angew. Chem., Int. Ed.* **2005**, *44*, 6367–6370.
(38) Ye, J.; Dixon, D. J.; Hynes, P. S. *Chem. Commun.* **2005**, 4481–4483.
(39) Wang, X.-F.; An, J.; Zhang, X.-X.; Tan, F.; Chen, J.-R.; Xiao, W.-J. *Org. Lett.* **2011**, *13*, 808–811.
(40) Li, D. R.; Murugan, A.; Falck, J. R. *J. Am. Chem. Soc.* **2007**, *130*, 46–48.
(41) Enders, D.; Hoffman, K. *Eur. J. Org. Chem.* **2009**, *2009*, 1665–1668.

(42) Zu, L.; Wang, J.; Li, H.; Xie, H.; Jiang, W.; Wang, W. *J. Am. Chem. Soc.* **2007**, *129*, 1036–1037.
(43) Zhu, N.; Ma, B.-C.; Zhang, Y.; Wang, W. *Adv. Synth. Catal.* **2010**, *352*, 1291–1295.
(44) Song, J.; Wang, Y.; Deng, L. *J. Am. Chem. Soc.* **2006**, *128*, 6048–6049.
(45) Dickmeiss, G.; De Sio, V.; Udmark, J.; Poulsen, T. B.; Marcos, V.; Jørgensen, K. A. *Angew. Chem., Int. Ed.* **2009**, *48*, 6650–6653.
(46) Wang, Y.-Q.; Song, J.; Hong, R.; Li, H.; Deng, L. *J. Am. Chem. Soc.* **2006**, *128*, 8156–8157.
(47) Doyle, A. G.; Jacobsen, E. N. *Chem. Rev.* **2007**, *107*, 5713–5743.
(48) Miyabe, H.; Takemoto, Y. *Bull. Chem. Soc. Jpn.* **2008**, *81*, 785–795.
(49) Iwabuchi, Y.; Nakatani, M.; Yokoyama, N.; Hatakeyama, S. *J. Am. Chem. Soc.* **1999**, *121*, 10219–10220.
(50) Li, H.; Wang, Y.; Tang, L.; Deng, L. *J. Am. Chem. Soc.* **2004**, *126*, 9906–9907.
(51) Matsui, K.; Takizawa, S.; Sasai, H. *J. Am. Chem. Soc.* **2005**, *127*, 3680–3681.
(52) Oh, S. H.; Rho, H. S.; Lee, J. W.; Lee, J. E.; Youk, S. H.; Chin, J.; Song, C. E. *Angew. Chem., Int. Ed.* **2008**, *47*, 7872–7875.
(53) Malerich, J. P.; Hagihara, K.; Rawal, V. H. *J. Am. Chem. Soc.* **2008**, *130*, 14416–14417.
(54) Wang, J.; Li, H.; Yu, X.; Zu, L.; Wang, W. *Org. Lett.* **2005**, *7*, 4293–4296.
(55) Marcelli, T.; van der Haas, R. N. S.; van Maarseveen, J. H.; Hiemstra, H. *Angew. Chem., Int. Ed.* **2006**, *45*, 929–931.
(56) Tsogoeva, S. B.; Wei, S. *Chem. Commun.* **2006**, 1451–1453.
(57) Wang, C.-J.; Zhang, Z.-H.; Dong, X.-Q.; Wu, X.-J. *Chem. Commun.* **2008**, 1431–1433.
(58) Jakubec, P.; Helliwell, M.; Dixon, D. J. *Org. Lett.* **2008**, *10*, 4267–4270.
(59) Pahadi, N. K.; Ube, H.; Terada, M. *Tetrahedron Lett.* **2007**, *48*, 8700–8703.
(60) Schwesinger, R.; Schlemper, H. *Angew. Chem., Int. Ed. English* **1987**, *26*, 1167–1169.
(61) *Superbases for organic synthesis : guanidines, amidines and phosphazenes and related organocatalysts*; Ishikawa, T., Ed.; John Wiley & Sons, Ltd, 2009.
(62) Caubere, P. *Chem. Rev.* **1993**, *93*, 2317–2334.
(63) Bordwell, F. G. *Acc. Chem. Res.* **1988**, *21*, 456–463.
(64) Selig, P. *Synthesis (Stuttg).* **2013**, *45*, 703–718.
(65) Fu, X.; Tan, C.-H. *Chem. Commun.* **2011**, *47*, 8210–8222.
(66) Jiang, Z.; Pan, Y.; Zhao, Y.; Ma, T.; Lee, R.; Yang, Y.; Huang, K.-W.; Wong, M. W.; Tan, C.-H. *Angew. Chem., Int. Ed.* **2009**, *48*, 3627–3631.
(67) Isobe, T.; Fukuda, K.; Ishikawa, T. *J. Org. Chem.* **2000**, *65*, 7770–7773.
(68) Ishikawa, T.; Araki, Y.; Kumamoto, T.; Seki, H.; Fukuda, K.; Isobe, T. *Chem. Commun.* **2001**, 245–246.
(69) Saito, N.; Ryoda, A.; Nakanishi, W.; Kumamoto, T.; Ishikawa, T. *Eur. J. Org. Chem.* **2008**, *2008*, 2759–2766.
(70) Merschaert, A.; Delbeke, P.; Daloze, D.; Dive, G. *Tetrahedron Lett.* **2004**, *45*, 4697–4701.
(71) Uraguchi, D.; Sakaki, S.; Ooi, T. *J. Am. Chem. Soc.* **2007**, *129*, 12392–12393.
(72) Uraguchi, D.; Ito, T.; Ooi, T. *J. Am. Chem. Soc.* **2009**, *131*, 3836–3837.
(73) Uraguchi, D.; Ueki, Y.; Ooi, T. *J. Am. Chem. Soc.* **2008**, *130*, 14088–14089.
(74) Uraguchi, D.; Ueki, Y.; Sugiyama, A.; Ooi, T. *Chem. Sci.* **2013**, *4*, 1308.
(75) Uraguchi, D.; Nakamura, S.; Sasaki, H.; Konakade, Y.; Ooi, T. *Chem. Commun.* **2014**, *50*, 3491–3493.
(76) Uraguchi, D.; Tsutsumi, R.; Ooi, T. *Tetrahedron* **2014**, *70*, 1691–1701.
(77) Uraguchi, D.; Ueki, Y.; Ooi, T. *Science* **2009**, *326*, 120–123.
(78) Komatsu, K.; Kitagawa, T. *Chem. Rev.* **2003**, *103*, 1371–1428.
(79) Bandar, J. S.; Lambert, T. H. *J. Am. Chem. Soc.* **2012**, *134*, 5552–5555.
(80) Bandar, J. S.; Lambert, T. H. *J. Am. Chem. Soc.* **2013**, *135*, 11799–11802.
(81) Kondo, Y. In *Superbases for Organic Synthesis*; John Wiley & Sons, Ltd, 2009; pp. 145–185.

Chapter 2: Organocatalyst Immobilisation

1. Introduction

The heterogenisation of reagents and catalysts can bring about many advantages, but due to the difficulties it can entail, is an area of ongoing development in organic synthesis.[1,2] The development of a supported reagent or catalyst is undertaken with the anticipation that its many benefits will outweigh the possible disadvantages and with the judicious choice of substrate and solid support, as well as careful study of their union, this positive outcome is possible in many cases.[3]

The primary benefits of heterogenisation are easy catalyst separation from the reaction mixture, the possibility of catalyst recycling and application in continuous flow processes.[4] From the point of view of organocatalysis, these benefits are highly relevant due to the chemical similarity of catalyst and product and the high value of some organocatalysts, due to their involved synthesis, combined with the use of relatively high catalyst loadings.[1] However, it has been argued by some that the main impediment to widespread adoption of immobilised organocatalysts is the prohibitive cost of the solid support compared to the low value of the catalyst itself.[2] Although functionalised solids are indeed expensive[2] and the above comparison certainly holds true for structurally simple and inexpensive catalysts such as proline, the preparation of many organocatalysts is non-trivial making them high-value compounds.[i]

The major disadvantages of immobilisation are perceived to be the concomitant loss of reactivity and enantioselectivity, the requirement of additional synthetic steps to affect immobilisation as well as the aforementioned high cost of the solid support. A decrease in reactivity and enantioselectivity can indeed be a consequence of catalyst immobilisation, however, this is not always the case and in many instances supported organocatalysts may perform similarly to, or even better than, their

[i] For example, enantiopure *trans*-1,2-cyclohexanediamine is a common scaffold in organocatalysis (e.g. Takemoto's and Jacobsen's catalysts). It must be either prepared by the resolution of racemic 1,2-cyclohexanediamine prior to use or it may be purchased from chemical suppliers, however it is very costly (~£200/g for the mono-Boc derivative from Sigma Aldrich at the time of writing).

homogeneous counterparts (*vide infra*).[1,3,4] In almost all cases, additional synthetic steps are required to introduce a linker into the catalyst structure which serves to attach the catalyst to the solid support. In some cases, the incorporation of a linker is seen to be important for minimising the effect of the support on reactivity or enantioselectivity (*vide infra*), however, the entailing structural modification of the catalyst may simultaneously lead to unwanted steric and/or electronic effects.[3] In order to learn how to address these disadvantages, it is important to have a good understanding of the nature of the solid support and its effect on the catalyst.

1.2 The nature of the solid support and the physical effects of immobilisation

It has been said (in the context of solid phase synthesis, but also applicable here) that the solid support is analogous to, and equally as important as, the solvent in a homogeneous reaction.[5] In this work, as we have predominantly used cross-linked polystyrene as the solid support as well as undertaking some investigations on silica, we will now focus on these two materials.

1.2.1 Cross-linked polystyrene

Cross-linked polystyrene is a co-polymer of styrene and divinylbenzene (most commercial resins contain about 1 – 2% divinylbenzene), typically synthesised by suspension polymerisation in order to form small spherical beads.[6] To form functionalised beads, a third monomer, a styrene derivative carrying the desired functional group, is added to the reaction mixture (Figure 11). When cross-linked polystyrene is placed in an appropriate solvent, it swells, increasing in volume. This is similar to the solvation of a non-crosslinked polymer, except the cross-links between polymer chains prevent complete freedom of motion and the solvent occupies the spaces between the chains.[6] As the majority of functionalised sites are within the volume of the polymer bead, it would follow that effective swelling is imperative for achieving good reaction rates.[6] Thus the reaction of a dissolved substrate with a polymer-supported catalyst consists of several stages: diffusion of the substrate from the bulk solution to the solution surrounding the polymer, diffusion through the bead volume to an active site, reaction, diffusion of the product out to the solution surrounding the polymer, then diffusion back into the bulk solution.[7] This lengthy series of steps may give the impression that a solid-supported

reaction is necessarily much slower than its homogeneous counterpart, but due to the nature of cross-linked polystyrene, this is not always the case.

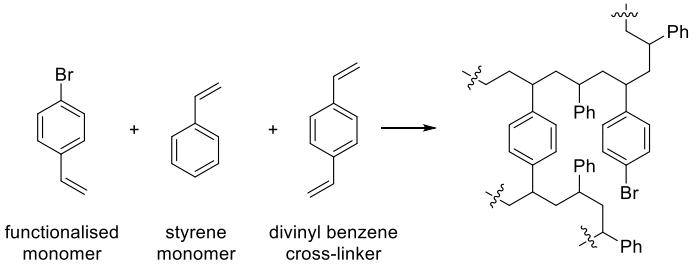

Figure 11. *Constitution and structure of cross-liked polystyrene featuring 4-bromophenyl functionality.*

Considering its physical appearance and depiction in chemical schemes, it is interesting to note how 'solution-like' the behaviour of swollen cross-linked polystyrene is. Indeed, it appears to bear greater resemblance to a viscous liquid than to a solid.[6] It has been shown that the rate of motion of the backbone and the aromatic groups of 1% cross-linked polystyrene swollen in dichloromethane is equivalent to that of soluble linear polystyrene.[8] Because of this, the tactic of incorporating a linker between a reagent or catalyst and a polystyrene solid support with the aim of increasing reactivity is often unnecessary, as the polymer chain to which it is connected is already highly mobile and flexible. Indeed, studies from the field of solid-phase synthesis show that the incorporation of a linker into a heterogeneous system does not necessarily improve the rate of reaction.[9,10] This high motility perhaps explains why even though reactions involving a solid-supported catalyst involve additional mass transfer and diffusion steps they may be quite fast and the rate of a heterogeneous reaction can still be comparable to the rate of the corresponding homogenous reaction, making cross-linked polystyrene a very useful solid support.

1.2.2 Silica

An alternative approach is to use an inorganic material as the solid support. Of these, silica has appropriate properties for this application due to its stability, high surface area (typically from 100 $m^2\ g^{-1}$ to more than 600 $m^2\ g^{-1}$) and large pore size (typically > 20 Å, however silicas with pore sizes of 5–500 Å may be prepared).[11,12] Functionalised silica may be prepared either by reacting pre-prepared silica with silanes bearing the desired functional group,[13] or by incorporating such

functionalised silanes into the process used to prepare the material.[12] A great variety of amorphous, microporous or macroporous silicas can be synthesised, many of which are also commercially available.[12] Silica may be subjected to post-synthetic modification due to the fact that the surface of silica consists of a mixture of siloxanes and free silanols, which are relatively reactive (Figure 12).[14] These can undergo a condensation reaction with a silane functionalising agent, or alternately, to reduce their reactivity, they may be converted to siloxanes by reaction with small reactive silanes (e.g. hexamethyldisilazane) in a process known as end-capping.[15] Presumably it is this versatility and accessibility that has made functionalised silica such a common solid support.

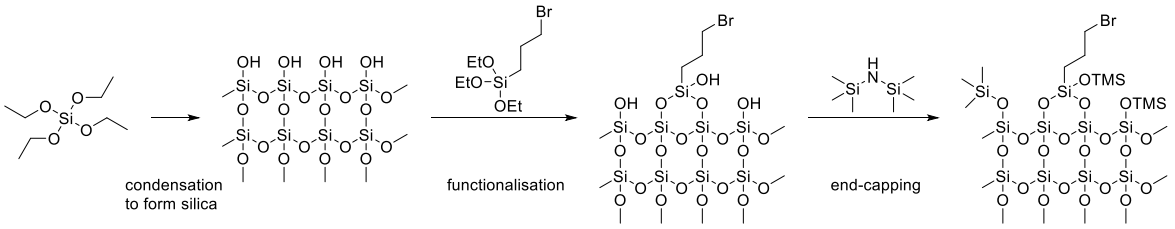

Figure 12. *Formation and structure of functionalised silica. TMS = trimethylsilyl.*

1.2.3 Beneficial effects of immobilisation

Intriguingly, in contrast to the detrimental effects of immobilisation on reactivity and selectivity discussed above, immobilisation may in some cases lead to an improvement in catalytic properties. There are two main physical processes which can lead to this outcome: site isolation and steric constraints brought about by the solid support.[16] Site isolation refers to the physical separation of catalytic sites, which can be beneficial in the case of catalysts which form inactive aggregates in solution. The advantages of site isolation have been well documented in metal-based catalysis,[17,18] however even though certain organocatalysts are well-known to form aggregates in solution[19,20] and have also been immobilised,[21,22] to the best of our knowledge, the effect of immobilisation on organocatalyst aggregation behaviour has not been explicitly investigated. The concept of site isolation can also be extended to the physical separation of two incompatible catalysts (e.g. an acidic and a basic catalyst), preventing mutual deactivation. This has been demonstrated by Pericàs and co-workers who used a combination of an immobilised proline-derived organocatalyst and an immobilised sulfonic acid to catalyse the *in situ* generation of acetaldehyde followed by its conjugate addition to nitrostyrene.[23]

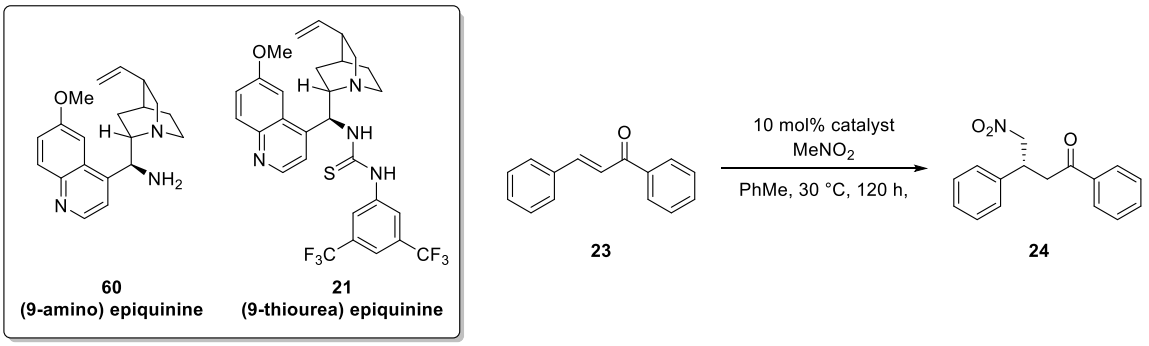

Catalyst	Pore size (nm)	Conversion (%)	e.e. (%)
60	homogenous	61	76 (*S*)
Immobilised **60**	4.7	29	57 (*S*)
	6.3	39	23 (*S*)
	9.6	25	12 (*S*)
21	homogenous	71	94 (*R*)
Immobilised **21**	4.7	25	75 (*R*)
	6.3	66	93 (*R*)
	10.2	58	39 (*R*)

Table 5. *Effect of immobilisation and solid support pore size on the Michael addition of nitromethane to chalcone catalysed by (9-amino) epiquinine **60** and (9-thiourea) epiquinine **21**.*

Steric constraints are particularly relevant to porous materials and refer to the confinement of the catalyst inside pores of a limited size inside the solid support.[16] In some cases, the reduction in freedom of motion due to confinement leads to improved organisation of the transition state and an increase in the enantioselectivity of the reaction. Similarly to site isolation, this phenomenon is well known in metal catalysis,[24,25] but little studied in the area of organocatalysis. A unique recent investigation on the effects of confinement on cinchona-based organocatalysts immobilised on mesoporous silica was undertaken by He and co-workers.[26] They demonstrated that confining immobilised (9-amino) epiquinine **60** and (9-thiourea) epiquinine **21** in small diameter pores resulted in a dramatic increase in enantioselectivity in the Michael addition of nitromethane to chalcone, compared to confinement in larger pores (Table 5). Computational modelling indicated that confinement increased the energy difference between the two diastereomeric transition states for the reaction. Furthermore, the authors suggest that organocatalysts may be particularly susceptible to steric constraints as many organocatalytic mechanisms rely on hydrogen bonding for activation and organisation and hydrogen bonding between the substrates and pore walls changes greatly with pore size.

1.3 Literature overview

Since the pioneering work of Merrifield on solid-phase peptide synthesis in the 1960's and 70's[27] the immobilisation of reagents and catalysts has been an area of active study[28] and the immobilisation of organocatalysts has often closely followed their discovery.[3] For instance, one of the earliest reports of the immobilisation of asymmetric catalysts, from 1974, describes the immobilisation of cinchona alkaloids in a polyacrylate.[29] Due to the great breadth of this field, both in the variety of catalysts and solid supports, we will focus on the achievements of immobilised organocatalysis since 2000, in particular those utilising insoluble polystyrene and silica-based supports.

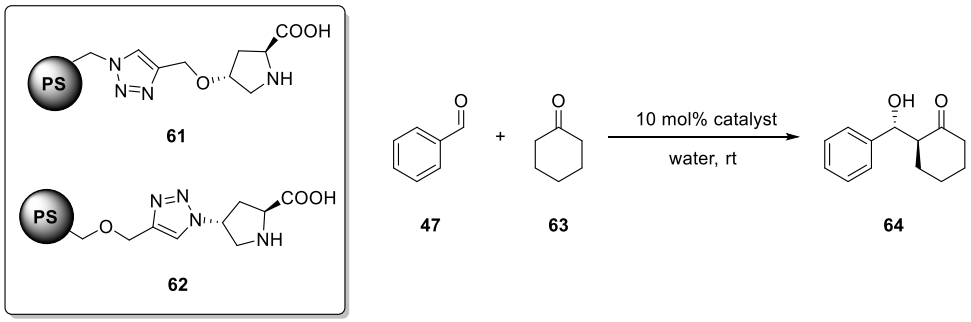

Catalyst	Additive	Time (h)	Yield (%)	d.r.	e.e. (%)
61	10 mol% diMePEG	84	67	95:5	95
62	–	24	74	96:4	98

Table 6. *Aldol reaction in water catalysed by polystyrene-supported proline derivatives.*

The immobilisation of proline-based organocatalysts has been extensively investigated since the first report of polystyrene-supported proline in 1985 and great advances in reactivity and selectivity have been made since that time.[30,31] In 2006, Pericàs and co-workers developed a polystyrene-supported proline catalyst that could be applied to the aldol reaction in water, analogously to hydrophobic proline derivatives which act as aldolase mimics.[32] The catalyst was immobilised *via* a triazole linker, joining it to cross-linked polystyrene resin (**61**, Table 6). Excellent stereoselectivity was obtained using water as a solvent, however these conditions resulted in a poor yield, presumably due to poor swelling of the support. The addition of 10 mol% dimethylpoly(ethyleneglycol) (DiMePEG) to aid diffusion through the resin ameliorated this situation and the aldol product was obtained in good yield, diastereoselectivity and e.e. The reaction rate was slightly slower than and the selectivity was equally as good as that obtained using analogous hydrophobic homogeneous proline-derived

catalysts in water.[33] This was followed by further development of the catalyst, specifically, the modification of the order of functional groups on the linker (**62**, Table 6), which remarkably enabled the swelling of the solid-supported catalyst in water.[34] An analogous catalytic system was then developed and adapted to application in a continuous flow system.[35]

Another noteworthy study is the 2005 work of Fernández-Mayoralas and co-workers on the development of proline-derived organocatalysts immobilised on mesoporous silica supports.[36] Proline was derivatised with triethoxy silane *via* a urea linker, immobilised on the surface of a range of silica-based materials, then tested in an aldol reaction. Proline immobilised on the mesoporous material MCM-41 (**65**) gave the best yield, d.r. and e.e. in the aldol reaction of hydroxyacetone and a small set of aliphatic and aromatic aldehydes such as **66**. Interestingly, for some substrates the diastereoselectivity of the reaction was reversed when using the immobilised catalyst, compared to a homogenous analogue. This was attributed to hydrogen bonding interactions between the substrates and surface silanol groups. Finally, the MCM-41-supported proline catalyst was amenable to reaction under microwave irradiation and performed comparably to its homogeneous analogue in this case (Table 7).

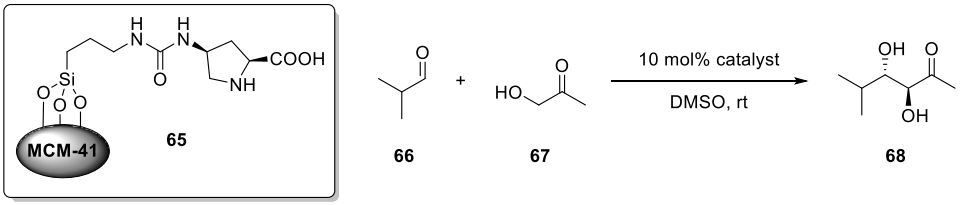

Catalyst	Time	Yield (%)	d.r.	e.e. (%)
L-proline	24 – 72 h	75	> 20:1	> 99
L-proline (microwave irradiation)	10 min	60	> 20:1	> 99
65	24 – 72 h	55	> 20:1	> 99
65 (microwave irradiation)	10 min	60	> 20:1	> 99

Table 7. *Aldol reaction catalysed by MCM-41-supported proline **65**, with and without microwave irradiation, with comparison to L-proline.*

In addition to proline, the second major class of covalent organocatalysts are the MacMillan imidazolidinones, the immobilisation of which has also been well-studied. In a study showcasing the broad applicability of the thiol-ene postmodification strategy for catalyst immobilisation (Scheme 9),[37–40] Gruttadauria and co-workers prepared polystyrene-supported imidazolidinone catalyst **69** and

applied it to the *α*-selenylation of aldehydes, obtaining their desired products in good yield and moderate e.r. (Scheme 9).[41] This is reasonably similar to the literature result with homogeneous MacMillan catalyst, where the *α*-selenylated aldehyde is obtained in > 95% conversion and 85% e.e. in 1 h.[42] The recycling of this immobilised catalyst was also demonstrated over three cycles.

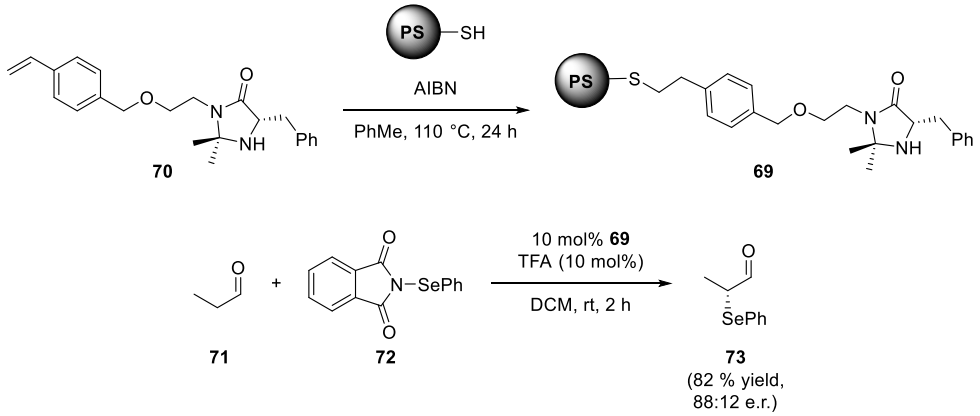

Scheme 9. *Immobilisation of MacMillan imidazolidinone using thiol-ene chemistry and α-selenylation of propanal using immobilised catalyst **69**.*

In an alternative approach, Pericàs and co-workers made use of a triazole linker to immobilise MacMillan imidazolidinones on to both polystyrene (**74**) and magnetic Fe_3O_4 nanoparticles.[43] Both immobilised catalysts performed very well in the asymmetric Friedel-Crafts reaction of pyrroles with *α*,*β*-unsaturated aldehydes. Impressively, enantioselectivity was comparable to that obtained with the homogeneous catalyst at higher temperatures than those used for the homogeneous reaction,[44] enabling the use of a shorter reaction time (Table 8). Furthermore, the immobilised catalysts could be recycled over six cycles. This was a particularly convenient operation for the magnetic nanoparticle-supported variant, as the catalyst could be easily recovered by magnetic decantation.

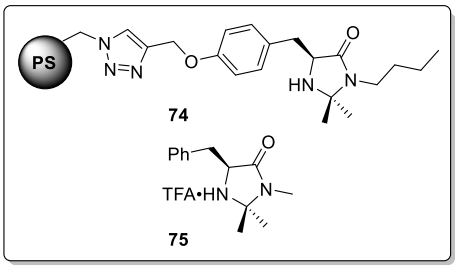

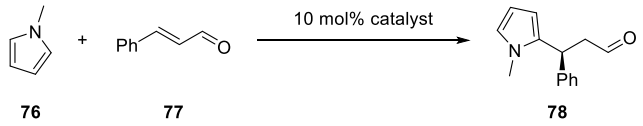

Catalyst	Loading (mol%)	Solvent	Temperature (°C)	Time (h)	Yield (%)	e.e. (%)
74	10	0.5 M aq. TFA/THF	0	12	65	93
75	20	THF/H_2O	−30	42	87	93

Table 8. *Comparison of Friedel-Crafts reaction catalysed by immobilised catalyst **74** and homogeneous MacMillan catalyst **75**.*

MacMillan imidazolidinones have also been immobilised on inorganic supports, for example in the recent work of Begnalia and Puglisi and co-workers.[45] In this study, commercial silica, without any special pre-treatment, was reacted with a trimethylsiloxy-functionalised MacMillan imidazolidinone to form immobilised catalyst **79**. This catalyst was then packed into a blank HPLC column and used in the continuous flow Diels-Alder reaction of cyclopentadiene and cinnamaldehyde (Scheme 10). Although the yield of the reaction appears to be good, it must be noted that with such a low flow rate the productivity of the system is very low.

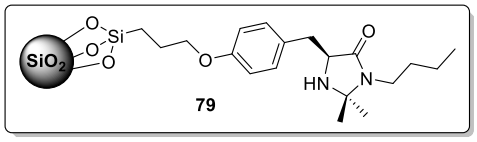

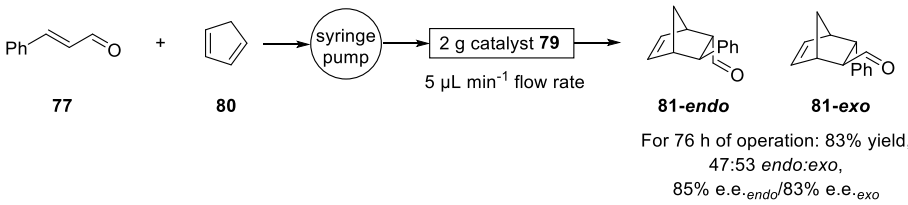

Scheme 10. *Silica-supported imidazolidinone catalyst and its application to a continuous flow Diels-Alder reaction.*

Another important class of organocatalyst whose immobilisation has been intensively investigated are the cinchona alkaloid-derived catalysts. An impressive application of immobilised cinchona alkaloid organocatalysts is the 2001 work of Lectka and co-workers on the asymmetric continuous flow synthesis of *β*-lactams using a series of immobilised catalysts and reagents.[46] Lectka and co-workers had previously demonstrated the synthesis of *β*-lactams from ketenes and imines, catalysed

by benzoylquinine and the base DMAN.[47] The main obstacle in the development of this reaction was that the use of reactive ketenes was required to obtain a high yield of *β*-lactam using benzoylquinine catalysis, but because of their instability these needed to be generated *in situ* by the treatment of acid chlorides with a base. However, the presence of a base interfered with the *β*-lactam formation, leading to racemic products. In the homogeneous system, this issue was resolved by the use of the strong, non-nucleophilic base DMAN in combination with benzoylquinine as a "shuttle base", which enabled a high yielding, highly enantioselective one-pot procedure. This issue was also elegantly resolved through the use of heterogenous catalysis. First, Lectka and co-workers found that ketenes could be successfully generated from acid chlorides by passing a solution of acid chloride through a fritted column packed with polystyrene-supported BEMP at −78 °C. Next, quinine and quinidine were immobilised on Wang resin *via* a biaryl linker attached at the C-9 position (e.g. **82**) and loaded into fritted columns. The BEMP column and the quinine column were then connected in series, with an inlet for the addition of imine between the two columns. A THF solution of acid chloride was eluted (under gravity) through the BEMP column, forming the ketene, which then immediately entered the quinine column together with the imine where the two reacted to form the corresponding *β*-lactam. A scavenger resin containing polystyrene-supported primary amine was used to trap any unreacted starting materials and by-products (Figure 13). The yields and e.e.'s of the prepared *β*-lactams were comparable to those obtained using the homogenous system, with the added advantages of a shorter reaction time (2 h vs. 5 h) and the possibility of reusing all of the columns multiple times.

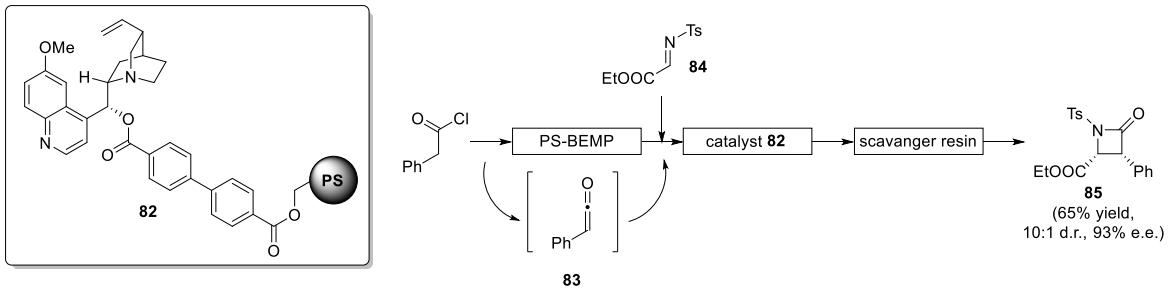

Figure 13. *Synthesis of β-lactams using solid-supported reagents and catalyst developed by Lectka and co-workers.*

A unique and highly efficient approach to immobilisation was developed by Soós and co-workers in their development of polystyrene-supported cinchona-derived squaramide organocatalysts, such as **86**, which were grafted directly to the solid support, without the need for a linker.[48] This was done

by using aminomethyl functionalised polystyrene as one of the substituents on the squaramide moiety (Scheme 11). The resulting catalyst was applied to the conjugate addition of 1,3-diketones and nitrostyrenes (Scheme 11) where it performed comparably to homogeneous cinchona-derived squaramide catalysts, although it was used at higher loadings than its homogeneous counterpart.[49] The recycling of this catalyst was also demonstrated over 10 cycles and it was used successfully in a 20 mmol scale continuous flow conjugate addition of acetylacetone and nitrostyrene.

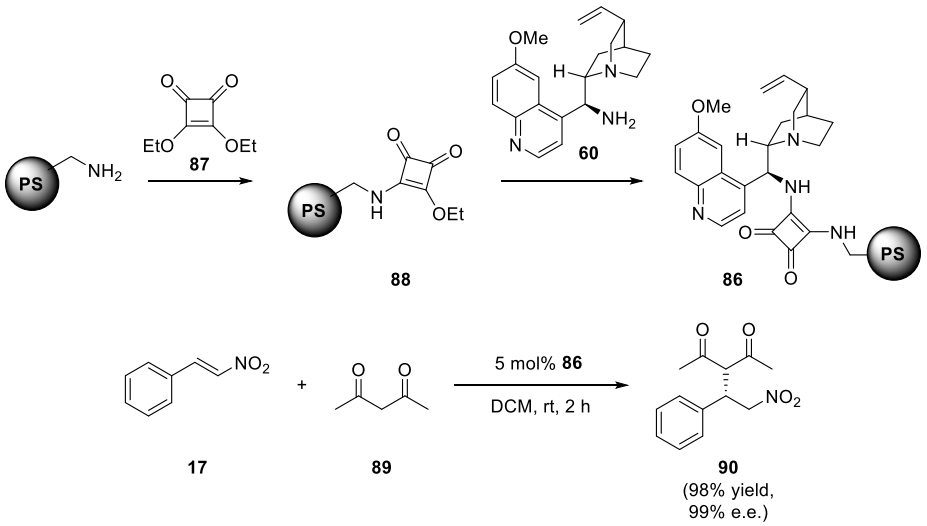

Scheme 11. *Tether-free immobilisation of cinchona-derived squaramide and application to the conjugate addition of acetylacetone to nitrostyrene.*

An alternative approach to the post-synthetic modification strategies discussed thus far for catalyst immobilisation is a "bottom up" approach. For polymer-supported catalysts this involves preparing a catalyst derivative containing a polymerisable functional group and co-polymerising it with a conventional monomer, such as acrylate or styrene, to form a functionalised polymer. A highly successful example of this approach is the formation of a polystyrene-supported cinchona-derived bifunctional sulfonamide catalyst demonstrated by Song and co-workers.[50] 9-Amino-(9-deoxy)-epiquinine (**40**) was reacted with 4-vinylbenzylsulfonyl chloride to form sulfonamide-derivatised epiquinine **91** that contained a polymerisable styrene moiety. This compound was then copolymerised with styrene and 2 mol% divinylbenzene under suspension polymerisation conditions to form solid-supported catalyst **92** (Scheme 12). This catalyst was then applied to the methanolytic desymmetrisation of *meso*-anhydrides (Scheme 12). Although the reported reaction times with immobilised catalyst **92** were approximately twice as long as with the corresponding homogeneous

catalyst, the yield and enantioselectivity were equally high.[51] Furthermore, this immobilised catalyst was described as being "indefinitely" stable and catalyst recycling at 1 mol% loading was successfully demonstrated over 10 cycles.

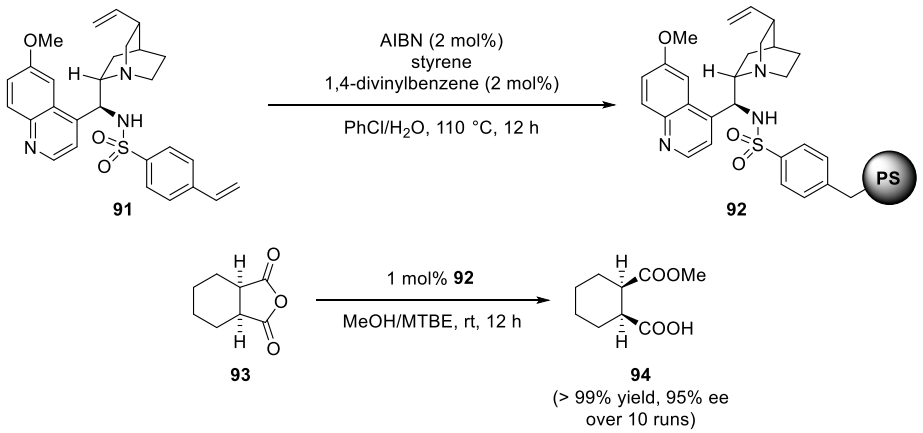

Scheme 12. *Preparation of catalyst **92** and application to the desymmetrisation of* meso-*anhydrides, with catalyst recycling.*

Another example of the immobilisation of the same cinchona-derived sulfonamide organocatalyst is the very recent work of List and co-workers on organotextile catalysis.[52] Although this work falls somewhat outside the scope of this introduction, it is worth discussing as it is a recent, highlighted development in the field of organocatalyst immobilisation.[53] List and co-workers immobilised cinchona-derived sulfonamide **95** (as well as an achiral DMAP analogue and sulfonic acid) onto nylon through the generation of surface radicals under UV irradiation. Catalyst **96** was then applied to the methanolytic desymmetrisation of *meso*-anhydrides. The resulting desymmetrised products were obtained in excellent yield and e.e. but a high catalyst loading and long reaction times were required (Scheme 13). The recycling of catalyst **96** was successfully demonstrated over an imposing 300 cycles and the catalyst was also utilised in a flow reactor; however iterative operation was required, presumably due to the low reaction rate. Although the immobilisation method developed by List and co-workers is very efficient and straightforward, it is not clear whether nylon has useful physical properties as a support compared to more conventional materials such as polystyrene or silica. For example, compared with polystyrene-supported cinchona-derived sulfonamide **92** (Scheme 12), the performance of catalyst **96** is clearly inferior. The recycling experiment does suggest that the support is very robust, but there appears to be no suitably long comparisons for other

supports in the literature. Perhaps with further development, for example increasing the surface area of the material, as suggested by the authors, the utility of a textile-based support may become more apparent.

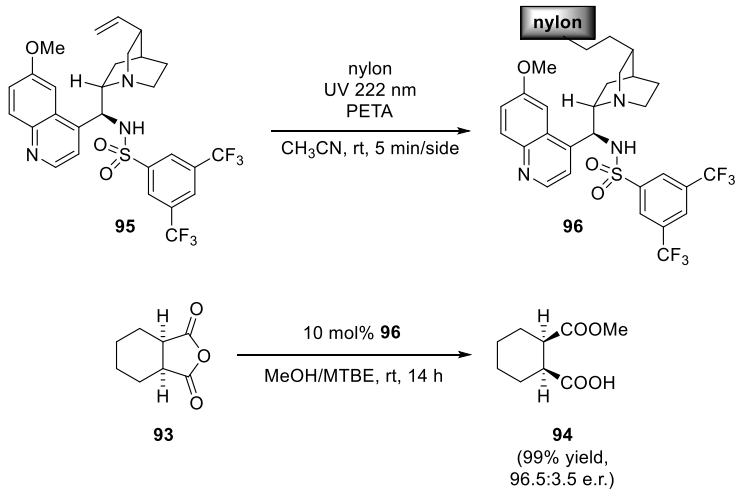

Scheme 13. *Immobilisation of cinchona-derived sulfonamide **95** onto nylon and application to the methanolytic desymmetrisation of an anhydride. PETA = penta-erythritol triacrylate (a cross-linking agent).*

Of the various classes of organocatalysts, the immobilisation of proline-derived organocatalysts, MacMillan imidazolidinones and cinchona alkaloid-derived organocatalysts has been studied most extensively, however other classes of organocatalyst have also been immobilised. Notably, Jacobsen's thiourea catalyst for the Strecker reaction was originally discovered as the polystyrene-supported variant, as discussed previously.[54] Further catalyst development also included a polystyrene-supported version of the catalyst, which performed comparably to its homogeneous counterpart (Scheme 14), although a like-for-like comparison is not possible as one catalyst contains a thiourea and the other a urea.[55] The bifunctional tertiary amine/thiourea organocatalyst developed by Takemoto has also been immobilised on polystyrene as well as PEG.[56]

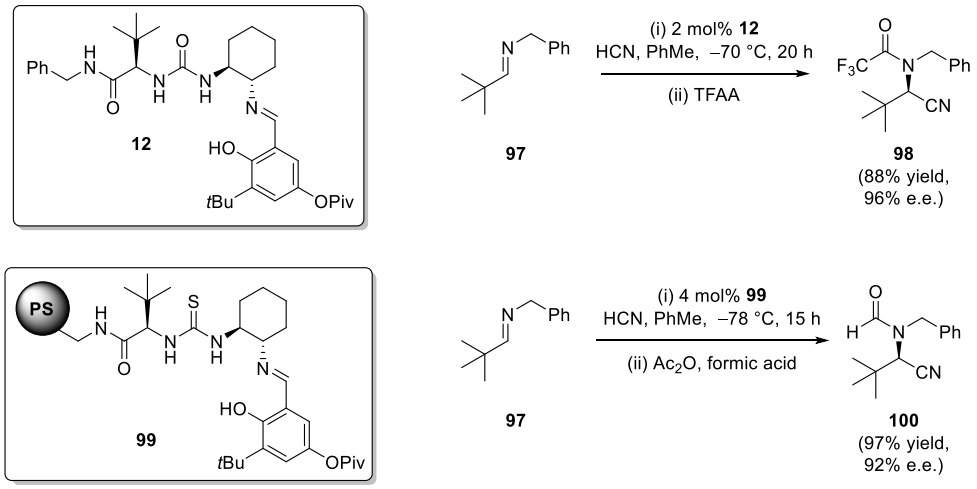

Scheme 14. *Comparison of homogeneous and polystyrene-immobilised Jacobsen's catalyst.*

Finally, as the present work concerns the immobilisation of a superbase organocatalyst it is important to review the literature in this specific category. Although many achiral superbases have been immobilised, for example, polystyrene-supported BEMP is a commercially available and widely used base,[57] to the best of our knowledge only one chiral superbase organocatalyst has been immobilised to date. In 2005 Ishikawa and co-workers reported the immobilisation of their chiral guanidine organocatalyst (see Chapter 1) on to a polystyrene support.[58] Two immobilisation approaches were investigated – grafting onto a chloromethyl functionalised polystyrene resin and polymerisation of a styrene-functionalised derivative of the catalyst (both with and without the addition of styrene), forming catalysts such as **101**. The resulting catalysts were then applied to the conjugate addition of glycine imine to methyl vinyl ketone. However, all three variants of the polystyrene-supported catalyst gave greatly reduced yields and e.e.'s compared to the homogeneous variant **102** (Table 9). The immobilisation of this catalyst was reported again by the same group in 2014, this time varying the position through which the catalyst was linked to the polystyrene support, from the guanidine nitrogen to the pendant benzyl group, forming catalyst **103**.[59] These new immobilised catalysts performed comparably to homogeneous catalyst **104** in the conjugate addition of glycine imine to methyl vinyl ketone (Table 9). Catalyst recycling over 3 cycles was also demonstrated.

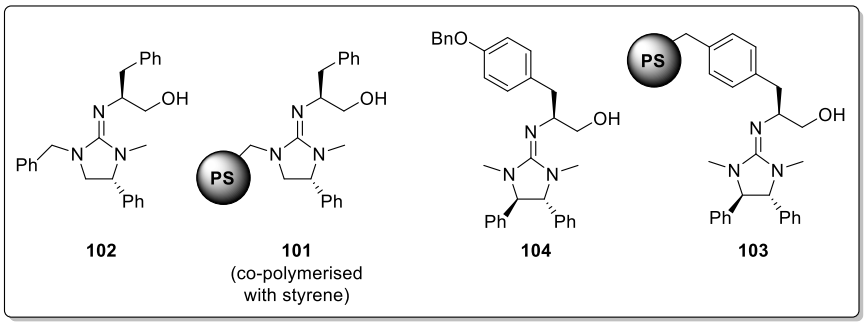

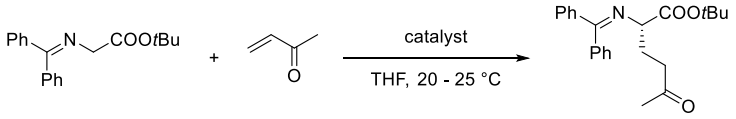

53 105 106

Catalyst	Loading	Time (d)	Yield (%)	e.e. (%)
102	20 mol%	7	75	74
101	240 wt%	9	32	45
104	20 mol%	4	89	82
103	20 mol%	2	87	85

Table 9. *Performance of immobilised guanidine organocatalysts.*

It appears that the main conclusion that emerges from the above brief review is how variable the outcomes of organocatalyst immobilisation may be, although some generalisations can be made. The above examples suggest that the reactivity of organocatalysts is more strongly affected by immobilisation than their enantioselectivity; with many immobilised catalysts exhibiting perhaps a decrease of at least 50% in reactivity while it appears rare for enantioselectivity to be significantly affected. However, there are also examples of organocatalysts that retain, or even increase their reactivity upon immobilisation. Unfortunately, few studies have been undertaken to explain the origins of this phenomenon. Indeed, perhaps due to the difficulty of characterising solid-supported small organic molecules, it appears there exists a gap in the knowledge of the physical processes affecting the reactions of immobilised organocatalysts. The decision of where and how to attach a catalyst to a solid support is, as expected, crucial to its performance. For some catalysts the linker may be incorporated into their core scaffold, making their immobilisation highly efficient, while others require more extensive modifications. However, linkers may have unexpected functional benefits, such as the development by Pericàs and co-workers of a polystyrene-supported proline-based catalyst that swells in water.[34] Overall however, it is most certainly possible for immobilised

organocatalysts to be highly performing tools for asymmetric synthesis, which offer added benefits such as easily workup, catalyst recycling and applications in flow chemistry.

2. Results and Discussion

2.1 Aims

The Dixon group has recently developed a novel class of bifunctional iminophosphorane organocatalysts. These catalysts are synthesised *via* a Staudinger reaction between a triarylphosphine and a chiral azide bearing the H-bond donor motif, forming the active iminophosphorane moiety in the final step (see Chapter 1).[60] As solid-supported triphenylphosphine is a widely-available commercial material,[61] we saw the opportunity to utilise it as a replacement for the soluble triarylphosphine component, thus forming an immobilised bifunctional iminophosphorane organocatalyst. The aims of this project were to investigate such immobilised bifunctional iminophosphorane organocatalysts, specifically:

- To demonstrate a proof of concept that solid-supported bifunctional iminophosphoranes could potentially be used as asymmetric organocatalysts
- To determine a suitable and readily available solid support
- To prepare the immobilised catalyst on a gram scale
- To attempt to characterise the immobilised catalyst
- To demonstrate the performance of the immobilised catalyst in a range of challenging asymmetric transformations that possessed some element of novelty and compare it to the corresponding homogeneous catalyst.
- To demonstrate catalyst recycling
- To demonstrate the use of the immobilised catalyst in a continuous flow system

We believed this would showcase the broad applicability and utility of immobilised bifunctional iminophosphoranes, while also expanding the scope of bifunctional iminophosphorane organocatalysis in general.

2.2 Proof of Concept

(N.B. Proof of concept was originally demonstrated by Dr. Marta Garcia Núñez, then reproduced by A.M.G. as described below)

Previous work in the Dixon group on homogeneous bifunctional iminophosphorane organocatalysts showed that these compounds were highly effective catalysts for the asymmetric nitro-Mannich reaction of diphenylphosphinoyl ketimines.[60] Therefore we decided to use this reaction in our proof of concept studies for catalyst immobilisation (Scheme 15). The solid-supported catalyst was prepared *in situ* following procedures developed previously for the homogeneous catalyst, with no modifications. Azide **107**, prepared following literature procedures,[60] was stirred with 2 equivalents of commercial polystyrene-supported triphenylphosphine (PS-PPh_3) in toluene at room temperature for 24 h, at which point TLC and mass spectrometry showed complete consumption of the azide. Ketimine **36a** and nitromethane were then added to this reaction mixture and after 28 h at room temperature the reaction was stopped by removal of the catalyst by filtration. The high conversion (83% by ^{1}H-NMR analysis of the crude reaction mixture) and enantiomeric ratio (12:88)[ii] of the product were taken as evidence of catalyst formation (neither the azide nor PS-PPh_3 catalyse product formation individually). With this encouraging result in hand, we set out to further develop our heterogeneous catalytic system.

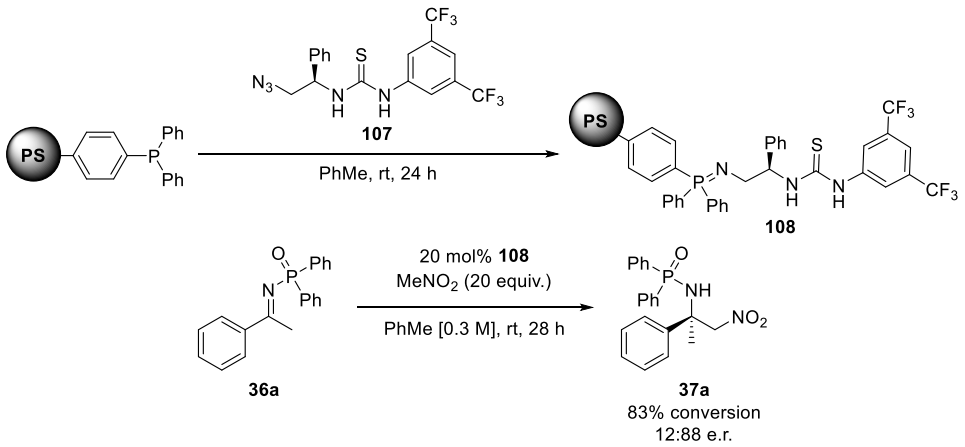

Scheme 15. *Proof of concept of catalyst immobilisation.*

[ii] Enantiomeric ratios for the nitro-Mannich reaction are stated as *R:S*.

2.3 Choice of solid support

Organocatalysts have been immobilised on a variety of solid supports such as silica, mesoporous silica, PEG and polystyrene (see Chapter 2, Introduction). As they are the most readily available solid supports, we decided to investigate the use of polystyrene and silica.

2.3.1 Polystyrene

Our initial experiments focused on comparing commercial PS-PPh_3 with PS-PPh_3 prepared following the method of Spring and co-workers (Scheme 16).[62] This method was appealing because it allowed the preparation of a variety of substituted polystyrene-supported phosphines. Also, Spring and co-workers claim that PS-PPh_3 prepared following their procedures exhibits superior performance as a chemical reagent, compared to commercial PS-PPh_3, due to its lower phosphine oxide content. Furthermore, this method allows for the functionalisation of large diameter (> 150 μm, commercially available functionalised resins are typically ~100 μm diameter) polystyrene beads, which have optimum handling properties. The method of Spring and co-workers uses the trialkylmagnesate complex *i*Pr(*n*Bu)$_2$MgLi developed by Oshima and co-workers,[63] to form a metallated polymer from poly(4-bromostyrene) which can react with a range of electrophiles, such as chlorophosphines. Oshima's trialkylmagnesate complex is a highly active metal-halogen exchange reagent and is able to successfully penetrate large diameter polystyrene beads, unlike simple organolithium or Grignard reagents.[62]

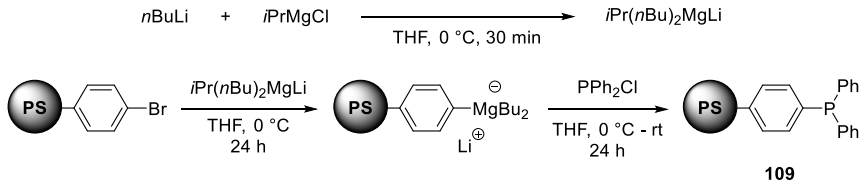

Scheme 16. *Preparation of polystyrene-supported phosphines following the method of Spring and co-workers.*

We found that synthesised PS-PPh_3 (**109**) formed immobilised catalysts which out-performed those formed from commercial PS-PPh_3 in terms of conversion in the nitro-Mannich reaction (Table 10). It was also much easier to handle and recover catalysts prepared using the synthesised PS-PPh_3, as the bead diameter was much larger than that of the commercially available material. A solvent screen

was simultaneously performed for the nitro-Mannich reaction and it was found that toluene gave the best conversion and e.r. (Table 10).

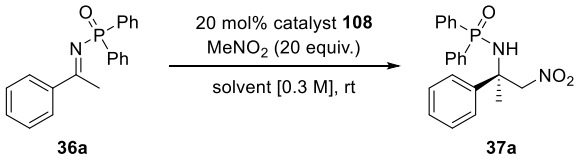

Solvent	PS-PPh_3	Time (h)	Conversion (%)[a]	e.r.[b]
Et_2O	commercial	NR	-	-
	109	10	93	40:60
THF	commercial	NR	-	-
	109	10	88	16:84
DCM	commercial	28	74	12:88
	109	24	86	13:87
PhMe	commercial	28	82	12:88
	109	10	89	10:90

Table 10. *Comparison of commercial and synthesised PS-PPh_3 and solvent screen. Catalyst prepared in situ using PS-PPh_3 (0.4 equiv) and azide **107** (0.2 equiv.) in PhMe. Ketimine **20a** (1.0 equiv.) and nitromethane (20 equiv.) then added to the reaction mixture. [a] Determined by ^{1}H-NMR analysis of the crude reaction mixture. [b] Determined by HPLC analysis on a chiral stationary phase.*

2.3.2 Silica

Silica is another common material for solid-supported reagents. Due to its high mechanical stability and because it does not swell, it can be tightly packed into cartridges for use in flow chemistry.[64] We initially planned to form immobilised catalysts with commercially available silica-supported diphenylphosphine (Si-PPh_2), however it was not possible to find a commercial source of this material which was end-capped. Attempts to form catalysts with un-end-capped Si-PPh_2 resulted in a lack of catalytic activity, possibly due to hydrolysis of the catalyst. Attempts to end-cap the commercial material were also unsuccessful. Finally we decided to prepare silica-supported triphenylphosphine from silica-supported propyl bromide, which was commercially available as the end-capped material (Scheme 17).

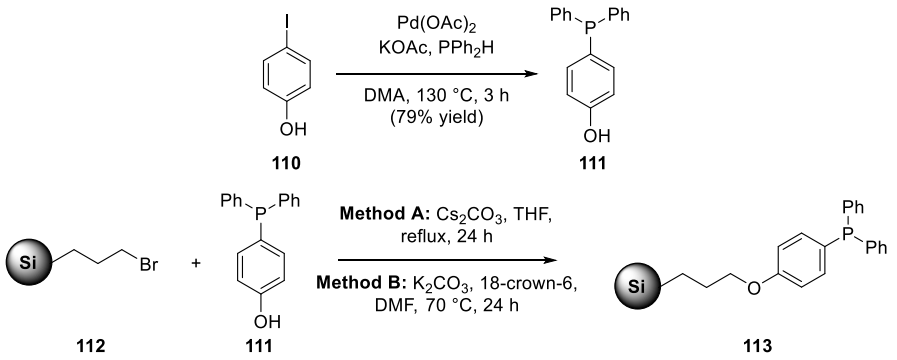

Scheme 17. *Preparation of Si-PPh$_3$ from silica-supported propyl bromide.*

TLC analysis of the functionalisation reaction showed significant quantities of residual **111** and consequently we were uncertain about the efficiency of the functionalisation. We therefore devised a method to measure the loading of **113** by reacting it with a known quantity of azide **114** and measuring the conversion to the iminophosphorane by analysis of a fully relaxed ^{1}H-NMR spectrum of the crude reaction mixture, relative to an internal standard (Table 11). This method had the added advantage of being analogous to our target reaction for catalyst formation.

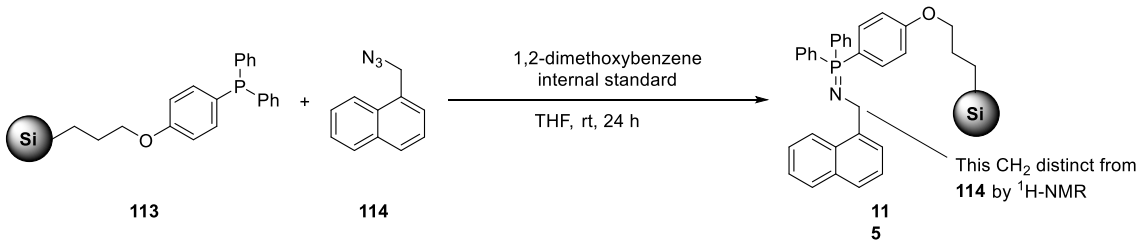

Method	Equivalents base	Loading (mmol g^{-1})
A	1	0.46
A	5	0.20
B	1.2	0.56
B	1.2	0.33

Table 11. *Results of measurement of phosphine loading of prepared silica. Methods A and B are described in Scheme 17. Expected loading from manufacturer's specifications for propyl bromide = 1.69 mmol g^{-1}.*

Unfortunately, we were not able to reproducibly prepare Si-PPh$_3$ **113** with high triphenylphosphine loadings (Table 11). Furthermore, formation of the silica-supported catalyst with azide **107** and application to the nitro-Mannich reaction of **36a** gave adduct **37a** in 54% conversion and 13:87 e.r. in 22 h. As this was an inferior result compared to those obtained with the polystyrene-supported

catalyst, the preparation of a silica-supported catalyst was not pursued further and we chose to focus on a polystyrene support.

2.4 Characterisation of polystyrene-supported catalyst

In the aforementioned reactions, catalyst formation was always conducted *in situ* with an excess of solid-supported phosphine. However, it was soon discovered that catalyst formation was quantitative with a single equivalent of PS-PPh_3 and subsequently that it could be performed on a gram scale and the catalyst isolated and stored in a sealed vial over several months. No optimisation of the reaction conditions for catalyst synthesis was required, the procedure used in the Proof of Concept was simply scaled up using an equimolar ratio of azide and PS-PPh_3.

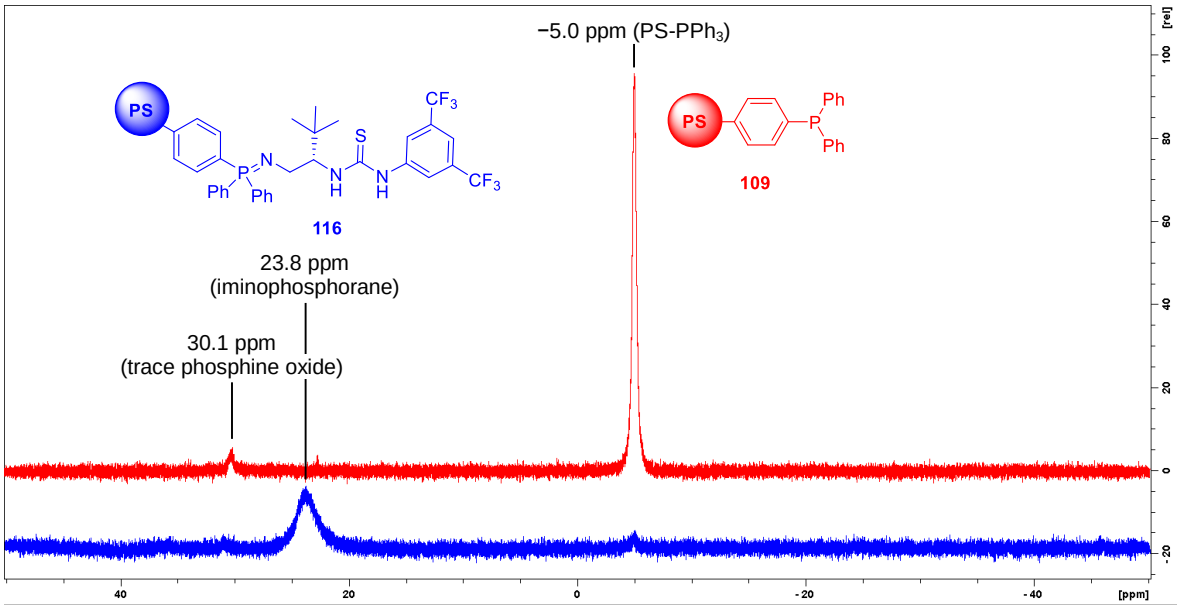

Figure 14. *Gel-phase ^{31}P-NMR ($CDCl_3$) of polystyrene-supported triphenylphosphine **109** (red, top) and polystyrene-supported catalyst **116** (blue, bottom).*

With large quantities of catalyst in hand, we were able to obtain spectroscopic evidence for catalyst formation in the form of gel-phase ^{31}P-NMR spectra of synthesised PS-PPh_3 **109** and catalyst **116** (Figure 14). Gel phase ^{31}P-NMR spectroscopy has long been known as a useful tool for monitoring solid phase reactions involving phosphorus atoms.[65,66] Our spectra distinctly show the disappearance of the "PPh_3" peak at −5.0 ppm and the formation of a new, broad peak at 23.8 ppm corresponding to the iminophosphorane (c.f. 21.9 ppm for the corresponding homogeneous catalyst). A minor peak

at 30.0 - 31.0 ppm which corresponds to a trace of polymer-bound triphenylphosphine oxide is visible in both spectra.

We next measured a series of variable temperature ^{31}P-NMR spectra of catalyst **116** (Figure 15). In the case of the homogeneous bifunctional iminophosphorane organocatalysts, solution phase NMR shows the presence of more than one chemical species. We hypothesise that the catalyst forms an inactive dimer in solution, which is in equilibrium with the active monomeric form (see Appendix).[67] This equilibrium may affect the catalyst activity and if it is absent in the immobilised catalyst, this could explain differences that may arise in the activity of the immobilised catalyst compared to the homogeneous system.

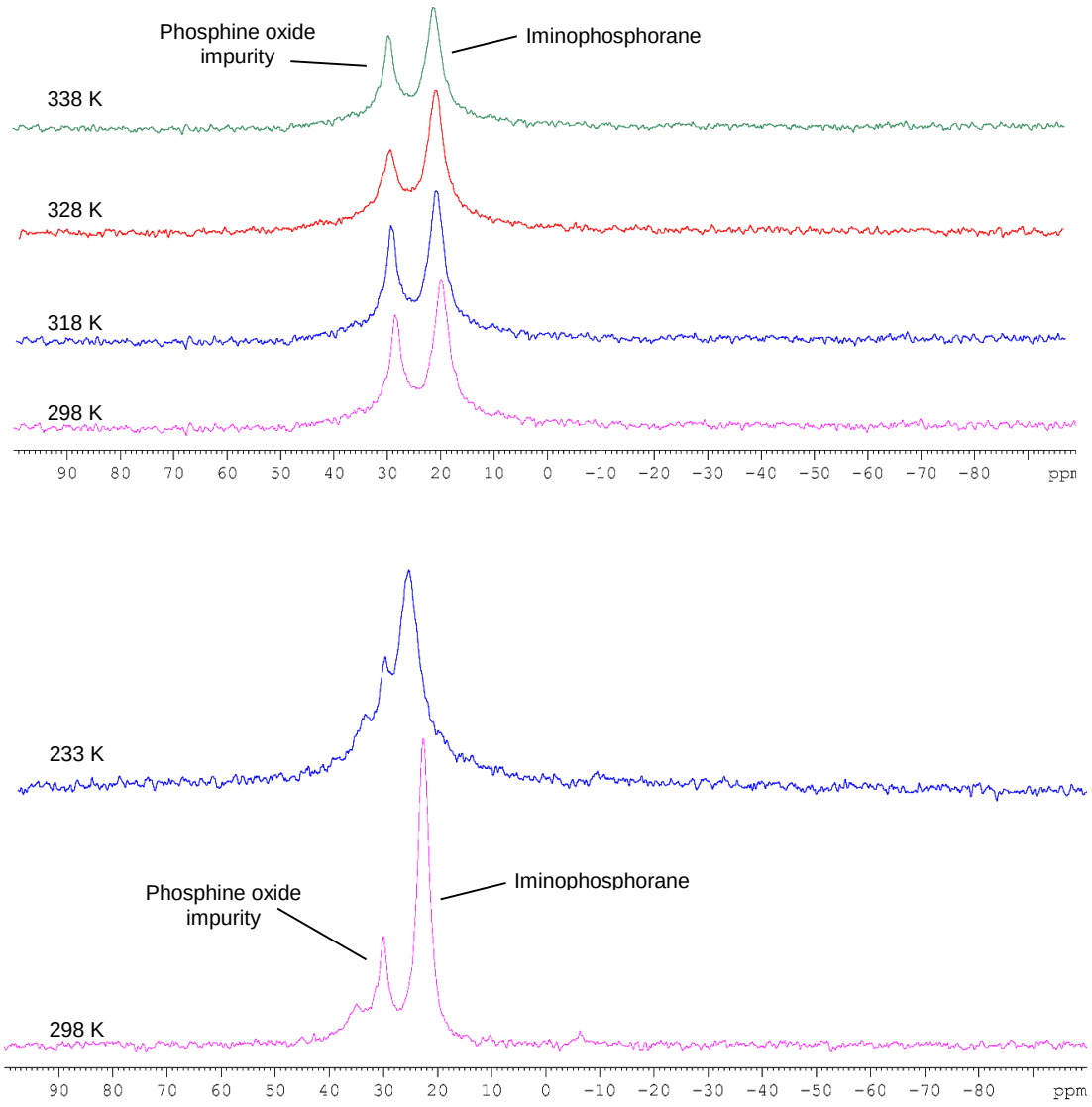

Figure 15. *Variable temperature gel-phase ^{31}P-NMR spectra of catalyst **116**.*

The variable temperature spectra show a batch of catalyst which is contaminated with a phosphine oxide impurity. This serves as a useful internal standard, as observing the effect of temperature on the impurity allows us to isolate the effect of temperature on the polystyrene beads themselves from the effect of temperature on putative catalyst aggregation. For example, gel phase spectra will typically sharpen with increasing temperature and broaden at lower temperatures.[68] This can be seen by observing the phosphine oxide peak in Figure 15, indicating that this effect in the iminophosphorane peak can be attributed to the resin itself. Fluorine spectra were also taken at variable temperature, however they remain unchanged across the measured temperature range. Therefore we have no indication of the existence of separate dimeric and monomeric species of the catalyst in the case of the polystyrene-supported bifunctional iminophosphoranes.

2.5 Nitro-Mannich reaction

2.5.1 Introduction

The nitro-Mannich reaction was first reported in 1896[69] and has been extensively studied due to the synthetic utility of its products, especially since the first reports of diastereoselective intramolecular nitro-Mannich reactions in 1998.[70] However, the majority of reports concern the nitro-Mannich reaction of aldimines. The reaction of ketimines, due to their much lower electrophilicity, is significantly less developed.[71] The first racemic organocatalysed nitro-Mannich reaction of ketimines was performed in 2007 by Terada and co-workers and is discussed in Chapter 1.[72] A small number of alternative racemic nitro-Mannich reactions of ketimines have been reported since.[73,74] The first catalytic enantioselective nitro-Mannich reaction of ketimines utilised Cu(I) in conjunction with a chiral *N,N*-dioxide ligand and gave the nitro-Mannich adduct of tosyl ketimines in modest yield and very good e.e.[75] However, very long reaction times (10 days) were required. The first organocatalytic enantioselective nitro-Mannich reaction of ketimines was reported by Wang and co-workers, using a bifunctional cinchona-derived organocatalyst (***pseudo*-31**, Scheme 18).[76] The nitro-Mannich adducts of cyclic trifluoromethyl ketimines could be obtained in excellent yields and e.e.'s, however the reaction conditions were specific to this particular trifluoromethylated substrate (**117**). More

general conditions for the nitro-Mannich rection of ketimines were reported in 2013 by Dixon and co-workers,[60] as discussed above in Chapter 1. This is the work we expand on in the present section.

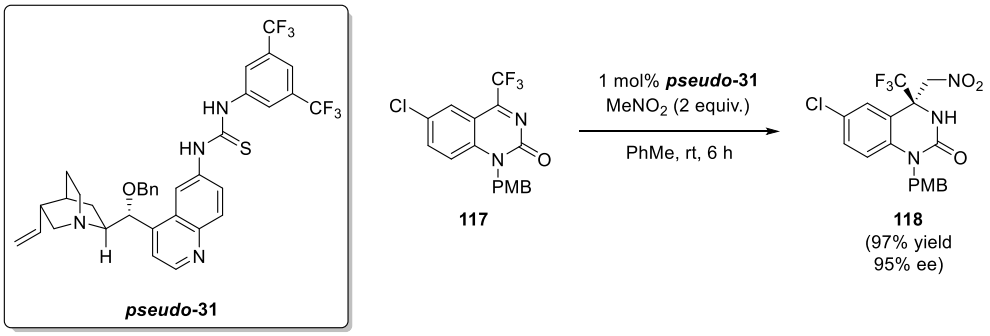

Scheme 18. *Nitro-Mannich reaction of trifluoromethyl ketimines demonstrated by Wang and co-workers. PMB = 4-(CH₃O)C₆H₄CH₂.*

2.5.2 Optimisation

As we had demonstrated in our proof of concept that polystyrene-supported bifunctional iminophosphoranes are effective at catalysing the nitro-Mannich reaction of ketimines, we set out to explore the scope of the reaction using this catalytic system. Having established toluene as the optimal solvent, it remained to optimise the reaction with respect to the catalyst loading and scaffold, reaction concentration, temperature and equivalents of nitromethane. We also returned to the preparation of the PS-PPh_3 and prepared a small set of variously-substituted polystyrene-supported phosphines and tested the performance of the derived catalysts in the nitro-Mannich reaction.

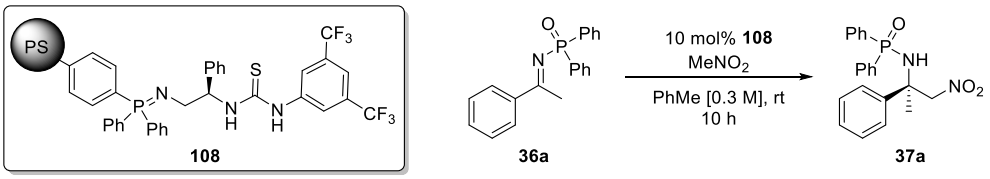

Equiv. $MeNO_2$	Conversion (%)[a]	e.r.[b]
10	80	18:82
5	67	22:78
1	35	32:68

Table 12. *Optimisation of nitro-Mannich reaction for equivalents of $MeNO_2$. [a] Measured by ^{1}H-NMR analysis of the crude reaction mixture. [b] Measured by HPLC analysis on a chiral stationary phase.*

We first investigated the effect of the number of equivalents of nitromethane on the conversion and enantiomeric ratio in the nitro-Mannich reaction (Table 12). We found that decreasing the

equivalents of nitromethane was detrimental to both parameters and consequently decided to continue the optimisation using 20 equivalents of nitromethane. The reduction in e.r. in conjunction with the reduction in equivalents of nitromethane is believed to be a result of the reversibility of the nitro-Mannich reaction (*vide infra*).

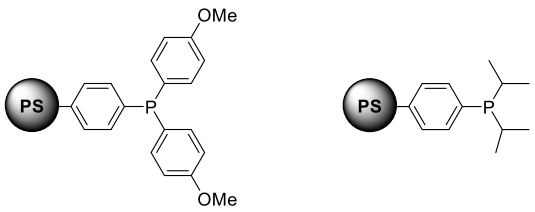

Figure 16. *Synthesised polystyrene-supported phosphines.*

We next synthesised two different polystyrene-supported phosphines (Figure 16) to investigate whether they could provide an improvement on conversion or e.r. in the nitro-Mannich reaction compared to PS-PPh_3. We chose to make these particular phosphines as we expected **119** to be more strongly basic and reactive than PS-PPh_3, based on pK_a measurements reported by the group.[60] Similarly with phosphine **120**, we knew from work within the group on the homogeneous system that alkyl substituted iminophosphoranes are also highly basic, however they are hydrolytically unstable. We were interested in investigating a mixed aryl-alkyl substituted iminophosphorane in the hope that it would be a stable, yet highly basic catalyst. Unfortunately, the increased reactivity of catalysts derived from **119** and **120** (prepared *in situ*) led to lowered e.r. in the nitro-Mannich reaction, although reaction times were reduced (Table 13). The synthesis of these phosphines was also more difficult than that of PS-PPh_3 due to their lower stability and difficult handling. Consequently, we decided to focus on using PS-PPh_3 in subsequent studies.

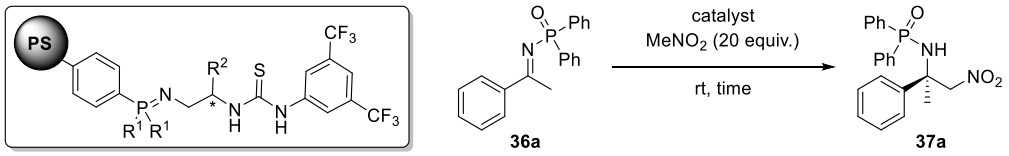

R^1	R^2	mol% cat.	Time (h)	Conversion (%)[a]	e.r.[b]
Ph	*t*Bu	10	24	99	96:4
*i*Pr			24	94	89:11
Ph	Ph	20	7	100	92:8
(4-OMe)Ph			3	100	89:11

Table 13. *Comparison of catalysts formed using PS-PPh_3 and with other polystyrene-supported phosphines in the nitro-Mannich reaction.* [a] *Determined by* ^{1}*H-NMR analysis of the crude reaction mixture.* [b] *Enantiomeric ratio (e.r.) was determined by HPLC analysis on a chiral stationary phase.*

We then prepared and isolated catalysts **108** and **116** (Scheme 19) and commenced optimisation with respect to the catalyst loading and scaffold, temperature and concentration (Table 14). It was rapidly established that the *tert*-butyl substituted catalyst **116** was optimal for the nitro-Mannich reaction. This is in line with results obtained in our group using homogeneous bifunctional iminophosphoranes.[60] Lower temperatures appeared to be beneficial for obtaining a high e.r., but simultaneously obtaining a high conversion with a reasonable catalyst loading was challenging. At first, even with 20 mol% catalyst the reaction required 48 h to reach full conversion, however 20 mol% was considered to be an unacceptably high loading. We resolved this issue by drastically increasing the reaction concentration. Interestingly, even though nitromethane is a non-swelling solvent for polystyrene beads, the reaction could be run neat at room temperature and good conversion and e.r. were achieved in 24 h. However, when we attempted the reaction at low temperature in order to improve the e.r., solubility issues resulted in low conversion. Finally, we found that performing the reaction at a high concentration in toluene at low temperature allowed us to obtain an excellent e.r., conversion and reaction time with an acceptable 10 mol% catalyst loading. These conditions were selected for our exploration of the reaction scope.

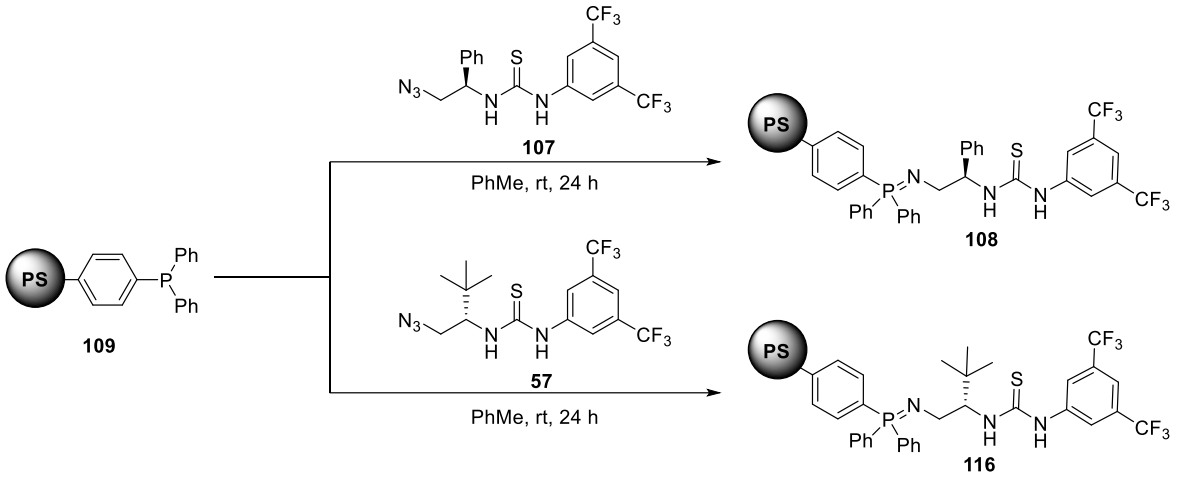

Scheme 19. *Preparation of catalysts **108** and **116**.*

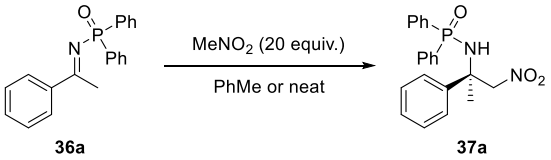

Catalyst	Temperature (°C)	Solvent	Catalyst loading (mol%)	Time (h)	Conversion (%)[a]	e.r.[b]
116	rt	PhMe	20	10	87	92:8
116	0	PhMe	20	24	97	98:2
116	−20	PhMe	20	48	99	99:1
108	rt	PhMe	20	10	85	13:87
108	0	PhMe	20	24	88	7:93
108	−20	PhMe	20	48	84	5:95
116	0	PhMe	10	48	88	94:6
108	0	PhMe	10	48	n.r.	n.d.
116	rt	neat	20	10	94	96:4
116	rt	neat	10	24	99	96:4
116	0	neat	10	48	35	n.d.
116	0	PhMe [4 M]	10	48	99	97:3
116	0	PhMe [8 M]	10	24	99	98:2

Table 14. *Optimisation of nitro-Mannich reaction for temperature, concentration, scaffold and loading. Concentration = 0.3 M unless otherwise stated. [a] Determined by ^{1}H-NMR analysis of the crude reaction mixture. [b] Determined by HPLC analysis on a chiral stationary phase.*

2.5.3 Substrate scope

We next examined the reaction scope by performing the nitro-Mannich reaction using our optimised conditions with a range of aryl ketimines (Figure 17). The yields and enantiomeric ratios of the nitro-Mannich products were comparable to those obtained previously with the homogeneous bifunctional

iminophosphorane under similar conditions.[60] A variety of diphenylphosphinoyl-protected ketimines were subjected to the nitro-Mannich reaction using the immobilized catalyst – electron withdrawing (**37d,e**) as well as electron donating (**37b,c,f**) substituents were all well-tolerated, as were heterocyclic substrates (**37h**) and extension of the methyl substituent of the ketimine to an ethyl group (**37g**). The discrepancy between the conversion, as determined by ^{1}H-NMR, and the isolated yield is due to the difficulty of isolating the product by flash column chromatography as the starting material and product co-elute. Performing the reaction in identical conditions with the corresponding homogeneous catalyst **182** and ketimine **36a**, we obtained the product in 92% conversion and 97:3 e.r. in 14 h.

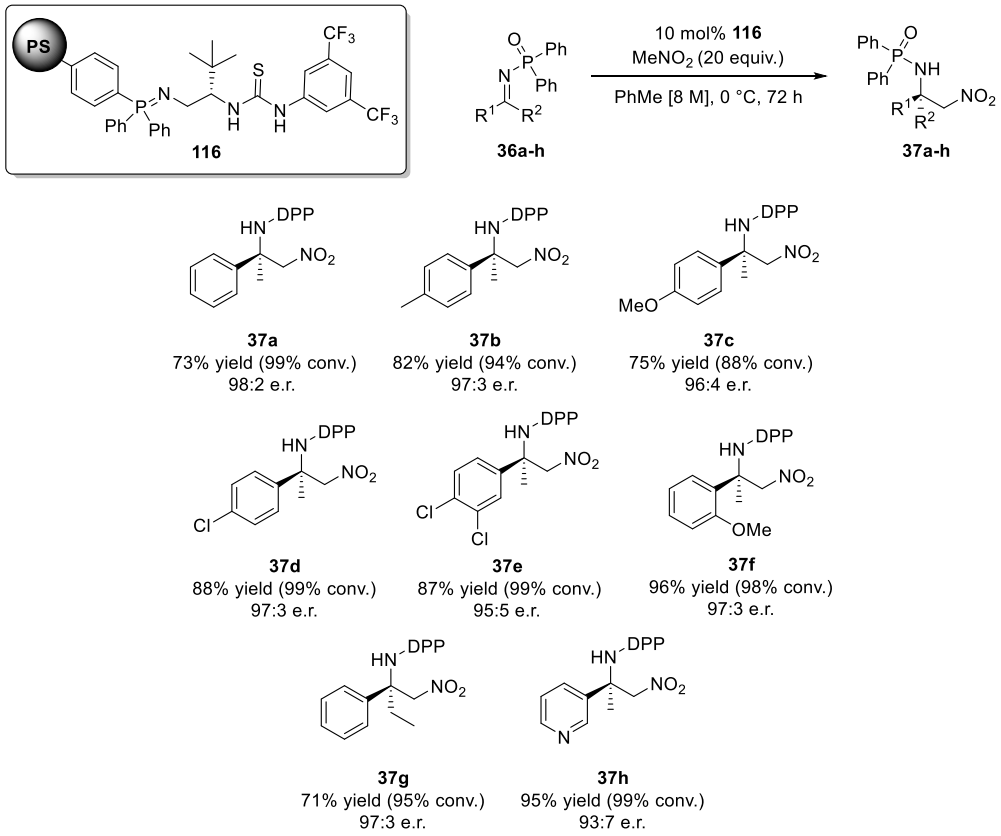

Figure 17. *General scheme and scope of the nitro-Mannich reaction. DPP = P(O)Ph$_2$. Absolute stereochemical configuration determined by comparison with literature compounds.*[60] *Conversion determined by ^{1}H-NMR analysis of the crude reaction mixture. Enantiomeric ratio (e.r.) was determined by HPLC analysis on a chiral stationary phase. The reaction time for **36a** was 24 h.*

2.6 Conjugate addition of alkylmalonates

2.6.1 Introduction

Malonates are a very common pronucleophile in the field of organocatalysis.[77–82] This can be related to a number of factors, for example their pK_a is well matched for tertiary amine-based catalysts, the ability of 1,3-dicarbonyl compounds to form dual hydrogen bonds and the versatility of the 1,3-diester functional group. Alkyl substituted malonates have a significantly higher pK_a (18.0 for dimethyl methylmalonate vs. 15.9 for dimethyl malonate, in DMSO)[83] and have been less extensively utilised, but can also form synthetically useful products. Conjugate adducts with nitrostyrene can be transformed into a variety of compounds such as lactams,[84] cyclopentanes,[85] 1-nitrobicyclo[3.1.0]hexanes, bicycloisoxazoline-*N*-oxides[86] or pyrrolidones[87] following literature procedures and a further variety of transformations could also be conceived. Isolated examples of the organocatalysed addition of substituted malonates to nitrostyrenes have been reported,[82,85,87,88] most notably using highly basic axially chiral guanidine catalysts such as **121** (Scheme 20).[89] However, these reports only feature the most reactive (i.e. lowest pK_a) methylmalonate and allylmalonate pronucleophiles and the scope of this reaction has not been systematically explored. Due to the high basicity of the bifunctional iminophosphorane organocatalysts we decided to investigate whether they could be used to develop a general method for the conjugate addition of substituted malonates.

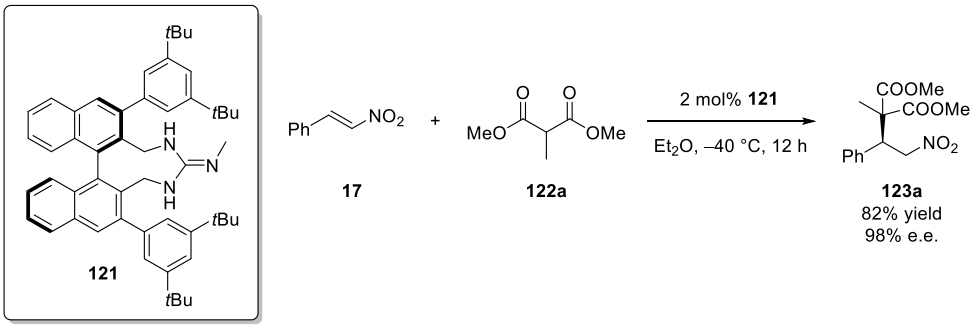

Scheme 20. *Conjugate addition of dimethyl methylmalonate to nitrostyrene by Terada and co-workers.*

2.6.2 Optimisation

After obtaining a promising 88% yield and 93:7 e.r. for our initial test of the addition of dimethyl methylmalonate to nitrostyrene using homogeneous bifunctional iminophosphorane organocatalyst **56**, we set out to optimise this reaction for polystyrene-supported catalyst **116**.

We commenced optimisation of this reaction with a temperature screen in toluene at room temperature, 0 °C and −20 °C (Table 15). Following our experience with the nitro-Mannich reaction, we chose a relatively high concentration (2 M) for this reaction. Low yields were obtained in toluene, which was attributed to the polymerisation of nitrostyrene, as TLC analysis indicated it was consumed in the course of the reaction. We found that lowering the reaction temperature led to an increase in e.r. to up to 95:5, but a large decrease in yield, possibly due to solubility issues. We therefore investigated the use of other solvents at low temperature, in conjunction with an increase in the number of equivalents of nitrostyrene to compensate for its polymerisation. The use of DCM at −20 °C with 3 equivalents of nitrostyrene gave an acceptable yield and e.r. but these results were surpassed by the use of THF. MTBE was also tested, but gave very low yield. We next investigated the use of varying equivalents of nitrostyrene and malonate in THF. An excess of nitrostyrene was found to be desirable in order to obtain both good yield and e.r. However, the relatively good yield obtained using 1:1 nitrostyrene and malonate indicated that a large excess was probably not necessary. We therefore attempted the reaction with 1.2 equivalents of nitrostyrene in THF at 0 °C and −20 °C and obtained excellent yields and e.r.'s. Finally, lowering the catalyst loading to 5 mol% gave a slight increase in yield, perhaps due to reduced nitrostyrene polymerisation, and an equally good e.r. as that obtained with 10 mol% catalyst loading. We thus concluded that these conditions (THF, −20 °C, 1.2 equivalents nitrostyrene and 5 mol% catalyst loading) gave the optimal yield and e.r. for the addition of dimethyl methylmalonate to nitrostyrene catalysed by **116**.

The possibility of using diethyl alkylmalonates was also investigated, but the reaction of diethyl methylmalonate with 3 equivalents of nitrostyrene in DCM at 0 °C with 10 mol% of **116** resulted in a yield of only 33% (e.r. not determined). We suspect that this is due to the increased pK_a of diethyl malonates, compared to dimethyl malonates.[83]

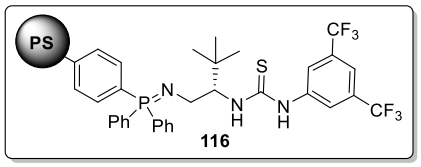

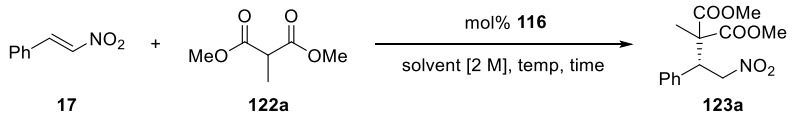

Temp. (°C)	Solvent	mol% 116	eq. nitrostyrene	eq. malonate	Time (h)	Yield (%)[a]	e.r.[b]
rt					4	50	93:7
0	PhMe	10	1.5	1	27	57	94:6
−20					144	11	95:5
−20	DCM	10	3	1	24	84	97:3
0	THF	10	3	1	24	90	96:4
−20					24	89	98:2
rt	MTBE	10	3	1	24	18	93:7
rt	THF	10	1	1	2	75	94:6
			3	1	2	90	94:6
			1	1.5	2	86	93:7
			1	3	2	88	92:8
0	THF	10	1.2	1	16	91	95:5
−20					16	91	98:2
0	THF	5	1.2	1	16	94	96:4
−20					16	93	98:2

Table 15. *Optimisation of nitro-Mannich reaction for temperature, concentration, scaffold and loading.* [a] *Isolated yield after flash column chromatography on silica.* [b] *Determined by HPLC analysis on a chiral stationary phase.*

2.6.3 Substrate synthesis

Before we commenced the substrate scope investigation it was necessary to synthesise a number of dimethyl alkylmalonates, as only a few of these are commercially available. Initially, we intended to alkylate dimethyl malonate using sodium hydride and an alkyl bromide in refluxing DMF as similar conditions had been used successfully in the group with diethyl malonate and were found to be necessary for the synthesis of branched alkylmalonates. However, in the case of dimethylmalonate this resulted in complete decomposition of the starting materials (no observable product or starting materials on TLC, ~ 6% mass return). Consequently, the dimethyl alkylmalonate substrates were synthesised by the alkylation of diethyl malonate, followed by transesterification to form the

dimethyl alkylmalonate (Figure 18). Although this method is indirect, the transesterification could be performed using the crude diethyl alkylmalonate so only a single purification step was required at the end of the sequence.

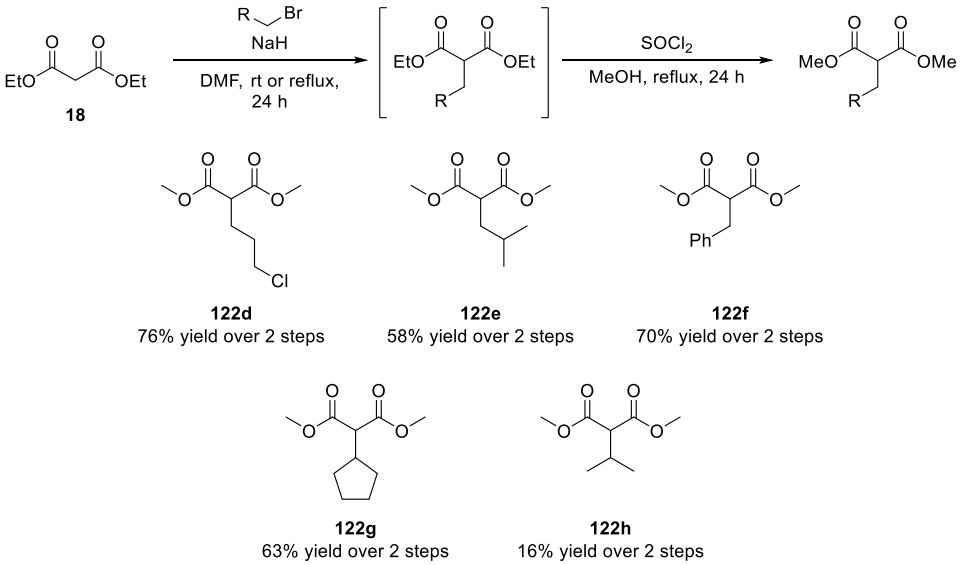

Figure 18. *General procedure for the synthesis of dimethyl alkylmalonates and substrates synthesised using this method.*

2.6.4 Substrate Scope

With a variety of dimethyl alkylmalonates in hand, we investigated their reactivity in the conjugate addition to nitrostyrene catalysed by **116** (Figure 19). Malonates with an unbranched alkyl substituents gave the best reactivity and enantioselectivity (**123a-d**) although the chloropropyl-substituted malonate **123d** required a somewhat longer reaction time. Branching at the γ position of the alkyl substituent was well-tolerated, but led to a reduction in yield and enantiomeric ratio (**123e,f**). Attempts to perform the reaction with *β*-branched alkylmalonates such as **123g** and **123h** led to a complete loss of reactivity, presumably due to the increased steric bulk but perhaps also due to increased pK_a. It is possible that performing these reactions at elevated temperature would have resolved this problem, but this was not attempted. Performing the reaction under identical conditions with corresponding homogeneous catalyst **182** and malonate **122a**, we obtained the product in 93% yield in 4 h and 97:3 e.r.

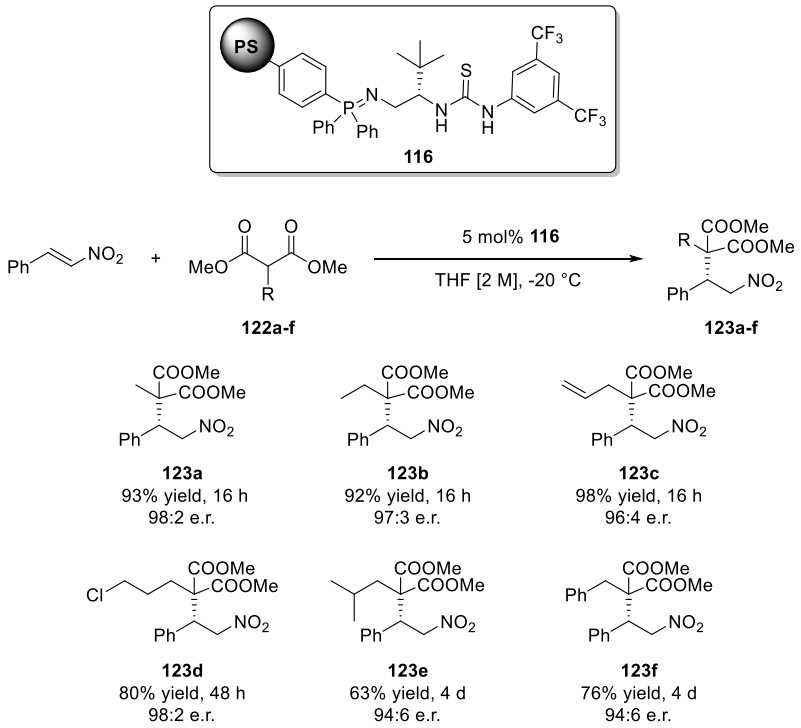

Figure 19. *General scheme and scope for the addition of dimethyl alkylmalonates to nitrostyrene. Absolute stereochemical configuration determined by comparison with literature compounds and by analogy. Yield represents isolated yield after flash column chromatography on silica. Enantiomeric ratio (e.r.) was determined by HPLC analysis on a chiral stationary phase.*

2.7 Conjugate addition of *β*-keto amides

2.7.1 Introduction

In a similar fashion to substituted malonates, *N*,*N*-dialkyl *β*-keto amides are high pK_a pro-nucleophiles (18.2 for *N*,*N*-dimethyl-3-oxobutanamide in DMSO)[83] which can form synthetically versatile conjugate adducts with nitroalkenes. The group of Constantieux and co-workers have undertaken extensive studies on the organocatalysed conjugate addition of *β*-keto amides to various electrophiles. Initial studies on cyclic substrates highlighted the importance of using secondary amides to stabilise *β*-keto amides in their more reactive, imidic form (Scheme 21) whereas cyclic *β*-keto amide substrates featuring a tertiary amide were shown to be unreactive (Scheme 22).[90–92]

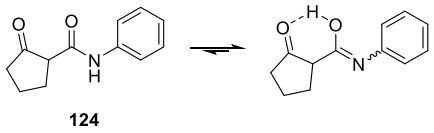

Scheme 21. *Equilibirum between amide and imidic forms of **124**.*

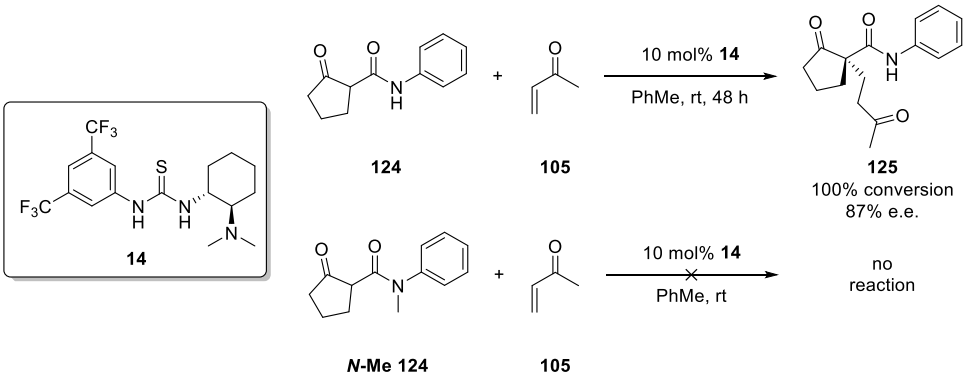

Scheme 22. *Reactivity of β-keto amides with secondary and tertiary amides in an organocatalysed conjugate addition.*[90]

In the case of acyclic substrates, presumably due to their lower pK_a, reactivity is retained even with a tertiary amide. However, these are still high pK_a pronucleophiles compared to other more commonly used substrates in organocatalysis such as *β*-keto esters.[49] The group of Constantieux and co-workers exploited this fact in their highly diastereoselective conjugate addition of *β*-keto Weinreb amides to nitroalkenes catalysed by cinchona-derived squaramides (Scheme 23).[93] To the best of our knowledge, this is the only report on the use of acyclic *β*-keto amides in organocatalysed conjugate additions.

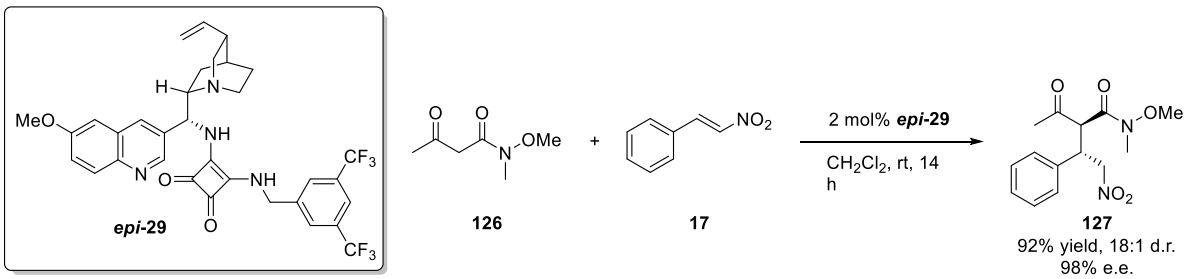

Scheme 23. *Conjugate addition of acyclic β-keto amides reported by Constantieux and co-workers.*

2.7.2 Optimisation

In our first attempt at this reaction, we used 10 mol% of homogeneous bifunctional iminophosphorane organocatalyst **56** to catalyse the conjugate addition of *N*,*N*-diethyl-3-oxobutanamide to nitrostyrene in toluene at room temperature (Table 16). This resulted in formation of the product in 57% yield, 71:29 d.r.[iii] and 88:12 e.r. (major diastereomer) and 89:11 (minor

[iii] Diastereomeric ratios for this reaction are quoted as 2*S*,3*S* : 2*S*,3*R*. The absolute configuration of the diastereomers of **129** was not determined, but it is assumed they follow the same trend as those of **131a** therefore are quoted following the same convention. Only two of the possible four stereoisomers were detected in all cases.

diastereomer). The use of catalyst **116** under the same conditions resulted in improved d.r. but decreased e.r. and yield.

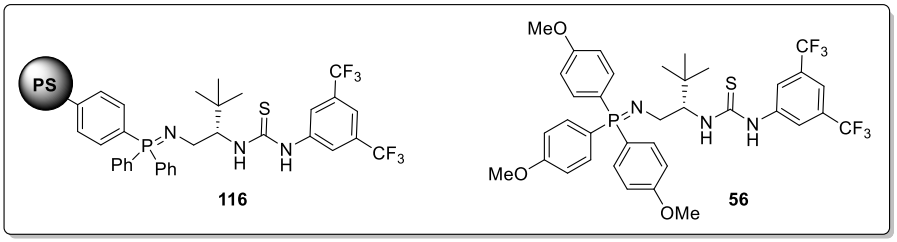

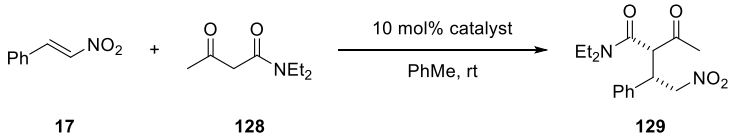

17 128 129

Catalyst	Equiv. nitrostyrene	Time (h)	Yield (%)[a]	d.r.[b]	e.r. (major)[c]	e.r. (minor)[c]
76	1.5	7	57	71:29	88:12	89:11
116	3	45	36	81:19	86:14	81:19

Table 16. *Preliminary results for the addition of β-keto amides to nitrostyrene. [a] Yield represents isolated yield after flash column chromatography on silica .[b] d.r. determined by mass ratio of isolated diastereomers. [c] Enantiomeric ratio (e.r.) was determined by HPLC analysis on a chiral stationary phase.*

We then decided to study *N,N*-dimethyl-3-oxobutanamide as we believed that smaller substituents at the nitrogen might improve reactivity by decreasing the steric clash upon enolisation. We did indeed achieve improved results with *N,N*-dimethyl-3-oxobutanamide and at room temperature in toluene, with 1.2 equivalents of nitrostyrene and 10 mol% **116**, we obtained adduct **129** in 57% yield, 37:63 d.r and 89:11 e.r. (major) and ~ 85:15 e.r. (minor). We therefore began optimisation of the conjugate addition of *N,N*-dimethyl-3-oxobutanamide to nitrostyrene with respect to temperature, solvent and catalyst loading.

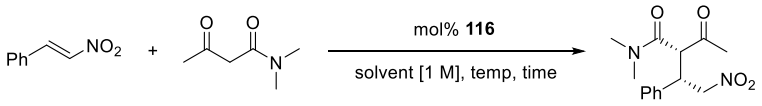

17 130a 131a

Temp (°C)	Solvent	mol% 116	Time (h)	d.r.[a]	Conversion (%)[a]	Yield (%)[b]	e.r. (major)[c]	Approx. e.r. (minor)[c]
rt	PhMe	10	18	37:63	n.d.	57	89:11	85:15
	DCM			37:63	n.d.	59	88:12	80:20
	THF			33:67	n.d.	75	91:9	85:15
	EtOAc			28:72	n.d.	69	88:12	81:19
rt	MTBE	5	48	26:74	57	n.d.	n.d.	n.d.
	THF		24	41:59	95	74	92:8	81:19
	EtOAc		24	43:57	89	74	89:11	79:21
	$CHCl_3$		24	54:46	75	52	86:14	77:23
0	MTBE	10	48	27:73	58	n.d.	n.d	n.d.
	THF		24	9:91	94	86	92:8	74:26
	EtOAc		24	8:92	91	77	89:11	79:21
	$CHCl_3$		24	19:81	76	60	89:11	64:36
−20	THF	10	24	74:26	96	82	95:5	94:6
	EtOAc			77:23	81	70	89:11	92:8
−40	THF	10	20	74:26	26	n.d.	n.d.	n.d.
40	THF	10	1	65:35	93	78	91:9	81:19
0	THF	10	2	40:60	97	74	93:7	89:11
rt			2	47:53	93	65	93:7	84:16
−20 then 0			24 + 24	20:80	91	74	96:4	86:14
−20 then 0			4 + 27	21:79	90	73	95:5	84:16

Table 17. *Optimisation of the conjugate addition of β-keto amides to nitrostyrene. All reactions performed with 1.2 equivalents of nitrostyrene at [1 M]. [a] Determined by ^{1}H-NMR analysis of the crude reaction mixture. [b] Isolated yield after flash column chromatography on silica. [c] Determined by HPLC analysis on a chiral stationary phase. The e.r. of the minor diastereomer is approximate due to poor peak resolution.*

Optimisation was commenced by performing a solvent screen at 5 mol% and 10 mol% catalyst loading at room temperature (Table 17). THF was found to be the optimal solvent, followed by ethyl acetate, however we continued to screen the reaction in the other solvents in case this trend changed with temperature. Reactivity and e.r. could be maintained when decreasing the catalyst loading from 10 mol% to 5 mol%, but this led to a reduced d.r. therefore we continued our optimisation with a 10 mol% loading. Reducing the temperature to 0 °C led to an increase in d.r. and a slight increase in yield, with the e.r. remaining roughly the same. Decreasing the temperature further to −20 °C led to an improvement in e.r., but the diastereoselectivity was reversed. Performing the reaction at −40 °C,

in the hope of obtaining a higher reversed d.r. led to drastically reduced reactivity with no accompanying increase in d.r.

At this point we began to contemplate the underlying cause behind these variations in diastereoselectivity. We hypothesised that the diastereomeric mixture obtained at room temperature favours the more thermodynamically stable diastereomer ("A"), while the diastereomeric mixture obtained at −20 °C favours the kinetic product ("B"). Indeed basic molecular modelling using PerkinElmer ChemBio3D which calculated a total minimised energy for diastereomer A of −11.2 kcal mol^{-1} and a total minimised energy of +5.0 kcal mol^{-1} for diastereomer B. We therefore suggest that this reaction takes place in two stages – the first, enantiodetermining step is the conjugate addition of the *β*-keto amide to nitrostyrene. Then, due to the basicity of the bifunctional iminophosphorane organocatalyst, epimerisation of the stereogenic centre *α*– to the two carbonyl groups takes place, establishing the d.r. This is consistent with the results obtained by Constantieux and co-workers, who obtain predominantly the kinetic diastereomer of **131a** using squaramide organocatalysts, which are not basic enough to epimerise the conjugate adduct.[93]

Using this hypothesis, we investigated different conditions for obtaining a high d.r. (in favour of either A or B) in this conjugate addition. First we tried conducting the reaction at elevated temperature (40 °C) for a short time, with the intention of rapidly forming the conjugate adduct and stopping the reaction before any significant epimerisation takes place. However this resulted in a d.r. of only 65:35 and a reduced e.r. A similar outcome was obtained at room temperature and 0 °C – stopping the reaction after a short time resulted in small excess of the kinetic diastereomer. It was clearly necessary to use low temperatures to obtain a good e.r., but reaction at at least 0 °C was required for sufficient epimerisation to take place to obtain a good d.r. Consequently, we decide to combine the two and conduct the reaction at −20 °C until the keto-amide was consumed (4 hours) and then stir the reaction mixture at 0 °C to effect epimerisation. This allowed us to obtain the adduct in 73% isolated yield, 21:79 d.r. and 95:5 e.r. of the major diastereomer.

Considering Table 17, it can be seen that there is a 10 – 20% discrepancy between the conversion as measured by ^{1}H-NMR and the isolated yield after flash column chromatography. Indeed, the isolated

mass after chromatography is less than would be expected from the mass of the crude reaction mixture. It may be that some product adheres to the silica and cannot be eluted under the chosen conditions or it may be that the conversion determined by ^{1}H-NMR (based on residual keto amide) is falsely inflated – although very little keto amide remains when the reaction is stopped, both it and the product may be decomposing under the reaction conditions. This is consistent with the appearance of of unidentified peaks in the ^{1}H-NMR spectra of the crude reaction mixture.

2.7.3 Substrate synthesis

Apart from the *N*,*N*-dimethyl-substituted *β*-keto amide *N*,*N*-dimethyl-3-oxobutanamide, many examples of this class of compounds are not commercially available. It was therefore necessary to devise a flexible synthetic route that would allow for the formation of a range of different *β*-keto amides. A variety of *β*-keto esters are commercially available, therefore our initial plan was to transamidate these with dimethylamine following literature procedures.[94] However, attempts to form *N*,*N*-dimethyl-3-oxobutanamide from methyl acetoacetate were unsuccessful (Scheme 24).

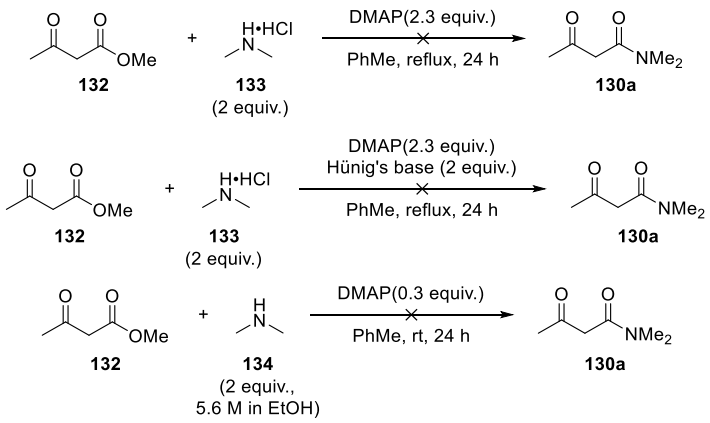

Scheme 24. *Unsuccessful attempts at transamidation.*

We next considered procedures which involved reacting dimethylamine with a ketene equivalent. We were aware of two possible reagents which can serve as ketene equivalents – diketene and diketene acetone adduct. The homodimerisation of acyl chlorides to form variously substituted diketenes is well known,[95] but for our substrate synthesis we required a procedure for heterodimerisation, which although known,[96] has not been well studied. We therefore chose to use diketene acetone adduct. Variously substituted diketene acetone adducts can be easily prepared by reaction of Meldrum's acid with acyl chlorides,[97] followed by reaction with dimethylamine to form

N,N-dimethyl *β*-keto amides.[98] This is the route we used to form the majority of substrates for this conjugate addition (Figure 20).

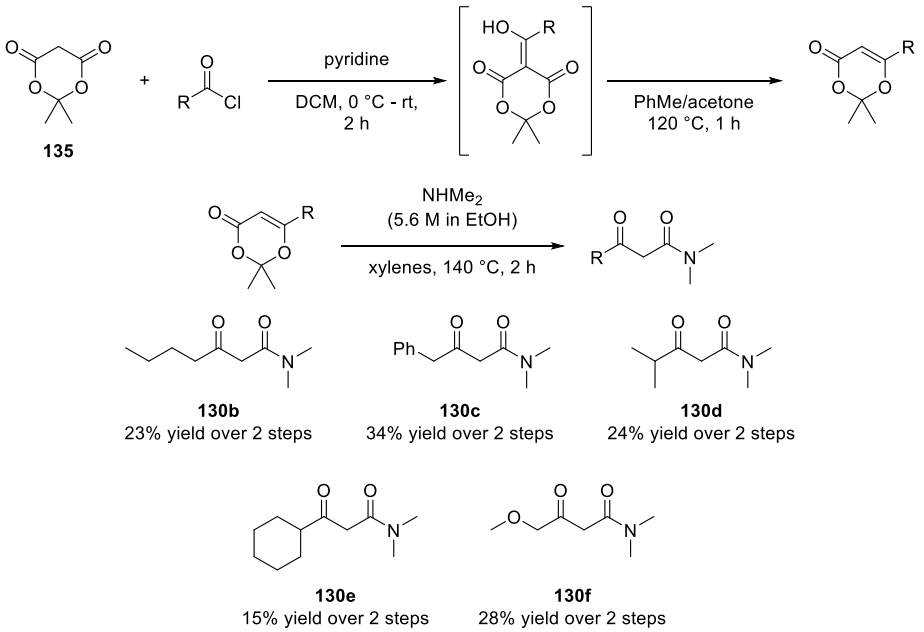

Figure 20. *General procedure for the synthesis of N,N-dimethyl β-keto amides and substrates synthesised using this method.*

The above method was not suitable for the synthesis of phenyl- and *tert*-butyl-substituted *β*-keto amides as the acylation of Meldrum's acid did not proceed with benzoyl chloride or trimethylacetyl chloride. But as these substrates featured unenolisable ketones, they could be formed in good yield by reacting the lithium enolate of *N,N*-dimethyl acetamide with the appropriate electrophile (Scheme 25).

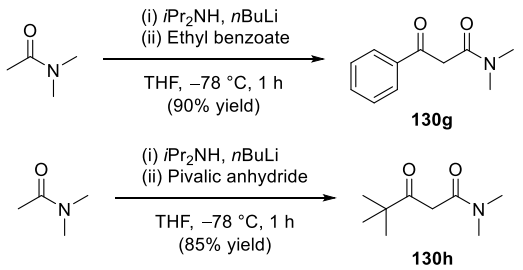

Scheme 25. *Synthesis of β-keto amides **130g** and **130h**.*

2.7.4 Substrate Scope

With a range of *N,N*-dimethyl *β*-keto amides in hand, we could commence our investigation of the substrate scope of this conjugate addition. The first substrate to be investigated was butyl-substituted

keto amide **130b** which was subjected to the reaction conditions developed for *N*,*N*-dimethyl-3-oxobutanamide **130a**. However, when the d.r. and e.r. were lower than expected we tried carrying out the reaction at −20 °C for 20 h and this resulted in improved d.r. and e.r. (Table 18). Consequently the other substrates were also subjected to these conditions.

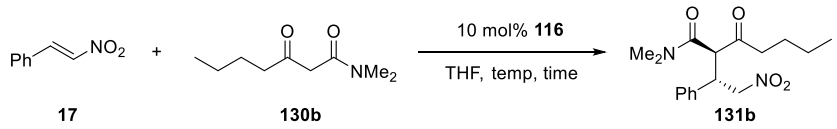

17 **130b** **131b**

Temp (°C)	Time (h)	d.r.[a]	Yield (%)[b]	e.r. (major)[c]
−20 then 0	4 then 28	85:15	66	92:8
−20	20	90:10	67	93:7

Table 18. *Conjugate addition of **130b** to nitrostyrene. [a] Determined by ^{1}H-NMR analysis of the crude reaction mixture. [b] Isolated yield after flash column chromatography on silica. [c] Determined by HPLC analysis on a chiral stationary phase.*

We were able to add a number of *N*,*N*-dimethyl *β*-keto amides, bearing a range of substituents at the ketone, to nitrostyrene in very good yields and diastereo- and enantiomeric ratios (Figure 21). Substrates with primary or secondary alkyl substituents (**131a-e**) gave the highest d.r. and e.r. The use of heteroatom-containing (**131f**) and aryl-substituted (**131g**) ketones resulted in reduced d.r. but very good e.r. The *tert*-butyl-substituted substrate (**131h**) required additional reaction time and also gave a reduced d.r. but very good e.r. Performing the reaction in identical conditions with the corresponding homogeneous catalyst **182** and ketoamide **130a**, we obtained the product in 77% yield, 38:62 d.r. and 94:6 e.r. (major diastereomer) in 2 h at −20 °C followed by 24 h at 0 °C. Interestingly, the homogeneous catalyst appears to be less effective at epimerising **131a** than the polystyrene-supported catalyst **116**. We believe this may be due to dimerization of the homogeneous catalyst in solution, which leads to reduced activity (*vide supra*).

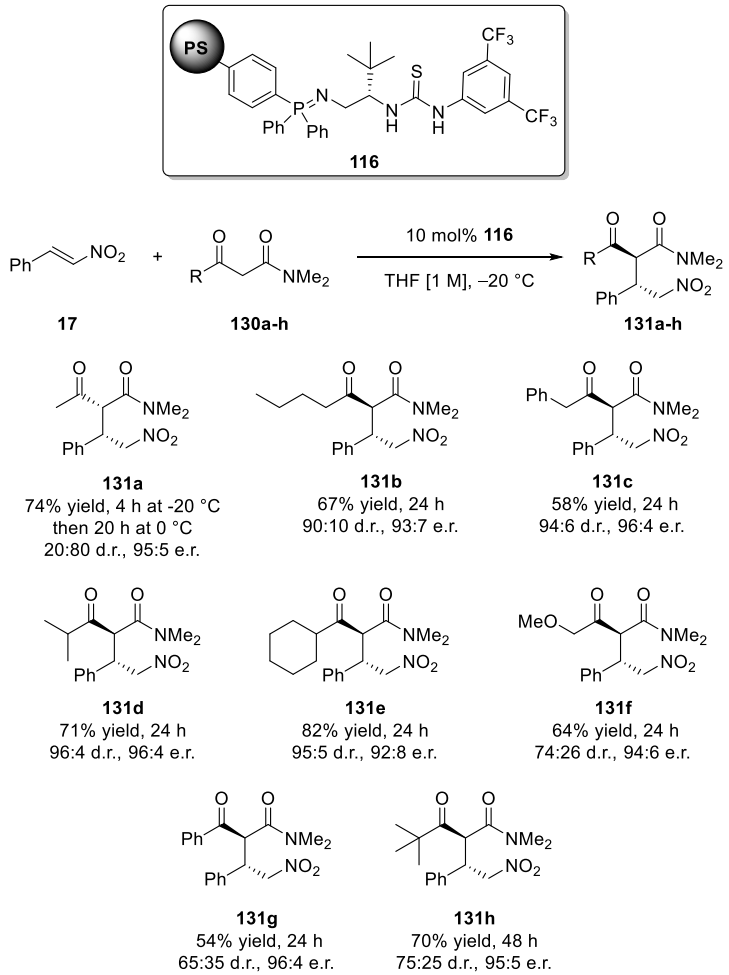

Figure 21. *General scheme and scope for the addition of β-keto amides to nitrostyrene. Absolute stereochemical configuration determined by comparison with literature compounds. Diastereomeric ratio determined by ^{1}H-NMR analysis of crude reaction mixture. Yield represents isolated yield after flash column chromatography over silica. Enantiomeric ratio (e.r.) was determined by HPLC analysis on a chiral stationary phase.*

The configuration of the major diastereomer of **131a** was established to be (2*R*, 3*S*) by comparison with the literature. The configuration of the major diastereomer of **131g** was also established by comparison to literature reports which indicate that it is (2*S*, 3*S*) (Figure 22).[93] We postulate that due its small size, the methyl ketone adduct **131a** does not exhibit high selectivity for either the (2*R*,3*S*) or (2*S*, 3*S*) configuration. At −20 °C the adduct is formed in 74:26 d.r. in favour of the (2*S*,3*S*) diastereomer. Through prolonged epimerisation the thermodynamic mixture of epimers is achieved, in which the (2*R*,3*S*) diastereomer predominates. By analogy, adducts **131b-h** are also formed as a kinetic mixture of diastereomers, with the (2*S*,3*S*) diastereomer predominating. Due to their steric bulk they exhibit higher selectivity and they also have a lower tendency to epimerise. This is due to two factors – the increased pK_a of these adducts relative to **131a** as well as the $A^{1,3}$ allylic strain of

the enolate (Figure 23). However, adducts **131f** and **131g** have a lower pK_a[83] and therefore suffer from epimerisation leading to a reduced d.r. The *tert*-butyl adduct **131h** appears to be a special case, as it has a low d.r. but presumably has too high a pK_a to be readily epimerisable. Perhaps the very large steric bulk of the *tert*-butyl group prevents it from assuming the same conformation in the transition state as the remaining adducts, resulting in a different d.r.

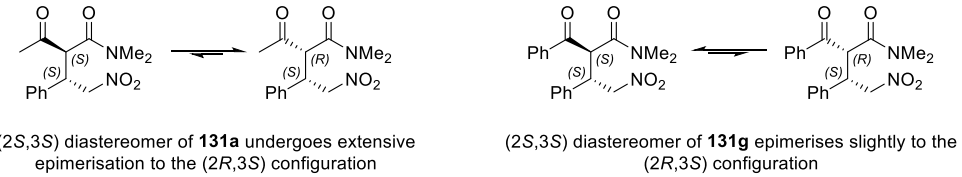

Figure 22. *Epimerisation and diastereoselectivity in the conjugate addition of β-keto amides to nitrostyrene.*

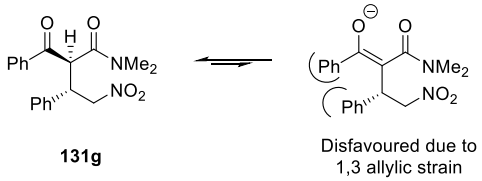

Figure 23. *1,3 allylic strain of the enolate form of the conjugate adducts makes enolisation unfavourable.*

2.8 Transition states for bifunctional iminophosphorane-catalysed reactions

It is possible to speculate on the transition states of the two main conjugate additions studied in this work. As they both involve 1,3-dicarbonyl pronucleophiles which should react in a similar fashion, for the sake of clarity we will first consider the transition states of a generic, symmetrical 1,3-dicarbonyl pronucleophile. This will allow us to narrow down the number of possible transition states by considering the stereochemistry of the newly formed benzyllic stereocenter. Furthermore, as we obtain the same stereoselectivity using the homogeneous and the polystyrene-supported catalysts, the homogeneous catalyst **182** is drawn below for clarity. We assume that this reaction proceeds *via* the deprotonation of the pronucleophile, after which the two substrates are hydrogen bonded to the catalyst and the bond-forming step takes place. It is the transition state for this bond-forming step that is depicted in Figures 26 and 27.

Following the computational studies of Soós and Pápai on the mode of action of bifunctional catalysts such as Takemoto's catalyst and cinchona-derived thioureas,[99] four possible transition states may be

conceived for the conjugate addition of 1,3-dicarbonyl compounds to nitrostyrenes catalysed by bifunctional iminophosphoranes (Figure 26): two with the nitrostyrene hydrogen-bonded to the thiourea, with different orientations of the nitrostyrene (A-1 and A-2), and two with the 1,3-dicarbonyl compound hydrogen-bonded to the thiourea, with different orientations of the nitrostyrene (B-1 and B-2). In this figure, due to the steric bulk of the *tert*-butyl group, pointing out of the page, the substrate associated with the iminophosphorane is orientated behind the plane of the pane. Therefore this substrate must be envisioned to approach the thiourea-bound substrate from behind (Figure 25).

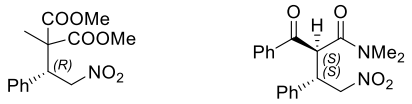

123a **131g**

Figure 24. *Compounds **123a** and **131g** re-drawn for comparison with the generic 1,3-dicarbonyl conjugate adduct in Figure 26.*

Considering these four possible transition states, in transition states A-2 and B-2 it appears as if there may be a steric clash between the nitrostyrene and the 1,3-dicarbonyl compound or the catalyst. Indeed, these two transition states give the incorrect stereochemistry compared to compounds **123** and **131** (see Figure 24), supporting their infeasibility. Transition states A-1 and B-1 do not entail this steric clash and both predict the correct stereochemical outcome compared to compounds **123** and **131**. It does not appear to be possible to determine whether A-1 or B-1 is the more favourable transition state, presumably computational modelling is required to determine their relative energies. Or it may be, as in the work of Soós and Pápai mentioned above, that both transition states are similarly feasible.

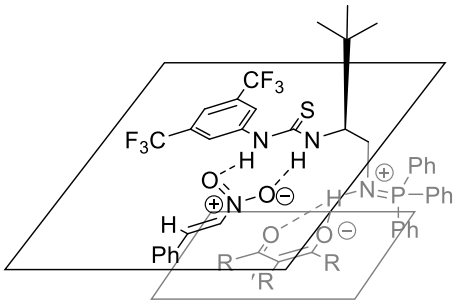

Figure 25. *Three dimensional representation of orientation of substrates in conjugate addition transition state (A-1).*

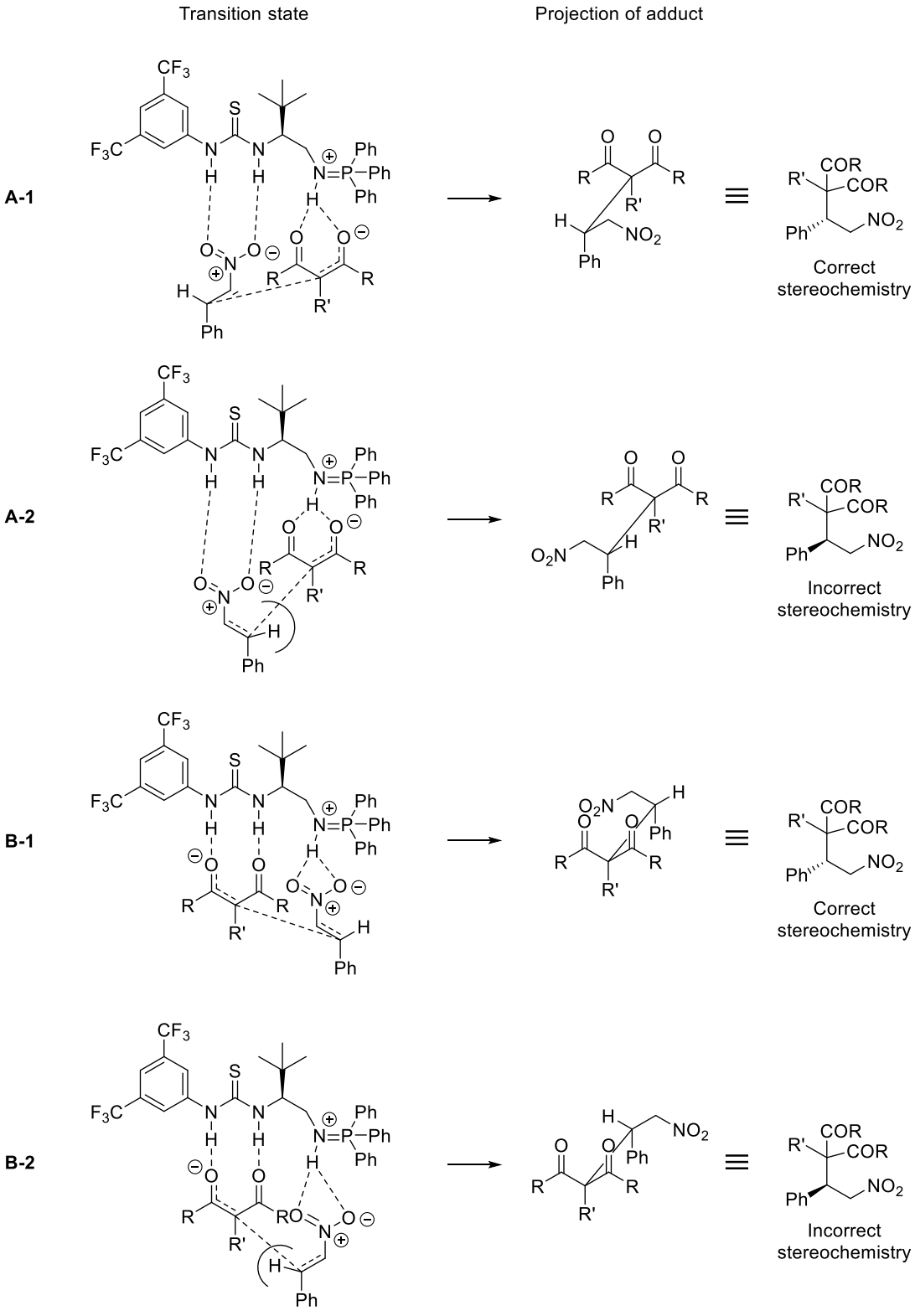

Figure 26. *Possible transition states for the conjugate addition of a 1,3-dicarbonyl compound to nitrostyrene catalysed by* ***116****. R = any alkyl, ester or amide functional group. R' = H or alkyl group.*

Now that we have identified A-1 and B-2 as feasible transition states within the two binding modes A and B, we may consider an asymmetrical pronucleophile and identify some possible transition states relating specifically to the conjugate addition of *β*-keto amides (Figure 27).

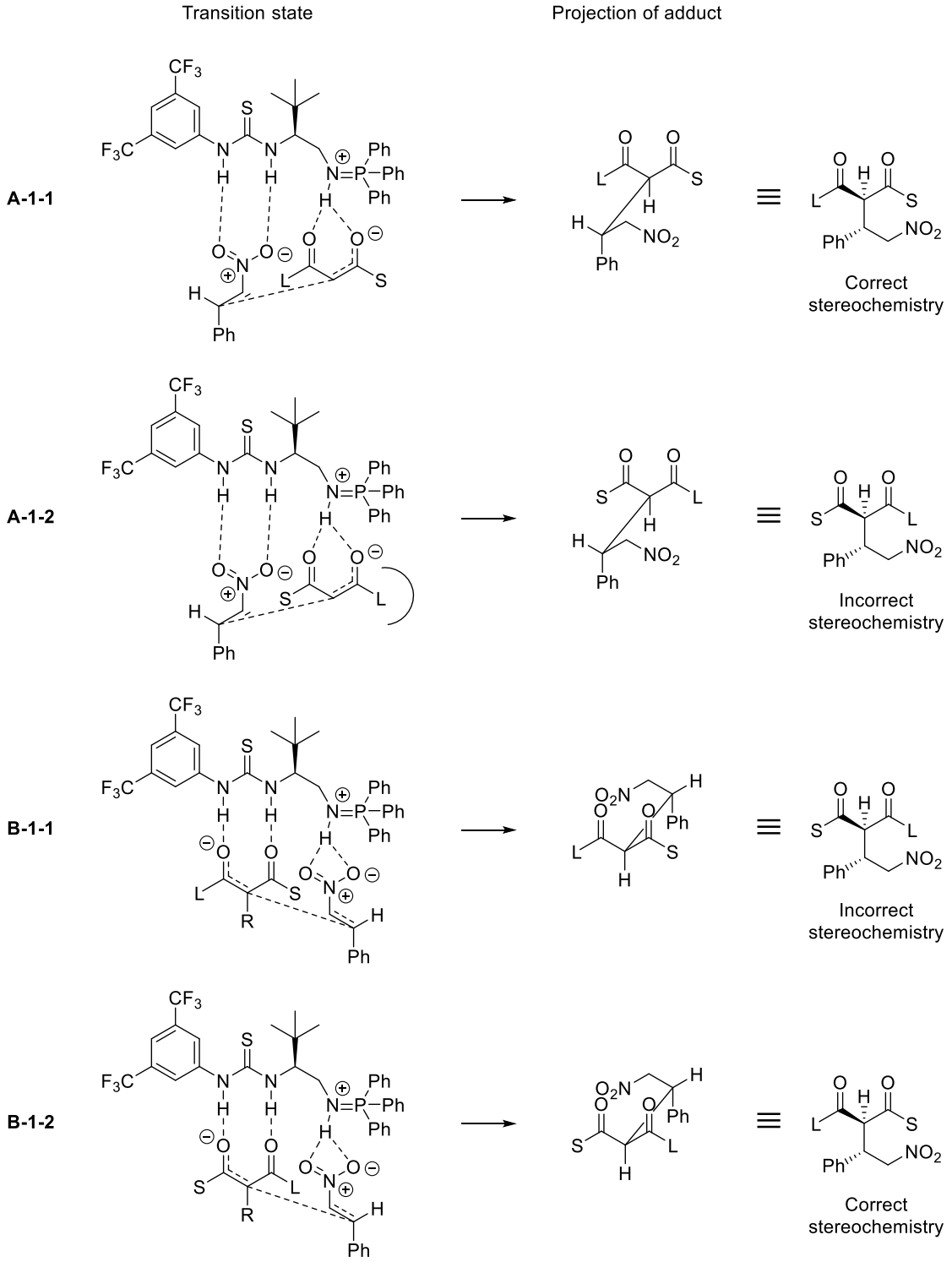

Figure 27. *Possible transition states for the conjugate addition of an asymmetrical 1,3-dicarbonyl compound to nitrostyrene catalysed by* ***116****. L = large substituent, S = small substituent. We consider the dimethylamide substituent as the "small" substituent for comparison with* ***131****.*

In binding mode A, the large substituent on the pronucleophile may be oriented either towards the thiourea or towards the phosphorus atom. In the latter case, there may be a steric clash between the large substituent and the bulky aryl groups on the phosphorus. Of these two possibilities, it is the former model transition state, A-1-1 that correctly predicts the stereochemistry of products **131**. Considering binding mode B it is more difficult to see *a priori* from a simple line drawing whether orientation B-1-1 or B-1-2 is more sterically favourable. However it is possible to make an electronic argument in favour of B-1-2 over B-1-1. In the deprotonated *β*-keto amide, the negative charge should be predominantly located on the ketonic oxygen, as the amide carbonyl has increased electron density due to donation from the nitrogen lone pair. The carbonyl with the greatest electron density will presumably hydrogen bond with the thiourea N-H with the least electron density, which is the one bearing the 3,5-bis(trfluoromethyl)phenyl substituent. This is the case in transition state B-1-2, considering the amide as the "small" substituent, which furthermore predicts the correct stereochemistry. However, this line of reasoning cannot explain the effect of the size of the ketone substituent on the initial d.r. although it does explain the overall selectivity.

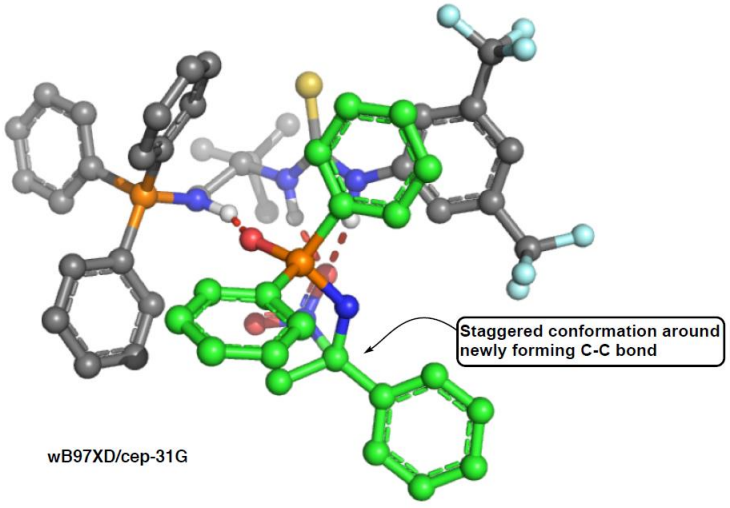

Figure 28. *Proposed working model of the nitro-Mannich transition state. Calculations by Prof. Robert Paton and Adam Madarasz: Quantum-guided molecular mechanics (Q2MM); Monte Carlo conformational search of the transition structures, followed by full DFT optimisations.*

For the nitro-Mannich reaction of ketimines, a working model has been proposed in collaboration with the group of Prof. Paton who undertook computational studies of this reaction. This model is

shown above in Figure 28 and represents the ketimine hydrogen bonded to the iminophosphorane nitrogen *via* the oxygen of the diphenylphosphinoyl group, while the thiourea-associated nitronate approaches the carbonyl carbon from behind the plane of the page. Again, as we obtain the same stereochemical outcome using the polystyrene-supported catalyst as with the homogeneous system, we assume that a similar transition state may be proposed for both.

2.9 Rate enhancement in conjugate additions of β-amido esters

As discussed in Chapter 1, the use of tertiary amines as the Brønsted basic motif in bifunctional organocatalysis can lead to very slow reaction rates due to their relatively low basicity. One approach to overcoming this issue is the use of organic superbases. Recent work within our group has demonstrated very large rate enhancements in the conjugate addition of cyclic β-amido esters to nitroalkenes when using bifunctional iminophosphorane organocatalysts instead of bifunctional cinchona alkaloid organocatalysts. The reactions studied were chosen from methodology and total synthesis studies published by the Dixon group which featured reactions with particularly slow rates under bifunctional tertiary amine catalysis. We were interested to see whether comparable rate enhancements could also be achieved using polystyrene-supported bifunctional iminophosphoranes, thus displaying the performance of this heterogeneous catalytic system. The reactions in Figure 29 were optimised under homogeneous conditions (*this work was carried out by Dr. Pavol Jakubec and Alistair Farley*) then using analogous reaction conditions, carried out using polystyrene-supported bifunctional iminophosphorane organocatalysts (*this work was carried out by A.M.G.*).

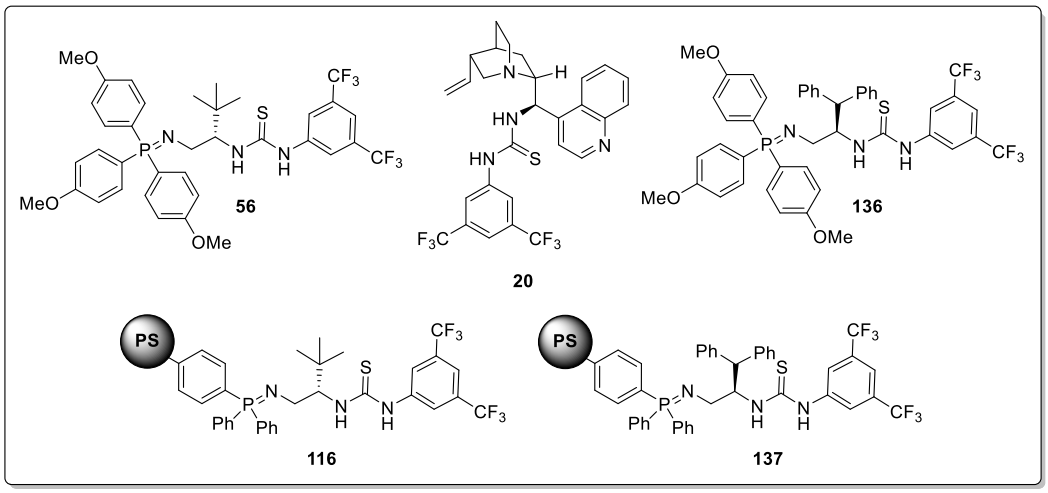

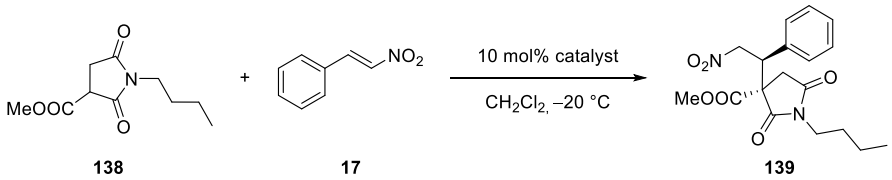

138 17 139

Procedure	Catalyst	Time	Crude d.r.[a]	d.r.[b]	e.r. (major)[c]	e.r. (minor)[c]	Yield (%)[d]
Literature[100]	**20**	2 d	-	66:34	97:3	95:5	81
Homogeneous	**136**	1 h	80:20	77:23	95:5	87:13	90
PS-supported	**137**	1 h	79:21	-	94:6	-	54 (major)

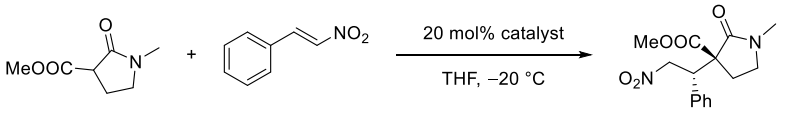

34 17 35

Procedure	Catalyst	Time	Crude d.r.[a]	d.r.[b]	e.r. (major)[c]	e.r. (minor)[c]	Yield (%)[d]
Literature[101, e]	**20**	14 d	84:16	84:16	96:4	76:24	92
Homogeneous	**136**	2 h	~89:11	88:12	96:4	61:39	95
PS-supported	**137**	3 h	79:21	79:21	89:11	61:39	78

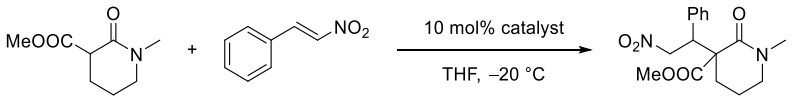

140 17 141

Procedure	Catalyst	Time	Crude d.r.[a]	d.r.[b]	e.r. (major)[c]	e.r. (minor)[c]	Yield (%)[d]
	20						NR
Homogeneous	**56**	22 h	74:26	74:26	96:4	-	98
PS-supported	**116**	16 h	76:24	76:24	96:4	78:22	69

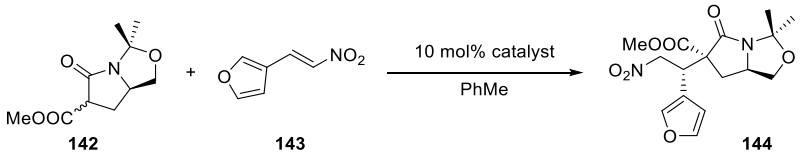

142 143 144

Procedure	Catalyst	Temp. (°C)	Time	Crude d.r.[a]	d.r.[b]	Yield (%)[d]
Literature[102]	**20**	30	2 d	94:6:0:0	single	80
Homogeneous	**136**	0	30 min	98:2:0:0	single	75
PS-supported	**137**	rt	1 h	96:4:0:0	single	66

Figure 29. *Conjugate addition of β-amido esters to nitroalkenes. [a] Crude diastereomeric ratio determined by [1]H-NMR analysis of crude reaction mixture. [b] Diastereomeric mixture determined by [1]H-NMR analysis after purification. [c] Enantiomeric ratio was determined by HPLC analysis on a chiral stationary phase. [d] Yield represents isolated yield after purification. [e] Only the reaction time for this reaction was reported in the cited publication, d.r., e.r. and yield were later determined by Dr. Pavol Jakubec.*

All the above reactions can be successfully carried out using polystyrene-supported bifunctional iminophosphorane organocatalysts. Furthermore, a similar magnitude of rate enhancement relative

to **20** that was observed using the homogeneous bifunctional iminophosphorane organocatalysts, was also observed with the polystyrene-supported system. However, all the yields obtained with catalysts **116** and **137** are 10 – 20% lower than those obtained with their homogeneous counterparts. This could be attributed to lower reaction rates with the heterogeneous catalysts due to impaired mass transfer or to the fact that the homogeneous catalysts feature the tris(4-methoxyphenyl) substituted iminophosphorane which is known to be more basic and reactive than the phenyl-substituted iminophosphorane. An interesting observation that can be derived from Figure 29 is the varying impact of immobilisation on the d.r. and e.r. of different reactions, even within the specific category studied here. The major diastereomers of **139**, **141** and **144** are all obtained with identical enantioselectivity (or diastereoselectivity in the case of **144**) using both homogeneous and heterogeneous catalysts, while the major diastereomer of **35** is obtained in 96:4 e.r. using catalyst **136** but only 89:11 e.r. using catalyst **137**. However, the minor diastereomer of **35** is obtained with identical e.r. using both systems. Furthermore, in the reactions where the e.r. is identical for the homogeneous and heterogeneous systems, the d.r. is also identical and for reactions where the e.r. is different, the d.r. is different also. It appears that attachment to a polystyrene-support may change the shape of the "chiral pocket" of bifunctional iminophosphorane organocatalysts, affecting both diastereo- and enantioselectivity. In the reactions we have studied, this effect appears to be rare and it is curious that it occurs with this particular nucleophile, while for instance the reaction of the analogous 6-membered pronucleophile **140** is unaffected. At this stage, we are unable to offer a more specific explanation for these observations other than to suggest that the transition state for this particular reaction is affected by unfavourable interactions between the catalyst and the solid support.

2.9.1 Bifunctional iminophosphoranes in the nitro-Mannich/lactamisation cascade

The reaction of nitroalkanes with imines in a nitro-Mannich/lactamisation cascade to form multicyclic piperidinones was first reported by the Dixon group in 2008[101] and developed further in subsequent years.[84] In this reaction a nitroalkane (formed by conjugate addition of a 1,3-dicarbonyl pronucleophile to a nitroalkene) undergoes a nitro-Mannich reaction with a cyclic imine to form an

amine, which reacts with one of the carbonyl groups derived from the 1,3-dicarbonyl pronucleophile to form a lactam (Figure 30).

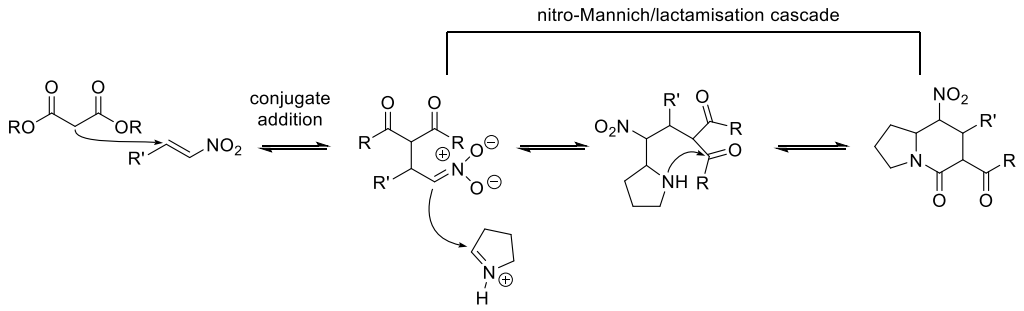

Figure 30. *General mechanism of the nitro-Mannich/lactamisation cascade.*

It is possible to combine the nitro-Mannich/lactamisation cascade with the conjugate addition for the formation of the nitroalkane in a one-pot procedure. This was demonstrated using **20** to form conjugate adduct **35**, which was then reacted directly with imine **145** (Scheme 26).[84]

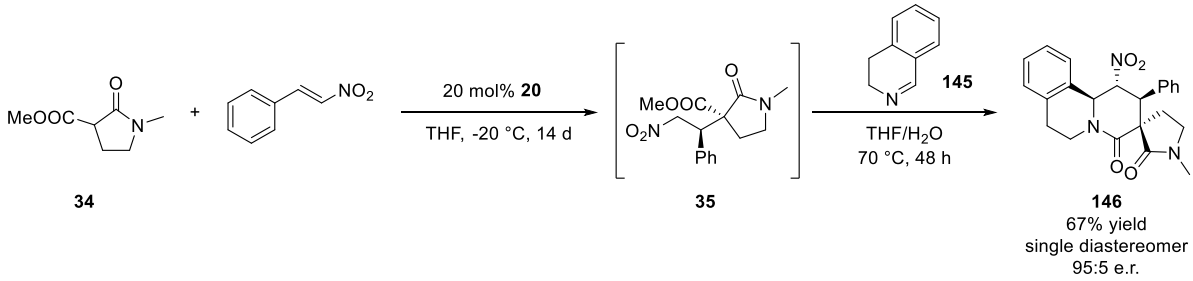

Scheme 26. *One-pot procedure for conjugate addition followed by nitro-Mannich/lactamisation cascade. Imine **145** and water were added directly to the conjugate addition reaction mixture.*

As discussed above, the rate of the conjugate addition in Scheme 26 may be greatly increased by using a bifunctional iminophosphorane organocatalyst. However, when the above one-pot procedure was attempted with catalyst **136**, the nitro-Mannich/lactamisation cascade did not proceed successfully *(reaction carried out by Dr. Pavol Jakubec and Alistair Farley)*. The presence of the strongly basic iminophosphorane interferes with the nitro-Mannich step by catalysing the reverse reaction, making it impossible to obtain piperidinone **146** in good yield.[iv] We considered that perhaps the use of the corresponding immobilised bifunctional iminophosphorane might offer a way to perform the above one-pot procedure whilst maintaining a short reaction time for the conjugate

[iv] It was possible to perform the one-pot procedure using the imine derived from allyl amine and formaldehyde. As it is much more reactive than **145**, the lactamisation step occured more quickly than the retro-Mannich and the piperidone final product was obtained in good yield.

addition. At first we simply repeated the procedure depicted in Scheme 26 using polystyrene-supported catalyst **137** in the hope that the use of a polar, non-swelling solvent (water) might reduce the activity of the catalyst and that the decrease in concentration in conjunction with the use of a heterogeneous catalyst will drastically slow the rate of any reactions involving the catalyst. The yield of **146** obtained using this method was less than 40% and the isolated product was of very low purity, even after column chromatography. It should be noted that water did not immediately hydrolyse the catalyst, as one might typically expect with an iminophosphorane. It was therefore necessary to filter the reaction mixture after the conjugate addition to remove catalyst **137** before subjecting the crude conjugate adduct to the nitro-Mannich lactamisation cascade. Although not as straightforward as the original one-pot procedure, this procedure was nevertheless very operationally simple and resulted in the formation of piperidinone **146** as a single diastereomer in 68% yield and 88:12 e.r. Our investigations towards carrying out this procedure using bifunctional iminophosphorane organocatalysts showcase one of the advantages of catalyst immobilisation, namely easy catalyst separation, without which it would be impossible to form piperidinone **146** without intermediate purifications steps and with a short reaction time.

2.10 Catalyst recycling

One of the advantages of catalyst immobilisation is the possibility of recycling. Unfortunately, not every reaction was found to be conducive to catalyst recycling over multiple cycles and it was necessary to test several reactions before we achieved successful recycling (sustained reactivity over 10 cycles was considered satisfactory). Our first attempt at catalyst recycling involved the conjugate addition of dimethyl methylmalonate to nitrostyrene as this reaction made use of commercial reagents, was relatively fast and purification was straightforward. However, on the second cycle, catalyst activity was already drastically diminished (Table 19). We suspect this may be due to the polymerisation of nitrostyrene, which then becomes caught in the polystyrene-beads thus inactivating the catalyst,[48] however this was not confirmed.

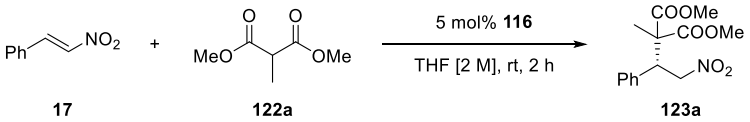

17 122a 123a

Cycle	Yield (%)[a]	e.r.[b]
1	76	93:7
2	35	94:6
3	trace	n.d.

Table 19. *Catalyst recycling with dimethyl methylmalonate conjugate addition. At the end of the indicated reaction time the reaction mixture was removed by syringe and the catalyst washed, dried and re-used.[a] Yield represents isolated yield after purification. [b] Enantiomeric ratio was determined by HPLC analysis on a chiral stationary phase.*

We next looked at the conjugate addition of nitromethane to chalcone.[103] Slightly better performance was obtained with this reaction, with the conversion only dropping drastically on the third cycle. We believed that this might be due to protonation of the catalyst by nitromethane, which, if the nitromethane anion was slow to react with chalcone and deprotonate the catalyst again, could inactivate it. Another possible catalyst deactivation pathway is *via* an aza-Wittig reaction with chalcone. The catalyst could be regenerated somewhat by washing with a BEMP solution between cycles, but the conversion dropped again soon after washing and the e.r. was decreased, perhaps due to residual BEMP catalysing the racemic reaction (Table 20).

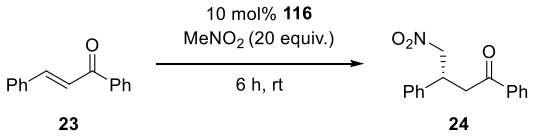

23 24

Cycle	Yield (%)[a]	e.r.[b]
1	93	89:11
2	88	88:12
3	38	n.d.
Catalyst washed with BEMP		
4	86	82:18
5	49	84:16

Table 20. *Catalyst recycling with nitromethane into chalcone conjugate addition. At the end of the indicated reaction time the reaction mixture was removed by syringe and the catalyst washed, dried and re-used.* [a] *Yield represents isolated yield after purification.* [b] *Enantiomeric ratio was determined by HPLC analysis on a chiral stationary phase.*

Another possible reason for the observed catalyst degradation was that while the catalyst was being stored overnight between cycles (under vacuum) it was absorbing moisture. We therefore repeated the recycling experiment using nitromethane and chalcone, this time storing the catalyst under vacuum over phosphorus pentoxide as a desiccating agent. This approach was much more successful for maintaining catalyst activity, but still did not meet our predetermined benchmark (Table 21).

Cycle	Yield (%)[a]	e.r.[b]
1	91	89:11
2	93	88:12
3	81	89:11
4	69	88:12
5	49	88:12
6	27	88:12
7	6	88:12

Table 21. *Catalyst recycling with nitromethane into chalcone conjugate addition. At the end of the indicated reaction time the reaction mixture was removed by syringe and the catalyst washed, dried over P_2O_5 and re-used.* [a] *Yield represents isolated yield after purification.* [b] *Enantiomeric ratio was determined by HPLC analysis on a chiral stationary phase.*

Finally, we attempted the recycling experiment using the nitro-Mannich reaction of ketimine **36a**. Catalyst recycling with this reaction was more successful, however, it still required several attempts to achieve a run of 10 cycles with greater than 90% conversion. As this reaction had a 24 h reaction time, we avoided the potential problems of storing the catalyst overnight by starting the next cycle immediately after the catalyst was washed and briefly dried under nitrogen flow. Using freshly prepared catalyst, we were able to achieve catalyst recycling over 10 cycles, maintaining excellent conversion and e.r. throughout the experiment (Figure 31).

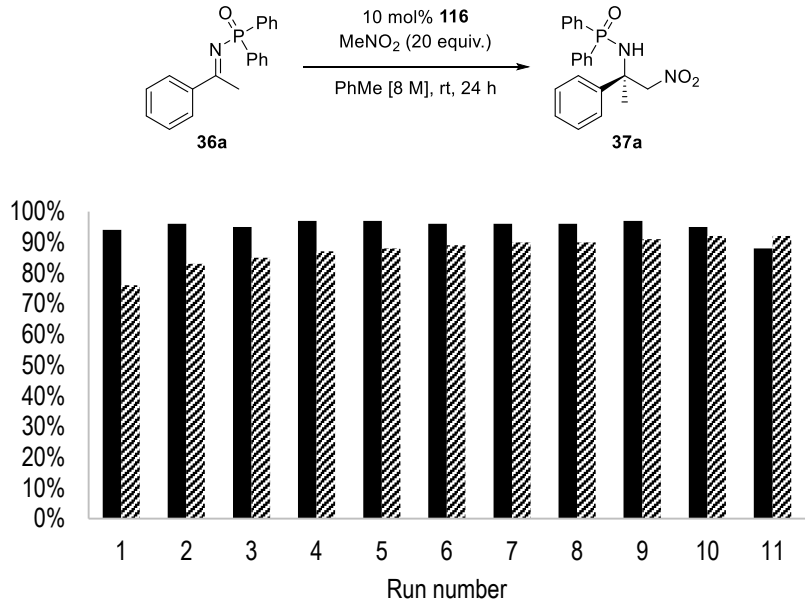

Figure 31. *Recycling of catalyst **116** in the nitro-Mannich reaction of ketimine **36a**. Solid columns represent conversion as measured by ^{1}H-NMR, dashed columns represent e.e.*

2.10.1 Nitro-Mannich reversibility

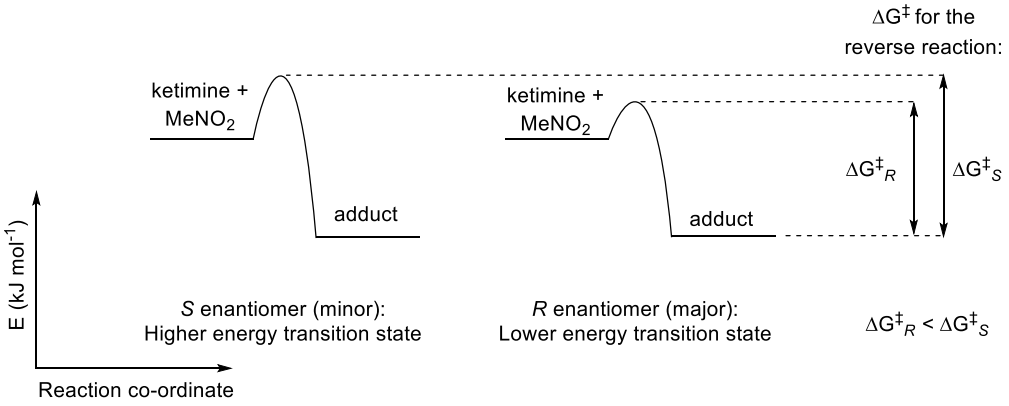

Figure 32. *Transition state diagrams for the nitro-Mannich reaction forming the R and S enantiomers of the product.*

In Figure 31 it can be seen that the e.e. of the nitro-Mannich reaction rises slightly over the course of the recycling experiment. We attribute this to decreasing racemisation, caused by the retro-nitro-Mannich reaction, as the catalyst activity decreases. We have observed that the e.r. of the nitro-Mannich adduct decreases over time in the presence of the bifunctional iminophosphorane organocatalyst (Table 22). We also note that *β*-nitro-amines are known to undergo the retro-Mannich reaction, expelling nitroalkane and reverting to their parent imine.[71,104] Following from these observations we propose that when the reverse reaction takes place under catalyst control, the fastest backwards reaction is the one of the major enantiomer (since the diastereomeric transition state leading to it is of lower energy, Figure 32). Also, the catalyst is more likely to react with the major enantiomer as it is in excess. As a result of this reverse reaction, some of the major enantiomer will be transformed to the minor enantiomer (as the enantiocontrol of the catalyst is not perfect). Thus there is an accumulation of the minor enantiomer as its reverse reaction is slower and as the system equilibrates the adduct racemises (Figure 33).

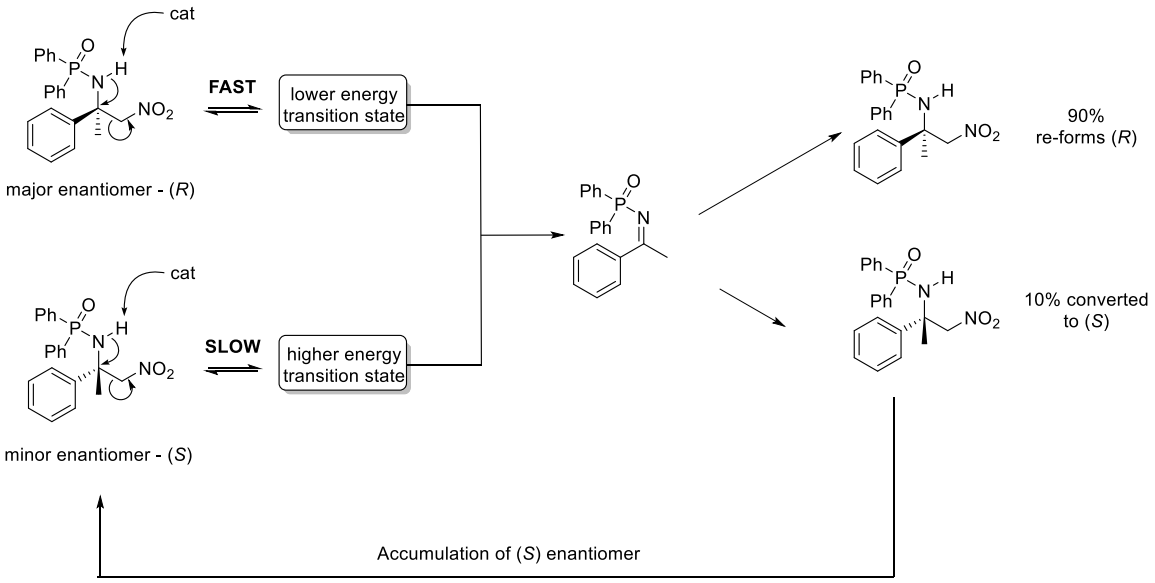

Figure 33. *Reversibility of the nitro-Mannich reaction leading to accumulation of minor enantiomer.*

In the recycling experiment, the catalyst activity slowly decreases, which may not be immediately apparent as the conversion remains very high. However, this is due to that fact that we have chosen a set time of 24 h for each run of the recycling experiment so the experiment may conveniently be carried out over many days (the reaction time required for full conversion at room temperature is approximately 10 h). Thus we propose that, as the catalyst activity slowly decreases so does the rate of the reverse reaction, decreasing the erosion of the e.r. This causes a net increase in the e.r. with each subsequent run.

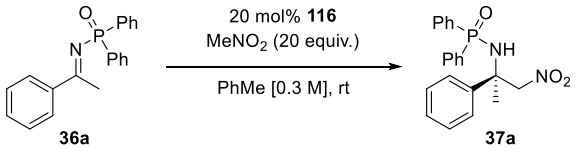

Time (h)	e.r.[a]
4	91:9
24	82:18
48	73:27

Table 22. *Change of e.r. of nitro-Mannich product with increasing reaction time.* [a] *Enantiomeric ratio (e.r.) was determined by HPLC analysis on a chiral stationary phase.*

2.11 Flow Chemistry

Another application of solid-supported reagents and catalysts is in continuous flow systems. We planned to demonstrate the use of our immobilised bifunctional iminophosphoranes in flow chemistry by using a HPLC-based set up – a blank HPLC column was filled with catalyst and a mixture of reagents was pumped through it using an HPLC pump. As with the catalyst recycling experiment, not every reaction was appropriate for flow chemistry. We expected that the best results would be achieved with a fast reaction as it would be mostly likely to reach full conversion in a single pass through the column. Our first attempt therefore was with the conjugate addition of *N,N*-dimethyl-3-oxobutanamide **130a** to nitrostyrene (Table 23).

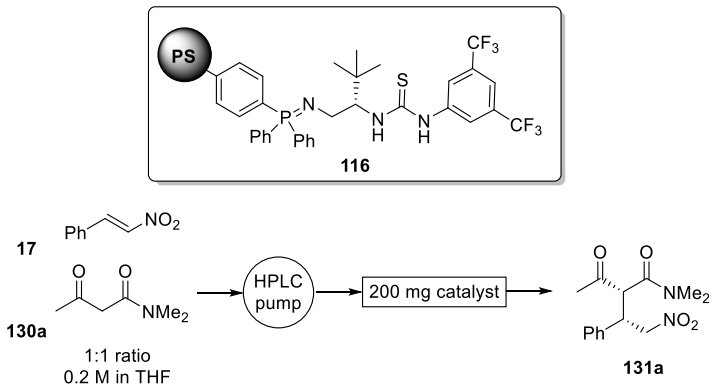

Flow rate (mL min^{-1})	Residence time (min)	Conversion (%)[a]	d.r.[a]	e.r. (major)[b]	e.r. (minor)[b]
0.5	5.4	66	64:36	66:34	~63:37
0.1	27	84	37:63	79:21	~70:30

Table 23. *Conjugate addition of N,N-dimethyl-3-oxobutanamide to nitrostyrene in flow. [a] Determined by ^{1}H-NMR analysis of the crude reaction mixture. [b] Determined by HPLC analysis on a chiral stationary phase. The e.r. of the minor diastereomer is approximate due to poor peak resolution.*

With this reaction we studied the conversion, d.r. and e.r. at two different flow rates. The conversion at 0.1 mL min^{-1} was reasonably good, however the d.r. was very poor and the e.r. was reduced. The poor d.r. is consistent with our optimisation studies which suggest that quite long reaction times are required to epimerise adduct **131a** to obtain a good d.r. As might be expected, with the higher flow rate there is less opportunity for the adduct to epimerise and the d.r. is in favour of the kinetic diastereomer.

Another fast reaction which we investigated under flow conditions was the conjugate addition of pyrrolidinone **34** to nitrostyrene. Initial studies using catalyst **137** showed high conversion at a flow rate of 0.1 mL min^{-1} and identical d.r. and e.r. to those obtained previously in batch (Table 24). These results were very promising and it was decided to investigate this reaction further.

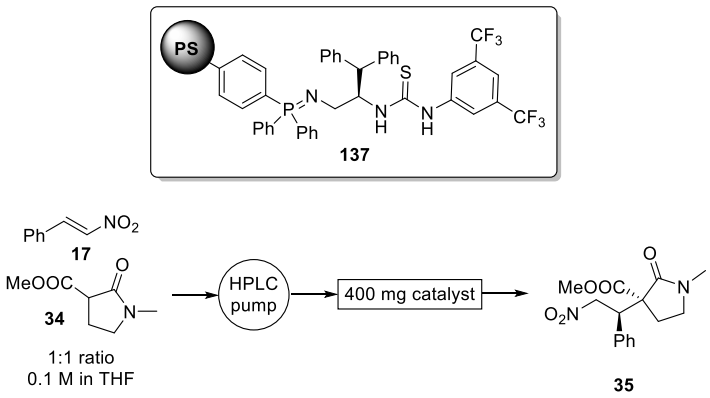

Flow rate (mL min^{-1})	Residence time (min)	Conversion (%)[a]	d.r.[a]	e.r. (major)[b]	e.r. (minor)[b]
1.0	2.7	35	79:21	n.d.	n.d.
0.5	5.4	42	79:21	n.d.	n.d.
0.1	27	82	79:21	89:11	59:41

Table 24. *Effect of flow rate on the conjugate addition of **34** to nitrostyrene in flow. [a] Determined by ^{1}H-NMR analysis of the crude reaction mixture. [b] Determined by HPLC analysis on a chiral stationary phase.*

We next ran the flow reaction continuously for 4 h at 0.1 mL min^{-1} to collect a sizeable amount of the product and confirm that the isolated yield corresponds with the conversion determined by ^{1}H-NMR. The collected product was purified by flash column chromatography over silica and we obtained a yield of 78%, with 80:20 d.r. and 89:11 e.r. (major) and 59:41 e.r. (minor). This correlated well with the conversion measured for this reaction (sampling every hour), which ranged from 74 – 80% (average of 77%).

Next we investigated the effect of reagent concentration on the flow reaction. As the flow rate is so low, it would be advantageous to use as high a reagent concentration as possible to enable the transformation of large amounts of material in a reasonable amount of time. Conversely, we also wanted to test whether using a lower reagent concentration relative to the catalyst would increase the reaction rate and allow us to use a higher flow rate. We found that the reagent concentration could

be increased to 0.2 M with no change in conversion, d.r. or e.r. while lowering the concentration resulted in decreased conversion (Table 25).

Conc. [M]	Conversion (%)[a]	d.r.[a]	e.r. (maj.)[b]	e.r. (min.)[b]
0.2	82	79:21	89:11	59:41
0.05	35	79:21	88:12	58:42

Table 25. *Effect of concentration of the conjugate addition of **34** to nitrostyrene in flow. [a] Determined by ^{1}H-NMR analysis of the crude reaction mixture. [b] Determined by HPLC analysis on a chiral stationary phase.*

Although these conditions gave good conversion at a reasonably high concentration, we wanted to develop a high performing method that could reliably be used for large scale flow reactions. From work carried out within the group using homogeneous bifunctional iminophosphoranes it was known that the *tert*-butyl substituted catalyst **56** gave a shorter reaction time for the conjugate addition of pyrrolidinone **34** to nitrostyrene than benzhydryl-substituted catalyst **136**. Therefore we investigated this reaction under flow conditions using polystyrene-supported *tert*-butyl substituted catalyst **116**. As with catalyst **137**, we began our investigation by studying the effect of flow rate, this time starting at a reagent concentration of 0.2 M (Table 26). Gratifyingly, at 0.1 mL min^{-1} flow rate, full conversion was achieved, with identical d.r. and e.r. to those achieved in the batch reaction with catalyst **116** or **137**.

Next we investigated the effect of concentration on the conversion, e.r. and d.r. We assumed that the effect of decreasing concentration would be the same as it was with catalyst **137** so only increased concentrations of 0.5 and 1.0 M were tested. We also investigated the effect of increasing the flow to 0.2 mL min^{-1}; since quantitative conversion was obtained at 0.1 mL min^{-1} we hoped that the conversion at 0.2 mL min^{-1} would also be high (Table 27). Unfortunately, it was not possible to increase the flow rate without a concomitant decrease in conversion. However, increasing the concentration even up to 1 M did not significantly affect the conversion (or e.r and d.r.).

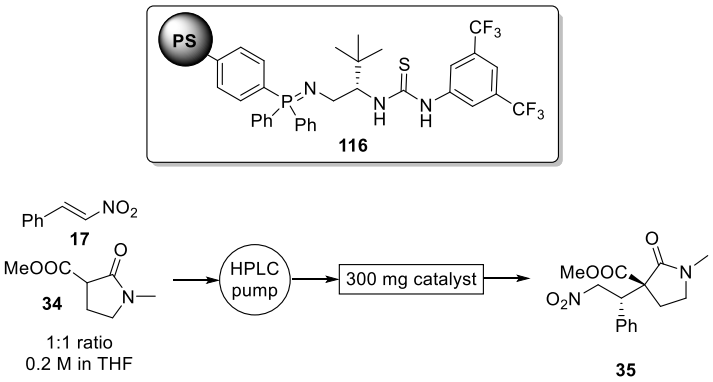

Flow (mL min^{-1})	Residence time (min)	Conversion (%)[a]	d.r.[a]	e.r. (maj.)[b]	e.r. (min.)[b]
1.0	2.7	55	79:21	n.d.	n.d.
0.5	5.4	79	79:21	n.d.	n.d.
0.1	27	99	79:21	89:11	70:30

Table 26. *Effect of flow rate on the conjugate addition of **34** to nitrostyrene in flow. [a] Determined by ^{1}H-NMR analysis of the crude reaction mixture. [b] Determined by HPLC analysis on a chiral stationary phase.*

Conc. [M]	Flow rate (mL min^{-1})	Conversion (%)[a]	d.r.[a]	e.r. (maj.)[b]	e.r. (min.)[b]
0.5	0.1	97	79:21	89:11	70:30
	0.2	87	78:22	n.d.	n.d.
1.0	0.1	95	78:22	89:11	71:29
	0.2	69	78:22	n.d.	n.d.

Table 27. *Effect of concentration and flow rate on the conjugate addition of **34** to nitrostyrene in flow. [a] Determined by ^{1}H-NMR analysis of the crude reaction mixture. [b] Determined by HPLC analysis on a chiral stationary phase.*

With conditions established for the successful conjugate addition of pyrrolidinone **34** to nitrostyrene under flow conditions, we attempted a large scale flow reaction to intensively test the performance of our immobilised catalytic system. We selected a concentration of 0.5 M for this reaction, as well as using freshly prepared catalyst, to ensure that conversion was as high as possible while maintaining a reasonable reaction time.

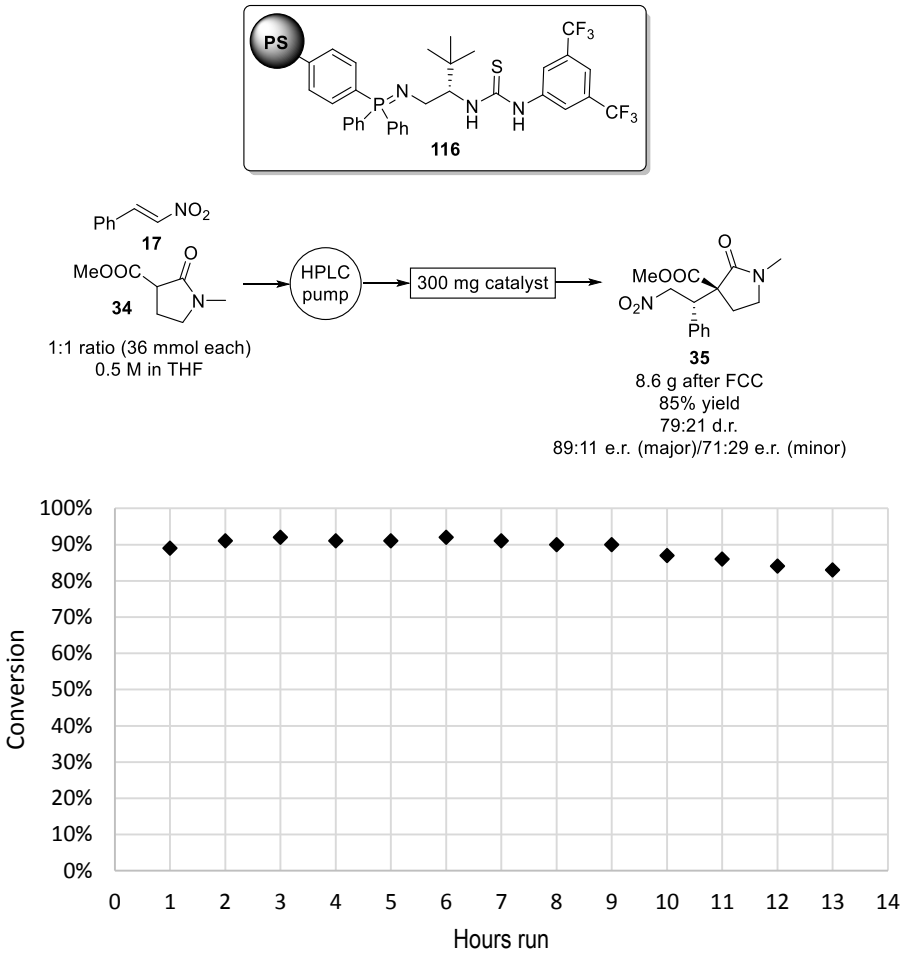

Figure 34. *Conversion vs. hours run in the large scale conjugate addition of **34** to nitrostyrene in flow. Conversion determined by ^{1}H-NMR analysis of the crude reaction mixture (separate fractions collected for each hour).*

The reaction was run continuously for 13 h at which point it was stopped as the reagent reservoir was almost depleted. ^{1}H-NMR analysis of the crude reaction mixture collected each hour showed that the conversion remained above 90% for 9 hours, then began to gradually decrease (Figure 34). Specifically, the conversion ranged from a maximum of 92%, decreasing to 83% at the end of the experiment, with an average of 89%. The d.r. remained constant at 79:21 throughout the experiment. The crude product from the entire experiment was combined and purified by flash column chromatography over silica to give 8.6 g of pure **35** in 85% yield, 79:21 d.r. and 89:11 e.r. for the major diastereomer and 71:29 e.r. for the minor diastereomer. The effective catalyst loading for this reaction was 0.8 mol% and the TON was 93. The productivity of the reactor was calculated to be 7.14 $mmol_{product}\ h^{-1}\ mmol_{catalyst}^{-1}$ (or 7.20 $mmol_{product}\ h^{-1}\ g_{catalyst}^{-1}$).

3. Conclusion

Starting from the bifunctional iminophosphorane organocatalysts discovered in the Dixon group,[60] we have developed polystyrene-supported variants. These catalysts can be easily prepared on a gram scale and have been characterised using gel phase ^{31}P-NMR spectroscopy. Their performance in several challenging asymmetric organocatalytic reactions has been tested and it was found that they typically retain excellent reactivity and stereoselectivity relative to the corresponding homogeneous catalyst. We then successfully demonstrated some of the unique advantages of catalyst immobilisation using our polystyrene-supported bifunctional iminophosphorane organocatalysts – namely straightforward catalyst separation, catalyst recycling and application in flow chemistry.

In terms of future applications we aim to further expand the scope of reactions that can be catalysed by polystyrene-supported bifunctional iminophosphorane organocatalysts. More thorough and extensive screening of different catalyst scaffolds and phosphines would also be desirable. With the discovery of appropriate reactions, this would also allow us to further expand the use of our immobilised catalysts in flow chemistry. It would also be interesting to further develop and study the solid-support and immobilisation itself. It is possible that immobilisation on silica is may be successfully demonstrated with further study and that such a material would have useful properties. Other means of immobilisation are also open to further investigation, such as immobilisation *via* the thiourea motif. Further investigations into the structure of the immobilised bifunctional iminophosphorane organocatalysts would also be worthwhile, specifically with a view to discovering any intermolecular interactions. One proposed experiment would be to investigate the effect of catalyst loading on gel phase ^{31}P-NMR spectra of the immobilised catalyst.

4. References

(1) Cozzi, F. *Adv. Synth. Catal.* **2006**, *348*, 1367–1390.
(2) Kristensen, T. E.; Hansen, T. *Eur. J. Org. Chem.* **2010**, *2010*, 3179–3204.
(3) Benaglia, M.; Puglisi, A.; Cozzi, F. *Chem. Rev.* **2003**, *103*, 3401–3430.
(4) Fan, Q.-H.; Li, Y.-M.; Chan, A. S. C. *Chem. Rev.* **2002**, *102*, 3385–3466.
(5) Czarnik, A. W. *Biotechnol. Bioeng.* **1998**, *61*, 77–79.
(6) Vaino, A. R.; Janda, K. D. *J. Comb. Chem.* **2000**, *2*, 579–596.
(7) Tomoi, M.; Ford, W. T. *J. Am. Chem. Soc.* **1981**, *103*, 3821–3828.
(8) Live, D.; Kent, S. B. H. In *Elastomers and Rubber Elasticity*; ACS Symposium Series; American Chemical Society, 1982; Vol. 193, pp. 27–501.
(9) Sarin, V. K.; Kent, S. B. H.; Mitchell, A. R.; Merrifield, R. B. *J. Am. Chem. Soc.* **1984**, *106*, 7845–7850.
(10) Li, W.; Yan, B. *J. Org. Chem.* **1998**, *63*, 4092–4097.
(11) Song, C. E.; Lee, S. *Chem. Rev.* **2002**, *102*, 3495–3524.
(12) Price, P. M.; Clark, J. H.; Macquarrie, D. J. *J. Chem. Soc. Dalt. Trans.* **2000**, 101–110.
(13) Brunel, D.; Blanc, A. C.; Galarneau, A.; Fajula, F. *Catal. Today* **2002**, *73*, 139–152.
(14) Corma, A.; Garcia, H. *Adv. Synth. Catal.* **2006**, *348*, 1391–1412.
(15) Jinno, K. In *Encyclopedia of Chromatography, Third Edition (Print Version)*; CRC Press, 2009.
(16) Song, C. E.; Park, Y. S. In *Advances in Organic Synthesis (Volume 1)*; Atta-ur-Rahman, P.; K. Laali, K., Eds.; Bentham Science Publishers, 2012; pp. 233–260.
(17) Pugin, B. *J. Mol. Catal. A Chem.* **1996**, *107*, 273–279.
(18) Shyu, S.-G.; Cheng, S.-W.; Tzou, D.-L. *Chem. Commun.* **1999**, 2337–2338.
(19) Tárkányi, G.; Király, P.; Varga, S.; Vakulya, B.; Soós, T. *Chem. – Eur. J.* **2008**, *14*, 6078–6086.
(20) Rho, H. S.; Oh, S. H.; Lee, J. W.; Lee, J. Y.; Chin, J.; Song, C. E. *Chem. Commun. (Camb).* **2008**, 1208–1210.
(21) Gleeson, O.; Davies, G.-L.; Peschiulli, A.; Tekoriute, R.; Gun'ko, Y. K.; Connon, S. J. *Org. Biomol. Chem.* **2011**, *9*, 7929–7940.
(22) Fredriksen, K. A.; Kristensen, T. E.; Hansen, T. *Beilstein J. Org. Chem.* **2012**, *8*, 1126–1133.
(23) Fan, X.; Rodríguez-Escrich, C.; Sayalero, S.; Pericàs, M. A. *Chem. – Eur. J.* **2013**, *19*, 10814–10817.
(24) Raynor, S. A.; Thomas, J. M.; Raja, R.; Johnson, B. F. G.; Bell, R. G.; Mantle, M. D. *Chem. Commun.* **2000**, 1925–1926.
(25) Gbery, G.; Zsigmond, A.; Balkus Jr., K. *Catal. Letters* **2001**, *74*, 77–80.
(26) Zhao, L.; Li, Y.; Yu, P.; Han, X.; He, J. *ACS Catal.* **2012**, *2*, 1118–1126.
(27) Merrifield, R. B. *J. Am. Chem. Soc.* **1963**, *85*, 2149–2154.
(28) Manecke, G.; Storck, W. *Angew. Chem., Int. Ed. English* **1978**, *17*, 657–670.
(29) Yamashita, T.; Yasueda, H.; Nakamura, N. *Chem. Lett.* **1974**, *3*, 585–588.
(30) Kondo, K.; Yamano, T.; Takemoto, K. *Die Makromol. Chemie* **1985**, *186*, 1781–1785.
(31) Dalko, P. I. (Ed. . *Comprehensive Enantioselective Organocatalysis: Catalysts, Reactions, and Applications*; Dalko, P. I., Ed.; Wiley-VCH, 2013.
(32) Font, D.; Jimeno, C.; Pericàs, M. A. *Org. Lett.* **2006**, *8*, 4653–4655.
(33) Aratake, S.; Itoh, T.; Okano, T.; Nagae, N.; Sumiya, T.; Shoji, M.; Hayashi, Y. *Chem. – Eur. J.* **2007**, *13*, 10246–10256.
(34) Font, D.; Sayalero, S.; Bastero, A.; Jimeno, C.; Pericàs, M. A. *Org. Lett.* **2008**, *10*, 337–340.
(35) Ayats, C.; Henseler, A. H.; Pericàs, M. A. *ChemSusChem* **2012**, *5*, 320–325.
(36) Calderón, F.; Fernández, R.; Sánchez, F.; Fernández-Mayoralas, A. *Adv. Synth. Catal.* **2005**, *347*, 1395–1403.
(37) Gruttadauria, M.; Giacalone, F.; Mossuto Marculescu, A.; Lo Meo, P.; Riela, S.; Noto, R. *Eur. J. Org. Chem.* **2007**, *2007*, 4688–4698.

(38) Gruttadauria, M.; Giacalone, F.; Marculescu, A. M.; Noto, R. *Adv. Synth. Catal.* **2008**, *350*, 1397–1405.
(39) Gruttadauria, M.; Salvo, A. M. P.; Giacalone, F.; Agrigento, P.; Noto, R. *Eur. J. Org. Chem.* **2009**, *2009*, 5437–5444.
(40) Dondoni, A. *Angew. Chem., Int. Ed. Engl.* **2008**, *47*, 8995–8997.
(41) Giacalone, F.; Gruttadauria, M.; Agrigento, P.; Campisciano, V.; Noto, R. *Catal. Commun.* **2011**, *16*, 75–80.
(42) Tiecco, M.; Carlone, A.; Sternativo, S.; Marini, F.; Bartoli, G.; Melchiorre, P. *Angew. Chem., Int. Ed. Engl.* **2007**, *46*, 6882–6885.
(43) Riente, P.; Yadav, J.; Pericàs, M. A. *Org. Lett.* **2012**, *14*, 3668–3671.
(44) Paras, N. A.; MacMillan, D. W. C. *J. Am. Chem. Soc.* **2001**, *123*, 4370–4371.
(45) Chiroli, V.; Benaglia, M.; Cozzi, F.; Puglisi, A.; Annunziata, R.; Celentano, G. *Org. Lett.* **2013**, *15*, 3590–3593.
(46) Hafez, A. M.; Taggi, A. E.; Dudding, T.; Lectka, T. *J. Am. Chem. Soc.* **2001**, *123*, 10853–10859.
(47) Taggi, A. E.; Hafez, A. M.; Wack, H.; Young, B.; Drury, W. J.; Lectka, T. *J. Am. Chem. Soc.* **2000**, *122*, 7831–7832.
(48) Kardos, G.; Soós, T. *Eur. J. Org. Chem.* **2013**, *2013*, 4490–4494.
(49) Malerich, J. P.; Hagihara, K.; Rawal, V. H. *J. Am. Chem. Soc.* **2008**, *130*, 14416–14417.
(50) Youk, S. H.; Oh, S. H.; Rho, H. S.; Lee, J. E.; Lee, J. W.; Song, C. E. *Chem. Commun.* **2009**, 2220–2222.
(51) Oh, S. H.; Rho, H. S.; Lee, J. W.; Lee, J. E.; Youk, S. H.; Chin, J.; Song, C. E. *Angew. Chem., Int. Ed.* **2008**, *47*, 7872–7875.
(52) Lee, J.-W.; Mayer-Gall, T.; Opwis, K.; Song, C. E.; Gutmann, J. S.; List, B. *Science* **2013**, *341*, 1225–1229.
(53) MacLellan, P. *Nat. Chem.* **2013**, *5*, 896–897.
(54) Sigman, M. S.; Jacobsen, E. N. *J. Am. Chem. Soc.* **1998**, *120*, 4901–4902.
(55) Sigman, M. S.; Vachal, P.; Jacobsen, E. N. *Angew. Chem., Int. Ed.* **2000**, *39*, 1279–1281.
(56) Miyabe, H.; Tuchida, S.; Yamauchi, M.; Takemoto, Y. *Synthesis (Stuttg).* **2006**, *2006*, 3295–3300.
(57) Schwesinger, R. In *Encyclopedia of Reagents for Organic Synthesis*; John Wiley & Sons, Ltd, 2001.
(58) Wannaporn, D.; Ishikawa, T. *Mol. Divers.* **2005**, *9*, 321–331.
(59) Ishikawa, T.; Heima, T.; Yoshida, M.; Kumamoto, T. *Helv. Chim. Acta* **2014**, *97*, 307–314.
(60) Núñez, M. G.; Farley, A. J. M.; Dixon, D. J. *J. Am. Chem. Soc.* **2013**, *135*, 16348–16351.
(61) Pelletier, J. C. In *Encyclopedia of Reagents for Organic Synthesis*; John Wiley & Sons, Ltd, 2001.
(62) Thomas, G. L.; Ladlow, M.; Spring, D. R. *Org. Biomol. Chem.* **2004**, *2*, 1679–1681.
(63) Kitagawa, K.; Inoue, A.; Shinokubo, H.; Oshima, K. *Angew. Chem., Int. Ed.* **2000**, *39*, 2481–2483.
(64) Akelah, A. *Br. Polym. J.* **1981**, *13*, 107–110.
(65) Johnson, C. R.; Zhang, B. *Tetrahedron Lett.* **1995**, *36*, 9253–9256.
(66) Bardella, F.; Eritja, R.; Pedroso, E.; Giralt, E. *Bioorg. Med. Chem. Lett.* **1993**, *3*, 2793–2796.
(67) *Unpublished results*.
(68) *Personal communication Prof. Tim Claridge*.
(69) Henry, L. *Bull. Acad. R. Belg.* **1896**, *32*, 33.
(70) Adams, H.; Anderson, J. C.; Peace, S.; Pennell, A. M. K. *J. Org. Chem.* **1998**, *63*, 9932–9934.
(71) Noble, A.; Anderson, J. C. *Chem. Rev.* **2013**, *113*, 2887–2939.
(72) Pahadi, N. K.; Ube, H.; Terada, M. *Tetrahedron Lett.* **2007**, *48*, 8700–8703.
(73) Hu, K.; Wang, C.; Ma, X.; Wang, Y.; Zhou, Z.; Tang, C. *Tetrahedron: Asymmetry* **2009**, *20*, 2178–2184.
(74) Wang, L.; Tan, C.; Liu, X.; Feng, X. *Synlett* **2008**.
(75) Tan, C.; Liu, X.; Wang, L.; Wang, J.; Feng, X. *Org. Lett.* **2008**, *10*, 5305–5308.

(76) Xie, H.; Zhang, Y.; Zhang, S.; Chen, X.; Wang, W. *Angew. Chem., Int. Ed. Engl.* **2011**, *50*, 11773–11776.
(77) Li, H.; Wang, Y.; Tang, L.; Deng, L. *J. Am. Chem. Soc.* **2004**, *126*, 9906–9907.
(78) Ye, J.; Dixon, D. J.; Hynes, P. S. *Chem. Commun.* **2005**, 4481–4483.
(79) Okino, T.; Hoashi, Y.; Takemoto, Y. *J. Am. Chem. Soc.* **2003**, *125*, 12672–12673.
(80) Song, J.; Wang, Y.; Deng, L. *J. Am. Chem. Soc.* **2006**, *128*, 6048–6049.
(81) McCooey, S. H.; Connon, S. J. *Angew. Chem., Int. Ed.* **2005**, *44*, 6367–6370.
(82) Andrés, J. M.; Manzano, R.; Pedrosa, R. *Chemistry* **2008**, *14*, 5116–5119.
(83) Bordwell, F. G. *Acc. Chem. Res.* **1988**, *21*, 456–463.
(84) Jakubec, P.; Cockfield, D. M.; Helliwell, M.; Raftery, J.; Dixon, D. J. *Beilstein J. Org. Chem.* **2012**, *8*, 567–578.
(85) Raimondi, W.; Lettieri, G.; Dulcere, J.-P.; Bonne, D.; Rodriguez, J. *Chem. Commun.* **2010**, *46*, 7247–7249.
(86) Kamimura, A.; Takeuchi, R.; Ikeda, K.; Moriyama, T.; Sumimoto, M. *J. Org. Chem.* **2012**, *77*, 2236–2245.
(87) Comer, E.; Rohan, E.; Deng, L.; Porco, J. A. *Org. Lett.* **2007**, *9*, 2123–2126.
(88) Wang, Y.; Luo, Y.-C.; Zhang, H.-B.; Xu, P.-F. *Org. Biomol. Chem.* **2012**, *10*, 8211–8215.
(89) Terada, M.; Ube, H.; Yaguchi, Y. *J. Am. Chem. Soc.* **2006**, *128*, 1454–1455.
(90) Sanchez Duque, M. del M.; Baslé, O.; Isambert, N.; Gaudel-Siri, A.; Génisson, Y.; Plaquevent, J.-C.; Rodriguez, J.; Constantieux, T. *Org. Lett.* **2011**, *13*, 3296–3299.
(91) Raimondi, W.; Sanchez Duque, M.; Goudedranche, S.; Quintard, A.; Constantieux, T.; Bugaut, X.; Bonne, D.; Rodriguez, J. *Synthesis (Stuttg).* **2013**, *45*, 1659–1666.
(92) Mailhol, D.; Duque, M. del M. S.; Raimondi, W.; Bonne, D.; Constantieux, T.; Coquerel, Y.; Rodriguez, J. *Adv. Synth. Catal.* **2012**, *354*, 3523–3532.
(93) Du, H.; Rodriguez, J.; Bugaut, X.; Constantieux, T. *Chem. – Eur. J.* **2014**, *20*, 8458–8466.
(94) Liu, Q.; Rovis, T. *Org. Lett.* **2009**, *11*, 2856–2859.
(95) Sung, K.; Wu, S.-Y. *Synth. Commun.* **2001**, *31*, 3069–3074.
(96) Ibrahim, A. A.; Nalla, D.; Van Raaphorst, M.; Kerrigan, N. J. *J. Am. Chem. Soc.* **2012**, *134*, 2942–2945.
(97) Mahulikar, P. P.; Mane, R. B. *Synth. Commun.* **2005**, *35*, 2139–2141.
(98) Sato, M.; Ogasawara, H.; Komatsu, S.; Kato, T. *Chem. Pharm. Bull.* **1984**, *32*, 3848–3856.
(99) Hamza, A.; Schubert, G.; Soós, T.; Pápai, I. *J. Am. Chem. Soc.* **2006**, *128*, 13151–13160.
(100) Jakubec, P.; Cockfield, D. M.; Hynes, P. S.; Cleator, E.; Dixon, D. J. *Tetrahedron: Asymmetry* **2011**, *22*, 1147–1155.
(101) Jakubec, P.; Helliwell, M.; Dixon, D. J. *Org. Lett.* **2008**, *10*, 4267–4270.
(102) Kyle, A. F.; Jakubec, P.; Cockfield, D. M.; Cleator, E.; Skidmore, J.; Dixon, D. J. *Chem. Commun.* **2011**, *47*, 10037–10039.
(103) Vakulya, B.; Varga, S.; Csámpai, A.; Soós, T. *Org. Lett.* **2005**, *7*, 1967–1969.
(104) Ahamed, M.; Thirukkumaran, T.; Leung, W. Y.; Jensen, P.; Schroers, J.; Todd, M. H. *Eur. J. Org. Chem.* **2010**, *2010*, 5980–5988.

Chapter 3: Organocatalytic Ring-Opening Polymerisation

1. Introduction

Ring-opening polymerisation (ROP) is a broad and varied field encompassing the reaction of chemically diverse monomers such as alkanes, alkenes, ethers, esters, sulfides, amides, phosphates and siloxanes *via* a range of anionic, cationic, radical and metathesis-based mechanisms.[1] The focus of this introduction will be organocatalytic ROP and in particular, the organocatalytic ROP of cyclic esters.

1.1 Basic concepts

It is helpful for the reader not familiar with polymer chemistry to first explain the basic process of ROP and define some of the terms used to describe and characterise polymers. ROP consists of two stages; initiation and propagation (Figure 35). In the initiation stage an initiator (**I**), which may for instance be a nucleophile such as an alkoxide that is added in a small amount to a cyclic ester, opens a molecule of monomer. This creates an active centre (**Y***), which is a reactive moiety capable of opening the next molecule of monomer thus elongating the polymer chain (propagation). A polymer chain which carries an active centre can be called a propagating, or active, chain. The process of propagation can become disrupted by unwanted events such as termination, where the active centre is intercepted by some agent which inactivates it – for example if the active centre is an alkoxide it might become protonated by some adventitious moisture. Or the active centre might react with the backbone of a polymer chain (either the one that carries it or a separate chain) and form a macrocycle or cause branching. This is referred to as chain transfer.

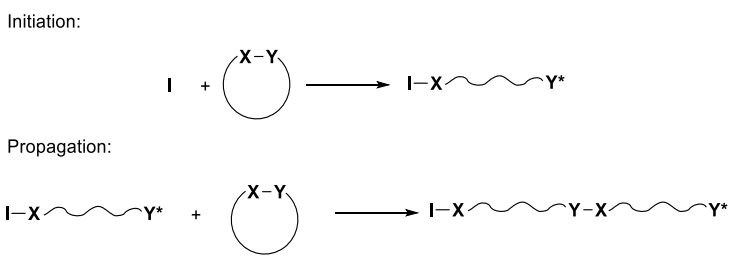

Figure 35. *Schematic for the initiation and propagation steps of ROP, where **I** represents an initiator molecule while **X** and **Y** are components of any functional group.*

As polymerisation is never entirely uniform and a polymer is an ensemble of many macromolecules, each possessing a different degree of polymerisation (consisting of a different number of monomer units, abbreviated as DP), its molecular mass must be considered in terms of a distribution. The three properties which are commonly used to characterise this distribution are the number average molar mass (M_n) and mass average molar mass (M_w), both of which are stated in g mol^{-1}, and the polydispersity index (PDI or simply "dispersity") which is unitless. The number average molar mass and mass average molar mass are defined by the following equations, where M_i is the mass of polymer molecules of size i and N_i is the number of polymer molecules of size i.

$$M_n = \frac{\sum M_i N_i}{\sum N_i} \qquad M_w = \frac{\sum M_i^2 N_i}{\sum M_i N_i}$$

The number average molar mass gives the molar mass of a polymer chain of the average size in the sample whereas the mass average molar mass gives the average molar mass as calculated from the weight fractions in the sample. Typically, the value of M_n is given when discussing the "molar mass" or "molecular weight" of a polymer.

Another important characteristic of a distribution is its broadness i.e. whether all the polymer chains in a particular sample are of very similar lengths and molecular masses or whether their masses are highly varied. This quality is described by the PDI, which is defined as the ratio of the mass average molar mass (M_w) to the number average molecular mass (M_n). A sample which consists of perfectly uniform polymer chains will have a PDI equal to 1. The value of the PDI is dependent on the mechanism of polymerisation, with the values for ROP typically ranging between 1 – 2, depending on the reaction conditions.[1]

The characterisation of the molecular mass distribution of a polymer is most commonly performed by gel permeation chromatography (GPC). This is a size exclusion chromatography technique wherein a volume of the polymer to be analysed is dissolved in an eluent and passed through a column packed with a porous gel. Smaller polymer chains can enter the pores of the gel and are eluted more slowly, whereas larger polymers elute more quickly. By measuring the elution time, the GPC thereby measures the intrinsic viscosity of the polymer. The instrument is calibrated with a series of

polystyrene standards of known molar mass to form a calibration curve from which the molar masses of other polymers can be calculated. This is done by applying the Mark-Houwink equation, which relates the intrinsic viscosity of a polymer to its molecular mass (shown below, where η is the intrinsic viscosity, M is the molecular mass and K and α are experimentally determined variables termed the Mark-Houwink parameters). The molar mass determined for each polymer fraction is then used to calculate the M_n, M_w and PDI for that sample.

$$[\eta] = KM^{\alpha}$$

The Mark-Houwink parameters K and α have been experimentally measured for many polymers, for instance for poly(lactide) or poly(caprolactone), however the parameters for some less common polymers such as poly(valerolactone) have not been determined. Also, the Mark-Houwink parameters for co-polymers are not typically known, making the determination of their molecular masses approximate. However, it is always true that the earlier a fraction elutes, the greater its molecular mass, making comparisons between samples possible.

MALDI-ToF spectrometry is also very useful in characterising polymers. MALDI is a soft ionisation technique which allows for the mass of entire polymer chains to be determined. MALDI spectra can directly show the molecular mass distribution, allowing for the calculation of M_n and M_w however it is more common to obtain these values from GPC. Analysing the mass of polymer chains observed by MALDI allows for the determination of the end-group fidelity – i.e. confirming whether each chain contains a molecule of the initiator on one end and the expected terminating agent on the other end.

1.2 Thermodynamic and kinetic aspects of ROP

For the majority of cyclic monomers, the change in enthalpy of polymerisation (ΔH_p) and the change in entropy of polymerisation (ΔS_p) are both negative (Table 28). Polymerisation is typically accompanied by a loss in the translational degrees of freedom of the monomer, thus the contribution of ΔH_p to the Gibb's free energy of the polymerisation (ΔG_p) becomes the deciding factor in the polymerisability of a monomer at a given temperature. The main contributor to ΔH_p is the release of

ring strain upon monomer opening, thus this is the main driving force for the polymerisation of cyclic monomers. In cyclic esters, the ring strain is mainly due to the presence of planar sp^2 carbons in the ring.

Monomer	ΔH_p^0 (kJ mol^{-1})	ΔS_p^0 (J mol^{-1} K^{-1})
cyclohexane	2.9	−10.5
L-lactide	−22.9	−41.1
δ-valerolactone	−27.4	−65
ε-caprolactone	−28.8	−53.9

Table 28. *Representative enthalpies and entropies of polymerisation for selected cyclic monomers.*[1]

The process of polymerisation of a monomer consists of several discrete reactions between the monomer and the initiator, propagating chains and the monomer or themselves and propagating chains and terminating agents. The main processes taking place in a polymerisation reaction can be expressed in the equations depicted in Table 29.

Event	Equation
Initiation of monomer *M* by initiating agent *I* and formation of an active center m^*	$I + M \overset{k_i}{\rightarrow} m^*$
Chain propagation/depropagation	$m_n m^* + M \overset{k_p/k_d}{\longleftrightarrow} m_{n+1} m^*$
Chain transfer, forming a new active center	$m_n m^* + M \overset{k_{tr}}{\rightarrow} m_n m + m^*$
Chain termination by terminating agent *X*	$m_n m^* + X \overset{k_t}{\rightarrow} m_n m X$

Table 29. *Reactions taking place during polymerisation, where m_n represents a polymer chain of length* n *monomers, while k_i, k_p, k_d, k_{tr} and k_t represent the rate constants of initiation, propagation, depropagation, chain transfer and termination, respectively.*

An important concept in ROP (and polymer chemistry in general) is that of a "living polymerisation". This is a polymerisation process in which chain termination or transfer events do not take place. Also, k_i is typically much greater than k_p resulting in a constant number of propagating chains which grow at a constant rate.[2] The consequences of this are that the products of a living polymerisation process have a very well controlled molecular weight that can be simply determined from the ratio of monomer to initiator ($[M]_0/[I]_0$) as well as very low polydispersity. Control over the molecular weight and dispersity of a polymer is advantageous since it influences the polymer's macroscopic properties. Also, the absence of termination events allows for easy end-capping by adding an end-capping agent

to the reaction once the monomer is consumed or for the formation of block co-polymers by adding a second monomer to the reaction mixture whose polymerisation will then be initiated by the existing active chains. For example, if there are 5 molecules of initiator for 100 molecules of monomer (an $[M]_0/[I]_0$ of 20) and the polymerisation is "living" then ideally, 5 propagating chains will form upon initiation and each will grow at a constant rate to a length of 20 monomer units at which point all the monomer will be consumed. If a further 100 molecules of monomer were to be added at this point, propagation would resume and chains with a degree of polymerisation of 40 would be formed. The PDI of this idealised polymer would be equal to 1.

Whether a polymerisation process is "living" can be determined by considering the plot of $ln\{([M]_0-[M]_{eq})/([M]-[M]_{eq})\}$ vs. time (or put more simply, if the equilibrium monomer concentration is negligible, the natural log of the inverse of the conversion vs. time) and the plot of M_n vs. monomer conversion. In the absence of any chain transfer or termination of events both of these plots should be linear, indicating that only propagation of a set number of active chains occurred during the polymerisation.

1.3 Discovery of organocatalytic ROP and development of bifunctional catalytic systems

Historically, the ring-opening polymerisation of cyclic esters has been most commonly undertaken using metal alkoxides, for example, the most common catalyst for the polymerisation of lactide is tin(II) octanoate.[1] However, despite the great achievements of metal-catalysed polymerisation,[3] there are some disadvantages to this approach. For certain applications, specifically medicine and electronics,[4,5] it is important to utilise materials that are entirely free of metal residues. This creates a demand for a metal-free method of preparing the required polymeric materials.

The discovery of organocatalytic ROP and the subsequent development of state-of-the-art catalytic systems for the polymerisation of cyclic esters can be attributed to the joint work of Hedrick and Weymouth in the early 2000's. Organocatalytic ROP was first demonstrated by Hedrick and co-workers who, motivated by the use of 4-(dimethylamino)pyridine (DMAP) as a transesterification

catalyst for poly(lactide),[6] investigated its use in the ROP of L-lactide (LA).[7] Good conversion and relatively low dispersity were achieved with superstoichiometric amounts of DMAP, but attempts at polymerisation with catalytic DMAP were met with limited success. Different alcohol initiators were tested, such as ethanol, benzyl alcohol and isopropanol, all of which were equally well-tolerated. It was postulated that this polymerisation proceeded through a monomer activation mechanism, in line with the typical reactivity of DMAP (Figure 36).

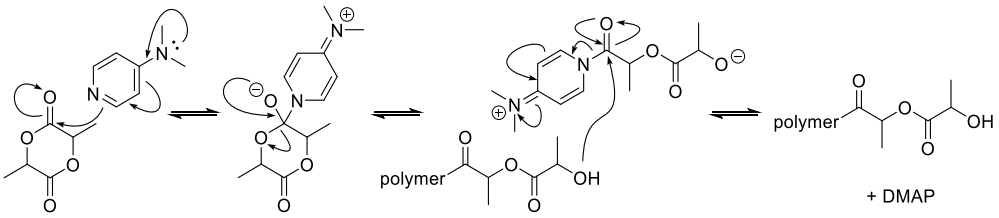

Figure 36. *Postulated mechanism for the polymerisation of lactide by DMAP.*

Hedrick, Weymouth and co-workers then turned their attention to bifunctional organocatalytic systems, consisting of an amine base combined with an H-bond donor. Citing the successes of the asymmetric organocatalysts developed by Jacobsen[8] and Takemoto[9] as their inspiration, they tested the use of Takemoto's catalyst (**14**) in the polymerisation of LA.[10] This catalyst performed very well, catalysing the formation of poly(LA) with high conversion, showing good agreement between theoretical and experimental molecular weight and exceptionally low dispersity. However, very long reaction times were required (48 h for the polymerisation of LA with $[M]_0/[I]_0$ of 100) and this catalyst is presumably unable to catalyse the polymerisation of less reactive monomers such as δ-valerolactone (VL) and ε-caprolactone (CL). This discovery led to the proposal of a new ROP mechanism, namely that of dual activation, (Figure 37) wherein the thiourea H-bond donor activates the monomer to nucleophilic attack and the tertiary amine base increases the nucleophilicity of the alcohol of the active chain (or initiator). Alternately it could be said that H-bonding with the thiourea stabilises the growing negative charge on the carbonyl oxygen in the transition state and the basic tertiary amine stabilises the growing positive charge on the alcohol in the transition state.

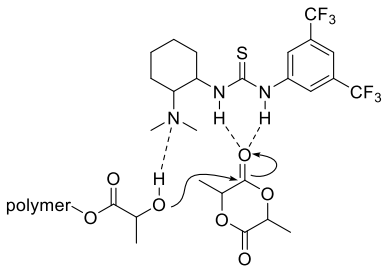

Figure 37. *Postulated dual activation mechanism of Takemoto's catalyst.*

Systematic studies on the nature of the basic and H-bond donor components of this catalyst led to the realisation that these two components do not need to be contained within a single molecule. At this point, a combination of sparteine and 1-[3,5-bis(trifluoromethyl)phenyl]-3-cyclohexylthiourea (**16**) was found to provide an improved catalytic system.[11] Further work identified amidine and guanidine bases in combination with thiourea **16** as successful ROP catalysts for cyclic esters.[12] In particular, 1,5,7-triazabicyclo-[4.4.0]dec-5-ene (TBD) is an interesting ROP catalyst. TBD is a very strong organic base with a pK_a of 26 in acetonitrile[13] that also has the potential for acting as a dual H-bond donor when protonated.[14] It is highly active in the ROP of cyclic esters with 0.1 mol% of TBD catalysing the polymerisation of LA with $[M]_0/[I]_0$ of 500 in 1 minute, obtaining a conversion of 95%, M_n of 62 600 g mol^{-1} and PDI of 1.11. It also successfully polymerises VL and CL in short reaction times, high conversion and with good control of the resulting molecular weight.[15] However, as TBD is so reactive it appears that some chain transfer events may occur during polymerisation and it is consequently not possible to achieve such low dispersity as with Takemoto's catalyst. Furthermore, TBD is very hygroscopic, which is particularly problematic for a moisture sensitive process such as ROP. Following NMR studies of acyl transfer reactions catalysed by TBD, a dual activation mechanism was proposed for the TBD-catalysed ROP of cyclic esters, shown here with VL (Figure 38). The highly nucleophilic TBD opens VL forming a tetrahedral intermediate, which collapses to give the alcohol, promoted by an interaction between the TBD N-H and the VL oxygen. This is the monomer activation step, which results in the formation of an amide bond between the monomer and TBD, which is presumably weakened relative to a typical amide bond by delocalisation over the other TBD nitrogens. Next, TBD acts as a base, promoting the attack of the terminal alcohol

of the growing polymer chain on the newly formed amide by (at least partially) deprotonating the alcohol. Once the transesterification is complete, the newly elongated polymer and TBD are released.

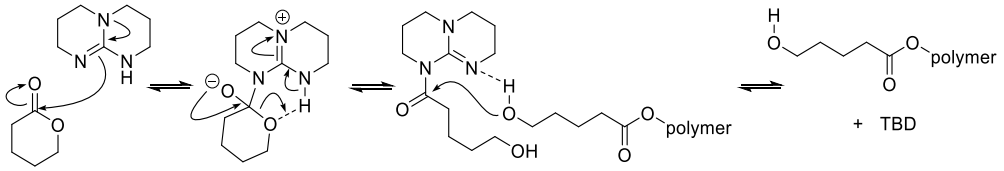

Figure 38. *Dual activation mechanism in the ROP of cyclic esters catalysed by TBD.*

If the *N*-methylated analogue of TBD, 7-methyl-1,5,7-triazabicyclo[4.4.0]dec-5-ene (MTBD) is used as a catalyst for the ROP of VL or CL, no conversion to polymer is observed unless thiourea **16** is added to the reaction mixture. This indicates the importance of the H-bonding interaction. In a similar fashion, DBU may also be used as a ROP catalyst in conjunction with thiourea **16**. In these cases, the dual activation mechanism described for Takemoto's catalyst (Figure 37) is presumed to apply. The combination of these guanidine and amidine bases with thiourea **16** represents the current state-of-the-art in the organocatalytic ROP of cyclic esters and is the most commonly used methodology (Table 30).

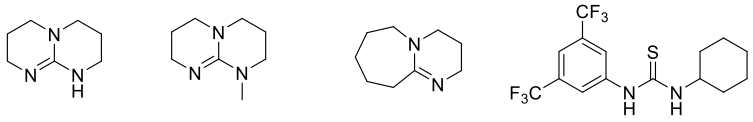

Catalyst	Monomer	Catalyst loading (%)	Time (h)	Conversion (%)	M_n (g mol^{-1})	PDI
TBD	LA	0.1	20 s	99	24 200	1.19
	VL	0.5	0.5	91	14 500	1.09
	CL	0.5	8	72	16 900	1.16
MTBD	LA	1	0.5	92	17 900	1.05
	VL	5 (+ **16**)	4	92	12 100	1.06
	CL	5 (+ **16**)	120	78	7 700	1.05
DBU	LA	1	1	99	21 000	1.05
	VL	5 (+ **16**)	4	95	8 300	1.05
	CL	5 (+ **16**)	120	78	8 100	1.04

Table 30. *Performance of amidines and guanidines (in conjunction with thiourea **16** additive, 5 mol% relative to monomer where indicated) in the ROP of cyclic esters, determined by Hedrick an co-workers.*[12] *For all entries, $[M]_0/[I]_0 = 100$.*

1.4 *N*-Heterocyclic carbene ROP catalysts

Another well studied class of organic ROP catalysts are *N*-heterocyclic carbenes (NHC). NHC's are highly basic and nucleophilic and have been used extensively as organocatalysts, perhaps most famously in the Stetter reaction.[16] After initial studies by Hedrick and Weymouth[17] and Nolan[18] demonstrating the use of NHC's as transesterification and acylation catalysts, the first example of NHC-catalysed living ROP was demonstrated by Hedrick and co-workers.[19] The ROP of LA, CL and *β*-butyrolactone catalysed by the NHC IMes (Figure 39) was shown to proceed in reasonable reaction times with good conversion and relatively low dispersity. For comparison with Table 30, the IMes-catalysed polymerisation of LA with $[M]_0/[I]_0$ of 100 reaches 92% conversion in 2 h and a PDI of 1.15 is obtained. This initial demonstration of NHC catalysis in ROP made use of isolated IMes; however, later studies by Hedrick and Weymouth used NHC's generated *in situ* by the deprotonation of the corresponding salt.[20] It was shown that imidazolium and imidazolinium-derived carbenes were more reactive ROP catalysts than thiazolium carbenes, however thiazolium-derived NHC's gave polymer products with lower dispersity. Also, it was found that less sterically bulky NHC's were more reactive ROP catalysts. NHC-catalysed ROP has been proposed to operate *via* a nucleophilic monomer activation mechanism (as shown in Figure 36 for DMAP) or *via* a H-bonding alcohol activation mechanism (Figure 39).

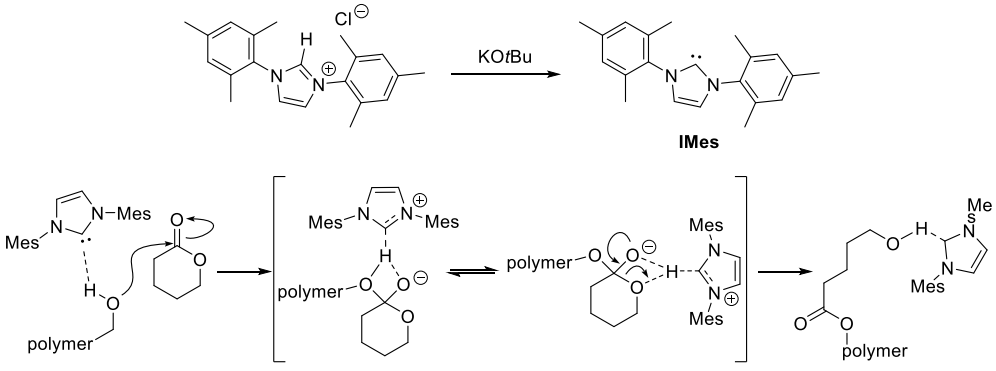

Figure 39. *Generation of IMes and H-bonding alcohol activation mechanism.*

An interesting development in NHC-catalysed ROP is the use of an imidazolium tetrafluoroborate ionic liquid as a catalyst precursor, enabling an interfacial biphasic polymerisation wherein the

polymer solution can be easily separated from the ionic liquid after polymerisation and the ionic liquid recycled for a subsequent polymerisation reaction.[20]

1.5 Phosphazene ROP catalysts

As strong organic bases, phosphazenes such as BEMP and Schwesinger's phosphazene bases[21] were also investigated for use as ROP catalysts. BEMP and P_1-*t*-Bu are capable of polymerising LA,[22] however their performance is inferior in terms of speed and conversion when compared to bifunctional systems (Table 31 vs. 30). VL can also be polymerised with BEMP or P_1-*t*-Bu, however attempts to polymerise CL resulted in very low conversion. P_2-*t*-Bu is significantly more active than P_1-*t*-Bu and is able to catalyse the rapid polymerisation of LA at low temperatures, leading to its application in the stereoselective ROP of LA (*vide infra*).[23] It is believed that phosphazene bases polymerise cyclic esters *via* an alcohol activation mechanism (Figure 39). Very recently, the use of BEMP in conjunction with thiourea **16** was reported in the ROP of cyclic esters.[24] This catalytic system in significantly more reactive than BEMP alone and allows for the well-controlled polymerisation of VL and CL in good reaction times.

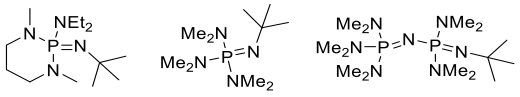

BEMP **P_1-*t*-Bu** **P_2-*t*-Bu**

Catalyst	Time (h)	Conversion (%)	M_n (g mol^{-1})	PDI
BEMP	23	76	13 100	1.08
P_1-*t*-Bu	70	82	16 000	1.06
P_2-*t*-Bu	0.4	84	13 000	1.08

Table 31. *Performance of phosphazene bases in the ROP of LA. All reactions at room temperature with 1 mol% catalyst loading and $[M]_0/[I]_0 = 100$.*

1.6 Choice of initiators

It should be noted that organocatalytic ROP is very tolerant of a variety of initiators, as long as they are suitably reactive. Alcohols are typically used as initiators (other nucleophiles such as amines and thiols are also acceptable)[11], however the non-participating structure of the initiator molecule does not appear to be very important, so long as it is inert to the reaction conditions. The most common initiators are benzyl alcohol and 1-pyrenebutanol, which is used due to its UV activity, so that its

incorporation into the polymer chain can be confirmed using a GPC equipped with a UV detector. The choice of initiator can be used to form interesting polymeric structures. For instance, the use of macroinitiators (macromolecules such as other polymers containing a suitable initiating moiety for example monohydroxyl-terminated PEG) can be used to form block co-polymers.[12] Alternatively, "dual headed" initiators can be used, for example, the initiator can contain an alcohol for initiating ROP in combination with an alkoxyamine for the initiation of nitroxide-mediated polymerisation (NMP) (Figure 40). Thus, at the conclusion of the ROP reaction, the resulting polymer can be used to initiate NMP and a di-block co-polymer will be formed. A similar approach has been demonstrated with ROP initiators containing dithioesters for initiating RAFT polymerisation.[11]

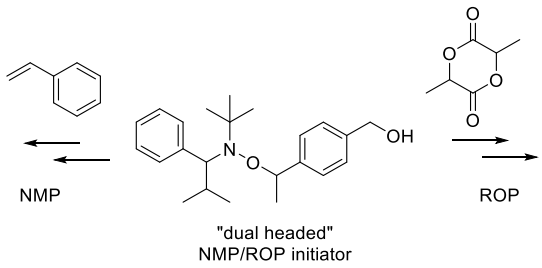

Figure 40. *A dual initiator for use in ROP and NMP.*

1.7 Stereocontrolled ROP of lactide

Thus far, we have discussed only the polymerisation of L-lactide, the stereochemical outcome of which is predetermined by the configuration of the monomer. However, lactide is also available in racemic (a 50:50 mixture of *R,R* and *S,S* lactide) and *meso* (*R,S* lactide) forms. When racemic lactide (*rac*-LA) is polymerised, the tacticity of the resulting polymer can be determined by the reaction conditions.

"Tacticity" refers to the relative configuration of adjacent stereocenters in the repeating units of a polymer. It is an important property, as it can affect the macroscopic properties of a polymer such as its crystallinity, melting point and solubility. Polymers may be isotactic, with all the stereocenters in the same relative configuration, syndiotactic, with the stereocenters in alternating configurations or atactic, with stereocenters in random relative configurations (Figure 41). Poly(L-lactide) is necessarily isotactic.

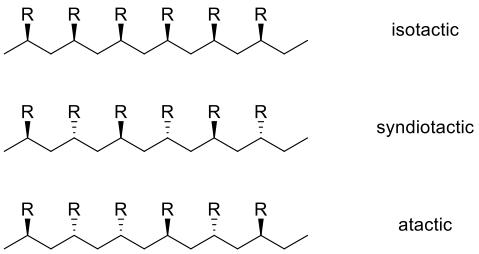

Figure 41. *Depictions of isotactic, syndiotactic and atactic polymers.*

Tacticity may also be defined for diads, triads, tetrads and so on; that is, the relative configuration of two, three or four adjacent stereocenters. Several conventions exist for the naming of these "*n*-ads"; in the present work we follow the nomenclature used in *J. of Polym. Sci. Part A: Polym. Sci*.(35) p. 1651 as this is the reference that we have followed for experimentally determining the tacticity of polymers of *rac*-LA prepared in this work. Diads are either isotactic or syndiotactic, while larger *n*-ads may be described as a series of adjacent diads, reading from left to right (Figure 42).

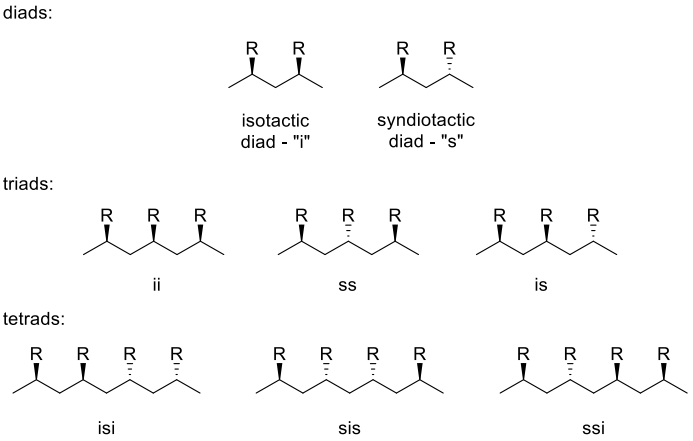

Figure 42. *Examples of the naming of diads, triads and tetrads of various configurations.*

The presence of variously configured tetrads can be observed in the ^{13}C-NMR and homodecoupled ^{1}H-NMR spectra of poly(*rac*-LA), and the chemical shifts of specific tetrads have been assigned.[25–27] When *rac*-LA is polymerised, depending on the stereocontrol imparted by the catalyst, there will be varying proportions of the different possible tetrads present in the polymer. For instance, polymerisation with a catalyst which imparts good, but not perfect, stereocontrol may result in the predominance of *iii* tetrads combined with small numbers of other possible combinations. The stereochemical composition of such a polymer is expressed by the parameter P_i, which represents the probability of finding an isotactic diad. This value may be calculated from the relative proportions

of the different tetrads present in the polymer (as observed by integration of the relevant tetrad signals in a homodecoupled ^{1}H-NMR spectrum) following literature procedures.[25] A P_i equal to 1 represents a completely isotactic polymer. One can conceive of two different approaches to preparing stereoregular poly(*rac*-LA); with a chiral catalyst it may be possible to perform a resolution, selectively polymerising one enantiomer of lactide, or with an achiral catalyst it may be possible to form a racemic, but uniformly isotactic polymer. This may take the form of a mixture of polymer chains where some chains contain all *R* stereocenters and some chains contain all *S* stereocenters, or of single chains consisting of long alternating series of isotactic *R* streocenters, followed by a series of *S* stereocenters (known as a "stereoblock" architecture).

A number of organocatalytic methods have been studied for the stereocontrolled ROP of lactide. The most successful catalysts for this process have been found to be sterically encumbered NHC's such as **147**[28] and the phosphazene base P$_2$-*t*-Bu[23] (Table 32). It is believed that the stereocontrol in these cases is due to "chain end control" wherein steric congestion at the active centre affects the orientation of the incoming monomer and results in an isotactic enhancement.

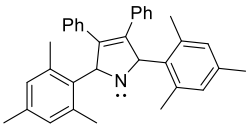

147

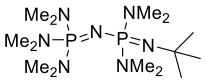

P$_2$-*t*-Bu

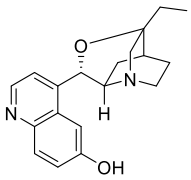

25

Catalyst	Temperature (°C)	Time (h)	Conversion (%)	PDI	P_i
147	−70	2	91	1.2	0.90
P$_2$-*t*-Bu	−75	3	99	1.1	0.95
25	rt	14	91	1.11	0.75

Table 32. *Stereocontrolled ROP of rac-lactide. For the top two entries $[M]_0/[I]_0 = 100$, for the third entry $[M]_0/[I]_0 = 10$ for added benzyl alcohol initiator.*

The kinetic resolution of *rac*-LA has also been demonstrated, using *β*-isocupreidine organocatalyst (**25**).[29] As this is a bifunctional tertiary amine catalysts of lower basicity than phosphazenes or NHC's, reaction times are relatively long. However, a P_i of up to 0.75 was attained and the catalyst was indeed selective for the polymerisation of the *S*,*S* enantiomer of lactide (L-lactide), with the e.e.

of remaining D-lactide reaching up to 71%. Although these results are modest, they do represent the first example of an organocatalytic kinetic resolution polymerisation reaction.

1.8 Conclusion

Organocatalytic ROP is now a well-developed alternative to the use of organometallic catalysts, offering comparative ease of operation for the well-controlled polymerisation of a wide range of monomers.[30] However, the perfect union of reactivity and control remains a goal to be pursued. Even with the most successful class of organocatalytic ROP systems, the bifunctional amidine-/guanidine-based systems, excellent reactivity often correlates with a less controlled polymerisation, and vice-versa. Also, although these organocatalysts are significantly easier to handle than the alternative organometallic species, polymerisations are nevertheless conducted in a glovebox, perhaps due to the highly hygroscopic nature of this class of compounds. This greatly limits the accessibility of ROP to many members of the general synthetic community, which is an obstacle to potential innovation. We hope to be able to contribute to this field through the development of an organic ROP catalyst that is both highly reactive and selective, while being easier to handle than its predecessors.

2. Results and Discussion

2.1 Aims

As bifunctional systems comprising a strong organic base in conjunction with a thiourea H-bond donor are known to be highly effective catalysts for the ROP of cyclic esters, we were inspired to investigate the use of bifunctional iminophosphorane organocatalysts in this reaction. The aims of this project were:

- To demonstrate proof of concept in the ROP of cyclic esters catalysed by bifunctional organic organocatalysts.
- To devise an achiral bifunctional iminophosphorane that could easily and rapidly be synthesised.
- Demonstrate the rapid and well-controlled polymerisation of LA, VL and CL and determine whether polymerisation could be reliably carried out without the use of a glovebox.
- Demonstrate the formation of block co-polymers through the use of macroinitiators and sequential monomer addition.
- Investigate whether bifunctional iminophosphoranes are effective catalysts for the stereocontrolled ROP of lactide.
- Investigate whether ROP catalysed by bifunctional iminophosphoranes may be considered a living polymerisation.
- Investigate the roles of the iminophosphorane and the thiourea components of the catalyst.

2.2 Proof of Concept

We first became aware of organocatalytic ROP through the 2005 publication of Hedrick and co-workers demonstrating the use of Takemoto's catalyst in the ROP of L-lactide (LA).[10] In our initial studies, we successfully duplicated the conditions described by Hedrick and co-workers using 5 mol% of catalyst **148** (Scheme 27).

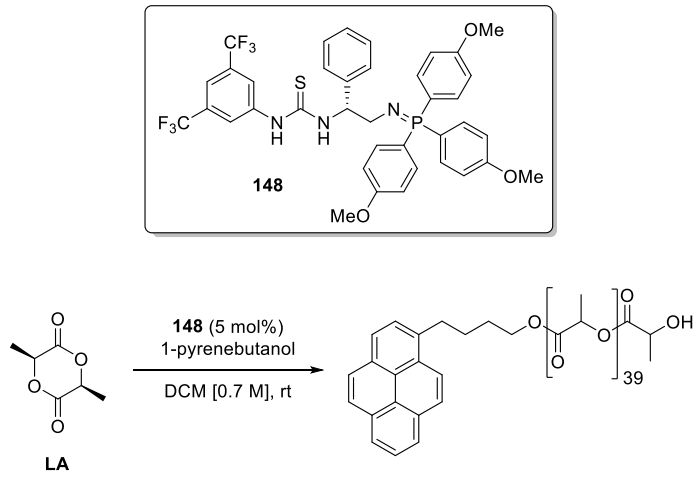

Scheme 27. *Proof of concept of ROP of LA using catalyst **148**.*

Performing the reaction with $[M]_0/[I]_0$ of 200, complete conversion was achieved in under 2 h. We were then able to analyse the resulting polymer by gel permeation chromatography (GPC), which indicated M_n of 12 300 g mol^{-1} and PDI of 1.08. The low PDI and high conversion within a relatively short reaction time encouraged us to further investigate the polymerisation of cyclic esters using bifunctional iminophosphorane organocatalysts.

It was extremely advantageous that our bifunctional iminophosphorane organocatalysts, unlike other systems used for organocatalytic ROP such as amidines and guanidines,[12] are not hygroscopic and could be weighed out in air. Organocatalytic ROP reactions are typically carried out in a glovebox as the presence of any moisture can lead to uncontrolled initiation or termination of polymerisation. As this facility was not available to us, it took considerable time to develop appropriate procedures for reagent and solvent purification and storage and reaction set up, despite the exceptional moisture stability of our catalyst. A major challenge in our studies of organocatalytic ROP was developing this technical capability.

2.3 Catalyst Synthesis

Although proof of concept was successfully demonstrated using catalyst **148**, it was not convenient to develop this methodology further using a chiral catalyst that required a multi-step synthesis from an amino acid precursor. Instead, we envisioned an achiral catalyst with a minimal carbon scaffold, which could be rapidly synthesised. We therefore sought to develop a route to azide **149**, which could then undergo a Staudinger reaction with an appropriate phosphine and form an achiral bifunctional

iminophosphorane organocatalyst. Several approaches were investigated which proved to be unsuccessful (Schemes 28 and 29).

We first attempted to synthesise **149** starting from 2-chloroethylamine. 2-Chloroethylamine hydrochloride was treated with triethylamine in the presence of 3,5-bis(trifluoromethyl)phenyl isothiocyanate in an attempt to convert the free amine to the thiourea, forming **150**. This resulted in the formation of 16% of an unidentified product as well as 50% of a product which was initially misidentified as the aziridine **151** due to the lack of analogous compounds in the literature. The procedure was optimised to increase the yield of the presumed aziridine **151** by basifying the 2-chloroethylamine hydrochloride prior to the addition of isothiocyanate, resulting in a 76% yield (Scheme 28). We planned to open aziridine **151** with a source of azide and thus form **149**, but at this point, the "aziridine" was correctly identified by NOESY and HMBC to in fact be compound **152**. This product may form either from **150** by the nucleophilic thiourea NH displacing the chloride, or perhaps by an intramolecular ring opening of aziridine **151**, leading to the formation of the less strained 5-membered ring.

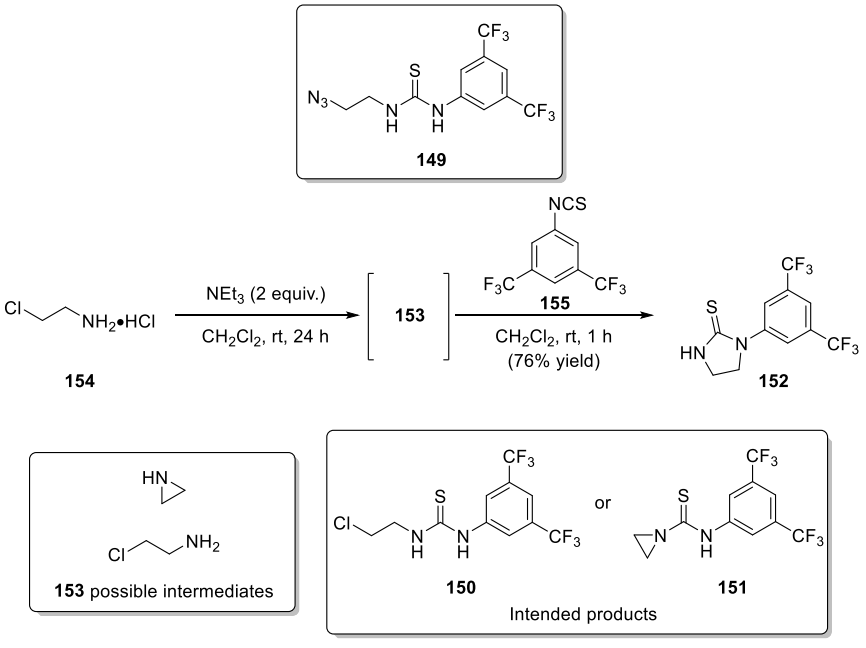

Scheme 28. *Failed route to **149** via 2-chloroethylamine.*

We next attempted to synthesise **149** by a diazo transfer reaction to amine **156** (Scheme 29). However, the diazo transfer step was low yielding, presumably due to the high nucleophilicity of the thiourea, and the proposed route was relatively long.

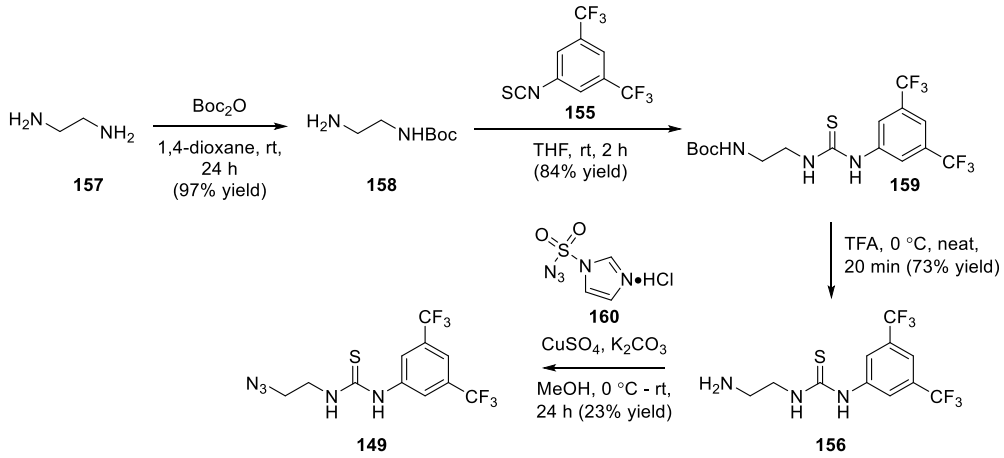

Scheme 29. *Failed route to **149** via diazo transfer.*

Finally we arrived at a successful route (Scheme 30), forming aminoazide **161** from 2-bromoethylamine hydrobromide following literature procedures,[31] and reacting it directly with 3,5-bis(trifluoromethyl)phenyl isothiocyanate to form **149** in a two-step procedure. Initial yields were low due to the unforeseen high aqueous solubility of **161**, but with thorough extraction yields of up to 60% over two steps could be achieved. Thiourea **149** was then reacted with tris(4-methoxy)phenylphosphine to form the achiral catalyst **162** in 88% yield.

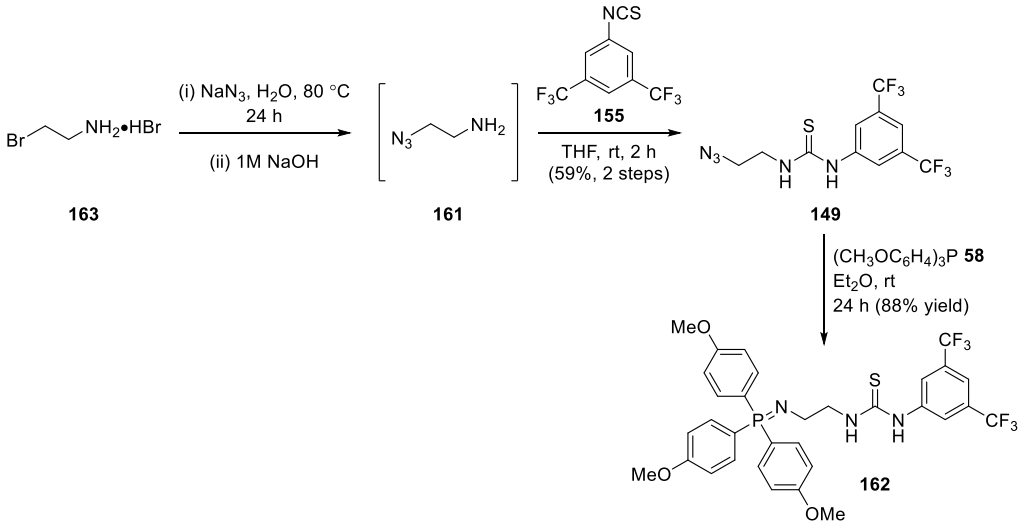

Scheme 30. *Synthesis of achiral catalyst **162**.*

A racemic version of phenylglycine-derived catalyst **148-*rac*** was also prepared, following modified literature procedures (Scheme 31).[32] The formation of the iminophosphorane was initially performed in diethyl ether at room temperature, however this repeatedly resulted in the formation of a 1:2 – 2:1 mixture of the phosphazide **164** (as indicated by mass spectrometry and ^{31}P-NMR) and the iminophosphorane. Heating the reaction mixture at 40 °C or performing the reaction in THF resulted in complete conversion to the iminophosphorane **148-*rac***. The preparation and isolation of phosphazides stabilised by hydrogen bonding (e.g. to amides) has previously been reported[33,34] and we suspect that hydrogen bonding between the azide nitrogen lone pair and one of the thiourea N-H groups may have stabilised the phosphazide in this case.

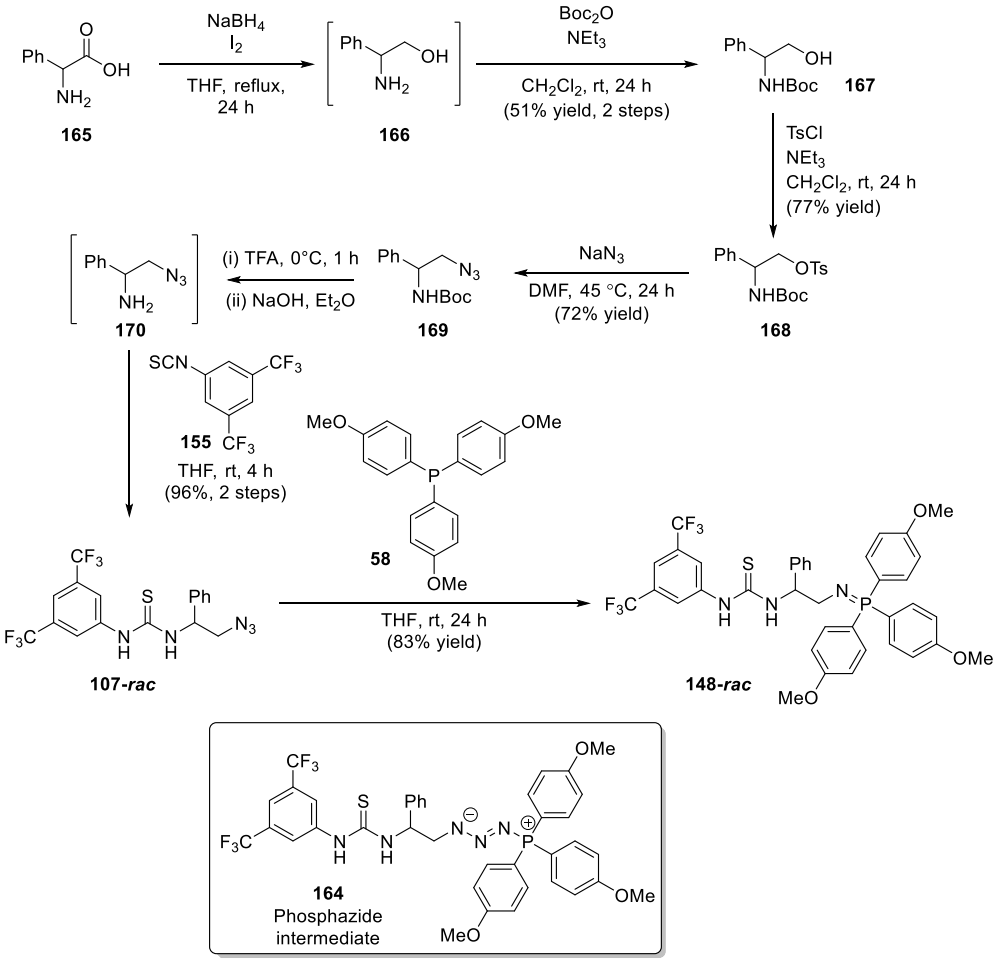

Scheme 31. *Preparation of racemic phenyl-substituted catalyst **148*-rac**.*

2.4 Synthesis of homopolymers

2.4.1 Polymerisation of L-lactide

After successfully establishing proof of concept, polymerisation of LA of various lengths was carried out under the same reaction conditions using 5 mol% of catalyst **162**. With $[M]_0/[I]_0$ of 50, 200 and 500 poly(LA) was formed in high conversion and short reaction times (Table 33). Although we investigated the use of benzyl alcohol as an alternative initiator, better accuracy and reproducibility was achieved by weighing out solid 1-pyrenebutanol than by preparing stock solutions of benzyl alcohol. Therefore we used 1-pyrenebutanol as the initiator for all polymerisation studies. This due to the fact that we were able weigh solids more accurately and precisely than measure volumes of liquid.

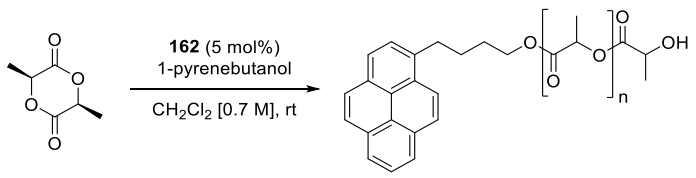

$[M]_0/[I]_0$	Time (min)	Conversion (%)[a]	M_n (g mol^{-1})[b]	PDI[b]	DP[a]
50	5	97	10 200	1.05	62
100	10	99	12 700	1.05	97
200	20	99	22 500	1.03	227
500	50	99	*c*	*c*	613

Table 33. *Polymerisation of LA using catalyst **162**. [a] Measured by ^{1}H-NMR. [b] Measured by GPC in THF. [c]Not soluble in THF.*

Encouraged by the fast reaction rate with 5 mol% of catalyst, we next investigated the reaction using a lower catalyst loading (Table 34).

162 loading (mol%)	[LA] (M)	Time (min)	Conversion (%)[a]
2	0.7	20	95
1.5	0.7	35	94
1	0.7	50	72
1.5	2.3	10	99
1	2.3	10	99
0.5	2.3	20	88
0.5	2.3	40	85

Table 34. *Optimisation of polymerisation of LA with low catalyst loading. $[M]_0/[I]_0 = 100$. [a] Measured by ^{1}H-NMR.*

At an LA concentration of 0.7 M, lowering the catalyst loading to 1 mol% resulted in incomplete conversion. However, when the concentration was increased to 2.3 M, full conversion could be achieved with 1 mol% catalyst in the same time as was required with a 5 mol% loading at the lower concentration. GPC analysis indicated that the poly(LA) prepared under these conditions had M_n = 23 200 g mol^{-1} and a PDI of 1.03. Having established optimal reaction conditions, poly(LA) with $[M]_0/[I]_0$ of 25, 50, 100, 200 and 500 was prepared using a catalyst loading of 1 mol% (Table 35).

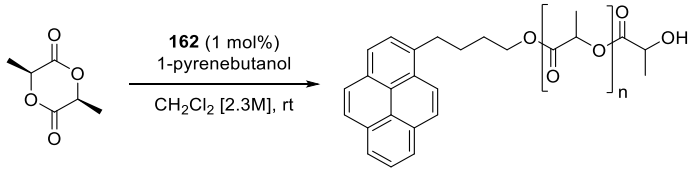

$[M]_0/[I]_0$	Time (min)	Conversion (%)[a]	M_n (g mol^{-1})[b]	PDI[b]	DP[a]
25	3	99	6 380	1.06	29
50	5	99	11 200	1.05	54
100	10	99	27 500	1.04	98
200	20	99	32 900	1.04	206
500	50	99	*c*	*c*	491

Table 35. *Polymerisation of LA using catalyst **162**. [a] Measured by ^{1}H-NMR. [b] Measured by GPC in THF. [c] Polymer not soluble in THF.*

GPC analysis showed that the M_n of the synthesised poly(LA) approximately agreed with the expected values (e.g. theoretical M_n for $[M]_0/[I]_0$ = 100 is 14 400 g mol^{-1}); overestimation of the molecular weight of poly(LA) in GPC analyses appears to be common in the literature.[10,12] The PDI for all lengths of poly(LA) is very close to unity, as is typical for organocatalytic ROP.

The end-group fidelity of the poly(LA) was established by analysis of ^{1}H-NMR spectra which clearly showed the presence of the terminal C<u>H</u>(OH) as well as the pyrenebutanol CH_2 adjacent to the first

ester linkage of the polymer chain. MALDI-ToF spectra of poly(LA) with $[M]_0/[I]_0$ of 25 indicated that the polymer chains were initiated by pyrenebutanol (see Experimental).

Homodecoupled ^{1}H-NMR showed a single peak corresponding to the C<u>H</u>(CH_3) in the polymer chain (see Appendix). This indicates that, within the limits of detection, no epimerisation took place during the polymerisation reaction.

Regular sampling of a polymerisation reaction of LA with $[M]_0/[I]_0$ of 100 allowed for the creation of a plot of conversion vs. M_n vs. PDI (Figure 43) as well as a plot of conversion vs. time (Figure 44). A linear relationship between the conversion and molecular weight and uniform polydispersity with respect to conversion indicates a well-controlled polymerisation (Figure 43).

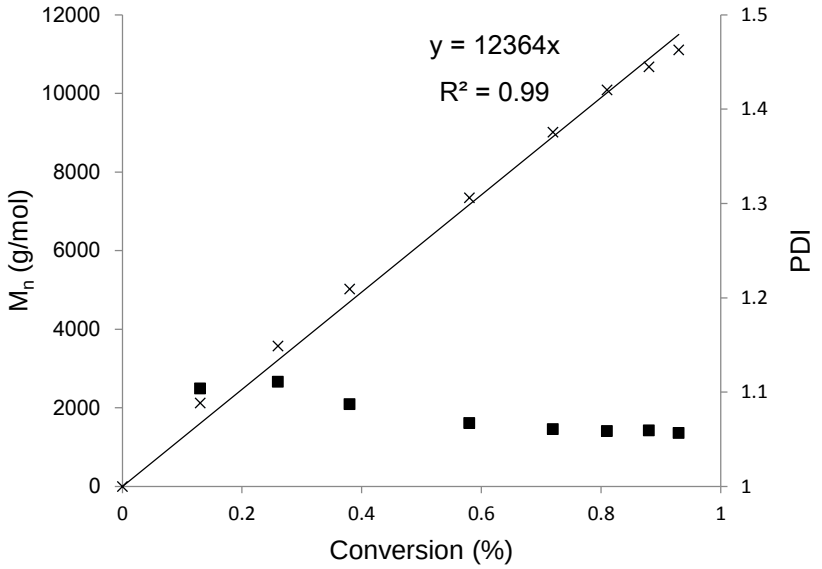

Figure 43. *Ring-opening polymerisation of LA with $[M]_0/[I]_0$ of 100 catalysed by **162**. Plot of M_n, (×) and PDI (■), as determined by GPC, vs. monomer conversion determined by ^{1}H-NMR.*

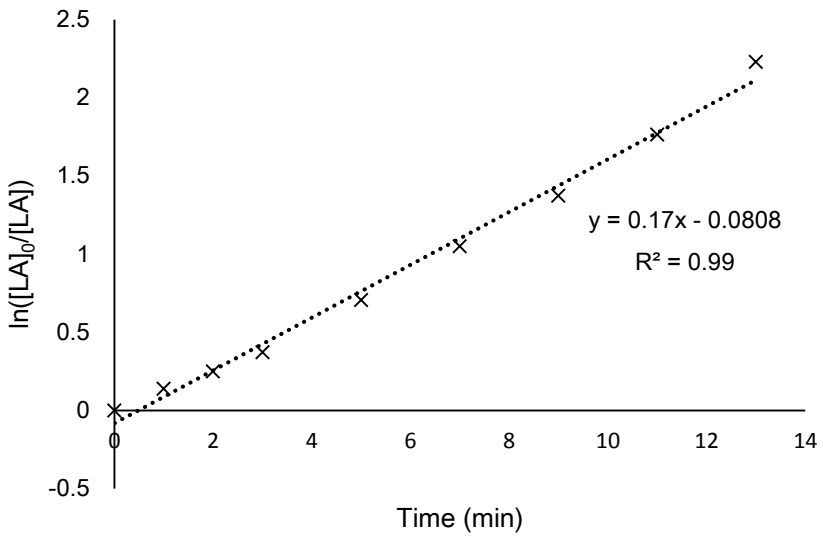

Figure 44. *Plot of ln([LA]$_0$/[LA]) vs. time with linear regression. Ring-opening polymerization of LA at room temperature with [M]$_0$/[I]$_0$ of 100 catalysed by* ***162****. Monomer conversion determined by* ^{1}*H-NMR.*

The linear relationship between $\ln([LA]_0/[LA])$ and time (Figure 44) indicates that the LA polymerisation data can be well-fitted by a first-order rate law:

$$ln\left(\frac{[LA]_0}{[LA]}\right) = kK_1K_2[catalyst]_0[ROH]_0t$$

Where *k* is the polymerisation rate constant, K_1 the equilibrium constant for the association between LA and the thiourea moiety, K_2 the equilibrium constant for the association between 1-pyrenebutanol and the iminophosphorane moiety, and $[catalyst]_0$, and $[ROH]_0$ are the concentrations of catalyst and 1-pyrenebutanol initiator at t = 0 min. It is assumed that the equilibrium constant K_2 for the catalyst and 1-pyrenebutanol is the same as for the catalyst and the propagating alcohol and that the alcohol concentration remains constant throughout the polymerisation.

Taken together, these two plots indicate that the polymerisation of LA by catalyst **162** fulfils the criteria for a living polymerisation (see Chapter 3 Introduction). This means that the rate of initiation is fast and no termination of chain transfer events take place during the polymerisation. This can be seen in Figures 43 and 44 from the constant growth of the polymer chains over the course of the reaction.

The polymerisation of *rac*-lactide (*rac*-LA) was also investigated, to ascertain whether our catalytic system could be used to control the tacticity of the resulting polymer or to selectively polymerise one enantiomer of lactide over the other. Using racemic catalysts **162** and **148-*rac***, the effect of temperature, solvent and catalyst loading on P_i was investigated (Table 36). Polymerisation of *rac*-LA with **162** or **148-*rac*** results in a slight isotactic enhancement (entries 1 and 2), with the use of the bulkier phenyl substituted catalyst having no significant effect on the tacticity of the resulting polymer. Conducting the reaction at −78 °C increased the P_i slightly to 0.74 (entry 5), however the reaction rate was greatly decreased. Changing the solvent to THF or lowering the catalyst loading did not significantly increase the isotactic enhancement (entries 7 – 11). A sample homodecoupled ^{1}H-NMR spectrum of poly(*rac*-LA) and corresponding P_i calculation can be found in the Appendix.

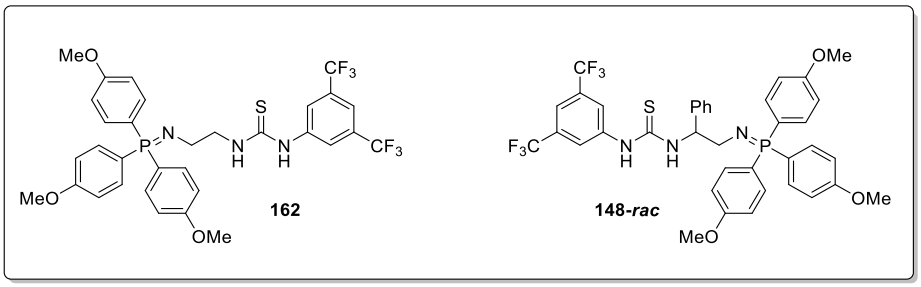

	Catalyst	Catalyst loading (mol%)	Solvent	Temp. (°C)	Time	Conversion (%)[a]	P_i^a
1	**162**	5	DCM	rt	10 min	97	0.64
2	**148-*rac***	5	DCM	rt	10 min	94	0.66
3	**162**	5	DCM	−20	24 h	99	0.66
4	**148-*rac***	5	DCM	−20	24 h	99	0.65
5	**162**	5	DCM	−78	3.5 h	36	0.74
6	**148-*rac***	5	DCM	−78	3.5 h	16	n.d.
7	**162**	5	THF	rt	90 min	96	0.65
8	**148-*rac***	5	THF	rt	90 min	97	0.68
9	**162**	1	DCM	rt	2 h	26	0.69
10	**148-*rac***	1	DCM	rt	2 h	22	0.65
11	**162**	0.5	DCM	rt	24 h	6	n.d.

Table 36. *Polymerisation of rac-LA. Reaction was conducted with $[M]_0/[I]_0$ of 100, at [LA] = 2.3 M with pyrenebutanol initiator. [a] Measured by ^{1}H-NMR.*

Next, polymerisation of *rac*-LA using enantiopure catalysts **56** and **148** was investigated to determine whether it was possible to selectively polymerise a single enantiomer of lactide. *rac*-LA was polymerised with 5 mol% catalyst following the typical procedure; however, in this instance the

reaction was stopped at partial conversion and any remaining monomer analysed by HPLC (Table 37). Unfortunately, using both catalyst **56** and **148** no enantioenrichment of the remaining monomer was observed, indicating no selectivity in the polymerisation.

Catalyst	Time (min)	Conversion (%)[a]	e.e. of monomer (%)[b]
148	5	66	7
56	5	53	3

Table 37. *Polymerisation of rac-LA. Reaction was conducted in DCM at room temperature, with $[M]_0/[I]_0$ of 100, [LA] = 0.7 M and pyrenebutanol initiator. [a] Measured by ^{1}H-NMR. [b] Measured by HPLC (Chiralpak IA, hexane/iso-propanol 70:30, 0.8 mL/min).*

2.4.2 Polymerisation of δ-valerolactone

Next the polymerisation of δ-valerolactone (VL) was investigated. At first a solvent screen using catalyst **162** was carried out (Table 38). The use of aromatic solvents gave the best conversion, but resulted in poor solubility of the catalyst, especially when polymerisations with larger $[M]_0/[I]_0$ were attempted.

Solvent	Time	Conversion (%)[a]
DCM	45 min	trace
PhMe	6 h	79
xylenes	6 h	94
PhCl	6 h	95

Table 38. *Solvent screen for VL polymerisation. Reaction was conducted at room temperature, with $[M]_0/[I]_0$ of 50, [VL] = 2.0 M and pyrenebutanol initiator. [a] Measured by ^{1}H-NMR.*

The problem of catalyst solubility was resolved through the use of phenyl-substituted catalyst **148-*rac***. Using this catalyst in chlorobenzene, poly(VL) with $[M]_0/[I]_0$ of 50, 100, 200 and 500 could be prepared (Table 39).

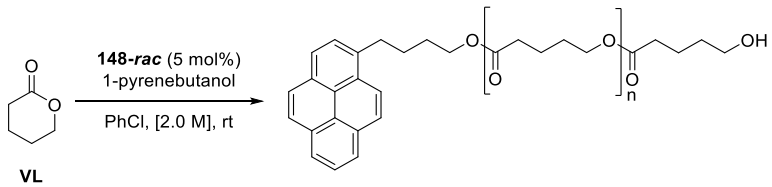

$[M]_0/[I]_0$	Time (h)	Conversion (%)[a]	M_n (g mol^{-1})[b]	PDI[b]
50	4	94	7 260	1.10
100	9	94	10 100	1.13
200	16	92	22 400	1.11
500	24	92	37 400	1.08

Table 39. *Polymerisation of VL using catalyst **148**-**rac**. [a] Measured by ^{1}H-NMR. [b] Measured by GPC in THF using Mark-Houwink parameters for polystyrene.*

The M_n of poly(VL) synthesised using this method agrees very well with the expected molecular weight, though it should be noted that these M_n values were adjudged directly using the polystyrene calibration curve of the GPC as no Mark-Houwink parameters for poly(VL) could be found in the literature. The PDI of these polymers are all in the very low range, indicating a well-controlled polymerisation.

The end-group fidelity of poly(VL) was established by analysis of MALDI-ToF spectra, which showed polymer chain molecular masses consistent with initiation by pyrenebutanol (see Experimental).

2.4.3 Polymerisation of ε-caprolactone

The organocatalytic ROP of ε-caprolactone (CL) is typically carried out in toluene or benzene,[12] nonetheless a solvent screen was carried out to confirm the optimal solvent for this monomer with our novel catalytic system (Table 40). Although solvent-free ROP gave good conversion, with larger $[M]_0/[I]_0$ these conditions resulted in poor stirring as the reaction progressed. Toluene performed comparably well and due to its prevalence in the literature, its use could facilitate a direct comparison with other catalyst systems. It was therefore chosen for further investigation of this reaction.

$[M]_0/[I]_0$	Solvent	Time (h)	Conversion (%)[a]
20	DCM	48	7
20	EtOAc	20	16
20	MeCN	20	trace
20	PhMe	24	90
50	PhCl	24	53
50	xylenes	24	31
50	neat	24	87

Table 40. *Solvent screen for CL polymerisation. Reaction was conducted at room temperature, with 5 mol% catalyst* ***162*** *[CL] = 2.0 M and pyrenebutanol initiator.* [a] *Measured by* ^{1}*H-NMR.*

As with the ROP of VL, catalyst **162** was poorly soluble in toluene, especially in reactions with larger $[M]_0/[I]_0$, and this was resolved by using the phenyl substituted catalyst **148-*rac***. Polymerisation of CL with $[M]_0/[I]_0$ of 50, 100, 200 and 500 was then successfully carried out (Table 41).

In the polymerisation of CL, an increasing discrepancy was seen between the target molecular weight and M_n as measured by GPC as $[M]_0/[I]_0$ increased. For example, poly(CL) with $[M]_0/[I]_0 = 50$ is expected to have a molecular weight of 5 700 g mol^{-1} while the experimental M_n is 3 000 g mol^{-1} (an error of 47% relative to the calculated value), but poly(CL) with $[M]_0/[I]_0 = 500$ is expected to have a molecular weight of 57 000 g mol^{-1} while its experimental M_n is only 9 310 g mol^{-1} (an error of 84% relative to the calculated value). We therefore believe that the polymerisation does not proceed in a controlled fashion due to the low reactivity of the CL monomer. The initiation step with pyrenebutanol is relatively slow and the propagation step is perhaps even slower, which allows for initiation from the catalyst itself (*vide infra*) to compete with chain propagation leading to shorter chain lengths than expected, as well as an increased PDI.

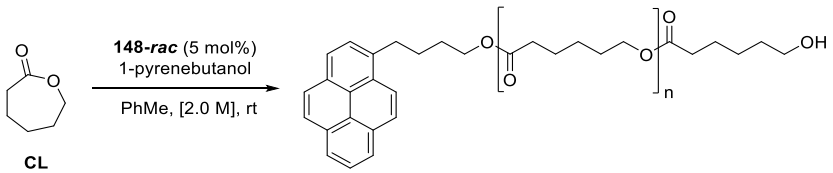

$[M]_0/[I]_0$	Time (h)	Conversion (%)[a]	M_n (g mol^{-1})[b]	PDI[b]
50	48	79	3 000	1.16
100	100	91	4 860	1.23
200	120	91	5 370	1.25
500	240	94	9 310	1.24

Table 41. *Polymerisation of CL using catalyst **148-rac**. [a] Measured by ^{1}H-NMR. [b] Measured by GPC in THF.*

The end-group fidelity of poly(CL) was established by analysis of MALDI-ToF spectra, which showed polymer chain molecular masses consistent with initiation by pyrenebutanol (see Experimental). Although we suspect some initiation from the catalyst occurred, no peaks corresponding to such polymer chains were observed in the MALDI-ToF spectra.

2.5 Synthesis of co-polymers

2.5.1 Sequential monomer addition

One advantage of living polymerisation is that as there are no chain termination events, polymerisation continues until all monomer is consumed and can resume once further monomer is added. This allows for the preparation of block co-polymers by the sequential addition of different monomers. Block copolymers of LA, VL and CL were prepared using this method.

In a typical example, VL was polymerised in chlorobenzene using 10 mol% of catalyst **148-*rac*** and 1-pyrenebutanol as the initiator with an $[M]_0/[I]_0$ of 50 for 5 h, at which point an aliquot was removed for NMR and GPC analysis. ^{1}H-NMR indicated 87% conversion, whilst GPC showed a peak with M_n of 4 050 g mol^{-1} and PDI of 1.10. 50 equivalents of CL (relative to the initiator) were then added and the reaction continued until 82% conversion (in CL) was reached, as indicated by ^{1}H-NMR, then quenched by addition of acetic acid. GPC analysis of the resulting polymer showed a single, unimodal peak with M_n of 5 920 g mol^{-1} and a PDI of 1.19, indicating that a diblock copolymer had been formed (see Appendix for representative trace). The final M_n compares favourably with the calculated molecular weight of 9 000 g mol^{-1}, given that this value was calculated directly from the

polystyrene calibration curve of the GPC. Poly(VL)-*block*-poly(LA) and poly(CL)-*block*-poly(LA) were also prepared in this fashion (Table 42).

Monomer 1	Conv.[b] (%)	M_n (g mol^{-1})		PDI[a]	Monomer 2	Conv.[b] (%)	M_n (g mol^{-1})		PDI[a]
		GPC[a]	NMR				GPC[a]	NMR	
VL	87	4 050	4 200	1.10	CL	82	5 920	8 000	1.19
VL	92	3 930	4 500	1.12	LA	99	7 530	11 000	1.13
CL	93	3 480	5 130	1.12	LA	99	5 670	14 100	1.16

Table 42. *Preparation of diblock co-polymers by sequential monomer addition. [a] Measured by GPC in THF using Mark-Houwink parameters for polystyrene. [b] Measured by ^{1}H-NMR. $[M]_0/[I]_0$ for monomer 1 relative to 1 pyrenebutanol = 50, then 50 equiv. of monomer 2 relative to 1-pyrenebutanol were added.*

The order of monomer addition was an important consideration when LA was used. Block co-polymerisation undertaken using LA as the first monomer was unsuccessful. Although the LA was consumed, incomplete consumption (< 30%) of the second monomer (VL or CL) was observed by ^{1}H-NMR at the expected reaction time for $[M]_0/[I]_0 = 50$ of the relevant monomer. Presumably this reflects the poor propensity of the terminal secondary alcohol of poly(LA) to initiate ROP.

2.5.2 Polymerisation using macroinitiators

Another method of forming block co-polymers is to use a polymer terminated with an appropriate nucleophile as the initiating species. We decided to investigate this approach using monomethoxy-terminated poly(ethylene glycol) with a length of 50 units ($mPEG_{50}$). The $mPEG_{50}$ was first analysed by MALDI-ToF and GPC to determine an accurate M_n and PDI, then it was used as an initiator in the polymerisation of LA, VL and CL (Table 43).

Monomer	$[M_0]/[I_0]$	Time	Conversion[b] (%)	M_n (g mol^{-1}) [a]	PDI[a]
LA	100	10 min	99	16 800	1.07
VL	50	5 h	99	4 600	1.04
CL	50	27 h	86	4 910	1.18

Table 43. *Synthesis of polymers from $mPEG_{50}$ macroinitiator. [a] Measured by GPC in THF using Mark-Houwink parameters for polystyrene. [b] Measured by ^{1}H-NMR. For $mPEG_{50}$: M_n = 2830 g mol^{-1} and PDI = 1.05 (measured by GPC in THF using Mark-Houwink parameters for polystyrene).*

^{1}H- NMR showed good conversion of the monomers to polymer and GPC analysis showed a single, unimodal peak with a higher M_n than $mPEG_{50}$, indicating that diblock co-polymers had been formed.

2.6 The mode of action of bifunctional iminophosphorane organocatalysts in ROP

Following our observation of unusual M_n values in the polymerization of CL, we sought to test the hypothesis that initiation from the catalyst itself was competing with chain propagation. This led us to undertake several control experiments to investigate the roles of both the iminophosphorane and thiourea moieties in the ROP reaction.

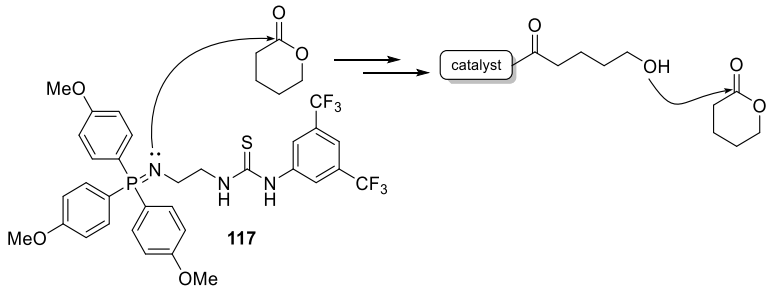

Figure 45. *Hypothesised initiation of polymerisation by catalyst **162**.*

The ability of the bifunctional iminophosphoranes to initiate polymerisation was first tested. In the presence of 5 mol% catalyst **162**, but with no additional initiating nucleophilic species, LA, VL and CL were all polymerised (Table 44). However longer reaction times were required to reach full conversion compared with the analogous reaction in the presence of an alcohol initiator. Based on the known reactivity between esters and iminophosphoranes to form amides in the Staudinger ligation,[35] it is likely that the nitrogen of the iminophosphorane acts as a nucleophile to open the monomer (Figure 45) We have also demonstrated that reaction between iminophosphorane **171** and VL leads to the opening of the cyclic ester and formation of the corresponding amide upon hydrolysis (Scheme 32).

Monomer	Time	Conversion (%)[a]
LA	10 min	75
VL	24 h	70
CL	24 h	20

Table 44. *Polymerization of monomers in the presence of 5 mol% of catalyst **162**. [a] Measured by ^{1}H-NMR.*

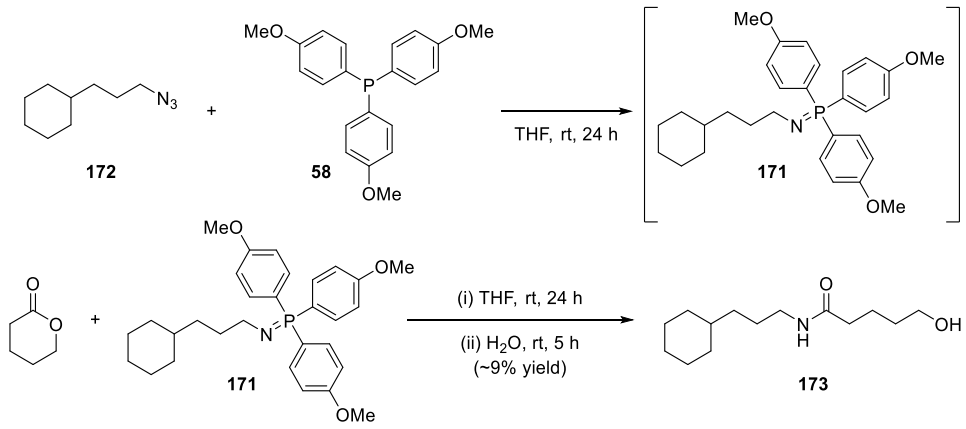

Scheme 32. *Reaction of VL with iminophosphorane **171**.*

Although we cannot completely rule out the possibility of initiation by adventitious moisture, no direct evidence of polymer chains initiated by H_2O could be observed in spite of several attempts at obtaining MALDI-ToF spectra of polymers synthesised in the absence of an alcohol initiator. However, it is important to note that polymer chains initiated by iminophosphoranes also could not be observed using MALDI-ToF.

The role of the thiourea moiety was next investigated by studying the ROP of LA catalysed by iminophosphorane **174**, which features an *N*-alkyl substituent rather than a linked H-bond donor. Iminophosphorane **174**, formed *in situ* from azide **175** and tris(4-methoxy)phenylphosphine **58** (Scheme 33), is able to catalyse the polymerization of LA initiated by 1-pyrenebutanol with a monomer to initiator ratio of 100:1 (Table 45, entry 1). However, the reaction rate is slower than that achieved with bifunctional catalyst **162**, requiring 1 h to reach 92% conversion and the polydispersity of the resulting polymer is greater than that obtained using the bifunctional catalyst (1.14 vs. $\leq$ 1.05). This increase in dispersity is consistent with the findings of Hedrick and co-workers who show that the association constant of valerolactone and caprolactone and 1-(3,5-bis(trifluoromethyl)phenyl)-3-cyclohexylthiourea is much greater than that of the thiourea and ethyl acetate.[12] From which it is inferred that the preferential activation of cyclic ester monomers over the polymer backbone suppresses transesterification. Thus the thiourea moiety increases the rate of polymerisation through monomer activation while also suppressing undesirable transesterification reactions. We attempted to measure the association constant between valerolactone and catalyst **162**, however this proved

untenable due to the complex and dynamic nature of the solution phase NMR spectra of the bifunctional iminophosphorane catalysts.

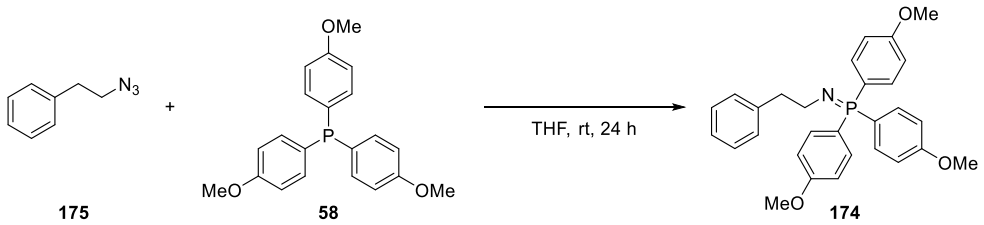

175 58 174

Scheme 33. *Preparation of iminophosphorane **174**.*

	$[M]_0/[I]_0$	Initiator	Time (h)	Conversion (%)[a]	M_n (g mol^{-1})[b]	PDI[b]	P_i[c]
1	100	1-PB	1	92	8 190	1.14	0.68
2	-	-	1	74	8 160	1.25	0.66

Table 45. *Polymerization of LA in the presence of 5 mol% **174** (relative to monomer). [a] Measured by ^{1}H-NMR. [b] Measured by GPC in THF. [c] Measured by homodecoupled ^{1}H-NMR.*

The slower reaction rate and higher PDI might also be explained by the possibility that iminophosphorane **174** may be more basic and/or more nucleophilic than catalyst **162**. Initiation from the more nucleophilic iminophosphorane **174** may successfully compete with initiation from the alcohol, leading to the formation of lower molecular weight oligomers as well as consumption of the catalyst, which would lead to lower monomer conversion. This is consistent with the low value of M_n when using iminophosphorane **174** (8 190 g mol^{-1} vs. 27 500 g mol^{-1} for $[M]_0/[I]_0$ = 100 using catalyst **162**). The increased basicity may also result in increased transesterification.

Iminophosphorane **174** also catalyses the polymerisation of LA in the absence of an initiating alcohol; with 5 mol% catalyst loading LA is polymerized in 74% conversion after 1 hour (Table 45, entry 2). This is slower than polymerisation in the absence of an alcohol initiator using bifunctional catalyst **162**, in agreement with the proposed activation of the monomer by thiourea.

Interestingly, significant epimerisation occurs when using iminophosphorane **174** as a polymerisation catalyst and the resulting polymer has a P_i of 0.66 – 0.68. Stirring a sample of poly(LA) (previously prepared using catalyst **162**) with iminophosphorane **174** in DCM for 1 h at room temperature does not result in any observable epimerization by homodecoupled ^{1}H-NMR.

Consequently we conclude that the reduced P_i of the polymer is caused by epimerisation of the LA monomer.

3. Conclusion

Bifunctional iminophosphorane organocatalysts **162** and **148-*rac*** were shown to be excellent catalysts for the synthesis of poly(LA) and poly(VL) with rapid reaction times, excellent monomer conversions, low polydispersity and high end-group fidelity. Poly(CL) could also be synthesised, however the utility of the catalysts was limited to relatively short lengths of polymer due to suspected competing initiation from the catalyst. Considering Table 30, it can be seen that the performance of our bifunctional iminophosphorane organocatalysts compares very favourably with that of the current state-of-the-art bifunctional systems. Although our catalysts do not match the reactivity of TBD, their performance exceeds that of the MTBD/thiourea system for LA and is comparable to this system for VL and CL. Notably, they are significantly easier to handle, enabling reaction set-up in open air. Diblock copolymers could successfully be synthesised through sequential monomer addition and our catalysts were also found to be compatible with the use of an mPEG macroinitiator. However, bifunctional iminophosphoranes did not prove to be effective for the stereocontrolled synthesis of poly(*rac*-LA). Finally, control experiments revealed the requirement for both the iminophosphorane and thiourea moiety in order to achieve rapid and well-controlled polymerisation thereby confirming the bifunctional nature of this novel class of ROP catalyst.

4. References

(1) Dubois, P.; Coulembier, O.; Raquez, J. M. *Handbook of Ring-Opening Polymerization*; Wiley, 2008.
(2) Jenkins, A. D.; Kratochvíl, P.; Stepto, R. F. T.; Suter, U. W. *Pure Appl. Chem.* **1996**, *68*.
(3) Hawker, C. J.; Wooley, K. L. *Science* **2005**, *309*, 1200–1205.
(4) Albertsson, A.-C.; Varma, I. K. *Biomacromolecules* **2003**, *4*, 1466–1486.
(5) Hedrick, J. L.; Magbitang, T.; Connor, E. F.; Glauser, T.; Volksen, W.; Hawker, C. J.; Lee, V. Y.; Miller, R. D. *Chem. – Eur. J.* **2002**, *8*, 3308–3319.
(6) Nederberg, F.; Connor, E. F.; Glausser, T.; Hedrick, J. L. *Chem. Commun.* **2001**, 2066–2067.
(7) Nederberg, F.; Connor, E. F.; Möller, M.; Glauser, T.; Hedrick, J. L. *Angew. Chem., Int. Ed.* **2001**, *40*, 2712–2715.
(8) Sigman, M. S.; Vachal, P.; Jacobsen, E. N. *Angew. Chem., Int. Ed.* **2000**, *39*, 1279–1281.
(9) Okino, T.; Hoashi, Y.; Takemoto, Y. *J. Am. Chem. Soc.* **2003**, *125*, 12672–12673.
(10) Dove, A. P.; Pratt, R. C.; Lohmeijer, B. G. G.; Waymouth, R. M.; Hedrick, J. L. *J. Am. Chem. Soc.* **2005**, *127*, 13798–13799.
(11) Pratt, R. C.; Lohmeijer, B. G. G.; Long, D. A.; Lundberg, P. N. P.; Dove, A. P.; Li, H.; Wade, C. G.; Waymouth, R. M.; Hedrick, J. L. *Macromolecules* **2006**, *39*, 7863–7871.
(12) Lohmeijer, B. G. G.; Pratt, R. C.; Leibfarth, F.; Logan, J. W.; Long, D. a; Dove, A. P.; Nederberg, F.; Choi, J.; Wade, C.; Waymouth, R. M.; Hedrick, J. L. *Macromolecules* **2006**, *39*, 8574–8583.
(13) Kaljurand, I.; Kütt, A.; Sooväli, L.; Rodima, T.; Mäemets, V.; Leito, I.; Koppel, I. A. *J. Org. Chem.* **2005**, *70*, 1019–1028.
(14) Corey, E. J.; Grogan, M. J. *Org. Lett.* **1999**, *1*, 157–160.
(15) Pratt, R. C.; Lohmeijer, B. G. G.; Long, D. A.; Waymouth, R. M.; Hedrick, J. L. *J. Am. Chem. Soc.* **2006**, *128*, 4556–4557.
(16) Enders, D.; Niemeier, O.; Henseler, A. *Chem. Rev.* **2007**, *107*, 5606–5655.
(17) Nyce, G. W.; Lamboy, J. A.; Connor, E. F.; Waymouth, R. M.; Hedrick, J. L. *Org. Lett.* **2002**, *4*, 3587–3590.
(18) Grasa, G. A.; Kissling, R. M.; Nolan, S. P. *Org. Lett.* **2002**, *4*, 3583–3586.
(19) Connor, E. F.; Nyce, G. W.; Myers, M.; Möck, A.; Hedrick, J. L. *J. Am. Chem. Soc.* **2002**, *124*, 914–915.
(20) Nyce, G. W.; Glauser, T.; Connor, E. F.; Möck, A.; Waymouth, R. M.; Hedrick, J. L. *J. Am. Chem. Soc.* **2003**, *125*, 3046–3056.
(21) Schwesinger, R.; Schlemper, H. *Angew. Chem., Int. Ed. English* **1987**, *26*, 1167–1169.
(22) Zhang, L.; Nederberg, F.; Pratt, R. C.; Waymouth, R. M.; Hedrick, J. L.; Wade, C. G. *Macromolecules* **2007**, *40*, 4154–4158.
(23) Zhang, L.; Nederberg, F.; Messman, J. M.; Pratt, R. C.; Hedrick, J. L.; Wade, C. G. *J. Am. Chem. Soc.* **2007**, *129*, 12610–12611.
(24) Kazakov, O. I.; Datta, P. P.; Isajani, M.; Kiesewetter, E. T.; Kiesewetter, M. K. *Macromolecules* **2014**, *47*, 7463–7468.
(25) Coudane, J.; Ustariz-Peyret, C.; Schwach, G.; Vert, M. *J. Polym. Sci. Part A Polym. Sci.* **1997**, *35*, 1651–1658.
(26) Bern, M.; Kasperczyk, J.; Jedlinski, Z. J. *Makromol. Chem* **1990**, *2296*, 2287–2296.
(27) Kasperczyk, J. *Macromolecules* **1995**, 3937–3939.
(28) Dove, A. P.; Li, H.; Pratt, R. C.; Lohmeijer, B. G. G.; Culkin, D. a.; Waymouth, R. M.; Hedrick, J. L. *Chem. Commun.* **2006**, 2881.
(29) Miyake, G.; Chen, E. *Macromolecules* **2011**, 4116–4124.
(30) Dove, A. P. *ACS Macro Lett.* **2012**, *1*, 1409–1412.
(31) Sinha, M. K.; Reany, O.; Yefet, M.; Botoshansky, M.; Keinan, E. *Chem. – Eur. J.* **2012**, *18*, 5589–5605.
(32) Núñez, M. G.; Farley, A. J. M.; Dixon, D. J. *J. Am. Chem. Soc.* **2013**, *135*, 16348–16351.

(33) Desamparados Velasco, M.; Molina, P.; Fresneda, P. M.; Sanz, M. A. *Tetrahedron* **2000**, *56*, 4079–4084.
(34) Bebbington, M. W. P.; Bourissou, D. *Coord. Chem. Rev.* **2009**, *253*, 1248–1261.
(35) van Berkel, S. S.; van Eldijk, M. B.; van Hest, J. C. M. *Angew. Chem., Int. Ed.* **2011**, *50*, 8806–8827.

Chapter 4: Experimental

General Experimental

General Experimental Techniques

For reactions requiring anhydrous conditions, glassware was dried in an oven at 100 °C and reactions were carried out under a nitrogen or argon atmosphere. For polymerisation studies glassware was flame-dried under vacuum and reaction assembly was performed on an open bench under a blanket of nitrogen. Room temperature (RT) refers to 20-25 °C. Temperatures of 0 °C and −78 °C were achieved using an ice-bath and dry ice in acetone respectively.

Solvents and Reagents

Bulk solutions were concentrated under reduced pressure using a Büchi rotary evaporator. All solvents were commercially supplied or provided by the communal stills of the Chemistry Research Laboratory, Oxford. These stills operate under the "Grubbs apparatus" method for solvent purification. Petroleum ether (PE) refers to distilled light petroleum with boiling points in the range of 30 - 40 °C. Commercially available reagents were used as received. Poly(4-bromostyrene) (Stratospheres^{TM} PL-PBS resin, 50-100 mesh, 2.0 mmol/g loading, 1% cross-linked with divinylbenzene), produced by Polymer Laboratories Ltd., was purchased from Sigma Aldrich. "Commercial" polystyrene-supported triphenylphosphine refers to triphenylphosphine, polymer-bound (100-200 mesh, ~3.0 mmol/g loading, 2 % cross-linked with divinylbenzene) purchased from Sigma Aldrich.

For polymerisation studies: L-Lactide was purchased from Alfa Aesar, DL-lactide was purchased from Sigma Aldrich. Both were recrystallized three times from toluene under anhydrous conditions then dried *in vacuo* before use. VL was purchased from Acros Organics and CL was purchased from Alfa Aesar. Both were distilled twice from calcium hydride before use. 1-pyrenebutanol and mono-methoxy-terminated poly(ethyleneglycol) (MW ~2000) were purchased from Sigma Aldrich and dried before use by dissolving in THF and stirring over calcium hydride for 24 h, followed by

filtration and recovery by removal of solvent under nitrogen flow. Anhydrous toluene and dichloromethane were obtained by filtration through activated alumina (powder ~150 mesh, pore size 58 Å, basic, Sigma-Aldrich) columns, followed by standing over activated 4 Å molecular sieves for 24 h. Chlorobenzene was distilled from calcium hydride. Solvents were stored in sealed Schlenk flasks over activated 4 Å molecular sieves, VL and CL were stored in sealed Schlenk flasks. LA was stored in a desiccator under vacuum over phosphorus pentoxide.

All other reagents purchased from commercial sources were used as supplied. The following compounds were synthesised by other members of the Dixon group and used as received:

Ketimines **36b-h** were synthesised by Alistair Farley, Dr. Marta Garcia Núñez and Dr. Irene Ortin Remón. Compounds **138**, **140**, **142**, **143** and **145** were synthesised by Dr. Pavol Jakubec. Compound **172** was synthesised by Dr. Marta Garcia Núñez.

Chromatography

All reactions were monitored by thin-layer chromatography (TLC) where appropriate using Merck Kiesel gel 60 F254 (230-400 mesh) silica plates which were visualised by UV-light (250 nm) or by staining using aqueous potassium permanganate or *p*-enisaldehyde solutions where appropriate. Flash column chromatography was carried out using Merck Kieselgel 60 silica gel (230-400 mesh).

Spectroscopy

All ^{1}H, ^{13}C and ^{31}P nuclear magnetic resonance (NMR) spectra were collected on either a Bruker DPX400 (400 MHz ^{1}H, 100 MHz ^{13}C), Bruker DQX400 (400 MHz ^{1}H, 100 MHz ^{13}C), Bruker AVC500 (500 MHz ^{1}H, 125 MHz ^{13}C), Bruker AVN400 (400 MHz ^{1}H, 100 MHz ^{13}C) and in the deuterated solvent stated. Chemical shift values (δ) are reported relative to tetramethylsilane (δ = 0 ppm) using the solvent residual peak as an internal reference. Assignments were aided by COSY, DEPT, HSQC, and NOESY experiments. The abbreviations s, d, t, q, quin, sept, br, m and e.g. “t” denote singlet, doublet, triplet, quartet, quintet, septet, broad, multiplet and apparent multiplicity respectively. All coupling constants, *J*, are quoted in Hz.

The NMR spectra of the bifunctional iminophosphoranes are dynamic in nature and depending on the solvent may show a mixture of monomeric and aggregated species. For this reason it is not always possible to observe all the expected protons and carbons in the NMR spectra (in particular the thiourea protons and low intensity carbon signals are often not observed). This appears to be typical for this class of compounds and NMR studies are ongoing in the Dixon group to better understand the solution phase behaviour of these catalysts.

Low resolution mass spectrometric (*m/z*) data was acquired by electrospray ionisation (ESI) on an LCT Premier Open Access instrument. High resolution mass spectra were recorded on a Bruker MicroTof mass spectrometer (ESI) by the internal service at the Department of Organic Chemistry, University of Oxford.

Infrared spectra (ν_{max}) were recorded on a Bruker Tensor 27 FT-IR spectrometer on a thin film on a diamond ATR module. Only selected maximum absorbances are reported.

For polymerisation studies: Conversion was measured by the ratio of the integrations of the NMR signals of the α-methylene or methine protons of the monomer compared to those of the polymers. The tacticity of synthesized poly(LA) was determined from the integration of the methine region of the homodecoupled ^{1}H-NMR spectrum. P_i, the probability of forming an isotactic dyad, was calculated using literature methods.[1]

MALDI-ToF

MALDI-ToF MS analysis was performed on a Waters MALDI micro equipped with a 337 nm nitrogen laser and an accelerating voltage of 25 kV. The polymer samples were dissolved in THF at a concentration of 1.0 mg mL^{-1}. The cationization agent used was potassium trifluoroacetate (Sigma Aldrich, >99%) dissolved in THF at a concentration of 5.0 mg mL^{-1}. The matrix used was *trans*-2-[3-(4-tert-butylphenyl)-2-methyl-2-propenylidene]-malononitrile (DCTB) (Sigma Aldrich) and was dissolved in THF at a concentration of 40 mg mL^{-1}. Solutions of matrix, salt and polymer were mixed in a volume ratio of 2 : 1 : 2, respectively. The mixed solution was hand spotted on a stainless steel MALDI target and left to air dry. The spectra were recorded in the reflectron mode.

Gel Permeation Chromatography

Polymer molecular weights (M_w, M_n and PDI) were determined by gel permeation chromatography (GPC) using a Polymer Laboratories PL-GPC50 Plus instrument equipped with a Polymer Laboratories PLgel MixedD column (300 mm length, 7.5 mm diameter) and refractive index (RI) detector. Samples were dissolved in THF (Fisher, HPLC grade, stabilized with BHT, 2.5 ppm) at a concentration of 2.0 mg mL^{-1} and filtered prior to injection. THF (Fisher, HPLC grade, stabilized with BHT, 2.5 ppm) was used as the eluent at 30 °C and the flow rate was set to 1.0 mL min^{-1}. Linear polystyrenes (Polymer Laboratories) were used as the primary calibration standards and the appropriate Mark-Houwink corrections for poly(LA) and poly(CL) in THF at 30 °C were used to calculate the experimental molecular weights.

Melting Points

Melting points (m.p.) were recorded in degrees Celsius (°C), using a Leica Galen III hot-stage microscope apparatus and are reported uncorrected.

Determination of enantiomeric ratios

Enantiomeric ratios were determined using analytical high performance liquid chromatography (HPLC) performed on an Agilent Technologies 1200 Series or 1260 Infinity Series systems (column and solvent conditions are given with the compound). For clarity, decimal places were avoided in tables and enantiomeric ratios were rounded up e.g. 97.5:2.5 becomes 98:2.

Optical rotations

Optical rotations were recorded using a Perkin-Elmer 241 polarimeter; specific rotation (SR) ($[\alpha]_D$) are reported in 10^{-1} deg·cm^2·g^{-1}; concentrations (c) are quoted in g/100 mL; D refers to the D-line of sodium (589 nm); temperatures (T) are given in degree Celsius (°C).

Naming

Compound names are those generated by ACD LABS 12.0 software and ACD iLab online chemical database service following the IUPAC nomenclature.

Chapter 2: Organocatalyst immobilisation

1. Catalyst synthesis

1.1 Azide thioureas

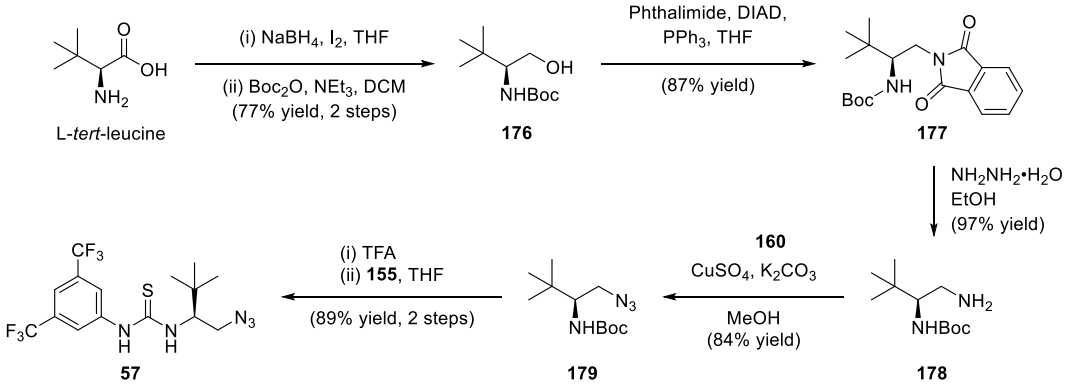

Scheme E1. *Synthesis of thiourea azide **57**.*

(S)-tert-Butyl (1-hydroxy-3,3-dimethylbutan-2-yl)carbamate (**176**)

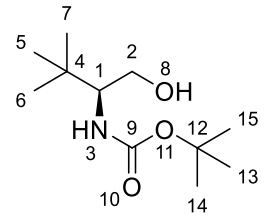

176

Following literature procedures, sodium borohydride (3.4 g, 92 mmol) was suspended in anhydrous THF (100 mL) under argon atmosphere. (L)-*tert*-leucine (4.5 g, 35 mmol) was added and the reaction mixture cooled to 0 °C. A solution of iodine (9.6 g, 38 mmol) in THF (25 mL) was added dropwise to the reaction *via* addition funnel over 30 min. After the addition was complete, the reaction mixture was stirred at room temperature for 15 min, then heated at reflux for 18 h. After cooling to room temperature, methanol was added until the solution became clear and it was stirred for 30 min. The solvent was removed *in vacuo* and the resulting colourless paste dissolved in aqueous KOH (20% w/w, 50 mL) and stirred at room temperature for 3 h. The reaction mixture was then extracted with CH_2Cl_2 (3 × 100 mL), washed with brine and dried over Na_2SO_4. Solvent was removed *in vacuo*, giving (L)-*tert*-leucinol as a colourless solid (4.2 g, quant.) which was used without further purification.

To a solution of (L)-*tert*-leucinol (4.2 g, 36 mmol) and triethylamine (5.9 mL, 43 mmol) in CH_2Cl_2 (114 mL) at 0 °C was added di-*tert*-butyl dicarbonate (9.3 g, 43 mmol) and the reaction mixture stirred for 1 h at 0 °C, then at room temperature for 24 h. The reaction mixture was washed with brine, dried over Na_2SO_4 and the solvent removed *in vacuo*. The residue was purified by flash column chromatography over silica (30% ethyl acetate in petroleum ether, then 50% ethyl acetate in petroleum ether) to give the product as a colourless solid (6.0 g, 77%). **$[\alpha]_D^{25}$** = −5.3 (*c* 1.3, $CHCl_3$), lit. $[\alpha]_D^{25}$ −5.5 (*c* 1.0, $CHCl_3$)[2]; **^{1}H-NMR** (400 MHz, $CDCl_3$) δ (ppm): 4.67 (1 H, d, *J*=5.8 Hz, NH-3), 3.52 - 3.41 (2 H, m, CH_2-2), 2.42 (1 H, br. s., OH-8), 1.44 (9 H, s, CH_3- 13,14,15), 0.92 (9 H, s, CH_3-5,6,7); **^{13}C-NMR** (100 MHz, $CDCl_3$) δ (ppm): 157.4 (C-9), 79.7 (C-12), 63.3 (C-2), 61.1 (C-1), 33.8 (C-4), 28.5 (C-12), 26.9 (C-4); **MP** 92 – 94 °C (lit. 102 – 103 °C). Spectroscopic data consistent with literature values.[2]

(*S*)-*tert*-Butyl (1-(1,3-dioxoisoindolin-2-yl)-3,3-dimethylbutan-2-yl)carbamate (**177**)

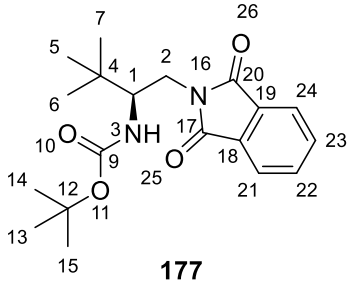

177

N-Boc *tert*-leucinol **176** (6.0 g, 27 mmol), phthalimide (4.1 g, 27 mmol) and triphenylphosphine (7.2 g, 27 mmol) were dissolved in THF (167 mL) under argon atmosphere and cooled to 0 °C. Diisopropyl azodicarboxylate (5.7 mL, 29 mmol) was added dropwise and the reaction stirred at room temperature for 72 h. The solvent was removed *in vacuo* and the residue purified by flash column chromatography over silica (10% ethyl acetate in petroleum ether, then 20% ethyl acetate in petroleum ether, then ethyl acetate) to give the product as a colourless solid (8.3 g, 87%). **$[\alpha]_D^{25}$** = + 45.9 (*c* 1.45, $CHCl_3$), lit. $[\alpha]_D$ + 48.7 (*c* 0.46, $CHCl_3$)[3]; **^{1}H-NMR** (400 MHz, $CDCl_3$) δ (ppm): 7.80 (2 H, dd, *J* = 5.3, 3.0 Hz, ArH), 7.66 (2 H, dd, J = 5.3, 3.0 Hz, ArH), 4.47 (1 H, d, *J*=10.6 Hz, NH-3), 3.84 - 3.76 (2 H, m, CH-1 and $C\underline{H}_a H_b$-2), 3.61 (1 H, dd, *J* = 12.1, 11.4 Hz, $CH_a\underline{H}_b$-2), 1.09 (9 H, s, CH_3-13,14,15), 1.01 (9 H, s, CH_3-5,6,7); **^{13}C-NMR** (100 MHz, $CDCl_3$) δ (ppm): 168.6 (C-17,20), 156.1 (C-9), 133.8 (C-22,23), 132.2 (C-18,19), 123.2 (C-21,24), 79.0 (C-12), 57.6 (C-1), 38.7 (C-2),

33.7 (C-4), 28.0 (C-13,14,15), 26.5 (C-5,6,7); **MP** 142 – 144 °C (lit. 146 – 147 °C); **MS** (ES+) 369.3 $[M+Na]^+$. Spectroscopic data consistent with literature values.[3]

(*S*)-*tert*-Butyl (1-amino-3,3-dimethylbutan-2-yl)carbamate (**178**)

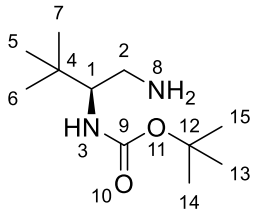

178

Hydrazine monohydrate (7.9 mL, 0.16 mol) was added to a solution of phthalimide **177** (8.3 g, 24 mmol) in absolute ethanol (120 mL) and the reaction mixture heated at reflux for 5 h. The solvent was removed under nitrogen flow and the residue was purified by flash column chromatography over silica (CH_2Cl_2 then 10% methanol in CH_2Cl_2) to give the product as a colourless solid (5.0 g, 97%). **$[\alpha]_D^{25}$** = + 7.2 (*c* 0.94, $CHCl_3$), lit. $[\alpha]_D$ = + 9.8 (*c* 0.48, $CHCl_3$)[3]; **^{1}H-NMR** (400 MHz, $CDCl_3$) δ (ppm): 4.44 (1 H, d, *J*=10.2 Hz, NH-3), 3.33 (1 H, td, *J*=10.5, 3.2 Hz, CH-1), 2.95 (1 H, dd, *J*=13.3, 3.1 Hz, C$\underline{H_a}H_b$-2), 2.38 (1 H, dd, *J*=13.3, 10.6 Hz, $CH_a\underline{H_b}$-2), 1.44 (9 H, s, CH_3-13,14,15), 0.90 (9 H, s, CH_3-5,6,7); **^{13}C-NMR** (100 MHz, $CDCl_3$) δ (ppm): 157.0 (C-9), 79.3 (C-12), 62.3 (C-1), 42.3 (C-2), 34.3 (C-4), 28.5 (C-13,4,15), 26.7 (C-5,6,7); **MP** 82 – 84 °C (lit. 84 °C). Spectroscopic data consistent with literature values.[3]

1*H*-Imidazole-1-sulfonyl azide hydrochloride (**160**)

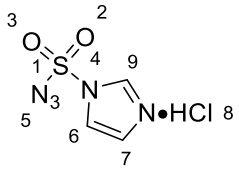

160

Sulfuryl chloride (2.8 mL, 34 mmol) was added dropwise to a solution of sodium azide (2.2 g, 34 mmol) in acetonitrile (34 mL) at 0 °C and the reaction mixture was stirred at room temperature for 24 h. The solution was then cooled to 0 °C and imidazole (4.4 g, 65 mmol) was added portionwise and the reaction stirred at room temperature for 3 h. The reaction mixture was then diluted with ethyl acetate (65 mL), washed with water (2 × 65 mL) and saturated aqueous $NaHCO_3$ (2 × 65 mL), then

dried over Na_2SO_4 and filtered. A solution of HCl in ethanol (6 M, 8.5 mL, obtained by adding acetyl chloride to ice-cooled absolute ethanol) was added dropwise with stirring to the filtrate. The mixture was then cooled in an ice bath until a colourless precipitate appeared, filtered and the filter-cake washed with ethyl acetate (3 × 10 mL). This gave the product as a colourless solid after drying under vacuum (4.3 g, 60%).**^{1}H-NMR** (400 MHz, D_2O) δ (ppm): 9.40 - 9.17 (1 H, m, CH-9), 7.97 (1 H, dd, *J*=2.0, 1.6 Hz, CH-6), 7.55 (1 H, dd, *J*=2.0, 1.2 Hz, CH-7); **^{13}C NMR** (100 MHz, D_2O) δ (ppm): 120.57 (C-9), 123.20 (C-7), 138.04 (C-6). Characterisation data is limited due to the potential explosive nature of this compound. Spectroscopic data consistent with literature values.[4,5]

(*S*)-*tert*-Butyl (1-azido-3,3-dimethylbutan-2-yl)carbamate (**179**)

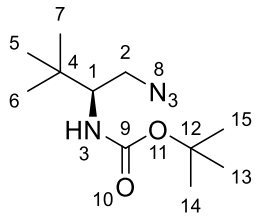

179

1*H*-Imidazole-1-sulfonyl azide hydrochloride **160** (2.9 g, 14 mmol) was added in portions to a solution of amine **178** (2.5 g, 11 mmol), copper sulfate pentahydrate (29 mg, 0.11 mmol) and potassium carbonate (2.7 g, 20 mmol) in methanol (57 mL) at 0 °C and the reaction mixture stirred at room temperature for 24 h. Solvent was removed under nitrogen flow and the residue partitioned between water (50 mL) and diethyl ether (50 mL). The organic layer was washed with brine (50 mL), dried over Na_2SO_4 and solvent removed under nitrogen flow. The residue was purified by flash column chromatography (petroleum ether then 10% ethyl acetate in petroleum ether) to give the product as a colourless solid (2.4 g, 84%). **$[\alpha]_D^{24}$** = −48 (*c* 1.0, $CHCl_3$), lit. $[\alpha]_D$ −46.6 (*c* 0.91, $CHCl_3$)[6]; **^{1}H-NMR** (400 MHz, $CDCl_3$) δ (ppm): 4.53 (1 H, d, *J*=8.9 Hz, NH-3), 3.71 - 3.53 (1 H, m, CH-1), 3.47 (1 H, dd, *J*=12.6, 3.6 Hz, C$\underline{H_a}H_b$-2), 3.22 (1 H, dd, *J*=12.6, 8.2 Hz, C$H_a\underline{H_b}$-2), 1.46 (9 H, s, $CH_3$13,14,15), 0.93 (9 H, s, CH_3-5,6,7); **^{13}C-NMR** (100 MHz, $CDCl_3$) δ (ppm): 155.9 (C-9), 79.6 (C-12), 58.3 (C-1), 52.0 (C-2), 34.2 (C-12), 28.4 (C-13,14,15), 26.6 (C-5,6,7); **MP** 58 – 60 °C; **MS** (ES+) 265.2 $[M+Na]^+$. Spectroscopic data consistent with literature values.[6]

(*S*)-1-(1-Azido-3,3-dimethylbutan-2-yl)-3-(3,5-bis(trifluoromethyl)phenyl)thiourea (**57**)

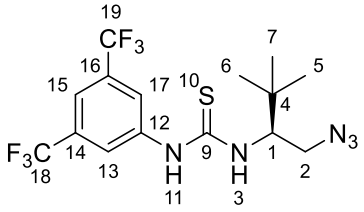

57

Trifluoroacetic acid (7.1 mL) was added dropwise, with stirring, to azide **179** (2.4 g, 9.7 mmol) at 0 °C. The reaction mixture was stirred for 1 h, allowing it to warm to room temperature. Trifluoroacetic acid was removed under nitrogen flow and the residue suspended in diethyl ether (10 mL). Aqueous sodium hydroxide (2 M) was added dropwise to the reaction mixture with vigorous stirring until a pH > 10 was obtained. The organic layer was separated and the aqueous layer extracted with diethyl ether (3 × 10 mL). The combined organic layers were washed with brine (20 mL) and dried over Na_2SO_4. Solvent was removed under nitrogen flow and the residue was dissolved in THF (33 mL) under argon atmosphere. 3,5-Bis(trifluoromethyl)phenyl isothiocyanate (1.8 mL, 9.7 mmol) was added dropwise to the reaction mixture, which was then stirred at room temperature for 24 h. Solvent was removed *in vacuo* and residue was purified by flash column chromatography over silica (5% ethyl acetate in petroleum ether, then 10% ethyl acetate in petroleum ether) to give the product as a colourless solid (3.6 g, 89%). **$[\alpha]_D^{25}$** = −7.8 (*c* 0.98, $CHCl_3$), lit. $[\alpha]_D$ −13.5 (*c* 1.05, $CHCl_3$)[6]; **^{1}H-NMR** (400 MHz, CD_3OD) δ (ppm): 8.24 (2 H, s, CH-13,17), 7.64 (1 H, s, CH-15), 4.73 (1 H, dd, *J*=7.0, 3.1 Hz, CH-1), 3.63 (1 H, dd, *J*=13.0, 3.8 Hz, C$\underline{H_a}H_b$-2), 3.42 (1 H, dd, *J*=12.9, 8.1 Hz, $CH_a\underline{H_b}$-2), 1.03 (9 H, s, CH_3-5,6,7); **^{13}C-NMR** (125 MHz, CD_3OD) δ (ppm): 184.1 (C-9), 143.4 (C-12), 132.7 (q, J_{FC}=33.3 Hz, C-14,16), 123.8 (br. s., C-13,17), 124.9 (q, J_{FC}=271.9 Hz, C-18,19), 118.0 (br. s., C-15), 62.8 (C-1), 52.7 (C-2), 35.8 (C-4), 27.3 (C-5,6,7); **MP** 159 – 160 °C, lit. 164 – 167 °C; **MS** (ES−) 412.1 $[M-H]^-$. Spectroscopic data consistent with literature values.[6]

(*R*)-1-(2-Azido-1-phenylethyl)-3-(3,5-bis(trifluoromethyl)phenyl)thiourea (**107**)

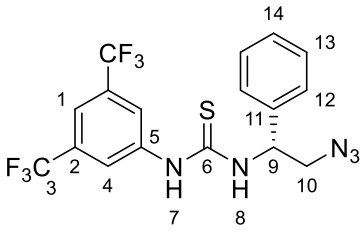

107

Trifluoroacetic acid (0.73 mL) was added dropwise, with stirring, to (*R*)-*tert*-butyl (2-azido-1-phenylethyl)carbamate (0.16 g, 0.62 mmol, synthesised by Dr. Marta Garcia Núñez) at 0 °C. The reaction mixture was stirred for 1 h, allowing to warm to room temperature. Trifluoroacetic acid was removed under nitrogen flow and the residue suspended in diethyl ether (5 mL). Aqueous sodium hydroxide (2 M) was added dropwise to the reaction mixture with vigorous stirring until a pH > 10 was obtained. The organic layer was separated and the aqueous layer extracted with diethyl ether (3 × 5 mL). The combined organic layers were washed with brine (5 mL) and dried over Na_2SO_4. Solvent was removed under nitrogen flow and the residue was dissolved in THF (3 mL) under argon atmosphere. 3,5-Bis(trifluoromethyl)phenyl isothiocyanate (0.12 mL, 0.68 mmol) was added dropwise to the reaction mixture, which was then stirred at room temperature for 24 h. Solvent was removed *in vacuo* and residue was purified by flash column chromatography over silica (5% ethyl acetate in petroleum ether, then 10% ethyl acetate in petroleum ether) to give the product as a colourless solid (0.23 g, 85%). **$[\alpha]_D^{25}$** = +16 (*c* 0.98, $CHCl_3$), lit. $[\alpha]_D^{25}$ = +16.8 (*c* 1.14, $CHCl_3$)[6]; **^{1}H-NMR** (400 MHz, $CDCl_3$) δ (ppm): 8.48 (1 H, br. s, NH-7), 7.77 - 7.29 (8 H, m, ArH), 6.91 (1 H, d, *J* = 6.1 Hz, NH-8), 5.68 (1 H, br. s, CH-9), 3.90 (1 H, dd, *J* = 12.6, 4.8 Hz, C$\underline{H_a}$CH_b-10), 3.77 (1 H, dd, *J* = 12.6, 5.1 Hz, C$H_a\underline{CH_b}$-10); **^{13}C-NMR** (100 MHz, $CDCl_3$) δ (ppm): 180.4 (C-6), 138.8 (C-11), 137.5 (C-5), 133.1 (q, J_{FC} = 35.1 Hz, C-2), 129.4 (C-13), 128.8 (C-14), 126.8 (C-12), 123.9 ('d', J_{FC} = 2.4 Hz, C-4), 119.7 ('dt', J_{FC} = 7.4, 3.9 Hz, C-1), 122.9 (q, J_{FC} = 273.3 Hz, C-3), 57.8 (C-9), 55.0 (C-10); **MP** 128 – 129 °C, lit. 136 – 137 °C; **MS** (ES−) 432.0 $[M-H]^-$. Spectroscopic data consistent with literature values.[6]

1-[(2*R*)-3-azido-1,1-diphenylpropan-2-yl]-3-[3,5-bis(trifluoromethyl)phenyl]thiourea (**180**)

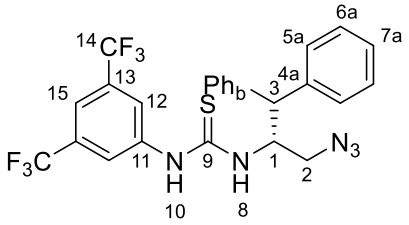

180

Trifluoroacetic acid (1.0 mL) was added dropwise, with stirring, to *tert*-butyl [(2*R*)-3-azido-1,1-diphenylpropan-2-yl]carbamate (0.30 g, 0.85 mmol, synthesised by Dr. Pavol Jakubec) at 0 °C. The reaction mixture was stirred for 1 h, allowing to warm to room temperature. Trifluoroacetic acid was removed under nitrogen flow and the residue suspended in diethyl ether (10 mL). Aqueous sodium hydroxide (2 M) was added dropwise to the reaction mixture with vigorous stirring until a pH > 10 was obtained. The organic layer was separated and the aqueous layer extracted with diethyl ether (3 × 10 mL). The combined organic layers were washed with brine (5 mL) and dried over Na_2SO_4. Solvent was removed under nitrogen flow and the residue was dissolved in THF (3.5 mL) under argon atmosphere. 3,5-Bis(trifluoromethyl)phenyl isothiocyanate (0.16 mL, 0.85 mmol) was added dropwise to the reaction mixture, which was then stirred at room temperature for 24 h. Solvent was removed *in vacuo* and residue was purified by flash column chromatography over silica (10% diethyl ether in petroleum ether) to give the product as a colourless foam (0.43 g, 96%). $\mathbf{[\alpha]_D^{25}}$ = −104 (*c* 1.0, $CHCl_3$), lit. $[\alpha]_D^{25}$ = − 103 (*c* 1.00, $CHCl_3$)[6]; **^{1}H-NMR** (400 MHz, $CDCl_3$) δ (ppm): 8.21 (1 H, s, NH-10), 7.63 (1 H, s, CH-15), 7.30 - 7.10 (12 H, m, ArH), 5.86 (1 H, d, *J*=8.1 Hz, NH-8), 5.42 (1 H, t, *J*=9.7 Hz, CH-1), 4.13 (1 H, d, *J*=11.5 Hz, CH-3), 3.83 (1 H, dd, *J*=12.6, 3.3 Hz, C$\underline{H_a}H_b$-2), 3.19 (1 H, dd, *J*=12.5, 2.2 Hz, $CH_a\underline{H_b}$-2); **^{13}C-NMR** (100 MHz, $CDCl_3$) δ (ppm): 180.0 (C-9), 140.7 (C-4a), 140.2 (C-4b), 137.8 (C-11), 133.5 (q, J_{FC}=33.4 Hz, C-13), 129.3 (C-5a), 129.2 (C-5b), 128.1 (C-6a), 127.9 (C-6b), 127.6 (C-7a), 127.5 (C-7b), 124.4 (br. s, C-12), 120.7 – 119.9 (m, C-15), 122.7 (q, J_{FC}=273.4 Hz, C-14), 57.2 (C-1), 53.0 (C-3), 51.9 (C-2); **MP** 48 – 52 °C, lit. 50 – 53 °C; **MS** (ES+) 524.1 $[M+H]^+$. Spectroscopic data consistent with literature values.[6]

1.2 Polystyrene-supported phosphines

Polystyrene-supported triphenylphosphine (**109**)

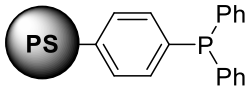

109

To a solution of *iso*-propyl magnesiumchloride (1.5 M, 2.6 mL, 4.0 mmol) in THF (20 mL) at 0 °C under argon atmosphere was added *n*-butyllithium (2.0 M, 4.0 mL, 8 mmol) and the resulting yellow solution was stirred at 0 °C for 30 min. Poly(4-bromostyrene) beads (2.0 mmol/g, 1.0 g, 2.0 mmol) were swollen in THF (20 mL) at 0 °C for 15 min under argon atmosphere. The *i*Pr(*n*Bu)$_2$MgLi solution was then added *via* cannula to the beads and the resulting mixture was stirred slowly at 0 °C for 24 h. Chlorodiphenylphosphine (2.2 mL, 12 mmol) was added dropwise and the reaction mixture was stirred slowly for 1 h at 0 °C, then left to warm to room temperature and stirred for 24 h. The beads were then collected on a sinter funnel and washed with THF (3 × 10 mL, 5 min), CH_2Cl_2: MeOH 1:1 (3 × 10 mL, 5 min) then CH_2Cl_2 (5 × 10 mL, 5 min). Drying under vacuum yielded free-flowing, colourless beads with a calculated loading of 1.65 mmol/g (based on the stated loading of poly(4-bromostyrene).

Polystyrene-supported bis(4-methoxyphenyl)(phenyl)phosphine (**119**)

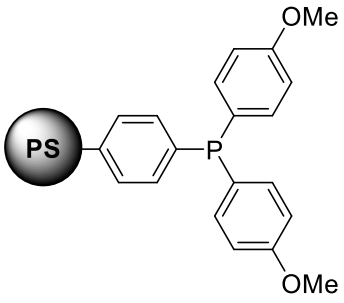

119

To a solution of *iso*-propyl magnesiumchloride (1.5 M, 0.52 mL, 0.80 mmol) in THF (4 mL) at 0 °C under argon atmosphere was added *n*-butyllithium (2.0 M, 0.80 mL, 1.6 mmol) and the resulting yellow solution was stirred at 0 °C for 30 min. Poly(4-bromostyrene) beads (2.0 mmol/g, 0.20 g, 0.40 mmol) were swollen in THF (4 mL) at 0 °C for 15 min under argon atmosphere. The *i*Pr(*n*Bu)$_2$MgLi solution was then added *via* cannula to the beads and the resulting mixture was stirred slowly at 0 °C

for 24 h. Bis(4-methoxyphenyl)chlorophosphine (0.45 g, 1.6 mmol) was dissolved in a minimal amount of THF and added dropwise. The reaction mixture was stirred slowly for 1 h at 0 °C, then left to warm to room temperature and stirred for 24 h. The beads were then collected on a sinter funnel and washed with THF (3 × 10 mL, 5 min), CH_2Cl_2: MeOH 1:1 (3 × 10 mL, 5 min) then CH_2Cl_2 (5 × 10 mL, 5 min). Drying under vacuum yielded free-flowing, colourless beads with a calculated loading of 1.50 mmol/g.

Polystyrene-supported diisopropyl(phenyl)phosphine (**120**)

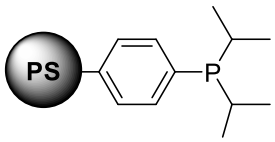

120

To a solution of *iso*-propyl magnesiumchloride (1.3 M, 0.65 mL, 0.8 mmol) in THF (4 mL) at 0 °C under argon atmosphere was added *n*-butyllithium (1.8 M, 0.89 mL, 1.6 mmol) and the resulting yellow solution was stirred at 0 °C for 30 min. Poly(4-bromostyrene) beads (2.0 mmol/g, 0.2 g, 0.4 mmol) were swollen in THF (4 mL) at 0 °C for 15 min under argon atmosphere. The *i*Pr(*n*Bu)$_2$MgLi solution was then added *via* cannula to the beads and the resulting mixture was stirred slowly at 0 °C for 24 h. Chlorodiisopropylphosphine (0.38 mL, 2.4 mmol) was added dropwise and the reaction mixture was stirred slowly for 1 h at 0 °C, then left to warm to room temperature and stir for 24 h. The beads were then collected on a sinter funnel and washed with THF (3 × 10 mL, 5 min), CH_2Cl_2: MeOH 1:1 (3 × 10 mL, 5 min) then CH_2Cl_2 (5 × 10 mL, 5 min). Drying under vacuum yielded free-flowing, colourless beads with a calculated loading of 1.86 mmol/g.

1.3 Polystyrene-supported catalysts

Polystyrene-supported *tert*-butyl/thiourea catalyst (**116**)

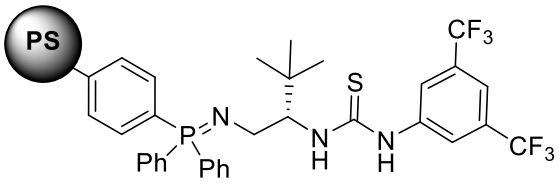

116

Polystyrene supported triphenylphosphine (242 mg, 0.399 mmol) and azide **57** (165 mg, 0.399 mmol) were taken up in anhydrous toluene (3 mL) in a sealed screw-cap glass vial and stirred at room temperature for 24 h after which the disappearance of the azide was observed by TLC. The solvent was carefully removed by syringe and the beads were washed with anhydrous CH_2Cl_2 (3 × 5 mL) in the reaction vial, each time removing the supernatant solution carefully with a syringe. Any remaining solvent was removed under gentle nitrogen flow and the resulting pale yellow beads were dried under vacuum for 24 h. The loading of the polystyrene-supported catalyst was calculated to be 1.01 mmol/g.

Polystyrene-supported phenyl/thiourea catalyst (**108**)

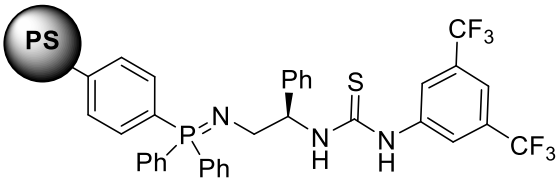

108

Polystyrene supported triphenylphosphine (0.20 g, 0.33 mmol) and azide **107** (0.14 g, 0.33 mmol) were taken up in anhydrous toluene (2.5 mL) in a sealed screw-cap glass vial and stirred at room temperature for 24 h after which the disappearance of the azide was observed by TLC. The solvent was carefully removed by syringe and the beads were washed with anhydrous CH_2Cl_2 (3 × 5 mL) in the reaction vial, each time removing the supernatant solution carefully with a syringe. Any remaining solvent was removed under gentle nitrogen flow and the resulting pale yellow beads were dried under vacuum for 24 h. The loading of the polystyrene-supported catalyst was calculated to be 0.99 mmol/g.

Polystyrene-supported benzhydryl/thiourea catalyst (**137**)

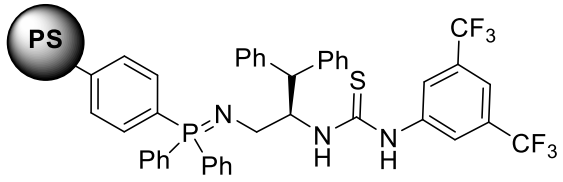

137

Polystyrene supported triphenylphosphine (0.23 g, 0.38 mmol) and azide **180** (0.20 mg, 0.38 mmol) were taken up in anhydrous toluene (2.9 mL) in a sealed screw-cap glass vial and stirred at room temperature for 24 h after which the disappearance of the azide was observed by TLC. The solvent was carefully removed by syringe and the beads were washed with anhydrous CH_2Cl_2 (3 × 5 mL) in the reaction vial, each time removing the supernatant solution carefully with a syringe. Any remaining solvent was removed under gentle nitrogen flow and the resulting pale yellow beads were dried under vacuum for 24 h. The loading of the polystyrene-supported catalyst was calculated to be 0.91 mmol/g.

1.4 Silica-supported catalyst

4-(diphenylphosphanyl)phenol (**111**)

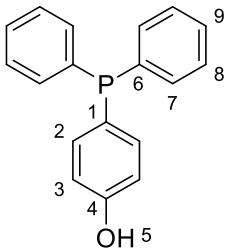

111

A solution of 4-iodophenol (1.1 g, 5.0 mmol), potassium acetate (0.59 g, 6.0 mmol) and $Pd(OAc)_2$ (1.1 mg, 0.005 mmol) in dimethyl acetamide (5.0 mL) was sparged with argon for several minutes. Diphenylphosphine (0.87 mL, 5.0 mmol) was added and the reaction mixture was heated at 130 °C for 3 h. The reaction mixture was then partitioned between CH_2Cl_2 and dilute aqueous lithium chloride. The organic portion was washed twice with dilute aqueous lithium chloride, once with brine and dried over Na_2SO_4. The solvent was removed *in vacuo* and the residue purified by flash column chromatography over silica (10% ethyl acetate in petroleum ether, gradually increasing to 30% ethyl acetate in petroleum ether) to give the product as a colourless solid (1.1 g, 79%). **^{1}H-NMR** (400

MHz, $CDCl_3$) δ (ppm): 7.35 - 7.21 (12 H, m, CH-2,6-9), 6.86 - 6.84 (2 H, m, CH-3), 5.54 (br. s, 1H, OH-5); **^{13}C-NMR** (125 MHz, $CDCl_3$) δ (ppm): 157.0 (C-4), 136.0 (d, J_{PC} = 21 Hz, C-3), 133.6 (d, J_{PC} = 19 Hz, C-8), 128.9 (C-9), 128.6 (d, J_{PC} = 8 Hz, C-7), 116.0 (d, J_{PC} = 9 Hz, C-2); **^{31}P-NMR** (162 MHz, $CDCl_3$) δ (ppm): −6.4; **MP** 100 – 102 °C; **MS** (ES−): 277.1 $[M-H]^-$. Spectroscopic data consistent with literature values.[7]

Si-supported triphenylphosphine (**113**)

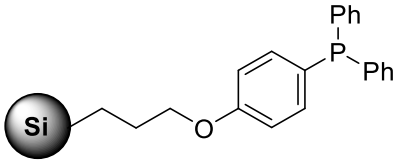

113

Method A:

Silica-supported propyl bromide (1.69 mmol/g, 0.16 g, 0.27 mmol; Silicycle Silia*Bond*®, 40-63 μm), Cs_2CO_3 (95 mg, 0.29 mmol) and phosphine **111** (74 mg, 0.27 mmol) were dissolved in THF (2.5 mL) and heated at reflux for 24 h under argon atmosphere. The reaction mixture was cooled, filtered through a sintered glass funnel and the resulting solid washed with THF (5 mL), distilled water (5 mL) then THF (10 mL). The solid was then dried for 24 h under vacuum over P_2O_5 to give a free flowing, colourless solid (135 mg, 58% of maximum calculated mass).

Method B:

Silica-supported propyl bromide (1.69 mmol/g, 0.15 g, 0.25 mmol; Silicycle Silia*Bond*®, 40-63 μm), K_2CO_3 (42 mg, 0.31 mmol), 18-crown-6 (7.0 mg, 0.025 mmol) and phosphine **111** (71 mg, 0.25 mmol) were dissolved in anhydrous DMF (1 mL) and heated at 70 °C for 24 h under argon atmosphere. The reaction mixture was cooled, filtered through a sintered glass funnel and the resulting solid washed with THF (5 mL), distilled water (5 mL) then THF (10 mL). The solid was then dried for 24 h under vacuum over P_2O_5 to give a free flowing, colourless solid (121 mg, 55% of maximum calculated mass).

1.5 Measurement of loading of Si-supported triphenylphosphine

1-(Azidomethyl)naphthalene (**114**)

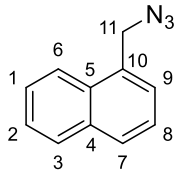

114

To a solution of 1-(chloromethyl)naphthalene (59 μL, 0.40 mmol) in acetonitrile (1 mL) was added sodium azide (39 mg, 0.59 mmol) and the reaction mixture heated at reflux for 24 h. The reaction was cooled to room temperature, solvent removed *in vacuo* and the residue partitioned between diethyl ether (5 mL) and water (5 mL). The aqueous portion was extracted with diethyl ether (2 × 2mL) and the combined organic portions were dried over Na_2SO_4. The solvent was removed *in vacuo* and residue purified by flash column chromatography over silica (2% diethyl ether in petroleum ether) to give the product as a colourless oil (63 mg, 87%). **^{1}H-NMR** (400 MHz, $CDCl_3$) δ (ppm): 8.05 - 7.45 (7 H, m, H1-3,6-9), 4.78 (2 H, s, CH_2-11); **^{13}C-NMR** (100 MHz, $CDCl_3$) δ (ppm): 134.0 (C-4), 131.5 (C-5), 131.1 (C-10), 129.6 (C-7), 128.9 (C-3), 127.4 (C-1), 126.9 (C-9), 126.3 (C-2), 125.3 (C-8), 123.6 (C-6), 53.1 (C-11). Spectroscopic data consistent with literature values.[8]

Measurement procedure

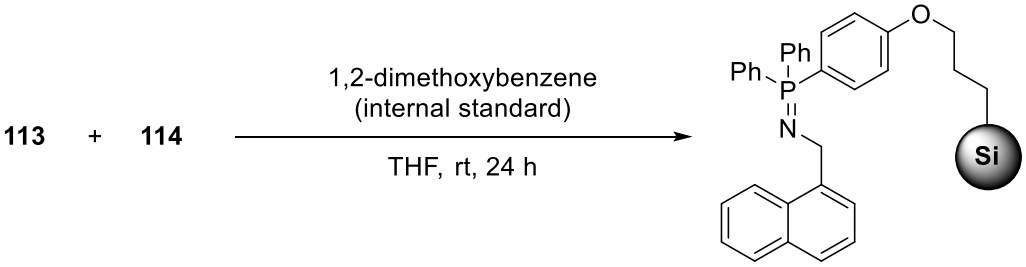

1-(Azidomethyl)naphthalene **114** (16 mg, 0.088 mmol) and 1,2-dimethoxybenzene (10 μL, 0.082 mmol) in THF (1 mL) were transferred to a flask containing triphenylphosphine-functionalised silica **113** (38 mg) under argon atmosphere. The reaction mixture was stirred at room temperature for 24 h, filtered to remove silica, and the solvent removed *in vacuo*. ^{1}H-NMR analysis of the residue enabled calculation of the triphenylphosphine content of the silica.

2. Proof of Concept procedure

In a screw-cap vial, polystyrene-supported triphenylphosphine (commercial – 13.0 mg, 3 mmol/g, 0.04 mmol or synthesised – 24 mg, 1.65 mmol/g, 0.04 mmol) and azide **107** (8.7 mg, 0.02 mmol) were stirred in anhydrous toluene (0.25 mL) at room temperature for 24 h. TLC analysis indicated the complete consumption of the azide. Ketimine **36a** (64 mg, 0.2 mmol) and nitromethane (0.22 mL, 4.0 mmol) were added and the reaction mixture was stirred at 0 °C for 24 h. The reaction mixture was then diluted with CH_2Cl_2 and filtered through a plug of cotton wool to remove the catalyst. The solvent was removed *in vacuo* and the conversion was measured by ^{1}H-NMR analysis of the crude reaction mixture. The crude reaction mixture was then purified by flash column chromatography over silica (50% ethyl acetate in petroleum ether). The enantiomeric excess was determined by HPLC analysis (Chiralpak OD-H, hexane/*iso*-propanol 80:20, λ 220 nm, 1.0 mL/min: t (minor) 8.1 min, t (major) = 20.3 min. See **37a** for full characterisation of product.

3. Nitro-Mannich with silica-supported catalyst

Silica-supported triphenylphosphine **113** (37 mg, 0.017 mmol) and azide **107** (6.8 mg, 0.016 mmol) were dissolved in anhydrous toluene (0.5 mL) and stirred at room temperature for 24 h under argon atmosphere. TLC analysis of the reaction mixture showed the complete consumption of the azide. Ketimine **36a** (50 mg, 16 mmol) and nitromethane (0.17 mL, 3.1 mmol) were added and the reaction mixture stirred 24 h at room temperature under argon atmosphere. The reaction mixture was then filtered through cotton wool to remove the solid-supported catalyst, which was washed with CH_2Cl_2. ^{1}H-NMR analysis of the crude reaction mixture indicated the product was obtained in 54% conversion. The solvent was removed *in vacuo* and the residue purified by flash column chromatography over silica (20% petroleum ether in ethyl acetate) to give a pure sample of the product as a colourless solid. The enantiomeric excess was determined by HPLC analysis (Chiralpak OD-H, hexane/*iso*-propanol 80:20, λ 220 nm, 1.0 mL/min: t (minor) 8.1 min, t (major) = 20.3 min (13:87 e.r.)). See **37a** for full characterisation of product.

4. Nitro-Mannich reaction

4.1 Preparation of phosphinoyl ketimines (General Procedure A)

Ketone (1.0 equiv.) was added to a solution of sodium acetate (1.5 equiv.) and hydroxylamine hydrochloride (1.5 equiv.) in 1:1 ethanol:water (1.8 M) and the reaction mixture was heated at 90 °C for 24 h. The reaction mixture was then cooled to room temperature, ethyl acetate added and the organic portion washed with brine and dried over Na_2SO_4. Solvent was removed *in vacuo* and the residue dried under high vacuum for 24 h to give the oxime which was used without further purification.

Triethylamine (1.1 equiv.) was added dropwise to a solution of oxime (1.0 equiv.) in 1:1 CH_2Cl_2: hexane (0.3 M) under argon atmosphere at −50 °C and the reaction mixture stirred for 10 min. Chlorodiphenylphosphine (1.1 equiv.) was then added *via* syringe pump over the course of 1 h, maintaining the temperature at −50 °C. The reaction mixture was stirred at −50 °C for 1 h, then stirred for 24 h, warming to room temperature. The solvent was removed *in vacuo* and the residue dissolved in CH_2Cl_2 and washed with water. The organic layer was then washed with brine, dried over Na_2SO_4 and the solvent removed *in vacuo*. The residue was purified by flash column chromatography over silica to give the diphenylphosphinoyl ketimine as a colourless solid.

(*E*)-*P*,*P*-diphenyl-*N*-(1-phenylethylidene)phosphinic amide (**36a**)

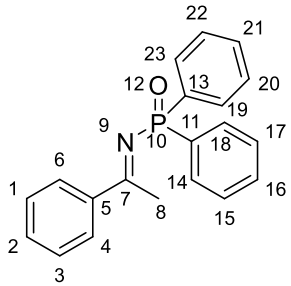

36a

Ketimine **36a** was isolated as a colourless solid (7.6 g, 55%) following General Procedure A. **^{1}H-NMR** (400 MHz, $CDCl_3$) δ (ppm): 8.14 - 7.38 (m, 15 H, ArH), 2.98 (3 H, d, J_{PH}=2.1 Hz, CH_3-8); **^{13}C-NMR** (100 MHz, $CDCl_3$) δ (ppm): 181.6 (d, J_{PC}=8.0 Hz, C-7), 139.5 (d, J_{PC}=24.0 Hz, C-5), 134.8 (d, J_{PC}=131.0 Hz, C-11,13), 132.5 (C-2), 131.7 (d, J_{PC}=8.8 Hz, C-14,18,19,23), 131.5 (d, J_{PC}=2.4 Hz, C-16,21), 128.6 (d, J_{PC}=6.4 Hz, C-15,17,20,22), 128.4 (C-1,3), 128.0 (C-4,6), 23.1 (d,

J_{PC}=12.0 Hz, C-8); **^{31}P-NMR** (162 MHz, $CDCl_3$) δ (ppm): 19.0; **MP** 134 – 136 °C, lit. 129 – 130 °C; **MS** (ES+) 319.0 $[M+H]^+$. Spectroscopic data consistent with literature values.[9]

4.2 Nitro-Mannich reaction (General Procedure B)

To polystyrene supported catalyst **116** (19.8 mg, 0.0200 mmol) and ketimine (0.200 mmol) in a screw-cap vial was added anhydrous toluene (25 µL) and nitromethane (215 µL, 4.00 mmol). The vial was sealed and the reaction mixture stirred at 0 °C for the indicated time. The reaction mixture was then diluted with CH_2Cl_2 and filtered through a plug of cotton wool to remove the catalyst. The solvent was removed *in vacuo* and the conversion was measured by ^{1}H-NMR of the crude reaction mixture. The crude reaction mixture was then purified by flash column chromatography over silica (50% ethyl acetate in petroleum ether) to give adducts **37a-h**.

Nitro-Mannich adducts **37a-h** have been reported and characterised previously in the literature.[6] Their physical and spectroscopic properties are in agreement to those reported.

N-[(2*R*)-1-Nitro-2-phenylpropan-2-yl]-*P*,*P*-diphenylphosphinic amide (**37a**)

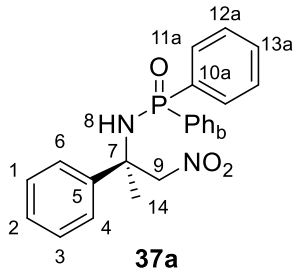

37a

Compound **37a** was obtained as a colourless solid (55.2 mg, 73%) following General Procedure B. The enantiomeric excess was determined by HPLC analysis (Chiralpak OD-H, hexane/*iso*-propanol 80:20, λ 220 nm, 1.0 mL/min: t (minor) 8.1 min, t (major) = 20.3 min (98:2 e.r.)). **$[\alpha]_D^{25}$** = −22 (*c* 0.50, $CHCl_3$, 98:2 e.r.), lit. $[\alpha]_D^{25}$ = −22.5 (*c* 0.50, $CHCl_3$, 95% e.e.)[6]; **^{1}H NMR** (400 MHz, $CDCl_3$) δ (ppm): 8.04 - 7.99 (2 H, m, CH-11a), 7.85 - 7.80 (2 H, m, CH-11b), 7.55 – 7.43 (8 H, m, CH-4,6,12a,13a,12b,13b), 7.37 (2 H, t, *J* = 7.7 Hz, CH-1,3), 7.29 - 7.28 (1 H, m, CH-2), 5.45 (1 H, d, *J*=13.4 Hz,C$\underline{H}_a$H$_b$-9), 5.05 (1 H, d, *J*=13.4 Hz, CH$_a$$\underline{H}_b$-9), 4.49 (1 H, d, *J*=4.3 Hz, NH-8), 1.55 (3 H, s, CH_3-14); **^{13}C NMR** (101 MHz, $CDCl_3$) δ (ppm): 143.1 (d, J_{CP}=7.6 Hz, C-5), 134.0 (d, J_{CP}=125.1 Hz, C-10a), 133.7 (d, J_{CP}=130.8 Hz, C-10b), 132.2 (d, J_{CP}=9.5 Hz, C-11a), 132.0 (d, J_{CP}=2.9 Hz, C-

13a), 132.0 (d, J_{CP}=2.9 Hz, C-13b), 131.0 (d, J_{CP}=9.5 Hz, C-11b), 128.9 (C-1,3), 128.8 (d, J_{CP}=12.4 Hz, C-12a), 128.6 (d, J_{CP}=13.4 Hz, C-12b), 127.9 (C-2), 124.6 (C-4,6), 84.3 (C-9), 59.9 (d, J_{CP}=2.9 Hz, C-7), 27.2 (d, J_{CP}=3.8 Hz, C-14); **^{31}P-NMR** (162 MHz, $CDCl_3$) δ (ppm): 22.8; **MP** 154 - 156 °C, lit. 161 – 163 °C; **MS** (ES+) 404.0 $[M+Na]^+$. Spectroscopic data consistent with literature values.[6]

N-[(2*R*)-2-(4-Methylphenyl)-1-nitropropan-2-yl]-*P*,*P*-diphenylphosphinic amide (**37b**)

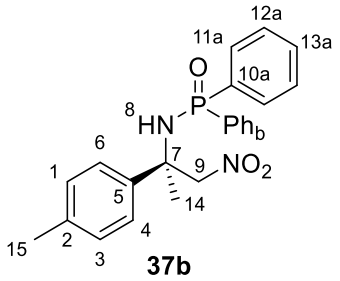

37b

Compound **37b** was obtained as a colourless solid (65.1 mg, 82%) following General Procedure B. The enantiomeric excess was determined by HPLC analysis (Chiralpak OD-H, hexane/*iso*-propanol 80:20, λ 220 nm, 1.0 mL/min: t (minor) 7.9 min, t (major) = 30.4 min (97:3 e.r.)). **$[\alpha]_D^{25}$** = −20 (*c* 0.51, $CHCl_3$, 97:3 e.r.), lit. $[\alpha]_D^{25}$ = −29.1 (*c* 0.98, $CHCl_3$, 89% e.e.)[6]; **^{1}H NMR** (400 MHz, $CDCl_3$) δ (ppm): 8.03 - 7.98 (2 H, m, CH-11a), 7.85 - 7.79 (2 H, m, CH-11b), 7.53 - 7.42 (6 H, m, CH-12a,12b,13a,13b), 7.39 (2 H, d, *J* = 8.3 Hz, CH-4,6), 7.16 (2 H, d, *J* = 8.0 Hz, CH-1,3), 5.42 (1 H, d, *J*=13.3 Hz, C$\underline{H}_a$H$_b$-9), 5.03 (1 H, d, *J*=13.3 Hz, CH$_a$$\underline{H}_b$-9), 4.47 (1 H, d, *J*=4.7 Hz, NH-8), 2.31 (3 H, s, CH_3-15), 1.53 (3 H, s, CH_3-14); **^{13}C NMR** (101 MHz, $CDCl_3$) δ (ppm): 140.2 (d, J_{CP}=7.8 Hz, C-5), 137.8 (C-2), 134.1 (d, J_{CP}=125.8 Hz, C-10a), 133.9 (d, J_{CP}=131.8 Hz, C-10b), 132.3 (d, J_{CP}=9.7 Hz, C-11a), 132.0 (“t”, J_{CP}=4.0 Hz, C-13a,13b), 131.1 (d, J_{CP}=9.7 Hz, C-11b), 129.7 (C-1,3), 128.9 (d, J_{CP}=12.9 Hz, C-12a), 128.7 (d, J_{CP}=13.0 Hz, C-12b), 124.7 (C-4,6), 84.6 (C-9), 59.8 (d, J_{CP}=2.4 Hz, C-7), 27.3 (d, J_{CP}=3.4 Hz, C-14), 21.0 (C-15); **^{31}P-NMR** (162 MHz, $CDCl_3$) δ (ppm): 22.6; **MP** 56 - 60 °C, lit. 46 – 50 °C; **MS** (ES+) 395.1 $[M+H]^+$. Spectroscopic data consistent with literature values.[6]

N-[(2*R*)-2-(4-Methoxyphenyl)-1-nitropropan-2-yl]-*P*,*P*-diphenylphosphinic amide (**37c**)

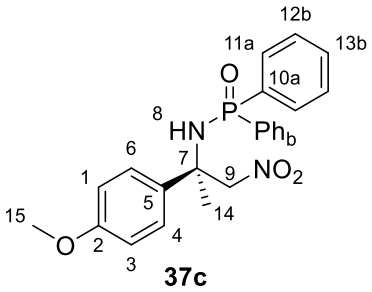

37c

Compound **37c** was obtained as a colourless solid (61.6 mg, 75%) following General Procedure B. The enantiomeric excess was determined by HPLC analysis (Chiralpak OD-H, hexane/*iso*-propanol 80:20, λ 220 nm, 1.0 mL/min: t (minor) 10.6 min, t (major) = 16.8 min (96:4 e.r.)). **$[\alpha]_D^{25}$** = − 30 (*c* 0.50, $CHCl_3$, 96:4 e.r.), lit. $[\alpha]_D^{25}$ = −33.0 (*c* 0.94, $CHCl_3$, 91% e.e.)[6]; **^{1}H NMR** (400 MHz, $CDCl_3$) δ (ppm): 7.99 (2 H, dd, *J*=11.6, 7.5 Hz, CH-11a), 7.82 (2 H, dd, *J*=11.9, 7.5 Hz, CH-11b), 7.52 - 7.40 (8 H, m, CH-12a,12b,13a,13b), 6.86 (d, *J*=8.8 Hz, 2 H, CH-1,3), 5.37 (1 H, d, *J*=13.2 Hz, C$\underline{H_a}H_b$-9), 5.02 (1 H, d, *J*=13.0 Hz, $CH_a\underline{H_b}$-9), 4.45 (1 H, d, *J*=3.7 Hz, NH-8), 3.77 (3 H, s, CH_3-15), 1.54 (3 H, s, CH_3-14); **^{13}C NMR** (101 MHz, $CDCl_3$) δ (ppm): 159.2 (C-2), 134.9 (d, J_{CP}=7.2 Hz, C-5), 134.1 (d, J_{CP}=126.8 Hz, C-10a), 134.0 (d, J_{CP}=116.7 Hz, C-10b), 132.3 (d, J_{CP}=9.5 Hz, C-11a), 132.1 (br. s., C-13a,13b), 131.2 (d, J_{CP}=9.5 Hz, C-11b), 128.9 (d, J_{CP}=11.1 Hz, C-12a), 128.7 (d, J_{CP}=10.3 Hz, C-12b), 126.2 (C-4,6), 114.2 (C-1,3), 84.7, (C-9), 59.6 (C-7), 55.4 (C-15), 27.3 (br. s., C-14); **^{31}P-NMR** (162 MHz, $CDCl_3$) δ (ppm): 22.5; **MP** 130 - 132 °C, lit. 148 – 151 °C; **MS** (ES+) 411.1 $[M+H]^+$. Spectroscopic data consistent with literature values.[6]

N-[(2*R*)-2-(4-Chloro)-1-nitropropan-2-yl]-*P*,*P*-diphenylphosphinic amide (**37d**)

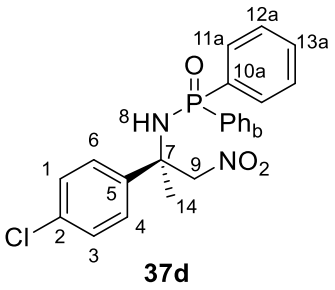

37d

Compound **37d** was obtained as a colourless solid (73.1 mg, 88%) following General Procedure B. The enantiomeric excess was determined by HPLC analysis (Chiralpak OD-H, hexane/*iso*-propanol 80:20, λ 220 nm, 1.0 mL/min: t (minor) 7.4 min, t (major) = 10.6 min (97:3 e.r.)). **$[\alpha]_D^{25}$** = − 45 (*c*

0.50, $CHCl_3$, 97:3 e.r.), lit. $[\alpha]_D^{25}$ = −37.9 (*c* 1.00, $CHCl_3$, 90% e.e.)[6]; **^{1}H NMR** (400 MHz, $CDCl_3$) δ (ppm): 7.99 - 7.94 (2 H, m, CH-11a), 7.83 - 7.78 (2 H, m, CH-11b), 7.55 - 7.43 (m, 8 H, CH-12a,12b,13a,13b,1,3), 7.32 - 7.29 (2 H, m, CH-4,6), 5.39 (1 H, d, *J*=13.2 Hz, C$\underline{H_a}H_b$-9), 5.01 (1 H, d, *J*=13.4 Hz, C$H_a\underline{H_b}$-9), 4.48 (1 H, d, *J*=4.4 Hz, NH-8), 1.53 (3 H, s, CH_3-14); **^{13}C NMR** (101 MHz, $CDCl_3$) δ (ppm): 141.6 (d, J_{CP}=7.2 Hz, C-5), 134.0 (C-2), 133.9 (d, J_{CP}=125.8 Hz, C-10a), 133.6 (d, J_{CP}=130.8 Hz, C-10b), 132.2 (C-13a,13b), 132.1 (C-11a), 131.2 (d, J_{CP}=9.5 Hz, C-11b)), 129.1 (C-1,3), 128.9 (d, J_{CP}=9.5 Hz, C-12a), 128.8 (d, J_{CP}=9.5 Hz, C-12b), 126.4 (C-4,6), 84.3 (C-9), 59.7 (d, J_{CP}=1.6 Hz, C-7), 27.2 (d, J_{CP}=3.2 Hz, C-14); **^{31}P-NMR** (162 MHz, $CDCl_3$) δ (ppm): 22.7; **MP** 136 - 140 °C, lit. 152 – 154 °C; **MS** (ES+) 415.1 $[M+H]^+$. Spectroscopic data consistent with literature values.[6]

N-[(2*R*)-2-(3,4-Dichloro)-1-nitropropan-2-yl]-*P*,*P*-diphenylphosphinic amide (**37e**)

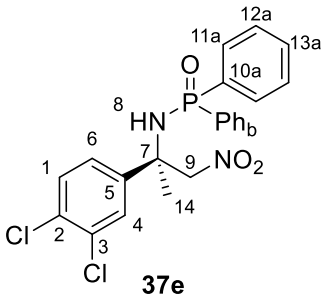

37e

Compound **37e** was obtained as a colourless solid (78.4mg, 87%) following General Procedure B. The enantiomeric excess was determined by HPLC analysis (Chiralpak OD-H, hexane/*iso*-propanol 80:20, λ 220 nm, 1.0 mL/min: t (minor) 8.8 min, t (major) = 15.8 min (95:5 e.r.)). **$[\alpha]_D^{25}$** = − 40 (*c* 0.50, $CHCl_3$, 95:5 e.r.), lit. $[\alpha]_D^{25}$ = −37.0 (*c* 1.06, $CHCl_3$, 87% e.e.)[6]; **^{1}H NMR** (400 MHz, $CDCl_3$) δ (ppm): 7.96 - 7.91 (2 H, m, CH-11a), 7.81 - 7.76 (2 H, m, CH-11b), 7.59 - 7.31 (m, 9 H, ArH), 5.37 (1 H, d, *J*=13.4 Hz, C$\underline{H_a}H_b$-9), 5.01 (1 H, d, *J*=13.4 Hz, C$H_a\underline{H_b}$-9), 4.47 (1 H, d, *J*=4.4 Hz, NH-8), 1.53 (3 H, s, CH_3-14); **^{13}C NMR** (101 MHz, $CDCl_3$) δ (ppm): 143.3 (d, J_{CP}=7.2 Hz, C-5), 133.2 (C-3), 133.5 (d, J_{CP}=125.8 Hz, C-10a), 133.3 (d, J_{CP}=130.8 Hz, C-10b), 132.3 (m, C-13a,13b), 132.3 (C-2), 132.1 (d, J_{CP}=9.5 Hz, C-11a), 131.2 (d, J_{CP}=10.3 Hz, C-11b), 130.9 (C-3), 128.9 (d, J_{CP}=12.7 Hz, C-12a), 128.9 (d, J_{CP}=12.7 Hz, C-12b), 127.5 (C-4), 124.5 (C-6), 84.0 (d, J_{CP}=1.6 Hz, C-9), 59.4 (d, J_{CP}=2.4 Hz, C-7), 27.1 (d, J_{CP}=4.0 Hz, C-14); **^{31}P-NMR** (162 MHz, $CDCl_3$) δ (ppm): 23.0; **MP**

132 - 135 °C, lit. 102 – 105 °C; **MS** (ES+) 449.0 $[M+H]^+$, 471.0 $[M+Na]^+$. Spectroscopic data consistent with literature values.[6]

N-[(2*R*)-2-(2-Methoxyphenyl)-1-nitropropan-2-yl]-*P*,*P*-diphenylphosphinic amide (**37f**)

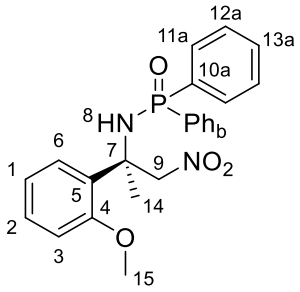

37f

Compound **37f** as a colourless oil (79.1 mg, 97%) following General Procedure B. The enantiomeric excess was determined by HPLC analysis (Chiralpak OD-H, hexane/*iso*-propanol 80:20, λ 220 nm, 1.0 mL/min: t (minor) 8.4 min, t (major) = 15.3 min (97:3 e.r.)). **$[\alpha]_D^{25}$** = + 29 (*c* 0.53, $CHCl_3$, 97:3 e.r.), lit. $[\alpha]_D^{25}$ = −31.0 (*c* 0.89, $CHCl_3$, 93% e.e.)[6]; **^{1}H NMR** (400 MHz, $CDCl_3$) δ (ppm): 7.88 (2 H, dd, *J*=12.0, 7.3 Hz, CH-11a), 7.81 (2 H, dd, *J*=11.2, 7.6 Hz, CH-11b), 7.36 - 7.59 (7 H, m, ArH), 7.27 - 7.35 (1 H, m, ArH), 6.99 (1 H, td, *J*=7.6, 1.0 Hz, ArH), 6.92 (1 H, dd, *J*=8.2, 0.9 Hz, ArH), 5.35 (1 H, d, *J*=11.7 Hz, C$\underline{H_a}H_b$-9), 5.23 (1 H, d, *J*=11.5 Hz, C$H_a\underline{H_b}$-9), 5.00 (1 H, d, *J*=4.9 Hz, NH-8), 3.83 (3 H, s, CH_3-15), 1.74 (3 H, s, CH_3-14); **^{13}C NMR** (101 MHz, $CDCl_3$) δ (ppm): 156.5 (C-4), 134.6 (d, J_{CP}=127.8 Hz, C-10a), 134.3 (d, J_{CP}=132.8 Hz, C-10b), 132.2 (d, J_{CP}=9.5 Hz, C-11a), 132.0 (br. s, C-13a), 131.9 (br. s, C-13b), 131.0 (d, J_{CP}=9.5 Hz, C-11b), 129.8 (C-6), 129.6 (d, J_{CP}=6.4 Hz, C-5), 128.8 (d, J_{CP}=12.7 Hz, C-12a), 128.6 (d, J_{CP}=12.7 Hz, C-12b), 127.4 (C-2), 121.5 (C-1), 111.9 (C-3), 84.4 (C-9), 59.6 (C-15), 55.5 C-7), 23.1 (d, J_{CP}=2.4 Hz, C-14); **^{31}P-NMR** (162 MHz, $CDCl_3$) δ (ppm): 21.8; **MS** (ES+) 411.1 $[M+H]^+$. Spectroscopic data consistent with literature values.[6]

N-[(2*R*)-1-Nitro-2-phenylbutan-2-yl]-*P*,*P*-diphenylphosphinic amide (**37g**)

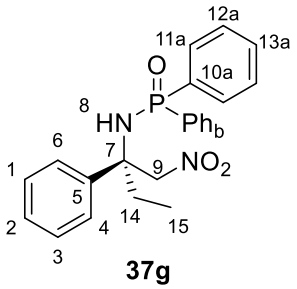

37g

Compound **37g** was obtained as a colourless solid (55.8 mg, 71%) following General Procedure B. The enantiomeric excess was determined by HPLC analysis (Chiralpak OD-H, hexane/*iso*-propanol 80:20, λ 220 nm, 1.0 mL/min: t (minor) 6.5 min, t (major) = 19.2 min (97:3 e.r.)). **$[\alpha]_D^{25}$** = −12 (*c* 0.52, $CHCl_3$, 97:3 e.r.), lit. $[\alpha]_D^{25}$ = −4.3 (*c* 1.05, $CHCl_3$, 92% e.e.)[6]; **^{1}H NMR** (400 MHz, $CDCl_3$) δ (ppm): 7.98 - 7.92 (2 H, m, CH-11a), 7.74 - 7.69 (2 H, m, CH-11b), 7.48 - 7.31 (7 H, m, ArH), 7.26 - 7.22 (2 H, m, ArH), 7.19 - 7.14 (m, 1 H), 5.47 (1 H, d, *J*=13.9 Hz, C$\underline{H}_a$H$_b$-9), 5.20 (1 H, d, *J*=13.7 Hz, CH$_a\underline{H}_b$-9), 4.26 (1 H, d, *J*=4.6 Hz, NH-8), 1.90 (2 H, q, *J*=7.3 Hz, CH_2-14), 0.37 (3 H, t, *J*=7.3 Hz, CH_3-15); **^{13}C NMR** (101 MHz, $CDCl_3$) δ (ppm): 140.5 (d, J_{CP}=7.9 Hz, C-5), 134.1 (d, J_{CP}=124.8 Hz, C-10a), 133.9 (d, J_{CP}=130.8 Hz, C-10b), 132.2 (d, J_{CP}=9.5 Hz, C-11a), 132.1 - 132.0 (C-13a,13b), 131.2 (d, J_{CP}=10.3 Hz, C-11b), 128.8 - 128.6 (C-1,3,12a,12b), 127.9 (C-2), 126.0 (C-4,6), 81.4 (C-9), 63.8 (d, J_{CP}=3.2 Hz, C-7), 32.3 (d, J_{CP}=3.2 Hz, C-14), 8.7 (C-15); **^{31}P-NMR** (162 MHz, $CDCl_3$) δ (ppm): 22.7; **MP** 128 - 132 °C, lit. 133 – 137 °C; **MS** (ES+) 395.2 $[M+H]^+$. Spectroscopic data consistent with literature values.[6]

N-[(2*R*)-2-(Pyridin-3-yl)-1-nitropropan-2-yl]-*P*,*P*-diphenylphosphinic amide (**37h**)

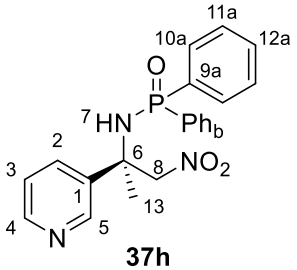

37h

Compound **37h** was obtained as a colourless solid (72.1 mg, 95%) following General Procedure B, with purification by flash column chromatography eluting with 10% methanol in CH_2Cl_2. The enantiomeric excess was determined by HPLC analysis (Chiralpak AD-H, hexane/*iso*-propanol

80:20, λ 220 nm, 1.0 mL/min: t (major) 15.3 min, t (minor) = 18.3 min (93:7 e.r.)). **$[\alpha]_D^{25}$** = − 28 (*c* 0.50, $CHCl_3$, 93:7 e.r.), lit. $[\alpha]_D^{25}$ = −17.8 (*c* 0.80, $CHCl_3$, 82% e.e.)[6]; **^{1}H NMR** (400 MHz, $CDCl_3$) δ (ppm): 8.73 (1 H, d, *J*=1.6 Hz, CH-5), 8.40 (1 H, d, *J*=4.0 Hz, CH-4), 7.90 - 7.84 (2 H, m, CH-10a), 7.75 - 7.68 (2 H, m, CH-10a), 7.45 - 7.32 (7 H, m, ArH), 7.19 - 7.16 (1 H, m, CH-3), 5.33 (1 H, d, *J*=13.0 Hz, C$\underline{H}_a$H$_b$-8), 4.96 (1 H, d, *J*=13.0 Hz, CH$_a$$\underline{H}_b$-8), 4.42 (1 H, d, *J*=4.3 Hz, NH-7), 1.47 (3 H, s, CH_3-13); **^{13}C NMR** (101 MHz, $CDCl_3$) δ (ppm): 149.3 (C-5), 146.8 (C-4), 138.7 - 138.7 (m, C-1), 133.6 (d, J_{CP}=126.4 Hz, C-9a), 132.9 (C-2), 133.4 (d, J_{CP}=131.1 Hz, C-9b), 132.3 ('t', J_{CP}=3.2 Hz, C-12a,12b), 132.1 (d, J_{CP}=9.5 Hz, C-10a), 131.2 (d, J_{CP}=10.3 Hz, C-10b), 129.0 (d, J_{CP}=12.7 Hz, C-11a), 128.9 (d, J_{CP}=12.7 Hz, C-11b), 123.6 (C-3), 83.9 (C-8), 58.8 (d, J_{CP}=2.4 Hz, C-6), 27.2 (d, J_{CP}=3.2 Hz, C-13); **^{31}P-NMR** (162 MHz, $CDCl_3$) δ (ppm): 22.0; **MP** 112 - 114 °C, lit. 70 – 72 °C; **MS** (ES+) 382.1 $[M+H]^+$, 404.1 $[M+Na]^+$. Spectroscopic data consistent with literature values.[6]

5. Conjugate addition of substituted malonates

5.1 Preparation of substituted dimethyl malonates (General Procedure C)

To a suspension of sodium hydride (96.0 mg, 2.40 mmol, 60% in mineral oil) in anhydrous DMF (10 mL) at 0 °C under argon atmosphere was added diethyl malonate (364 μL, 2.40 mmol) dropwise. The resulting mixture was stirred for 30 min at 0 °C. Alkyl bromide (2.00 mmol) was then added and the reaction mixture stirred at room temperature for 24 h (**122d**) or heated at 80 °C for 24 h (**122e-h**). The reaction mixture was then partitioned between water and diethyl ether, the organic phase separated and the aqueous phase extracted twice with diethyl ether. The combined organic phases were washed with brine, dried over anhydrous Na_2SO_4 and the solvent removed *in vacuo* to yield the crude substituted diethyl malonate as a yellow oil.

The crude substituted diethyl malonate was dissolved in methanol (10 mL), treated with thionyl chloride (1.5 mL, 20 mmol) and the resulting mixture was heated at reflux for 24 h. The volatiles were removed *in vacuo* and the residue purified by flash column chromatography over silica (5% ethyl acetate in petroleum ether, then 10% ethyl acetate in petroleum ether) to yield the substituted dimethyl malonate as a colourless oil.

Dimethyl 2-(3-chloropropyl)malonate (**122d**)

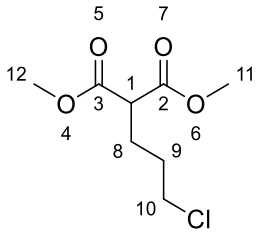

122d

Compound **122d** was isolated as a colourless oil (267 mg, 76% over 2 steps) following General Procedure C. **^{1}H NMR** (400 MHz, $CDCl_3$) δ (ppm): 3.73 (6 H, s, CH_3-11,12), 3.53 (2 H, t, *J*=6.5 Hz, CH_2-10), 3.38 (1 H, t, *J*=7.5 Hz, CH-1), 2.10 - 1.97 (2 H, m, CH_2-9), 1.88 - 1.73 (2 H, m, CH_2-8); **^{13}C NMR** (101 MHz, $CDCl_3$) δ (ppm): 169.6 (C-2,3), 52.7 (C-11,12), 51.0 (C-1), 44.2 (C-10), 30.2 (C-9), 26.3 (C-8); **IR** ν_{max}/cm^{-1} 2956, 1731, 1436, 1199, 1147, 1064; **MS** (ES+) 209.0 $[M+H]^+$; **HRMS** (ES+) calcd. for $C_8H_{13}ClNaO_4$ $[M+Na]^+$ 231.0395, found 231.0395.

Dimethyl 2-isobutylmalonate (**122e**)

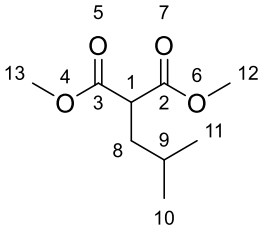

122e

Compound **122e** was isolated as a colourless oil (220 mg, 58% over 2 steps) following General Procedure C. **^{1}H NMR** (400 MHz, $CDCl_3$) δ (ppm): 3.72 (6 H, s, CH_3-12,13), 3.44 (1 H, t, *J*=7.7 Hz, CH-1), 1.78 (2 H, t, *J*=7.3 Hz, CH_2-8), 1.53 (1 H, dquin, *J*=13.5, 6.8 Hz, CH-9), 0.90 (6 H, d, *J*=6.6 Hz, CH_3-10,11); **^{13}C NMR** (101 MHz, $CDCl_3$) δ (ppm): 170.2 (C-2,3), 52.6 (C-12,13), 50.1 (C-1), 37.7 (C-8), 26.3 (C-9), 22.3 (C-10,11); **IR** ν_{max}/cm^{-1} 2957, 1734, 1436, 1243, 1323, 1243, 1196, 1153, 1124, 1062, 1016; **MS** (ES+) 189.1 $[M+H]^+$; **HRMS** (ES+) calcd. for $C_9H_{16}NaO_4$ $[M+Na]^+$ 211.0941, found 211.0949.

Dimethyl 2-benzylmalonate (**122f**)

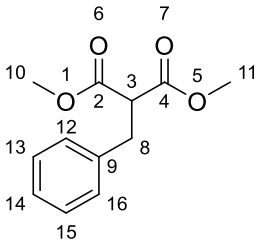

122f

Compound **122f** was isolated as a colourless oil (311 mg, 70% over 2 steps) following General Procedure C. **^{1}H NMR** (400 MHz, $CDCl_3$) δ (ppm): 7.33 - 7.21 (5 H, m, ArH), 3.73 (6 H, s, CH_3-10,11), 3.72 - 3.68 (1 H, m, CH-3), 3.25 (2 H, d, *J*=7.8 Hz, CH_2-8); **^{13}C NMR** (101 MHz, $CDCl_3$) δ (ppm): 169.3 (C-2,4), 137.9 (C-9), 128.9 (C-13,15), 128.7 (C-12,16), 126.9 (C-14), 53.7 (C-10,11), 52.7 (C-3), 34.9 (C-8); **MS** (ES+) 245.0 $[M+Na]^+$. Spectroscopic data are in agreement with literature values.[10]

Dimethyl cyclopentylpropanedioate (**122g**)

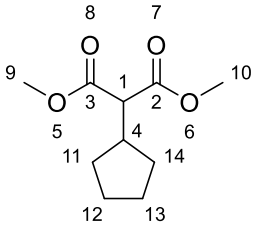

122g

Compound **122g** was isolated as a colourless oil (253 mg, 63% over 2 steps) following General Procedure C. **^{1}H NMR** (400 MHz, $CDCl_3$) δ (ppm): 3.73 (6 H, s, CH_3-9,10), 3.22 (1 H, d, *J*=10.3 Hz, CH-1), 2.49 (1 H, dq, *J*=17.7, 8.6 Hz, CH-4), 1.90 - 1.78 (2 H, m, CH_{eq}-11,14), 1.71 - 1.51 (4 H, m, CH_2-12,13), 1.31 - 1.14 (2 H, m, CH_{ax}-11,14); **^{13}C NMR** (101 MHz, $CDCl_3$) δ (ppm): 169.6 (C-2,3), 57.1 (C-1), 52.4 (C-9,10), 39.8 (C-4), 30.9 (C-11,14), 25.0 (C-12,13); **IR** ν_{max}/cm^{-1} 2954, 2872, 1733, 1435, 1324, 1198, 1146, 1022; **MS** (ES+) 329.1 $[M+Na]^+$. **HRMS** (ES+) calcd. for $C_{10}H_{16}NaO_4$ $[M+Na]^+$ 223.09408, found 223.09354.

Dimethyl propan-2-ylpropanedioate (**122h**)

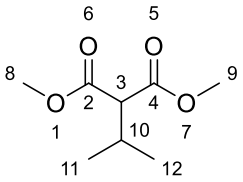

122h

Compound **122h** was isolated as a colourless oil (55 mg, 16% over 2 steps) following General Procedure C. **^{1}H NMR** (500 MHz, $CDCl_3$) δ (ppm): 3.72 (6 H, s, CH_3-8,9), 3.15 (1 H, d, *J*=8.7 Hz, CH-3), 2.44 - 2.33 (1 H, m, CH-10), 0.99 (6 H, d, *J*=6.8 Hz, CH_3-11,12); **^{13}C NMR** (125 MHz, $CDCl_3$) δ (ppm): 169.4 (C-2,4), 58.9 (C-3), 52.4 (C-8,9), 29.0 (C-10), 20.5 (C-11,12); **IR** ν_{max}/cm^{-1} 2959, 1735, 1436, 1301, 1238, 1198, 1152, 1128, 1024; **MS** (ES+) 197.1 $[M+Na]^+$. Spectroscopic data consistent with literature values.[11]

5.2 Addition of substituted dimethyl malonates to nitrostyrene (Racemic procedure)

Potassium *tert*-butoxide (22 mg, 0.20 mmol) was added to a solution of malonate (0.24 mmol) in THF (1.4 mL) at room temperature under argon atmosphere. The reaction mixture was then cooled to −35 °C and a solution of nitrostyrene (54 mg, 0.36 mmol) in THF (0.12 mL) was added. The reaction mixture was then stirred for 1 h at −35 °C. Saturated aqueous NH_4Cl was added and the resulting mixture extracted with ethyl acetate (3 × 10 mL). The combined organic phases were dried over Na_2SO_4 and the solvent removed *in vacuo*. The residue was purified by flash column chromatography over silica (ethyl acetate in petroleum ether).

5.3 Addition of substituted dimethyl malonates to nitrostyrene (General Procedure D)

To *trans*-β-nitrostyrene (35.8 mg, 0.240 mmol) and catalyst **116** (9.91 mg, 0.0100 mmol) in a screw-cap vial was added anhydrous THF (0.1 mL), followed by the indicated substituted dimethyl malonate (0.200 mmol). The vial was promptly sealed and cooled to the indicated temperature. At the conclusion of the indicated reaction time, the reaction mixture was filtered through a plug of cotton wool, the solvent removed *in vacuo* and the residue subjected to flash column chromatography over silica (5% ethyl acetate in petroleum ether, then 10% ethyl acetate in petroleum ether) to yield the adducts **123a-f**.

Dimethyl (*R*)-2-methyl-2-(2-nitro-1-phenylethyl)malonate (**123a**)

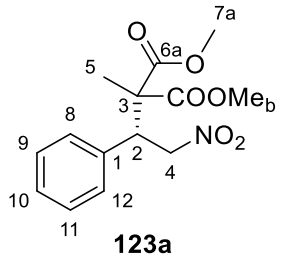

123a

Compound **123a** was isolated as a colourless solid (54.8 mg, 93%) following General Procedure D. The enantiomeric excess was determined by HPLC analysis (Chiralpak AD-H, hexane/*iso*-propanol 90:10, λ 210 nm, 1.0 mL/min: t (major) = 8.2 min, t (minor) = 8.9 min (98:2 e.r.)). **$[\alpha]_D^{25}$** = −33 (*c* 0.51, $CHCl_3$, 98:2 e.r.), lit. $[\alpha]_D^{25}$ = +29.7 (*c* 0.15, $CHCl_3$, 98% e.e., *S* enantiomer)[12]; **^{1}H NMR** (400 MHz, $CDCl_3$) δ (ppm): 7.37 - 7.09 (5 H, m, ArH), 5.05 (1 H, d, *J*=6.6 Hz, C$\underline{H_a}H_b$-4), 5.03 (1 H, d, *J*=1.7 Hz, $CH_a\underline{H_b}$-4), 4.17 (1 H, dd, *J*=9.7, 4.8 Hz, CH-2), 3.77 (3 H, s, CH_3-7a), 3.73 (3 H, s, CH_3-7b), 1.35 (3 H, s, CH_3-5). **^{13}C NMR** (101 MHz, $CDCl_3$) δ (ppm): 171.5 (C-6a), 170.9 (C-6b), 135.1 (C-1), 129.1 (C-9,11), 128.9 (C-8,12), 128.6 (C-10), 77.6 (C-4), 56.9 (C-3), 53.2 (C-7a), 53.0 (C-7b), 48.5 (C-2), 20.5 (C-5); **MP** 124 - 128 °C, lit. 130 °C; **MS** (ES+) 296.0 $[M+H]^+$. Spectroscopic data consistent with literature values.[12]

Dimethyl (*R*)-2-ethyl-2-(2-nitro-1-phenylethyl)malonate (**123b**)

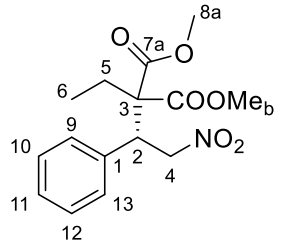

123b

Compound **123b** was isolated as a colourless oil (57.1 mg, 92%) following General Procedure D. The enantiomeric excess was determined by HPLC analysis (Chiralpak AD-H, hexane/*iso*-propanol 95:5, λ 210 nm, 1.0 mL/min: t (major) = 9.9 min, t (minor) = 10.8 min (97:3 e.r.)). **$[\alpha]_D^{25}$** = −64 (*c* 0.53, $CHCl_3$, 97:3 e.r.); **^{1}H NMR** (400 MHz, $CDCl_3$) δ (ppm): 7.31 - 7.08 (5 H, m, ArH), 5.05 (1 H, dd, *J*=13.6, 3.2 Hz, C$\underline{H_a}H_b$-4), 4.97 (1 H, dd, *J*=14.2, 11.0 Hz, $CH_a\underline{H_b}$-4), 4.20 (1 H, dd, *J*=10.7, 3.2 Hz, CH-2), 3.80 (3 H, s, CH_3-8a), 3.78 (3 H, s, CH_3-8b), 1.85 (1 H, dq, *J*=14.6, 7.4 Hz, C$\underline{H_a}H_b$-5),

1.55 (1 H, dq, *J*=14.5, 7.4 Hz, $CH_a\underline{H_b}$-5), 0.88 (3 H, t, *J*=7.6 Hz, CH_3-6); **^{13}C NMR** (101 MHz, $CDCl_3$) δ (ppm) 170.8 (C-7a), 170.5 (C-7b), 135.2 (C-1), 129.0 (C-10,12), 128.8 (C-9,13), 128.6 (C-11), 78.7 (C-4), 61.1 (C-3), 53.0 (C-8a), 52.7 (C-8b), 46.5 (C-2), 27.3 (C-5), 9.0 (C-6); **IR** ν_{max}/cm^{-1} 2955, 1728, 1553, 1434, 1379, 1303, 1283, 1234, 1130, 1100, 1022; **MS** (ES+) 310.1 $[M+H]^+$, 332.0 $[M+Na]^+$. **HRMS** (ES+) calcd. for $C_{15}H_{19}NNaO_6$ $[M+Na]^+$ 332.11046, found 332.10970.

Dimethyl (*R*)-2-allyl-2-(2-nitro-1-phenylethyl)malonate (**123c**)

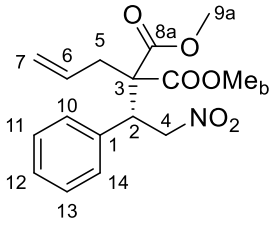

123c

Compound **123c** was isolated as a colourless oil (63.0 mg, 98%) following General Procedure D. The enantiomeric excess was determined by HPLC analysis (Chiralpak AD-H, hexane/*iso*-propanol 98:2, λ 210 nm, 1.0 mL/min: t (major) = 12.8 min, t (minor) = 14.5 min (96:4 e.r.)). **$[\alpha]_D^{25}$** = − 42 (*c* 0.55, $CHCl_3$, 96:4 e.r.), lit. $[\alpha]_D^{20}$ = +38.5 (*c* 1, $CHCl_3$, 92% e.e., *S* enantiomer)[13]; **^{1}H NMR** (400 MHz, $CDCl_3$) δ (ppm): 7.31 - 7.10 (5 H, m, ArH), 5.76 - 5.70 (1 H, m, CH-6), 5.13 (1 H, d, *J*=10.1 Hz, CH_{cis}-7), 5.10 - 5.02 (2 H, m, CH_{trans}-7, $C\underline{H_a}H_b$-4), 4.99 (1 H, dd, *J*=14.2, 11.0 Hz, $CH_a\underline{H_b}$-4), 4.20 (1 H, dd, *J*=11.0, 3.2 Hz, CH-2), 3.80 (3 H, s, CH_3-9a), 3.74 (3 H, s, CH_3-9b), 2.57 (1 H, dd, *J*=14.5, 6.6 Hz, $C\underline{H_a}H_b$-5), 2.27 (1 H, dd, *J*=14.5, 7.9 Hz, $CH_a\underline{H_b}$-5); **^{13}C NMR** (101 MHz, $CDCl_3$) δ (ppm): 170.2 (C-8a), 170.1 (C-8b), 134.9 (C-1), 131.9 (C-6), 129.0 (C-11,13), 128.9 (C-10,14), 128.7 (C-12), 120.0 (C-7), 78.4 (C-4), 60.9 (C-3), 52.9 (C-9a), 52.9 (C-9b), 46.9 (C-5), 38.6 (C-2); **MS** (ES+) 322.1 $[M+H]^+$, 344.1 $[M+Na]^+$. Spectroscopic data consistent with literature values.[13]

Dimethyl (*R*)-2-(3-chloropropyl)-2-(2-nitro-1-phenylethyl)malonate (**123d**)

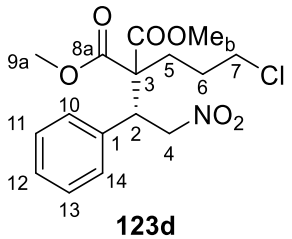

123d

Compound **123d** was isolated as a colourless oil (56.9 mg, 80%) following General Procedure D. The enantiomeric excess was determined by HPLC analysis (Chiralpak OD-H, hexane/*iso*-propanol 95:5, λ 210 nm, 1.0 mL/min: t (major) = 15.5 min, t (minor) = 25.3 min (98:2 e.r.)). $\mathbf{[\alpha]_D^{25}}$ = − 30 (*c* 0.41, $CHCl_3$, 98:2 e.r.); **^{1}H NMR** (400 MHz, $CDCl_3$) δ (ppm): 7.32 - 7.08 (5 H, m, ArH), 5.03 (1 H, dd, *J*=13.2, 4.2 Hz, C$\underline{H_a}H_b$-4), 4.98 (1 H, dd, *J*=13.2, 9.8 Hz, C$H_a\underline{H_b}$-4), 4.18 (1 H, dd, *J*=9.8, 4.2 Hz, CH-2), 3.81 (3 H, s, CH_3-9a), 3.80 (3 H, s, CH_3-9b), 3.40 (2 H, t, *J*=6.0 Hz, CH_2-7), 1.92 - 1.86 (1 H, m, C$\underline{H_a}H_b$-5), 1.84 - 1.76 (1 H, m, C$H_a\underline{H_b}$-5), 1.75 - 1.58 (2 H, m, CH_2-6); **^{13}C NMR** (101 MHz, $CDCl_3$) δ (ppm): 170.6 (C-8a), 170.1 (C-8b), 134.8 (C-1), 129.1 (C-11,13), 128.8 (C-12), 128.8 (C-10,14), 78.5 (C-4), 60.3 (C-3), 53.2 (C-9a), 52.9 (C-9b), 47.2 (C-7), 44.4 (C-2), 31.7 (C-6), 27.8 (C-5); **IR** ν_{max}/cm^{-1} 2956, 1728, 1553, 1434, 1379, 1283, 1252, 1211, 1165, 1090; **MS** (ES+) 380.0 $[M+Na]^+$. **HRMS** (ES+) calcd. for $C_{16}H_{20}NNaO_6$ $[M+Na]^+$ 380.0871, found 380.0873.

Dimethyl (*R*)-2-isobutyl-2-(2-nitro-1-phenylethyl)malonate (**123e**)

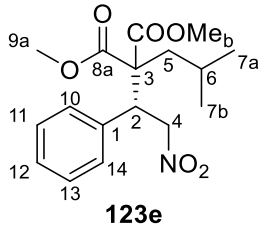

123e

Compound **123e** was isolated as a colourless oil (42.6 mg, 63%) following General Procedure D. The enantiomeric excess was determined by HPLC analysis (Chiralpak AD-H, hexane/*iso*-propanol 98:2, λ 210 nm, 1.0 mL/min: t (major) = 9.8 min, t (minor) = 10.8 min (94:6 e.r.)). $\mathbf{[\alpha]_D^{25}}$ = − 45 (*c* 0.51, $CHCl_3$, 94:6 e.r.); **^{1}H NMR** (400 MHz, $CDCl_3$) δ (ppm): 7.32 - 7.05 (5 H, m, ArH), 5.07 (1 H, dd, *J*=13.5, 3.1 Hz, C$\underline{H_a}H_b$-4), 4.92 (1 H, dd, *J*=13.4, 11.0 Hz, C$H_a\underline{H_b}$-4), 4.26 (1 H, dd, *J*=11.0, 3.2 Hz, CH-2), 3.79 (3 H, s, CH_3-9a), 3.77 (3 H, s, CH_3-9b), 1.90 - 1.73 (1 H, m, CH-6), 1.73 - 1.62 (1 H, dd, *J* = 14.7, 7.3 Hz, C$\underline{H_a}H_b$-5), 1.47 (1 H, dd, *J*=14.4, 3.9 Hz, C$H_a\underline{H_b}$-5), 0.79 (6 H, "d", *J*=6.7

Hz, CH_3-7a,7b); **^{13}C NMR** (101 MHz, $CDCl_3$) δ (ppm): 171.3 (C-8a), 170.7 (C-8b), 135.3 (C-1), 129.0 (C-10,14), 128.9 (C-11,13), 128.6 (C-12), 78.8 (C-4), 59.9 (C-3), 52.8 (C-9a), 52.7 (C-9b), 47.5 (C-5), 42.8 (C-2), 24.5 (C-7a), 24.0 (C-7b), 23.2 (C-6); **IR** ν_{max}/cm^{-1} 2958, 1729, 1553, 1434, 1379, 1283, 1225, 1130, 1036; **MS** (ES+) 338.2 $[M+H]^+$, 360.1 $[M+Na]^+$. **HRMS** (ES+) calcd. for $C_{17}H_{23}NNaO_6$ $[M+Na]^+$ 360.1418, found 360.1429.

Dimethyl (*R*)-2-benzyl-2-(2-nitro-1-phenylethyl)malonate (**123f**)

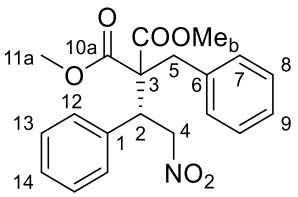

123f

Compound **123f** was isolated as a colourless solid (56.6 mg, 76%) following General Procedure D. The enantiomeric excess was determined by HPLC analysis (Chiralpak AD-H, hexane/*iso*-propanol 95:5, λ 210 nm, 1.0 mL/min: t (major) = 11.8 min, t (minor) = 18.6 min (94:6 e.r.)). **$[\alpha]_D^{25}$** = + 5.8 (*c* 0.52, $CHCl_3$, 94:6 e.r.); **^{1}H NMR** (400 MHz, $CDCl_3$) δ (ppm): 7.29 - 7.01 (10 H, m, ArH), 4.92 - 4.77 (2 H, m, CH_2-4), 4.20 (1 H, dd, *J*=9.0, 5.1 Hz, CH-2), 3.74 (3 H, s, CH_3-11a), 3.47 (3 H, s, CH_3-11b), 3.13 (1 H, d, *J*=14.2 Hz, C$\underline{H}_a$H$_b$-5), 2.82 (1 H, d, *J*=14.2 Hz, CH$_a$$\underline{H}_b$-5); **^{13}C NMR** (101 MHz, $CDCl_3$) δ (ppm): 170.2 (C-10a), 170.2 (C-10b), 135.6 (C-1 or -6), 135.1 (C-1 or -6), 130.2 (ArC), 129.3 (ArC), 129.0 (ArC), 128.8 (ArC), 128.4 (ArC), 127.5 (ArC), 78.7 (C-4), 62.5 (C-3), 52.8 (C-11a), 52.7 (C-11b), 48.6 (C-5), 40.7 (C-2); **MP** 50 - 52 °C; **IR** ν_{max}/cm^{-1} 3012, 1726, 1554, 1496, 1434, 1380, 1257, 1177, 1088; **MS** (ES+) 372.1 $[M+H]^+$, 394.1 $[M+Na]^+$. **HRMS** (ES+) calcd. for $C_{20}H_{21}NNaO_6$ $[M+Na]^+$ 394.1261, found 394.1271.

Diethyl methyl(2-nitro-1-phenylethyl)propanedioate (**181**)

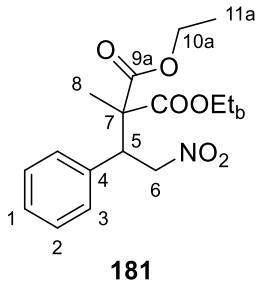

181

To *trans*-β-nitrostyrene (89 mg, 0.60 mmol) and catalyst **116** (20 mg, 0.020 mmol) in a screw-cap vial was added anhydrous CH_2Cl_2 (50 μL), followed by diethyl methylmalonate (34 μL, 0.20 mmol). The vial was promptly sealed and stirred at 0 °C for 24 h. The reaction mixture was then filtered through a plug of cotton wool, the solvent removed *in vacuo* and the residue subjected to flash column chromatography over silica (10% ethyl acetate in petroleum ether) to give the product as a colourless solid (21 mg, 33%). **^{1}H NMR** (400 MHz, $CDCl_3$) δ (ppm): 7.33 - 7.14 (5 H, m, ArH), 5.09 - 5.01 (2 H, m, CH_2-6), 4.25 (2 H, q, *J*=7.3 Hz, CH_2-10a), 4.21 - 4.12 (3 H, m, CH_2-10b, CH-5), 1.33 (3 H, s, CH_3-8), 1.28 (3 H, t, *J*=6.5 Hz, CH_3-11a), 1.25 (3 H, t, *J*=6.5 Hz, CH_3-11b); **^{13}C NMR** (101 MHz, $CDCl_3$) δ (ppm): 171.1 (C-9a), 170.4 (C-9b), 135.2 (C-4), 129.2 (C-2), 128.9 (C-3), 128.5 (C-1), 77.8 (C-6), 62.2 (C-10a), 62.1 (C-10b), 56.8 (C-7), 48.4 (C-5), 20.4 (C-8), 14.1 (C-11a), 14.1 (C-11b); **MP** 54 – 56 °C; **MS** (ES+) 346.1 $[M+Na]^+$. Spectroscopic data consistent with literature values.[14]

6. Conjugate addition of *β*-keto-amides

6.1 Preparation of *β*-keto-amides (General Procedure E).

Meldrum's acid (0.72 g, 5.0 mmol, 1.0 equiv.) was dissolved in CH_2Cl_2 (12 mL) and pyridine (0.89 mL, 11 mmol, 2.2 equiv.) at −10 °C and stirred for 10 min. The indicated acyl chloride (5.5 mmol, 1.1 equiv.) was added dropwise and the reaction mixture stirred 1 h at −10 °C, then 1 h at room temperature. The reaction mixture was treated with aqueous HCl (1M, 5 mL) and washed with water (5 mL). The aqueous phase was then extracted with CH_2Cl_2 (2 × 5 mL). The combined organic phases were washed with brine, dried over anhydrous Na_2SO_4 and the solvent removed *in vacuo*.

The crude residue was immediately dissolved in anhydrous toluene (5 mL) and acetone (2.5 mL) and heated at 120 °C in a sealed microwave vial for 1 h. The solvent was removed *in vacuo* and the

residue purified by flash column chromatography over silica (50% CH_2Cl_2 in petroleum ether) to give the acetonide as a yellow oil.

The acetonide (1.0 equiv.) was dissolved in xylenes and dimethylamine (5.6 M in EtOH, 4.0 equiv.) was added. The resulting mixture was heated at 140 °C in a sealed microwave vial for 2 h. The solvent was removed *in vacuo* and the residue was purified by flash column chromatography over silica (50% ethyl acetate in petroleum ether) to give the corresponding keto-amide.

N,*N*-Dimethyl-3-oxoheptanamide (**130b**)

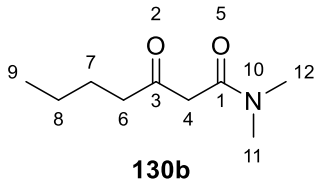

130b

Compound **130b** was isolated as a yellow oil (0.19 g, 23% from Meldrum's acid) following General Procedure E. **^{1}H NMR** (400 MHz, $CDCl_3$) δ (ppm): 3.51 (2 H, s, CH_2-4), 2.97 (3 H, s, CH_3-11), 2.95 (3 H, s, CH_3-12), 2.54 (2 H, t, *J*=7.3 Hz, CH_2-6), 1.55 (2 H, quin, *J*=7.5 Hz, CH_2-7), 1.36 - 1.23 (2 H, m, CH_2-8), 0.97 - 0.79 (3 H, t, *J* = 7.1 Hz, CH_3-9); **^{13}C NMR** (101 MHz, $CDCl_3$) δ (ppm): 204.9 (C-3), 166.9 (C-1), 49.4 (C-4), 42.8 (C-6), 38.0 (C-11), 35.6 (C-12), 25.7 (C-7), 22.3 (C-8), 13.9 (C-9); **IR** ν_{max}/cm^{-1} 3946, 2980, 1814, 1624, 1404, 1478, 1352, 1268, 1201, 1234, 1004; **MS** (ES+) 172.2 $[M+H]^+$, 194.1 $[M+Na]^+$. **HRMS** (ES+) calcd. For $C_9H_{17}NNaO_2$ $[M+Na]^+$ 194.1151, found 194.1154.

N,*N*-Dimethyl-3-oxo-4-phenylbutanamide (**130c**)

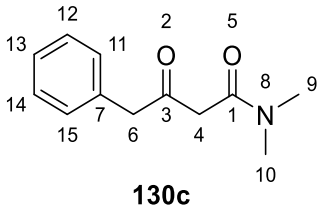

130c

Compound **130c** was isolated as an orange oil (0.35 g, 34% from Meldrum's acid) following General Procedure E. **^{1}H NMR** (400 MHz, $CDCl_3$) δ (ppm): (approx. 20% of compound **130c** is present as the enol in $CDCl_3$) 7.38 - 7.25 (5 H, m, ArH), 3.88 (2 H, s, CH_2-4), 3.55 (2 H, br. s, CH_2-6), 2.96 (3 H, m, CH_3-9), 2.86 (3 H, m, CH_3-9); **^{13}C NMR** (101 MHz, $CDCl_3$) δ (ppm): (ketone and enol peaks)

202.3 (C-3), 176.4, 166.7, 136.5 (ArC), 133.7 (ArC), 129.7 (ArC), 129.3 (ArC), 128.9 (ArC), 128.6 (ArC), 127.4 (ArC), 126.9 (ArC), 87.3, 50.0 (C-4), 48.3 (C-6), 42.3, 37.9 (C-9), 35.5 (C-10); **MS** (ES+) 206.1 $[M+H]^+$, 228.1 $[M+Na]^+$. Spectroscopic data consistent with literature values.[15]

N,*N*,4-Trimethyl-3-oxopentanamide (**130d**)

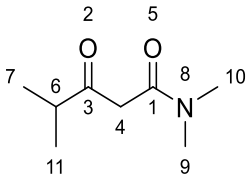

130d

Compound **130d** was isolated as a yellow oil (0.35 g, 24% from Meldrum's acid) following General Procedure E. **^{1}H NMR** (400 MHz, $CDCl_3$) δ (ppm): 3.59 (2 H, br. s., CH_2-4), 2.96 (6 H, s, CH_3-9,10), 2.78 (1 H, m, CH-6), 1.12 (6 H, d, *J*=6.8 Hz, CH_3-7,11); **^{13}C NMR** (101 MHz, $CDCl_3$) δ (ppm): 208.3 (C-3), 167.1 (C-1), 47.1 (C-4), 41.0 (C-6), 38.0 (C-9), 35.4 (C-10), 18.0 (C-7,11); **IR** ν_{max}/cm^{-1} 3952, 2970, 1714, 1630, 1504, 1467, 1360, 1323, 1262, 1207, 1144, 1074; **MS** (ES+) 158.1 $[M+H]^+$, 180.1 $[M+Na]^+$; **HRMS** (ES+) calcd. for $C_8H_{15}NNaO_2$ $[M+Na]^+$ 180.0995, found 180.1000.

3-Cyclohexyl-*N*,*N*-dimethyl-3-oxopropanamide (**130e**)

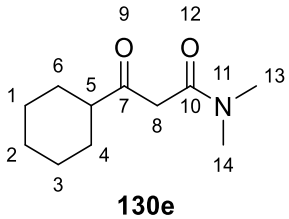

130e

Compound **130e** was isolated as an orange oil (0.15 g, 15% from Meldrum's acid) following General Procedure E. **^{1}H NMR** (400 MHz, $CDCl_3$) δ (ppm): (approx. 20% of compound **130e** is present as the enol in $CDCl_3$) 3.56 (2 H, s, CH_2-8), 2.95 - 2.94 (6 H, m, CH_3-14,13), 2.53 - 2.46 (1 H, m, CH-5), 1.88 - 1.63 (5 H, m, CH_{eq}-1,2,3,4,6), 1.38 - 1.08 (5 H, m, CH_{ax}-1,2,3,4,6); **^{13}C NMR** (101 MHz, $CDCl_3$) δ (ppm): (ketone peaks) 207.8 (C-7), 167.2 (C-10), 50.8 (C-5), 47.4 (C-8), 38.1 (C-14), 35.5 (C-13), 28.4 (C-4,6), 25.8 (C-2), 25.6 (C-1,3); **MS** (ES+) 198.2 $[M+H]^+$, 220.1 $[M+Na]^+$; **HRMS** (ES+) calcd. for $C_{11}H_{19}NNaO_2$ $[M+Na]^+$ 220.1308, found 220.1313. Spectroscopic data consistent with literature values.[16]

4-Methoxy-*N*,*N*-dimethyl-3-oxobutanamide (**130f**)

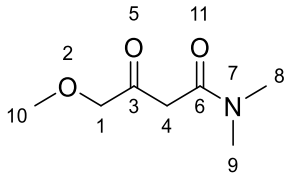

130f

Compound **130f** was isolated as an orange oil (0.22 g, 28% from Meldrum's acid) following General Procedure E. **^{1}H NMR** (400 MHz, $CDCl_3$) δ (ppm): (approx. 40% of compound **130f** is present as the enol in $CDCl_3$) 4.11 (2 H, s, CH_2-1), 3.54 (2 H, s, CH_2-4), 3.39 (3 H, s, CH_3-10), 2.98 (6 H, s, CH_3-9,8); **^{13}C NMR** (101 MHz, $CDCl_3$) δ (ppm): (ketone peaks) 202.8 (C-3), 166.6 (C-6), 77.5 (C-1), 59.5 (C-10), 45.3 (C-4), 38.0 (C-9), 35.5 (C-8); **IR** ν_{max}/cm^{-1} 3954, 2934, 1730, 1635, 1504, 1396, 1261, 1197, 1102; **MS** (ES+) 160.1 $[M+H]^+$; **HRMS** (ES+) calcd. for $C_7H_{13}NNaO_3$ $[M+Na]^+$ 182.0788, found 182.0790.

N,*N*-Dimethyl-3-oxo-3-phenylpropanamide (**130g**)

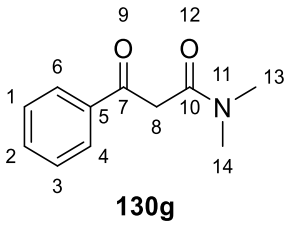

130g

To diisopropylamine (0.56 mL, 4.0 mmol) in THF (8 mL) at −78 °C under argon atmosphere was added *n*-butyllithium (1.9 mL, 2.21 M, 4.2 mmol) and the reaction mixture was stirred for 0.5 h. *N*,*N*-dimethylacetamide (0.19 mL, 2.0 mmol) was added and the reaction mixture stirred for 0.5 h. Ethyl benzoate (0.29 mL, 2.0 mmol) was then added and the reaction mixture stirred for a further 0.5 h. The reaction mixture was poured onto saturated aqueous NH_4Cl and extracted with ethyl acetate (3 × 10 mL). The combined organic extracts were washed with brine, dried over Na_2SO_4 and the solvent removed *in vacuo*. The residue was purified by flash column chromatography over silica (50% ethyl acetate in petroleum ether) yielding **130g** as an off-white solid (0.35 g, 90%). **^{1}H NMR** (400 MHz, CD_3OD) δ (ppm): (ketone peaks) 8.01 - 7.42 (5 H, m, ArH), 3.13 (1 H, br. s., $C\underline{H_a}H_b$-8), 3.05 (3 H, s, CH_3-14), 3.02 (1 H, br. s., $CH_a\underline{H_b}$-8), 2.98 (3 H, s, CH_3-13); **^{13}C NMR** (101 MHz, CD_3OD) δ (ppm): (ketone and enol peaks) 196.0 (C-7), 170.3 (C-10), 137.6 (ArC), 134.8 (ArC), 129.8 (ArC),

129.6 (ArC), 129.5 (ArC), 126.9 (ArC), 38.4 (C-14), 37.5 (br. s., C-8), 35.7 (C-13); **MP** 64 - 66 °C; **MS** (ES+) 192.1 $[M+H]^+$, 214.1 $[M+Na]^+$. Spectroscopic data consistent with literature values.[17]

N,*N*,4,4-Tetramethyl-3-oxopentanamide (**130h**)

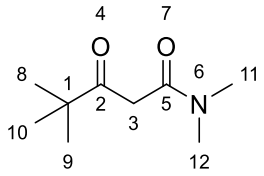

130h

To diisopropylamine (0.56 mL, 4.0 mmol) in THF (8 mL) at −78 °C under argon atmosphere was added *n*-butyllithium (1.9 mL, 2.21 M, 4.2 mmol) and the reaction mixture was stirred for 0.5 h. *N*,*N*-dimethylacetamide (0.19 mL, 2.0 mmol) was added and the reaction mixture stirred for 0.5 h. Pivalic anyhydride (0.41 mL, 2.0 mmol) was then added and the reaction mixture stirred for a further 0.5 h. The reaction mixture was poured onto saturated aqueous NH_4Cl and extracted with ethyl acetate (3 × 10 mL). The combined organic extracts were washed with brine, dried over Na_2SO_4 and the solvent removed *in vacuo*. The residue was purified by flash column chromatography over silica (2% MeOH in CH_2Cl_2) yielding **130h** as a colourless oil (0.29 g, 85%). **^{1}H NMR** (400 MHz, $CDCl_3$) δ (ppm): (approx. 15% of compound **130h** is present as the enol in $CDCl_3$) 3.65 (2 H, s, CH_2-3), 2.99 - 2.94 (6 H, m, CH_3-12,11), 1.16 (9 H, s, CH_3-8,9,10); **^{13}C NMR** (101 MHz, $CDCl_3$) δ (ppm): (ketone peaks) 209.6 (C-2), 167.6 (C-5), 44.8 (C-1), 43.6 (C-3), 38.0 (C-11), 35.4 (C-12), 26.3 (C-8,9,10); **IR** ν_{max}/cm^{-1} 2962, 1707, 1618, 1501, 1393, 1369, 1351, 1313, 1271, 1218, 1167, 1140, 1062; **MS** (ES+) 172.2 $[M+H]^+$, 194.1 $[M+Na]^+$; **HRMS** (ES+) calcd. for $C_9H_{17}NNaO_2$ $[M+Na]^+$ 194.11515, found 194.11485.

6.2 Addition of *β*-keto amides to nitrostyrene (Racemic procedure)

To a suspension of sodium hydride (8.0 mg, 0.20 mmol, 60% in mineral oil) in THF (0.3 mL) at 0 °C under argon atmosphere was added *β*-keto amide (0.20 mmol) in THF (0.2 mL) and the reaction stirred for 10 min. A solution of nitrostyrene (36 mg, 0.24 mmol) in THF (0.5 mL) was added dropwise and the reaction stirred for 3 h, warming to room temperature. The solvent was then removed *in vacuo* and the residue purified by flash column chromatography over silica (ethyl acetate in petroleum ether).

6.3 Addition of *β*-keto amides to nitrostyrene (General Procedure F)

To catalyst **116** (19.8 mg, 0.0200 mmol) and nitrostyrene (35.8 mg, 0.240 mmol) in a screw-cap glass vial was added a solution of ketoamide (0.200 mmol) in THF (0.2 mL) in one portion. The vial was immediately cooled to the indicated temperature and the reaction stirred for the indicated time. The reaction mixture was then diluted with CH_2Cl_2 and filtered through cotton wool to remove the catalyst. The solvent was removed *in vacuo* and the diastereomeric ratio was determined by ^{1}H-NMR of the crude reaction mixture. The residue was then purified by flash column chromatography over silica to give adducts **131a-h**.

(2*R*, 3*S*)-2-Acetyl-*N*,*N*-dimethyl-4-nitro-3-phenylbutanamide (**131a**)

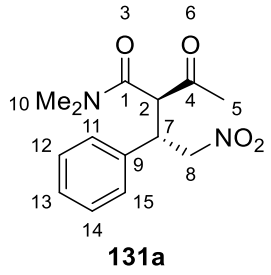

131a

Compound **131a** was isolated as an off-white solid (42.1 mg, 74%) following General Procedure F. The diastereomeric ratio was determined to be 20:80 by ^{1}H-NMR analysis of the crude reaction mixture. The enantiomeric excess of the major diastereomer was determined by HPLC analysis (Chiralpak AD-H, hexane/*iso*-propanol 85:15, λ 210 nm, 1.0 mL/min: t (major) = 11.7 min, t (minor) = 17.6 min (96:4 e.r.)). **$[\alpha]_D^{25}$** = +60 (*c* 1.0, $CHCl_3$, 20:80 d.r., 96:4 e.r.), minor diastereomer: $[\alpha]_D^{25}$ = +18 (*c* 0.49, $CHCl_3$, ~85:15 e.r.), lit. $[\alpha]_D^{25}$ = +23.9 (*c* 0.51, $CHCl_3$, 98% e.e.),[18] matched with minor diastereomer of **131a**; **^{1}H NMR** (400 MHz, $CDCl_3$) *δ* (ppm): (major diastereomer) 7.26 - 7.15 (5 H, m, ArH), 4.78 (1 H, dd, *J*=13.4, 8.4 Hz, C$\underline{H}_a$H$_b$-8), 4.72 (1 H, dd, *J*=13.1, 4.1 Hz, CH$_a$$\underline{H}_b$-8), 4.22 - 4.17 (1 H, m, CH-7), 4.14 (1 H, d, *J*=9.9 Hz, CH-2), 2.83 (3 H, s, CH_3-10a), 2.68 (3 H, s, CH_3-10b), 2.17 (3 H, s, CH_3-5); (minor diastereomer) 7.34 - 7.08 (5 H, m, ArH), 4.75 (1 H, dd, *J*=12.8, 4.7 Hz, C$\underline{H}_a$H$_b$-8), 4.69 (1 H, dd, *J*=12.7, 8.2 Hz, CH$_a$$\underline{H}_b$-8), 4.30 (1 H, td, *J*=8.5, 4.7 Hz, CH-7), 4.16 (1 H, d, *J*=9.0 Hz, CH-2), 2.94 (3 H, s, CH_3-10a), 2.85 (3 H, s, CH_3-10b), 1.96 (3 H, s, CH_3-5); **^{13}C NMR** (101 MHz, $CDCl_3$) *δ* (ppm) 202.2 (C-4), 166.7 (C-1), 137.0 (C-9), 129.0 (C-12,14), 128.3 (C-13), 128.0 (C-11,15), 77.6 (C-8), 59.6 (C-2), 43.4 (C-7), 37.9 (C-10a), 36.0 (C-10b), 28.7 (C-5);

(minor diastereomer, selected peaks) 201.8, 166.7, 136.5, 129.3, 128.5, 128.0, 78.1, 59.9, 43.2, 36.3, 27.4; **IR** ν_{max}/cm^{-1} 2976, 1723, 1631, 1546, 1498, 1384, 1359, 1266, 1137; **MP** 130 - 140 °C; **MS** (ES+) 279.1 $[M+H]^+$, 301.1 $[M+Na]^+$; **HRMS** (ES+) calcd. for $C_{14}H_{18}N_2NaO_4$ $[M+Na]^+$ 301.11588, found 301.11521. Spectroscopic data consistent with literature values.[18]

(*S*)-*N*,*N*-Dimethyl-2-((*S*)-2-nitro-1-phenylethyl)-3-oxoheptanamide (**131b**)

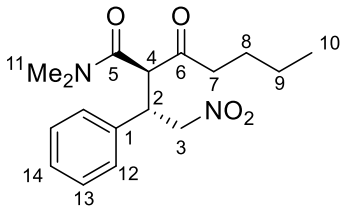

131b

Compound **131b** was isolated as a colourless oil (42.2 mg, 67%) following General Procedure F. The diastereomeric ratio was determined to be 90:10 by ^{1}H-NMR analysis of the crude reaction mixture. The enantiomeric excess of the major diastereomer was determined by HPLC analysis (Chiralpak IA, hexane/*iso*-propanol 90:10, λ 210 nm, 1.0 mL/min: t (major) = 14.7 min, t (minor) = 16.5 min (93:7 e.r.)). **$[\alpha]_D^{25}$** = +14 (*c* 1.0, $CHCl_3$, 90:10 d.r., 93:7 e.r. major diastereomer); **^{1}H NMR** (400 MHz, $CDCl_3$) δ (ppm): (major diastereomer) 7.27 - 7.12 (5 H, m, ArH), 4.77 (1 H, d, *J*=13.0, 4.4 Hz, $C\underline{H_a}H_b$-3), 4.71 (1 H, d, *J*=13.0, 8.6 Hz, $CH_a\underline{H_b}$-3), 4.31 (1 H, td, *J*=8.6, 4.4 Hz, CH-2), 4.14 (1 H, d, *J*=8.6 Hz, CH-4), 2.93 (3 H, s, CH_3-11a), 2.81 (3 H, s, CH_3-11b), 2.37 - 2.12 (2 H, m, CH_2-7), 1.34 - 1.20 (2 H, m, CH_2-8), 1.04 (2 H, sxt, *J*=7.4 Hz, CH_2-9), 0.72 (3 H, t, *J*=7.3 Hz, CH_3-10); (minor diastereomer, selected peaks) 2.82 (3 H, s), 2.67 (3 H, s), 2.41 (1 H, m,), 1.49 (2 H, m), 0.82 (3 H, t, *J*=7.3 Hz); **^{13}C NMR** (101 MHz, $CDCl_3$) δ (ppm) (major diastereomer) 203.8 (C-6), 166.8 (C-5), 136.6 (C-1), 129.1 (C-13), 128.3 (C-14), 128.0 (C-12), 78.0 (C-3), 59.4 (C-4), 43.1 (C-2), 39.5 (C-7), 37.8 (C-11a), 36.2 (C-11b), 25.2 (C-8), 21.9 (C-9), 13.7 (C-10); (minor diastereomer, selected peaks) 204.3, 166.7, 137.1, 128.9, 128.1, 127.9, 77.6, 59.0, 43.3, 41.0, 35.9, 25.5, 22.1, 13.8; **IR** ν_{max}/cm^{-1} 2958, 1717, 1635, 1549, 1496, 1455, 1399, 1379, 1259, 1140; **MS** (ES+) 321.2 $[MH]^+$, 343.2 $[M+Na]^+$; **HRMS** (ES+) calcd. for $C_{17}H_{24}N_2NaO_4$ $[M+Na]^+$ 343.1628, found 343.1629.

(2*S*, 3*S*)-*N*,*N*-Dimethyl-4-nitro-3-phenyl-2-(2-phenylacetyl)butanamide (**131c**)

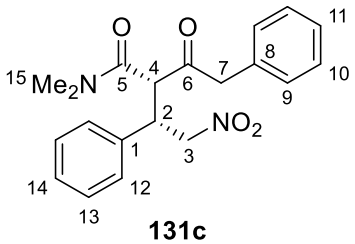

131c

Compound **131c** was isolated as a colourless solid (41.3 mg, 58%) following General Procedure F. The diastereomeric ratio was determined to be 94:6 by ^{1}H-NMR analysis of the crude reaction mixture. The enantiomeric excess of the major diastereomer was determined by HPLC analysis (Chiralpak AD-H, hexane/*iso*-propanol 80:20, λ 220 nm, 1.0 mL/min: t (minor) = 17.2 min, t (major) = 19.9 min (96:4 e.r.)). **$[\alpha]_D^{25}$** = −39 (*c* 1.0, $CHCl_3$, 94:6 d.r., 96:4 e.r. major diastereomer); **^{1}H NMR** (400 MHz, $CDCl_3$) δ (ppm): (major diastereomer) 7.40 - 6.84 (10 H, m, ArH), 4.84 (1 H, dd, *J*=13.2, 4.4 Hz, C$\underline{H_a}H_b$-3), 4.76 (1 H, dd, *J*=13.2, 9.3 Hz, C$H_a\underline{H_b}$-3), 4.36 (1 H, ddd, *J*=9.3, 7.3, 4.4 Hz, CH-2), 4.05 (1 H, d, *J*=7.3 Hz, CH-4), 3.68 (1 H, d, *J* = 15.9 Hz, C$\underline{H_a}H_b$-7), 3.51 (1 H, d, *J* = 16.1 Hz, C$H_a\underline{H_b}$-7), 2.80 (3 H, s, CH_3-15a), 2.27 (3 H, s, CH_3-15b), (minor diastereomer, selected peaks) 2.58 (3 H, s) , 2.45 (3 H, s); **^{13}C NMR** (101 MHz, $CDCl_3$) δ (ppm) (major diastereomer, minor diastereomer not observed) 201.7 (C-6), 166.8 (C-5), 136.7 (C-1 or -8), 133.1 (C-1 or -8), 129.7 (ArC), 129.2 (ArC), 128.7 (ArC), 128.4 (ArC), 128.0 (ArC), 127.4 (ArC), 77.3 (C-3), 58.4 (C-4), 47.4 (C-7), 42.9 (C-2), 37.4 (C-15a), 36.0 (C-15b); **MP** 140 - 144 °C; **IR** ν_{max}/cm^{-1} 2953, 1719, 1636, 1550, 1496, 1455, 1380, 1140; **MS** (ES+) 355.2 $[MH]^+$, 377.1 $[M+Na]^+$; **HRMS** (ES+) calcd. for $C_{20}H_{22}N_2NaO_4$ $[M+Na]^+$ 377.1472, found 377.1482.

(*S*)-*N*,*N*,4-Trimethyl-2-((*S*)-2-nitro-1-phenylethyl)-3-oxopentanamide (**131d**)

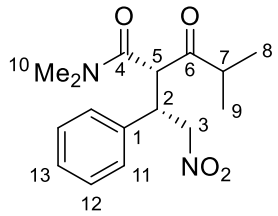

131d

Compound **131d** was isolated as a colourless solid (43.2 mg, 71%) following General Procedure F. The diastereomeric ratio was determined to be 96:4 by ^{1}H-NMR analysis of the crude reaction

mixture. The enantiomeric excess of the major diastereomer was determined by HPLC analysis (Chiralpak IB, hexane/*iso*-propanol 85:15, λ 210 nm, 1.0 mL/min: t (minor) = 10.6 min, t (major) = 11.7 min (96:4 e.r.)). **$[\alpha]_D^{25}$** = −42 (*c* 1.0, $CHCl_3$, 96:4 d.r., 96:4 e.r. major diastereomer); **^{1}H NMR** (400 MHz, $CDCl_3$) δ (ppm): (major diastereomer) 7.26 - 7.12 (5 H, m, ArH), 4.85 (1 H, dd, *J*=13.2, 4.8 Hz, C$\underline{H_a}H_b$-3), 4.76 (1 H, dd, *J*=13.2, 9.0 Hz, $CH_a\underline{H_b}$-3), 4.32 (1 H, ddd, *J*=9.1, 7.5, 4.2 Hz, CH-2), 4.19 (1 H, d, *J*=7.3 Hz, CH-5), 2.91 (3 H, s, CH_3-10a), 2.69 (3 H, s, CH_3-10b), 2.67 - 2.62 (1 H, m, CH-7), 0.89 (3 H, d, *J*=7.1 Hz, CH_3-8), 0.76 (3 H, d, *J*=6.6 Hz, CH_3-9); (minor diastereomer, selected peaks) 2.80 (3 H, s), 1.00 (3 H, d, *J*=1.0 Hz), 0.99 (3 H, d, *J*=1.5 Hz); **^{13}C NMR** (101 MHz, $CDCl_3$) δ (ppm): (major diastereomer, minor diastereomer not observed) 208.0 (C-6), 167.0 (C-4), 137.1 (C-1), 129.2 (C-12), 128.4 (C-13), 128.1 (C-11), 77.6 (C-3), 58.0 (C-5), 42.9 (C-2), 38.5 (C-7), 37.8 (C-10a), 36.2 (C-10b), 19.9 (C-8), 18.1 (C-9); **MP** 112 – 114 °C; **IR** ν_{max}/cm^{-1} 2974, 1716, 1638, 1551, 1381, 1142; **MS** (ES+) 307.2 $[M+H]^+$, 329.1 $[M+Na]^+$; **HRMS** (ES+) calcd. for $C_{16}H_{22}N_2NaO_4$ $[M+Na]^+$ 329.14718, found 329.14638.

(2*S*, 3*S*)-2-(Cyclohexanecarbonyl)-*N*,*N*-dimethyl-4-nitro-3-phenylbutanamide (**131e**)

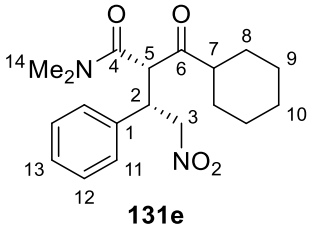

131e

Compound **131e** was isolated as a colourless solid (56.6 mg, 82%) following General Procedure F. The diastereomeric ratio was determined to be 95:5 by ^{1}H-NMR analysis of the crude reaction mixture. The enantiomeric excess of the major diastereomer was determined by HPLC analysis (Chiralpak AD-H, hexane/*iso*-propanol 80:20, λ 220 nm, 1.0 mL/min: t (major) = 8.4 min, t (minor) = 9.8 min (93:7 e.r.)). **$[\alpha]_D^{25}$** = −16 (*c* 1.0, $CHCl_3$, 95:5 d.r., 93:7 e.r. major diastereomer); **^{1}H NMR** (400 MHz, $CDCl_3$) δ (ppm): (major diastereomer) 7.26 - 7.12 (5 H, m, ArH), 4.83 (1 H, dd, *J*=13.4, 4.2 Hz, C$\underline{H_a}H_b$-3), 4.75 (1 H, dd, *J*=13.2, 9.2 Hz, $CH_a\underline{H_b}$-3), 4.35 - 4.30 (1 H, m, CH-2), 4.17 (1 H, d, *J*=7.8 Hz, CH-5), 2.90 (3 H, s, CH_3-14a), 2.70 (3 H, s, CH_3-14b), 2.40 - 2.33 (1 H, m, CH-7), 1.64 - 1.52 (4 H, m, CH_{eq}-8,9), 1.21 - 1.02 (6 H, m, CH_2-10, CH_{ax}-8,9); (minor diastereomer, selected peaks) 2.80 (3 H, s), 2.66 (3 H, s); **^{13}C NMR** (101 MHz, $CDCl_3$) δ (ppm): (major diastereomer, minor

diastereomer not observed) 207.0 (C-6), 166.9 (C-4), 137.2 (C-1), 129.2 (C-12), 128.3 (C-13), 128.0 (C-11), 77.7 (C-3), 58.1 (C-5), 48.7 (C-7), 42.9 (C-2), 37.8 (C-14a), 36.2 (C-14b), 30.2 (C-8), 27.9 (C-10), 25.6 (C-9); **MP** 144 - 116 °C; **IR** ν_{max}/cm^{-1} 2932, 2855, 1715, 1636, 1551, 1496, 1453, 1379, 1146; **MS** (ES+) 347.2 $[MH]^+$, 369.2 $[M+Na]^+$; **HRMS** (ES+) calcd. for $C_{19}H_{26}N_2NaO_4$ $[M+Na]^+$ 369.1785, found 369.1790.

(*S*)-4-Methoxy-*N*,*N*-dimethyl-2-((*S*)-2-nitro-1-phenylethyl)-3-oxobutanamide (**131f**)

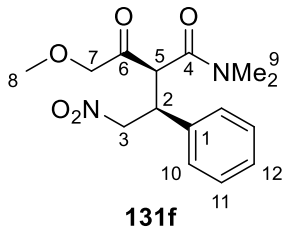

131f

Compound **131f** was isolated as a colourless oil (39.4 mg, 64%) following General Procedure F. The diastereomeric ratio was determined to be 74:26 by ^{1}H-NMR analysis of the crude reaction mixture. The enantiomeric excess of the major diastereomer was determined by HPLC analysis (Chiralpak AD-H, hexane/*iso*-propanol 80:20, λ 220 nm, 1.0 mL/min: t (minor) = 15.0 min, t (major) = 18.3 min (94:6 e.r.)). **$[\alpha]_D^{25}$** = −16 (*c* 1.0, $CHCl_3$, 74:26 d.r., 94:6 e.r. major diastereomer); **^{1}H NMR** (400 MHz, $CDCl_3$) δ (ppm): (major diastereomer) 7.27 - 7.13 (5 H, m, ArH), 4.94 (1 H, dd, *J*=13.4, 3.9 Hz, C$\underline{H}_a$H$_b$-3), 4.79 (1 H, dd, *J*=13.4, 9.5 Hz, CH$_a\underline{H}_b$-3), 4.31 (1 H, d, *J*=6.3 Hz, CH-5), 4.28 - 4.23 (1 H, m, CH-2), 3.89 (1 H, d, *J*=16.6 Hz, C$\underline{H}_a$H$_b$-7), 3.70 (1 H, d, *J*=16.6 Hz, CH$_a\underline{H}_b$-7), 3.18 (3 H, s, CH$_3$-8), 2.87 (3 H, s, CH$_3$-9a), 2.52 (3 H, s, CH$_3$-9b); (minor diastereomer, selected peaks) 4.90 - 4.83 (2 H, m), 4.40 (1 H, d, *J*=9.0 Hz), 4.12 (1 H, td, *J*=9.3, 4.4 Hz), 3.27 (3 H, s), 2.75 (3 H, s), 2.64 (3 H, s); **^{13}C NMR** (101 MHz, $CDCl_3$) δ (ppm): (major diastereomer) 202.8 (C-6), 166.9 (C-4), 137.1 (C-1), 129.1 (C-11), 128.9 (ArC, either diastereomer), 128.3 (ArC, either diastereomer), 128.2 (ArC, either diastereomer), 128.0 (ArC, either diastereomer), 127.9 (C-10), 76.6 (C-3), 76.4 (C-7), 59.3 (C-8), 55.4 (C-5), 42.2 (C-2), 37.6 (C-9a), 36.0 (C-9b); (minor diastereomer, selected peaks) 203.1, 166.8, 137.0, 130.9, 129.0, 76.8, 59.4, 55.0, 42.9, 37.9, 35.8; **IR** ν_{max}/cm^{-1} 2935, 1727, 1633, 1550, 1496, 1455, 1380, 1201, 1137; **MS** (ES+) 309.1 $[MH]^+$, 331.1 $[M+Na]^+$; **HRMS** (ES+) calcd. for $C_{15}H_{20}N_2NaO_5$ $[M+Na]^+$ 309.14450, found 309.14399.

(2*S*, 3*S*)-2-Benzoyl-*N*,*N*-dimethyl-4-nitro-3-phenylbutanamide (**131g**)

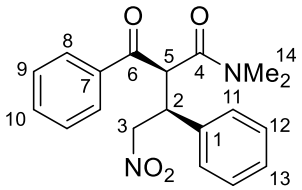

131g

Compound **131g** was isolated as a colourless oil (36.8 mg, 54%) following General Procedure F. The diastereomeric ratio was determined to be 65:35 by ^{1}H-NMR analysis of the crude reaction mixture. The enantiomeric excess of the major diastereomer was determined by HPLC analysis (Chiralpak AD-H, hexane/*iso*-propanol 98:2 ramp to 80:20 over 30 min, then 80:20 (15 min), λ 210 nm, 1.0 mL/min: t (major) = 31.0 min, t (minor) = 40.4 min (96:4 e.r.)). $\mathbf{[\alpha]_D^{25}}$ = +13 (*c* 1.0, $CHCl_3$, 65:35 d.r., 96:4 e.r. major diasteroemer); **^{1}H NMR** (400 MHz, $CDCl_3$) δ (ppm): (major diastereomer) 7.78 - 7.11 (10 H, m, ArH), 5.08 (1 H, dd, J=13.6, 4.0 Hz, C$\underline{H_a}H_b$-3), 5.01 – 4.84 (1 H, m, $CH_a\underline{H_b}$-3), 4.79 (1 H, d, *J*=7.1 Hz, CH-5), 4.45 - 4.38 (1 H, m, CH-2), 2.84 (3 H, s, CH_3-14a), 2.67 (3 H, s, CH_3-14a); (minor diastereomer, selected peaks) 2.74 (3 H, s), 2.63 (3 H, s); **^{13}C NMR** (101 MHz, $CDCl_3$) δ (ppm): (major diastereomer) 194.2 (C-6), 167.0 (C-4), 137.3 (C-1 or -7), 133.7 (C-1 or -7), 129.1 (C-9 or -12), 128.9 (C-9 or -12), 128.3 (C-10 or -13), 128.2 (br. s, C-8,11), 128.1 (C-10 or -13), 77.3 C-3), 55.8 (C-5), 43.7 (C-2), 37.7 (C-14a), 36.2 (C-14b); (minor diastereomer, selected peaks) 194.3, 166.9, 137.1, 136.4, 133.9, 129.0, 128.9, 55.0, 53.6, 36.0; **IR** ν_{max}/cm^{-1} 2890, 1688, 1634, 1551, 1496, 1448, 1398, 1265, 1134; **MS** (ES+) 341.1 $[M+H]^+$, 363.1 $[M+Na]^+$; **HRMS** (ES+) calcd. for $C_{19}H_{20}N_2NaO_4$ $[M+Na]^+$ 363.13153, found 363.13114.

(*S*)-*N*,*N*,4,4-Tetramethyl-2-((*S*)-2-nitro-1-phenylethyl)-3-oxopentanamide (**131h**)

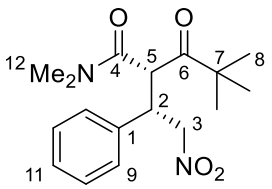

131h

Compound **131h** was isolated as a colourless solid (44.2 mg, 70%) following General Procedure F. The diastereomeric ratio was determined to be 75:25 by ^{1}H-NMR analysis of the crude reaction

mixture. The enantiomeric excess of the major diastereomer was determined by HPLC analysis (Chiralpak AD-H, hexane/*iso*-propanol 85:15, λ 210 nm, 1.0 mL/min: t (minor) = 13.1 min, t (major) = 15.3 min (95:5 e.r.)). **$[\alpha]_D^{25}$** = −114 (*c* 1.0, $CHCl_3$, 75:25 d.r., 95:5 e.r. major diastereomer); **^{1}H NMR** (400 MHz, $CDCl_3$) δ (ppm): (major diastereomer) 7.32 - 7.12 (5 H, m, ArH), 5.16 (1 H, dd, *J*=13.8, 4.0 Hz, $C\underline{H_a}H_b$-3), 4.80 (1 H, dd, *J*=13.9, 10.8 Hz, $CH_a\underline{H_b}$-3), 4.32 (1 H, d, *J*=5.9 Hz, CH-5), 4.21 - 4.16 (1 H, m, CH-2), 2.86 (3 H, s, CH_3-12a), 2.53 (3 H, s, CH_3-12b), 0.99 (9 H, s, CH_3-8); (minor diastereomer, selected peaks) 5.40 (1 H, dd, *J*=10.6, 4.0 Hz), 4.45 (1 H, d, *J*=8.1 Hz), 3.74 (1 H, dt, *J*=10.5, 3.9 Hz), 3.08 (3 H, s), 2.73 (3 H, s), 0.83 (9 H, s); **^{13}C NMR** (101 MHz, $CDCl_3$) δ (ppm): (major diastereomer) 207.9 (C-6), 166.4 (C-4), 137.9 (C-1), 129.1 (C-10), 127.7 (C-9), 127.2 (C-11), 76.3 (C-3), 53.5 (C-5), 44.8 (C-7), 43.3 (C-2), 37.7 (C-12a), 35.9 (C-12b), 26.6 (C-8); (minor diastereomer, selected peaks) 208.1, 165.5, 135.2, 129.3, 128.1, 73.7, 46.8, 45.0, 44.0, 38.0, 35.8, 26.5; **MP** 60 - 62 °C; **IR** ν_{max}/cm^{-1} 2968, 1713, 1636, 1553, 1478, 1394, 1134, 1062; **MS** (ES+) 321.2 $[M+H]^+$, 343.1 $[M+Na]^+$; **HRMS** (ES+) calcd. for $C_{17}H_{24}N_2NaO_4$ $[M+Na]^+$ 343.16283, found 343.16267.

2-Acetyl-N,N-diethyl-4-nitro-3-phenylbutanamide (**129**)

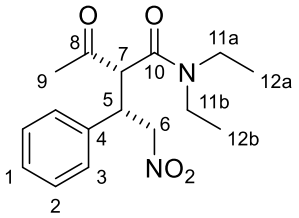

129

To *trans*-β-nitrostyrene (89 mg, 0.60 mmol), *N*,*N*-diethyl-3-oxobutanamide (31 mg, 0.20 mmol) and catalyst **116** (20 mg, 0.020 mmol) in a screw-cap vial was added anhydrous toluene (0.2 mL). The vial was promptly sealed and stirred at room temperature for 45 h. The reaction mixture was then filtered through a plug of cotton wool, the solvent removed *in vacuo* and the residue subjected to flash column chromatography over silica (50% ethyl acetate in petroleum ether) to give the product as an off-white solid (major diastereomer – 18 mg, 29%, minor diastereomer – 4.3 mg, 7%). The enantiomeric excess of the major diastereomer was determined by HPLC analysis (Chiralpak AD-H, hexane/*iso*-propanol 85:15, λ 210 nm, 1.0 mL/min: major diastereomer - t (major) 9.8 min, t (minor)

= 11.5 min (86:14 e.r.), minor diastereomer - t (major) 8.9 min, t (minor) = 11.5 min (81:19 e.r.)). Characterisation follows for the major diastereomer: **$[\alpha]_D^{25}$** = −5.9 (*c* 0.8, $CHCl_3$, 86:14 e.r.); **^{1}H NMR** (400 MHz, $CDCl_3$) δ (ppm): 7.29 - 7.12 (5 H, m, ArH), 4.79 (1 H, dd, *J*=9.5, 1.7 Hz, C$\underline{H_a}H_b$-6), 4.74 (1 H, dd, *J*=9.5, 4.9 Hz, $CH_a\underline{H_b}$-6), 4.33 (1 H, td, *J*=8.1, 5.3 Hz, CH-5), 3.96 (1 H, d, *J*=8.1 Hz, CH-7), 3.33 (2 H, q, *J*=6.9 Hz, CH_2-11a), 3.09 - 3.25 (1 H, m, C$\underline{H_a}H_b$-11b), 2.89 (1 H, dq, *J*=14.9, 7.2 Hz, $CH_a\underline{H_b}$-11b), 2.00 (3 H, s, CH_3-9), 1.07 (3 H, t, *J*=7.1 Hz, CH_3-12a), 0.97 (3 H, t, *J*=7.2 Hz, CH_3-12b); **^{13}C NMR** (101 MHz, $CDCl_3$) δ (ppm): 202.2 (C-8), 166.1 (C-10), 136.5 (C-4), 129.3 (C-2), 128.5 (C-1), 128.1 (C-3), 77.7 (C-6), 60.3 (C-7), 43.2 (C-5), 42.4 (C-11b), 41.2 (C-11a), 27.3 (C-9), 14.1 (C-12b), 12.7 (C-12a); **MP** 62 – 64 °C; **IR** ν_{max}/cm^{-1} 2978, 1719, 1626, 1550, 1495, 1455, 1435, 1380, 1360, 1313, 1275, 1215, 1169, 1139, 1097; **MS** (ES+) 329.1 $[M+Na]^+$. **HRMS** (ES+) calcd. for $C_{16}H_{22}NNaO_4$ $[M+Na]^+$ 329.14718, found 329.14612.

7. Rate enhancement in conjugate additions

Methyl 1-methyl-2-oxopyrrolidine-3-carboxylate (**34**)

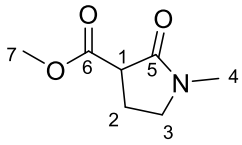

34

To a solution of diisopropylamine (14 mL, 0.10 mol) in THF (50 mL) at −78 °C under argon atmosphere was added *n*-butyllithium (42 mL, 0.11 mol, 2.5 M in hexanes) and the mixture stirred at −78 °C for 0.5 h. *N*-methylpyrrolidinone (4.9 mL, 50 mmol) was added and the mixture stirred at −78 °C for 1 h. Dimethylcarbonate (4.3 mL, 50 mmol) was then added dropwise with vigorous stirring and the resulting suspension was stirred for 4 h at room temperature. The reaction mixture was poured onto saturated aqueous NH_4Cl and extracted with CH_2Cl_2 (3 × 50 mL). The combined organic extracts were dried over Na_2SO_4 and the solvent removed *in vacuo*. The residue was purified by flash column chromatography over silica (ethyl acetate) to give the product as a pale yellow oil (5.8 g, 74% yield). **^{1}H NMR** (400 MHz, $CDCl_3$) δ (ppm): 3.76 (3 H, s, CH_3-7), 3.50 (1 H, td, *J*=9.1, 5.2 Hz, C$\underline{H_a}H_b$-2), 3.43 (1 H, dd, *J*=9.5, 6.6 Hz, CH-1), 3.35 (1 H, ddd, *J*=9.5, 8.5, 5.6 Hz, $CH_a\underline{H_b}$-2), 2.87 (3 H, s, CH_3-4), 2.41 (1 H, dddd, *J*=13.1, 8.6, 6.5, 5.8 Hz, C$\underline{H_a}H_b$-3), 2.32 - 2.20 (1 H, m,

CH_aH_b-2); **^{13}C NMR** (101 MHz, $CDCl_3$) δ (ppm): 170.8 (C-5), 169.7 (C-6), 52.6 (C-7), 48.1 (C-1), 47.8 (C-2), 30.0 (C-4), 22.1 (C-3); **MS** (ES+) 158.1 $[M+H]^+$. Spectroscopic data in agreement with literature values.[19]

Methyl (3*S*)-1-butyl-3-[(1*S*)-2-nitro-1-phenylethyl]-2,5-dioxopyrrolidine-3-carboxylate (**139**)

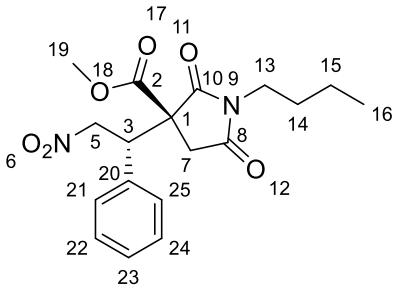

139

Maleimide **138** (43 mg, 0.20 mmol) and nitrostyrene (45 mg, 0.30 mmol) in CH_2Cl_2 (0.2 mL) were cooled to -20 °C then added to catalyst **137** (22 mg, 0.020 mmol) in a screw-cap vial. The vial was immediately placed in a −20 °C cold bath and the reaction mixture was stirred at that temperature for 1 h. The catalyst was removed by filtration through a plug of cotton wool, the solvent removed *in vacuo* and the residue subjected to flash column chromatography over silica (10% EtOAc/petroleum ether, then 20% EtOAc in petroleum ether) to give the product **139** as a colourless oil (major diastereomer - 39 mg, 54%). The diastereomeric ratio was determined to be 79:21 by ^{1}H-NMR analysis of the crude reaction mixture. The enantiomeric excess was determined by HPLC analysis (Chiralpak IB, hexane/*iso*-propanol 85:15, λ 210 nm, 1.0 mL/min: t (minor) 16.7 min, t (major) = 23.0 min (94:6 e.r.)). **$[\alpha]_D^{25}$** (major diastereomer) = +69.4 (*c* 1.0, $CHCl_3$, 94:6 e.r.), (lit. $[\alpha]_D^{25}$ = +89 (*c* 0.70, $CHCl_3$)[20]; **^{1}H NMR** (400 MHz, $CDCl_3$) δ (ppm): (major diastereomer) 7.33 - 7.13 (m, 5 H, ArH), 5.30 (dd, *J*=14.3, 10.4 Hz, 1 H, CH-5a), 5.12 (dd, *J*=13.9, 3.4 Hz, 1 H, CH-5b), 4.26 (dd, *J*=11.0, 3.4 Hz, 1 H, CH-3), 3.82 (s, 3 H, CH_3-19), 3.52 - 3.37 (m, 2 H, CH_2-13), 2.83 (d, *J*=18.3 Hz, 1 H, CH-7a), 2.65 (d, *J*=18.3 Hz, 1 H, CH-7b), 1.59 - 1.37 (m, 2 H, CH_2-14), 1.33 - 1.10 (m, 2 H, CH_2-15), 0.91 (t, *J*=7.3 Hz, 3 H, CH_3-16); **^{13}C NMR** (100 MHz, $CDCl_3$) δ (ppm): 174.7 (C-10), 173.5 (C-8), 169.8 (C-2), 133.8 (C-20), 129.6 (C-22,24), 129.4 (C-23), 129.1 (C-21,25), 76.9 (C-5), 56.4 (C-1), 54.0 (C-19), 46.6 (C-13), 39.4 (C-7), 38.3 (C-3), 29.3 (C-14), 20.0 (C-15), 13.6 (C-16); **MS** (ES+) 385.2 $[M+Na]^+$. Spectroscopic data consistent with literature values.[20]

Methyl (3*S*)-1-methyl-3-[(1*S*)-2-nitro-1-phenylethyl]-2-oxopyrrolidine-3-carboxylate (**35**)

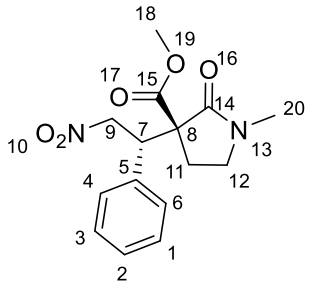

35

Pyrrolidinone **34** (41 mg, 0.26 mmol) and nitrostyrene (30 mg, 0.20 mmol) in THF (0.2 mL) were cooled to −20 °C then added to catalyst **137** (22 mg, 0.020 mmol) in a screw-cap vial. The vial was immediately placed in a −20 °C cold bath and the reaction mixture was stirred at that temperature for 2 h. The catalyst was removed by filtration through a plug of cotton wool, the solvent removed *in vacuo* and the residue subjected to flash column chromatography over silica (50% EtOAc/petroleum ether) to give the product **35** as a colourless oil (48 mg, 78%). The diastereomeric ratio was determined to be 79:21 by ^{1}H-NMR analysis of the crude reaction mixture. The enantiomeric excess was determined by HPLC analysis (Chiralpak AS-H, hexane/*iso*-propanol 90:10, λ 210 nm, 1.0 mL/min: major diastereomer - t (minor) 30.2 min, t (major) = 42.1 min (88:12 e.r.), minor diastereomer - t (major) 39.6 min, t (minor) 53.4 min (61:39 e.r.)). **$[\alpha]_D^{25}$** = +34 (*c* 0.90, $CHCl_3$, 79:21 d.r., 88:12 e.r. (major), 61:39 (minor)); **^{1}H NMR** (400 MHz, $CDCl_3$) δ (ppm): (major diastereomer) 7.37 - 7.16 (m, 5 H, ArH), 5.21 (dd, *J*=13.8, 11.1 Hz, 1 H, CH-9a), 4.95 (dd, *J*=13.7, 3.4 Hz, 1 H, CH-9b), 4.14 (dd, *J*=11.1, 3.3 Hz, 1 H, CH-7), 3.73 (s, 3 H, CH_3-18), 3.02 (td, *J*=9.0, 4.5 Hz, 1 H, CH-12a), 2.69 (s, 3 H, CH_3-20), 2.29 - 2.17 (m, 1 H, CH-12b), 2.15 - 2.05 (m, 1 H, CH-11a), 2.03 - 1.90 (m, 1 H, CH-11b); (minor diastereomer, selected peaks) 5.44 (1 H, dd, *J*=13.7, 3.7 Hz), 5.04 (1 H, dd, *J*=13.7, 11.0 Hz), 4.06 (1 H, dd, *J*=11.2, 3.7 Hz), 3.72 (3 H, s), 3.23 (1 H, ddd, *J*=9.4, 8.3, 6.2 Hz), 2.87 (1 H, td, *J*=9.2, 4.4 Hz), 2.67 (3 H, s), 2.35 (1 H, ddd, *J*=13.3, 8.5, 4.4 Hz); **^{13}C NMR** (101 MHz, $CDCl_3$) δ (ppm): (major diastereomer) 172.0 (C-14), 170.7 (C-15), 135.3 (C-5), 129.2 (C-1,3), 129.0 (C-2), 128.9 (C-4,6), 76.6 (C-9), 57.9 (C-8), 53.3 (C-18), 47.4 (C-12), 46.7 (C-20), 30.1 (C-7), 28.5 (C-11); (minor diastereomer, selected peaks) 170.5, 170.1, 135.6, 128.7, 128.4, 58.2, 53.2,

47.3, 46.6, 30.3, 26.8; **MS** (ES+) 307.1 $[M+H]^+$, 329.1 $[M+Na]^+$. Spectroscopic data consistent with literature values.[21]

Methyl 1-methyl-3-(2-nitro-1-phenylethyl)-2-oxopiperidine-3-carboxylate (**141**)

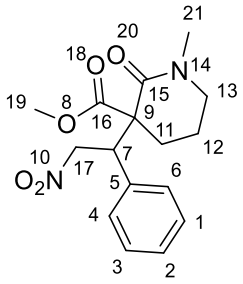

141

Lactam **140** (34 mg, 0.20 mmol) and nitrostyrene (36 mg, 0.24 mmol) in THF (0.2 mL) were cooled to −20 °C then added to catalyst **116** (20 mg, 0.020 mmol) in a screw-cap vial. The vial was immediately placed in a −20 °C cold bath and the reaction mixture was stirred at that temperature for 16 h. The catalyst was removed by filtration through a plug of cotton wool, the solvent removed *in vacuo* and the residue subjected to flash column chromatography over silica (50% EtOAc/petroleum ether) to give the product **141** as a colourless amorphous solid (44 mg, 69%). The diastereomeric ratio was determined to be 76:24 by ^{1}H-NMR analysis of the crude reaction mixture. The enantiomeric excess was determined by HPLC analysis (Chiralpak AD, hexane/*iso*-propanol 90:10, λ 210 nm, 1.0 mL/min: major diastereomer - t (major) 24.3 min, t (minor) = 49.9 min (96:4 e.r.), minor diastereomer t (minor) 21.3 min, t (major) 26.6 min (77:23)). $\mathbf{[\alpha]_D^{25}}$ = −66 (*c* 1.0, $CHCl_3$, 76:34 d.r., 96:4 e.r.(major), 78:22 e.r. (minor)); **^{1}H NMR** (400 MHz, $CDCl_3$) δ (ppm): (major diastereomer) 7.34 - 7.15 (m, 5 H, ArH), 5.35 (dd, *J*=13.9, 10.5 Hz, 1 H, CH-17a), 4.85 (dd, *J*=13.9, 2.7 Hz, 1 H, CH-17b), 3.96 (dd, *J*=10.6, 2.6 Hz, 1 H, CH-7), 3.75 (s, 3 H, CH_3-19), 3.16 - 3.01 (m, 1 H, CH-13a), 2.90 (s, 3 H, CH_3-21), 2.83 (m, 1 H, CH-13b), 2.05 - 1.92 (m, 1 H, CH-11a), 1.80 - 1.56 (m, 2 H, CH-11b and CH-12a), 1.47 - 1.27 (m, 1 H, CH-12b); (minor diastereomer, selected peaks) 5.32 (1 H, dd, *J*=13.7, 3.7 Hz), 4.98 (1 H, dd, *J*=13.4, 11.0 Hz), 4.18 (1 H, dd, *J*=10.8, 3.7 Hz), 3.65 (3 H, s), 2.80 (3 H, s); **^{13}C NMR** (101 MHz, $CDCl_3$) δ (ppm): (major diastereomer) 173.2 (C-16), 167.1 (C-15), 136.4 (C-5), 129.8 (C-2), 128.9 (C-1,3), 128.4 (C-4,6), 79.6 (C-17), 57.8 (C-9), 53.3 (C-19), 50.2 (C-7), 49.6 (C-13), 35.4 (C-21), 32.0 (C-11), 19.7 (C-12); (minor diastereomer, selected peaks)

171.9, 167.3, 135.9, 129.9, 128.5, 128.2, 77.8, 56.5, 52.9, 49.5, 48.3, 35.7, 28.9, 19.6; **IR** ν_{max}/cm^{-1} 2952, 1731, 1637, 1548, 1496, 1454, 1434, 1433, 1402, 1379, 1331, 1309, 1291, 1242, 1197, 1182, 1148, 1110, 1086, 1035, 1002; **MS** (ES+) 321.1 $[M+H]^+$, 343.1 $[M+Na]^+$; **HRMS** (ES+) calcd. for $C_{16}H_{21}N_2O_5$ $[M+H]^+$ 321.14450, found 321.14395.

Methyl (7a*R*)-6-[1-(furan-3-yl)-2-nitroethyl]-3,3-dimethyl-5-oxotetrahydro-1H-pyrrolo[1,2-*c*][1,3]oxazole-6-carboxylate (**144**)

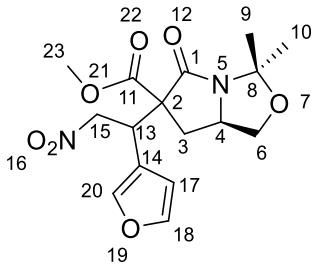

144

Bicycle **142** (85 mg, 0.40 mmol) and nitroalkene **143** (28 mg, 0.20 mmol) were dissolved in toluene (0.6 mL) then added to catalyst **137** (22 mg, 0.020 mmol) in a screw-cap vial. The vial was stirred at room temperature for 1 h. The catalyst was removed by filtration through a plug of cotton wool and the solvent removed *in vacuo* to give the crude product with a d.r. of 96:4:0:0, determined by ^{1}H-NMR analysis. The crude product was then subjected to flash column chromatography over silica (10% EtOAc/petroleum ether then 70% EtOAc/petroleum ether). The resulting colourless solid was then triturated with diethyl ether at −30 °C to give pure **144** as a colourless solid (46 mg, 66%). The diastereomeric ratio of the product after trituration was determined to be >99:1 by ^{1}H-NMR analysis. **$[\alpha]_D^{25}$** = −2.7 (*c* 1.0, $CHCl_3$), lit. $[\alpha]_D^{26}$ = +2.1 (*c* 0.75, $CHCl_3$)[22]; **^{1}H NMR** (400 MHz, $CDCl_3$) δ (ppm): 7.45 (s, 1 H, CH-18), 7.43 (m, 1 H, CH-20), 6.42 (s, 1 H, CH-17), 4.99 (dd, *J*=13.3, 4.0 Hz, 1 H, CH-15a), 4.93 (dd, *J*=13.4, 10.5 Hz, 1 H, CH-15b), 4.15 (dd, *J*=10.6, 3.9 Hz, 1 H, CH-13), 3.91 (dd, *J*=7.8, 5.3 Hz, 1 H, CH-6a), 3.83 (s, 3 H, CH_3-23), 3.40 (dd, *J*=9.6, 7.9 Hz, 1 H, CH-6b), 3.25 - 3.35 (m, 1 H, CH-4), 2.18 (dd, *J*=7.2, 1.7 Hz, 2 H, CH_2-3), 1.67 (s, 3 H, CH_3-9/10), 1.42 (s, 3 H, CH_3-9/10); **^{13}C NMR** (101 MHz, $CDCl_3$) δ (ppm): 171.8 (C-1), 167.4 (C-11), 144.1 (C-18), 142.1 (C-20), 119.3 (C-14), 109.6 (C-17), 92.0 (C-8), 76.9 (C-15), 70.0 (C-6), 63.6 (C-2), 58.7 (C-4), 53.5 (C-23), 38.7 (C-13), 33.4 (C-3), 26.4 (C-9/10), 23.4 (C-9/10); **MP** 148 - 150 °C (lit. 157 °C); **MS** (ES+) 375.1 $[M+Na]^+$, Spectroscopic data consistent with literature values.[22]

(1*R*,2*S*,3*S*,11b*S*)-1′-Methyl-1-nitro-2-phenyl-1,6,7,11b-tetrahydro-2*H*,2′*H*-spiro[pyrido[2,1-a]isoquinoline-3,3′-pyrrolidine]-2′,4-dione (**146**)

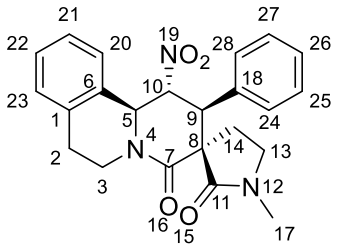

146

Pyrrolidinone **34** (41 mg, 0.26 mmol) and nitrostyrene (30 mg, 0.20 mmol) in THF (0.2 mL) were cooled to −20 °C then added to catalyst **137** (22 mg, 0.020 mmol) in a screw-cap vial. The vial was immediately placed in a −20 °C cold bath and the reaction mixture was stirred at that temperature for 2 h. The catalyst was removed by filtration through a plug of cotton wool and the solvent removed *in vacuo*. The crude residue and imine **145** (53 mg, 0.40 mmol) were suspended in water (1.5 mL) and heated at 70 °C for 48 h. The reaction mixture was then cooled to room temperature and extracted with CH_2Cl_2. The organic extracts were washed with brine, dried with anhydrous Na_2SO_4 and the solvent removed *in vacuo*. The residue was subjected to flash column chromatography over silica (20% EtOAc/petroleum ether then 50% EtOAc/petroleum ether) to give the product **146** as a pale yellow solid (56 mg, 68%). The diastereomeric ratio of the product was determined to be >99:1 by ^{1}H-NMR analysis. The enantiomeric excess was determined by HPLC analysis (Chiralpak OD, hexane/*iso*-propanol 80:20, λ 210 nm, 1.0 mL/min: t (major) 21.0 min, t (minor) = 24.8 min (88:12 e.r.)). **$[\alpha]_D^{25}$** = +197 (*c* 1.0, $CHCl_3$, 88:12 e.r.), lit. $[\alpha]_D^{25}$ = +219.8 (*c* 1.0, $CHCl_3$, 96% e.e.)[19]; **^{1}H NMR** (400 MHz, $CDCl_3$) δ (ppm): 7.47 - 6.99 (m, 9 H, ArH), 6.47 (dd, *J*=12.2, 8.3 Hz, 1 H, CH-10), 5.34 (d, *J*=8.3 Hz, 1 H, CH-5), 4.40 (dt, *J*=12.7, 5.3 Hz, 1 H, CH-3a), 3.72 (d, *J*=12.2 Hz, 1 H, CH-9), 3.21 (ddd, *J*=12.9, 9.0, 4.3 Hz, 1 H, CH-3b), 3.14 - 3.06 (m, 1 H, CH-13a), 3.05 - 2.99 (m, 1 H, CH-2a), 2.94 (ddd, *J*=13.1, 9.5, 6.5 Hz, 1 H, CH-14a), 2.76 (dt, *J*=16.0, 5.0 Hz, 1 H, CH-2b), 2.55 (s, 3 H, CH_3-17), 2.05 (td, *J*=8.8, 6.6 Hz, 1 H, CH-13b), 1.79 (ddd, *J*=12.8, 8.7, 3.7 Hz, 1 H, CH-14b); **^{13}C NMR** (101 MHz, $CDCl_3$) δ (ppm): 171.1 (C-11), 167.8 (C-7), 135.9 (C-18), 134.3 (C-6), 133.4 (C-1), 131.6 (br. s., ArC), 129.2 (ArC), 129.0 (ArC), 128.9 (ArC), 128.1 (ArC), 127.3 (ArC), 126.6 (br. s., ArC), 123.8 (ArC), 87.5 (C-10), 58.6 (C-5), 55.8 (C-8), 51.3 (C-9), 47.2 (C-13), 43.1

(C-3), 30.0 (C-17), 28.5 (C-2), 27.3 (C-14); **MP** 196 - 200 °C; **MS** (ES+) 428.2 $[M+Na]^+$. Spectroscopic data consistent with literature values.[21]

8. Comparisons with homogeneous bifunctional iminophosphorane organocatalyst (**182**)

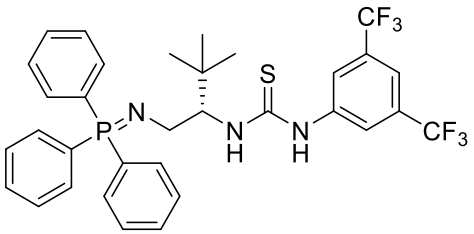

182

Azide **57** (8.3 mg, 0.020 mmol) and triphenylphosphine (5.2 mg, 0.020 mmol) were dissolved in diethyl ether (0.1 mL) and stirred at room temperature for 24 h in a sealed screw-cap vial. TLC analysis indicated the complete consumption of azide and triphenylphosphine and mass spectrometry indicated the presence of the iminophosphorane catalyst **182**. Solvent was removed under a flow of nitrogen to give the crude catalyst **182** as a colourless oil. Spectroscopic data consistent with literature values.[6]

General Procedures B, D and F were repeated using catalyst **182** in the place of catalyst **116**.

9. Catalyst recycling experiment

9.1 Conjugate addition of nitromethane to chalcone

4-nitro-1,3-diphenylbutan-1-one (**24**)

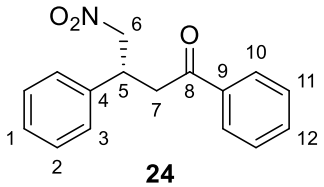

24

To polystyrene supported catalyst **116** (40 mg, 0.040 mmol) and chalcone (83 mg, 0.40 mmol) in a screw-cap vial was added nitromethane (0.43 mL, 8.0 mmol). The vial was sealed and the reaction mixture stirred at room temperature for 6 h. The reaction mixture was then diluted with anhydrous CH_2Cl_2 and stirred for several minutes. The supernatant solution containing the product was removed carefully with a syringe and transferred to a flask, leaving the catalyst in the vial. This washing

procedure was repeated 3-4 times (5 mL total volume CH_2Cl_2). The solvent from the combined supernatant solutions was removed *in vacuo* and the crude reaction mixture was then purified by flash column chromatography over silica (10% ethyl acetate in petroleum ether) and the enantiomeric excess was determined by HPLC analysis (Chiralpak IA, hexane/*iso*-propanol 95:5, λ 210 nm, 1.0 mL/min: t (minor) 22.7 min, t (major) = 29.6 min). The catalyst remaining in the screw-cap vial was dried under nitrogen flow and the procedure repeated. **$[\alpha]_D^{25}$** = +17 (*c* 1.0, $CHCl_3$, 89:11 e.r.); **^{1}H NMR** (400 MHz, $CDCl_3$) δ (ppm): 7.87 - 7.78 (2 H, m, ArH), 7.52 - 7.45 (1 H, m, ArH), 7.43 - 7.28 (2 H, m, ArH), 7.31 - 7.15 (5 H, m, ArH), 4.75 (1 H, dd, *J*=12.5, 6.6 Hz, C$\underline{H_a}H_b$-6), 4.60 (1 H, dd, *J*=12.5, 8.1 Hz, $CH_a\underline{H_b}$-6), 4.15 (1 H, quin, *J*=7.2 Hz, CH-5), 3.40 (1 H, dd, *J*=18.1, 6.8 Hz, C$\underline{H_a}H_b$-7), 3.33 (1 H, dd, *J*=18.1, 7.8 Hz, $CH_a\underline{H_b}$-7); **^{13}C NMR** (101 MHz, $CDCl_3$) δ (ppm): 197.0 (C-8), 139.2 (C-4), 136.4 (C-9), 133.7 (C-12), 129.2 (C-10), 128.8 (C-11), 128.1 (C-3), 128.0 (C-1), 127.6 (C-2), 79.7 (C-6), 41.6 (C-7), 39.4 (C-5); **MS** (ES+) 292.1 $[M+Na]^+$. Spectroscopic data in agreement with literature values.[23]

9.2 Nitro-Mannich reaction

To polystyrene supported catalyst **116** (19.8 mg, 0.0200 mmol) and phenyl ketimine **36a** (63.9 mg, 0.200 mmol) in a screw-cap vial was added anhydrous toluene (25 µL) and nitromethane (215 µL, 4.00 mmol). The vial was sealed and the reaction mixture stirred at room temperature for 24 h. The reaction mixture was then diluted with anhydrous CH_2Cl_2 and stirred for several minutes. The supernatant solution containing the product was removed carefully with a syringe and transferred to a flask, leaving the catalyst in the vial. This washing procedure was repeated 3-4 times (5 mL total volume CH_2Cl_2). The solvent from the combined supernatant solutions was removed *in vacuo* and the conversion was measured by ^{1}H-NMR of the crude reaction mixture. The crude reaction mixture was then purified by flash column chromatography over silica (80% ethyl acetate in petroleum ether) and the enantiomeric excess was determined by HPLC analysis (Chiralpak OD-H, hexane/*iso*-propanol 80:20, λ 220 nm, 1.0 mL/min: t (minor) 8.1 min, t (major) = 20.3 min). The catalyst remaining in the screw-cap vial was dried under nitrogen flow and the procedure repeated.

Run	Conversion by ^{1}H-NMR	e.e.
1	94%	76%
2	96%	83%
3	95%	85%
4	97%	87%
5	97%	88%
6	96%	89%
7	96%	90%
8	96%	90%
9	97%	91%
10	95%	92%
11	88%	92%

Table E1. *Results of catalyst recycling experiment.*

10. Flow chemistry representative procedure

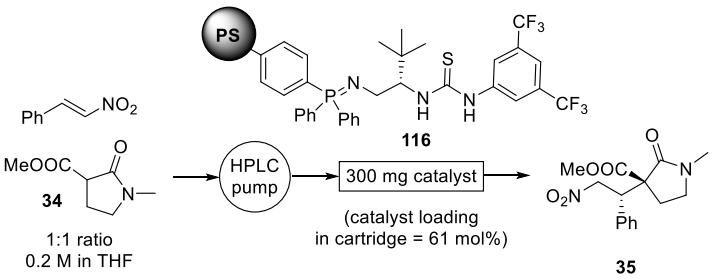

A blank HPLC column (150 mm length, I.D. 4.6 mm, 2.7 mL internal volume) was partially filled with catalyst **116** (300 mg, 0.303 mmol) and connected to an HPLC pump (HP Model 1050). THF (0.5 mL/min) was pumped through the column for approximately 30 min to swell the polystyrene support. A solution of **34** and nitrostyrene (in a 1:1 molar ratio, 0.2 M each) in THF was pumped through the column at the indicated flow rate. The product was collected in vials. The solvent was removed *in vacuo* and the residue analysed by ^{1}H-NMR to obtain the conversion and diastereomeric ratio. The residue was then purified by flash column chromatography over silica (50% EtOAc/petroleum ether) to give the product **35** as a colourless oil. The enantiomeric excess was

determined by HPLC analysis (Chiralpak AS-H, hexane/*iso*-propanol 90:10, λ 210 nm, 1.0 mL/min: major diastereomer - t (minor) 30.2 min, t (major) = 42.1 min, minor diastereomer - t (major) 39.6 min, t (minor) 53.4 min). Spectroscopic data in agreement with characterisation data for **35**.

Chapter 3: Organocatalytic Ring-Opening Polymerisation

1. Catalyst Synthesis

1.1 Achiral catalyst

1-[3,5-bis(trifluoromethyl)phenyl]imidazolidine-2-thione (**152**)

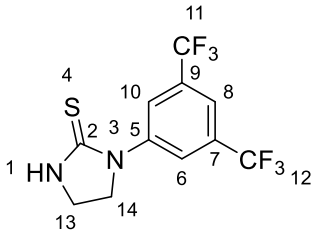

152

To a suspension of 2-chloroethylamine hydrochloride (0.12 g, 1.0 mmol) in CH_2Cl_2 (1.5 mL) was added triethylamine (0.28 mL, 2.0 mmol) and the reaction mixture stirred at room temperature for 24 h. 3,5-bis(trifluoromethyl)phenyl isothiocyanate (0.18 mL, 1.0 mmol) was then added and the reaction mixture stirred at room temperature for 1 h. The reaction mixture was washed with water, then brine, then dried over Na_2SO_4. The solvent was removed *in vacuo* and the residue purified by flash column chromatography over silica (20% ethyl acetate in petroleum ether) to give the product as a colourless solid (0.24 g, 76%). **^{1}H NMR** (500 MHz, $CDCl_3$) δ (ppm): 7.52 (1 H, s, CH-8), 7.47 (2 H, s, CH-6,10), 5.41 (1 H, br. s, NH-1), 3.74 (2 H, t, J=6.9 Hz, CH_2-13), 3.36 (2 H, t, J=6.9 Hz, CH_2-14); **^{13}C NMR** (125 MHz, $CDCl_3$) δ (ppm): 165.2 (C-2), 151.4 (C-5), 132.3 (q, J_{FC}=33.5 Hz, C-7,9), 123.5 (q, J_{FC}=273.2 Hz, C-11,12), 122.3 ('d', J_{FC}=3.2 Hz, C-6,10), 116.6 ('dt', J_{FC}=7.4, 3.9 Hz, C-8), 46.9 (C-14), 31.2 (C-13); **MP** 118 – 120 °C; **IR** (ν_{max}/cm^{-1}) 3092, 2093, 1646, 1474, 1378, 1280, 1166, 1113, 1076; **HRMS** (ES+) calcd. for $C_{11}H_9F_6N_2S$ $[M+H]^+$ 315.0385, found 315.0377.

tert-Butyl (2-aminoethyl)carbamate (**158**)

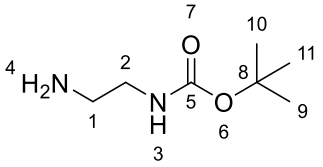

158

To a solution of ethylenediamine (0.33 mL, 5.0 mmol) in dioxane (1.5 mL) at room temperature was added dropwise di-*tert*-butyl dicarbonate (0.11 g, 0.50 mmol) in dioxane (0.5 mL) and the reaction stirred at room temperature for 24 h. The solvent was removed *in vacuo* and the residue purified by flash column chromatography over silica (30% methanol in ethyl acetate) to give the product as a colourless oil (78 mg, 97%). **^{1}H NMR** (500 MHz, $CDCl_3$) δ (ppm): 4.95 (1 H, br. s, NH-3), 3.15 (2 H, q, *J*=5.3 Hz, CH_2-2), 2.78 (2 H, t, *J*=5.8 Hz, CH_2-1), 1.42 (9 H, s, CH_3-9,10,11); **^{13}C NMR** (100 MHz, $CDCl_3$) δ (ppm): 156.4 (C-5), 79.3 (br. s, C-8), 43.4 (br. s., C-1), 42.0 (C-2), 28.5 (C-9,10,11); **MS** (ES+) 161.2 $[M+H]^+$. Spectroscopic data consistent with literature values.[24]

tert-Butyl [2-({[3,5-bis(trifluoromethyl)phenyl]carbamothioyl}amino)ethyl]carbamate (**159**)

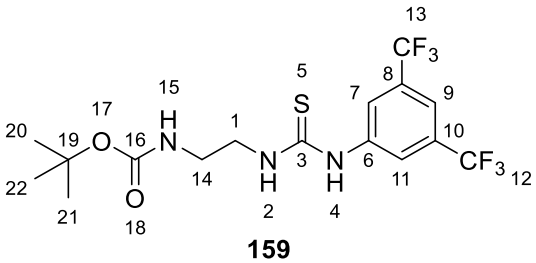

159

To a solution of **158** (60 mg, 0.37 mmol) in THF (1.8 mL) at room temperature was added 3,5-bis(trifluoromethyl)phenyl isothiocyanate (72 μL, 0.39 mmol) and the reaction mixture stirred for 2 h. The solvent was removed *in vacuo* and the residue purified by flash column chromatography over silica (20% ethyl acetate in petroleum ether, then 30% ethyl acetate in petroleum ether) to give the product as a colourless solid (0.14 g, 84%). **^{1}H NMR** (500 MHz, $CDCl_3$) δ (ppm): 9.47 (1 H, br. s, NH-4), 8.32 (2 H, br. s, CH-7,11), 7.84 (1 H, br. s, NH-2), 7.72 (1 H, s, CH-9), 6.26 (1 H, br. s, NH-15), 3.72 (2 H, br. s, CH_2-1), 3.36 (2 H, q, *J*=6.1 Hz, CH_2-14), 1.39 (9 H, s, CH_3-20,21,22); **^{13}C NMR** (125 MHz, d_6-acetone) δ (ppm): 182.5 (br. s, C-3), 157.5 (br. s, C-16), 142.7 (br. s, C-6), 132.0 (q, J_{FC}=33.3 Hz, C-8,10), 123.7 (br. s, C-7,11), 124.4 (q, J_{FC}=271.7 Hz, C-12,13), 117.6 ('t', J_{FC}=3.8 Hz, C-9), 79.2 (br. s, C-19), 46.0 (br. s, C-1), 40.2 (C-14), 28.5 (C-20,21,22); **^{19}F NMR** (470 MHz,

$CDCl_3$) δ (ppm): −63.5; **MP** 142 – 144 °C. **IR** (ν_{max}/cm^{-1}) 3287, 1683, 1522, 1472, 1383, 1278, 1174, 1134; **HRMS** (ES+) calcd. for $C_{16}H_{19}F_6N_3NaO_2S$ $[M+Na]^+$ 454.0994, found 454.0988.

1-(2-Aminoethyl)-3-[3,5-bis(trifluoromethyl)phenyl]thiourea (**156**)

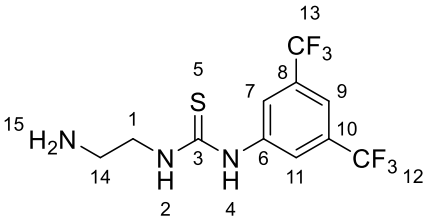

156

To **159** (50 mg, 0.12 mmol) at 0 °C was added trifluoroacetic acid (0.2 mL) and the reaction mixture stirred for 20 min at room temperature. The trifluoroacetic acid was removed under nitrogen flow and the residue dissolved in diethyl ether. Aqueous NaOH (1 M) was added dropwise with stirring until pH > 10 was obtained. The organic portion was separated and the aqueous portion extracted with diethyl ether (3 ×). The organic portions were combined and the solvent removed *in vacuo*. The residue was purified by flash column chromatography over silica (30% methanol in ethyl acetate with 5 drops triethylamine/100 mL eluent) to give the product as a colourless oil (28 mg, 73%). **^{1}H NMR** (200 MHz, CD_3OD) δ (ppm): 8.19 (2 H, s, CH-7,11), 7.63 (1 H, s, CH-9), 3.67 (2 H, t, *J*=5.2 Hz, CH_2-1), 2.90 (2 H, t, *J*=6.2 Hz, CH_2-14); **MS** (ES+) 332.0 $[M+H]^+$.

1-(2-Azidoethyl)-3-[3,5-bis(trifluoromethyl)phenyl]thiourea (**149**) *via* diazo transfer

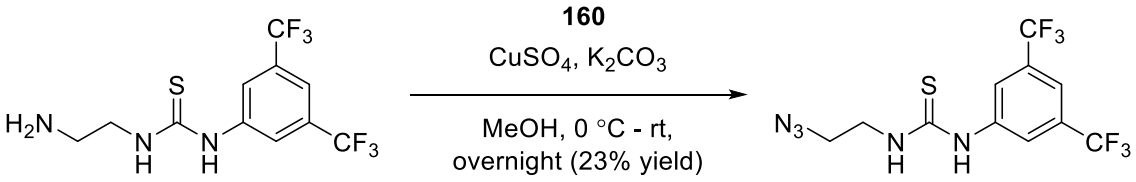

156 **149**

1*H*-Imidazole-1-sulfonyl azide hydrochloride **160** (21 mg, 0.10 mmol) was added in portions to a solution of **156** (28 mg, 0.085 mmol), copper sulfate pentahydrate (0.2 mg, 0.8 μmol) and potassium carbonate (20 mg, 0.14 mmol) in methanol (0.64 mL) at 0 °C and the reaction mixture stirred at room temperature for 24 h. Solvent was removed under nitrogen flow and the residue partitioned between water and diethyl ether. The organic layer was washed with brine, dried over Na_2SO_4 and solvent removed under nitrogen flow. The residue was purified by flash column chromatography (20% ethyl

acetate in petroleum ether) to give the product as a colourless oil (7 mg, 23%). For full characterisation see compound **149** below.

1-(2-Azidoethyl)-3-[3,5-bis(trifluoromethyl)phenyl]thiourea (**149**)

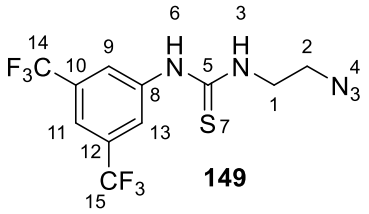

149

To a solution of bromoethylamine hydrobromide (1.00 g, 4.88 mmol) in water (5 mL) at room temperature was added sodium azide (0.952 g, 14.6 mmol) and the reaction mixture was heated at 80 °C for 24 h. The reaction mixture was allowed to cool to room temperature then basified with potassium hydroxide (1.60 g, 28.5 mmol). The reaction mixture was then extracted with diethyl ether (3 × 50 mL) and the combined organic extracts washed with brine, dried over anhydrous Na_2SO_4 and the solvent removed under a flow of nitrogen. The crude aminoazide was dissolved in anhydrous THF (25 mL), treated with 3,5-bis(trifluoromethyl)phenyl isothiocyanate (0.664 mL, 3.64 mmol) and the reaction mixture stirred under argon atmosphere for 3 h. The solvent was removed *in vacuo* and the crude reaction mixture purified by flash column chromatography over silica (petroleum ether, followed by 10% ethyl acetate in petroleum ether, then 20% ethyl acetate in petroleum ether) to give the product as a colourless solid (1.03 g, 2.89 mmol, 59% over 2 steps)**.** **^{1}H NMR** (500 MHz, $CDCl_3$) δ (ppm): 8.54 (1 H, br. s., NH-6), 7.81 (2 H, s, CH-9,13), 7.74 (1 H, s, CH-11), 6.54 (1 H, br. s., NH-3), 3.94 - 3.74 (2 H, m, CH_2-1), 3.72 - 3.54 (2 H, m, CH_2-2); **^{13}C NMR** (125 MHz, $CDCl_3$) δ (ppm): 181.1 (C-5), 138.6 (C-8), 133.4 (q, J_{FC} = 34.3 Hz, C-10,12), 124.3 (‘d’, J_{FC} = 3.8 Hz, C-9,13), 122.8 (q, J_{FC} = 272.8 Hz, C-14,15), 120.1 (‘t’, J_{FC} = 3.8 Hz, C-11), 50.4 (C-2), 44.4 (C-1)**; ^{19}F NMR** (470 MHz, $CDCl_3$) δ (ppm): −63.1; **MP** 84 – 85 °C. **IR** (ν_{max}/cm^{-1}) 3238, 2116, 1537, 1469, 1379, 1336, 1270, 1166, 1127, 971, 894, 847, 713, 680, 649. **HRMS** (ES+) calcd. for $C_{11}H_9F_6N_5NaS$ $[M+Na]^+$ 380.0375, found 380.0366.

1-[3,5-bis(trifluoromethyl)phenyl]-3-(2-{[tris(4-methoxyphenyl)-λ^5-phosphanylidene]amino}ethyl)thiourea (**162**)

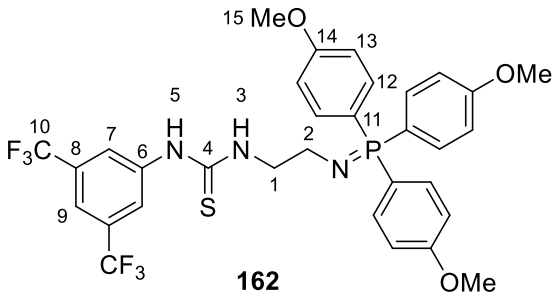

162

Azide **149** (0.945 g, 2.64 mmol) and tris(4-methoxy)phenylphosphine (0.932 g, 2.64 mmol) were dissolved in anhydrous diethyl ether (8 mL) and stirred at room temperature under argon atmosphere for 24 h. The resulting colourless precipitate was collected by filtration, washed with pentane (10 mL) and dried under vacuum for 24 h, yielding **162** (1.59 g, 2.33 mmol, 88%) as a colourless solid. **^{1}H NMR** (500 MHz, $CDCl_3$) δ (ppm): 7.46 (6 H, dd, J = 11.9, 8.8 Hz, CH-12), 7.28 (1 H, br. s., CH-9), 7.26 (2 H, s, CH-7), 6.96 (6 H, dd, J = 8.9, 2.6 Hz, CH-13), 3.84 (9 H, s, CH_3-15), 3.64 (2 H, br. s., CH_2-1), 3.10 - 3.07 (2 H, m, CH_2-2); **^{13}C NMR** (125 MHz, $CDCl_3$) δ (ppm): 182.1 (C-4), 163.9 (C-14), 134.9 (d, J_{PC} = 11.4 Hz, C-13), 130.7 (q, J_{FC} = 32.4 Hz, C-8), 124.3 (br. s., C-7), 123.8 (q, J_{FC} = 272.8 Hz, C-10), 116.0 (br. s., C-6), 115.2 (d, J_{PC} = 13.4 Hz, C-12), 115.0 - 114.7 ('t', J_{FC} = 2.9 Hz, C-9), 77.4 (C-15), 55.6 (C-1), 46.5 (br. s., C-2) *(N.B. C-11 not observed)*; **^{19}F NMR** (470 MHz, $CDCl_3$) δ (ppm): −62.1; **^{31}P NMR** (202 MHz, $CDCl_3$) δ (ppm): 27.9 (br. s.). **M.P.** 96 – 98 °C. **IR** (ν_{max}/cm^{-1}) 1595, 1502, 1466, 1416, 1374, 1299, 1273, 1179, 1114, 1013, 867, 836, 804, 699, 678. **HRMS** (ES+) calcd. for $C_{32}H_{31}F_6N_3O_3PS$ $[M+H]^+$ 682.1722, found 682.1772.

1.2 Phenyl-substituted catalyst

tert-Butyl (2-hydroxy-1-phenylethyl)carbamate (**167**)

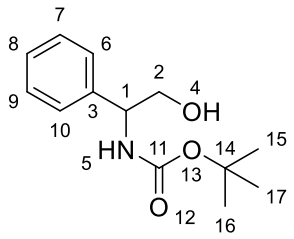

167

Sodium borohydride (3.0 g, 79 mmol) was suspended in anhydrous THF (87 mL) under argon atmosphere. (±)-phenylglycine (5.0 g, 33 mmol) was added and the reaction mixture cooled to 0 °C. A solution of iodine (8.4 g, 33 mmol) in THF (22 mL) was added dropwise to the reaction *via* addition funnel over 30 min. After the addition was complete, the reaction mixture was stirred at room temperature for 15 min, then heated at reflux for 18 h. After cooling to room temperature, methanol was added until the solution became clear and it was stirred for 30 min. The solvent was removed *in vacuo* and the resulting colourless paste dissolved in aqueous KOH (20% w/w, 50 mL) and stirred at room temperature for 3 h. The reaction mixture was then extracted with CH_2Cl_2 (3 × 100 mL), washed with brine and dried over Na_2SO_4. Solvent was removed *in vacuo*, giving (±)-phenylglycinol as a colourless solid (4.5 g) which was used without further purification.

To a solution of (±)-phenylglycinol (4.5 g, 33 mmol) and triethylamine (5.5 mL, 40 mmol) in CH_2Cl_2 (106 mL) at 0 °C was added di-*tert*-butyl dicarbonate (8.6 g, 40 mmol) and the reaction mixture stirred for 1 h at 0 °C, then at room temperature for 24 h. The reaction mixture was washed with brine, dried over Na_2SO_4 and the solvent removed *in vacuo*. The residue was purified by flash column chromatography over silica (20% ethyl acetate in petroleum ether gradually increasing to 50% ethyl acetate in petroleum ether) to give the product as a colourless solid (4.0 g, 51%). **^{1}H-NMR** (400 MHz, d_6-acetone) δ (ppm): 7.46 - 7.18 (5 H, m, ArH), 6.33 (1 H, br. s., NH-5), 4.75 - 4.69 (1 H, m, CH-1), 3.97 (1 H, t, *J*=5.9 Hz, OH-4), 3.78 - 3.68 (2 H, m, CH_2-2), 1.38 (9 H, br. s., CH_3-15,16,17); **^{13}C-NMR** (100 MHz, d_6-acetone) δ (ppm): 156.3 (C-11), 142.6 (C-3), 129.0 (C-7,9), 127.7 (C-6), 127.7 (C-8,10), 78.8 (C-14), 66.4 (C-2), 57.9 (C-1), 28.6 (C-15,6,17); **MP** 140 – 142 °C (lit. 138 – 140 °C); **MS** (ES+) 260.2 $[M+H]^+$. Spectroscopic data consistent with literature values.[25]

2-[(*tert*-butoxycarbonyl)amino]-2-phenylethyl 4-methylbenzenesulfonate (**168**)

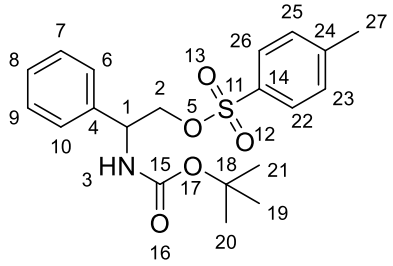

168

To a solution of alcohol **167** (4.0 g, 17 mmol) and triethylamine (4.7 mL, 34 mmol) in CH_2Cl_2 (12 mL) at room temperature was added *para*-toluenesulfonyl chloride (3.2 g, 17 mmol) and the reaction stirred at room temperature for 24 h. Water (30 mL) was then added to the reaction mixture and the resulting mixture extracted with CH_2Cl_2 (3 × 20 mL). The combined organic portions were washed with saturated aqueous NH_4Cl and dried over Na_2SO_4. The solvent was removed *in vacuo* and the residue purified by flash column chromatography over silica (10% ethyl acetate in petroleum ether, then 20% ethyl acetate in petroleum ether) to give the product as a colourless solid (5.0 g, 77%). **^{1}H-NMR** (400 MHz, $CDCl_3$) δ (ppm): 7.68 - 7.15 (m, 9 H, ArH), 5.14 (br. s., 1 H, NH-3), 4.89 (br. s., 1 H, CH-1), 4.28 - 4.19 (m, 1 H, C$\underline{H_a}H_b$-2), 4.19 - 4.11 (m, 1 H, C$H_a\underline{H_b}$-2), 2.41 (s, 3 H, CH_3-27), 1.39 (br. s., 9 H, CH_3-19,20,21); **^{13}C-NMR** (100 MHz, $CDCl_3$) δ (ppm): 155.0 (C-15), 145.1 (C-24), 137.9 (C-4), 132.5 (C-14), 130.0 (C-23,25), 128.9 (C-7,9), 128.1 (C-8), 128.0 (C-22,26), 126.7 (6,10), 80.3 (C-18), 71.6 (C-2), 53.5 (C-1), 28.4 (C-19,20,21), 21.8 (27); **MP** 154 – 156 °C (lit. 157– 160 °C); **MS** (ES+) 414.1 $[M+Na]^+$. Spectroscopic data consistent with literature values.[25]

tert-Butyl (2-azido-1-phenylethyl)carbamate (**169**)

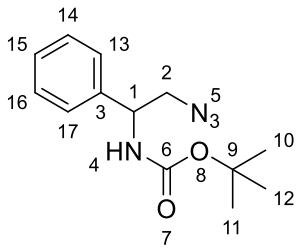

169

To tosylate **168** (5.1 g, 13 mmol) in *N*,*N*-dimethylformamide (43 mL) at room temperature was added sodium azide (0.92 g, 14 mmol) and the reaction mixture stirred at 45 °C for 24 h. The reaction mixture was cooled to room temperature and partitioned between water (90 mL) and diethyl ether

(60 mL). The organic portion was separated and the aqueous portion was further extracted with diethyl ether (2 × 30 mL). The combined organic portions were washed with brine, dried over Na_2SO_4. The solvent was removed *in vacuo* and the residue purified by flash column chromatography over silica (petroleum ether, then 10% ethyl acetate in petroleum ether) giving the product as a colourless solid (2.6 g, 72%). **^{1}H-NMR** (400 MHz, $CDCl_3$) δ (ppm): 7.41 - 7.27 (5 H, m, ArH), 5.15 - 5.05 (1 H, m, NH-4), 4.88 (1 H, br. s., CH-1), 3.69 - 3.56 (2 H, m, CH_2-2), 1.44 (9 H, br. s., CH_3-10,11,12); **^{13}C-NMR** (100 MHz, $CDCl_3$) δ (ppm): 155.2 (C-6), 139.4 (C-3), 129.0 (C-14,16), 128.2 (C-3), 126.6 (C-13,17), 80.2 (C-9), 55.8 (C-2), 54.2 (C-1), 28.5 (C-10,11,12); **MP** 80 – 82 °C (lit. 82 – 84 °C); **MS** (ES+) 285.1 $[M+Na]^+$. Spectroscopic data consistent with literature values.[6]

1-(2-azido-1-phenylethyl)-3-[3,5-bis(trifluoromethyl)phenyl]thiourea (**107-*rac***)

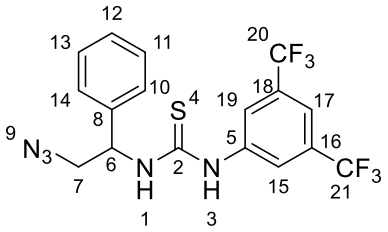

107-*rac*

Trifluoroacetic acid (11 mL) was added dropwise, with stirring, to azide **169** (2.6 g, 9.2 mmol) at 0 °C. The reaction mixture was stirred for 1 h, allowing to warm to room temperature. Trifluoroacetic acid was removed under nitrogen flow and the residue suspended in diethyl ether (10 mL). Aqueous sodium hydroxide (2 M) was added dropwise to the reaction mixture with vigorous stirring until a pH > 10 was obtained. The organic layer was separated and the aqueous layer extracted with diethyl ether (3 × 20 mL). The combined organic layers were washed with brine (20 mL) and dried over Na_2SO_4. Solvent was removed under nitrogen flow and the residue was dissolved in THF (32 mL) under argon atmosphere. 3,5-Bis(trifluoromethyl)phenyl isothiocyanate (1.7 mL, 9.2 mmol) was added dropwise to the reaction mixture, which was then stirred at room temperature for 24 h. Solvent was removed *in vacuo* and residue was purified by flash column chromatography over silica (5% ethyl acetate in petroleum ether, then 10% ethyl acetate in petroleum ether) to give the product as a colourless solid (3.8 g, 96%). **^{1}H-NMR** (400 MHz, $CDCl_3$) δ (ppm): 8.48 (br. s., 1 H, NH-3), 7.77 - 7.29 (8 H, m, ArH), 6.91 (1 H, d, *J*=6.1 Hz, NH-1), 5.68 (1 H, br. s., CH-6), 3.90 (1 H, dd, *J*=12.6,

4.8 Hz, C<u>H</u>$_a$H$_b$-7), 3.77 (1 H, dd, *J*=12.6, 5.1 Hz, CH$_a$<u>H</u>$_b$-7); **^{13}C-NMR** (100 MHz, $CDCl_3$) δ (ppm): 180.4 (C-2), 138.8 (C-8), 137.5 (C-5), 133.1 (q, J_{FC}=35.1 Hz, C-16,18), 129.4 (C-11,13), 128.8 (C-12), 126.8 (C-10,14), 123.9 ('d', J_{FC}=2.4 Hz, C-15,19), 119.7 ('dt', J_{FC}=7.4, 3.9 Hz, C-17), 122.9 (q, J_{FC}=273.3 Hz, C-20,21), 57.8 (C-6), 55.0 (C-7); **MP** 128 – 129 °C (lit. 136 – 137 °C; **MS** (ES−) 432.0 $[M-H]^-$. Spectroscopic data consistent with literature values.[6]

1-[3,5-bis(trifluoromethyl)phenyl]-3-(1-phenyl-2-{[tris(4-methoxyphenyl)-λ^5-phosphanylidene]amino}ethyl)thiourea (**148-*rac***)

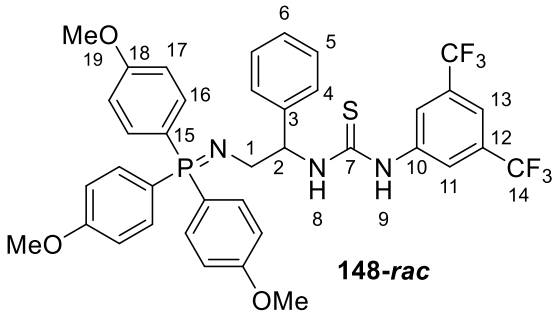

148-*rac*

Thiourea **107-*rac*** (0.70 g, 1.6 mmol) and tris(4-methoxy)phenylphosphine (0.57 g, 1.6 mmol) were dissolved in THF (8 mL) at room temperature under argon atmosphere and stirred for 24 h. The solvent was removed under a flow of nitrogen and the residue dried under vacuum. Diethyl ether (3 mL) and was added and the reaction stirred for several minutes until a colourless precipitate formed. Pentane (3 mL) was then added and the mixture stirred a further 15 min. The precipitate was collected by filtration giving the product as a colourless solid (1.0 g, 83%). **^{1}H-NMR** (400 MHz, $CDCl_3$) δ (ppm): 7.67 (2 H, br. s., CH-11), 7.49 (6 H, dd, *J*=11.9, 8.8 Hz, CH-16), 7.35 - 7.27 (5 H, m, CH-4,5,6), 6.95 (6 H, dd, *J*=9.0, 2.6 Hz, CH-17), 5.35 (1 H, br. s., CH-2), 3.83 (9 H, s, CH_3-18), 3.36 (1 H, q, *J*=10.1 Hz, C<u>H</u>$_a$H$_b$-1), 3.26 - 3.09 (1 H, m, CH$_a$<u>H</u>$_b$-1); **^{13}C-NMR** (100 MHz, $CDCl_3$) δ (ppm): 163.7 (C-18), 134.7 (d, J_{PC}=11.4 Hz, C-17), 130.6 (q, J_{FC}=32.7 Hz, C-12), 129.6 (C-6), 128.8 (br. s., C-5), 128.1 - 127.8 (m, C-11), 127.0 (C-4), 126.9 (C-3), 123.6 (q, J_{FC}=272.8 Hz, C-14), 115.9 (C-10), 115.0 (d, J_{PC}=13.4 Hz, C-16), 62.4 (br. s., C-2), 55.5 (C-19), 52.9 (C-1) *(N.B. C-7,8,9,13 and 15 not observed)*; **MP** 136 – 140 °C (lit. 136 – 142 °C); **MS** (ES+) 758.2 $[M+H]^+$. Spectroscopic data consistent with literature values.[6]

2. Synthesis and characterisation of homopolymers

2.1 Poly(L-lactide) representative procedure

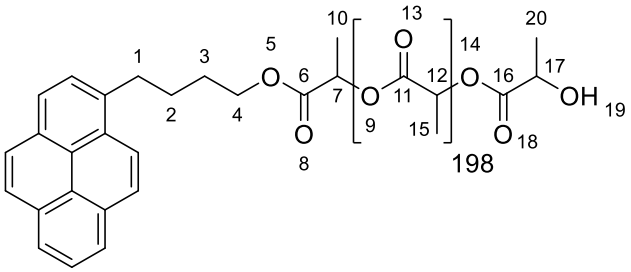

To a stirred solution of L-lactide (100 mg, 0.694 mmol, 100 equiv.) in CH_2Cl_2 (0.1 mL) under argon atmosphere was added a solution of catalyst **162** (4.7 mg, 0. 0069 mmol, 1.0 equiv.) and 1-pyrenebutanol (1.9 mg, 0.0069 mmol, 1.0 equiv.) in CH_2Cl_2 (0.2 mL). The reaction mixture was stirred for 10 minutes at room temperature, then quenched by the addition of acetic acid (0.05 mL, 1 M in CH_2Cl_2). Solvent was removed *in vacuo* and the crude reaction mixture analysed by ^{1}H-NMR to determine conversion. The crude polymer was dissolved in a minimum amount of CH_2Cl_2, then precipitated from methanol and isolated by filtration. The purified polymer was analysed by GPC to determine its molecular weight and polydispersity. **^{1}H NMR** (400 MHz, $CDCl_3$) δ (ppm): (selected peaks) 8.25 - 7.83 (9 H, m, ArH), 5.15 (196 H, q, J = 7.2 Hz, CH-12), 4.35 (1 H, q, J = 6.9 Hz, CH-17), 4.20 (2 H, td, J = 6.4, 1.6 Hz, CH_2-4), 1.57 (608 H, d, J = 7.3 Hz, CH_3-15); **^{13}C NMR** (100 MHz, $CDCl_3$) δ (ppm): (selected peaks) 169.7 (C-11), 69.1 (CH-12), 16.8 (CH_3-15); **GPC** (RI) M_n (PDI) = 27 500 g mol^{-1} (1.04). Spectroscopic data consistent with literature values.[26]

MALDI-ToF data for poly(LA)

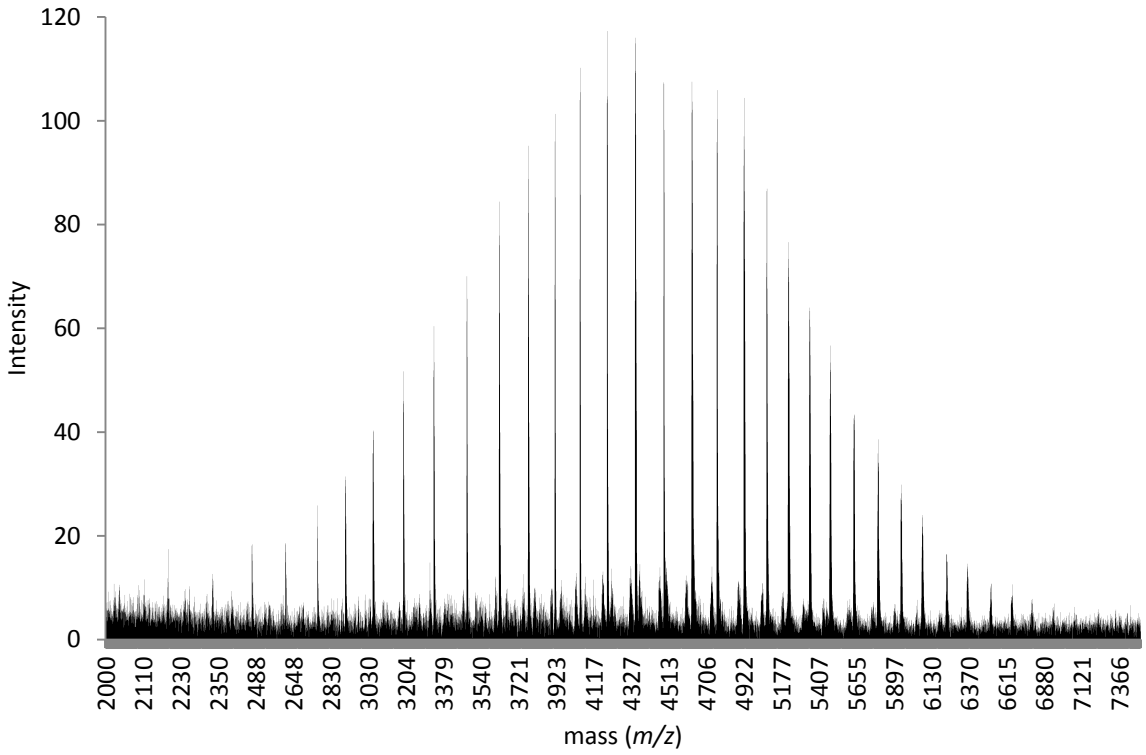

Figure E1. *MALDI-ToF spectrum of poly(LA) with $[M]_0/[I]_0 = 25$.*

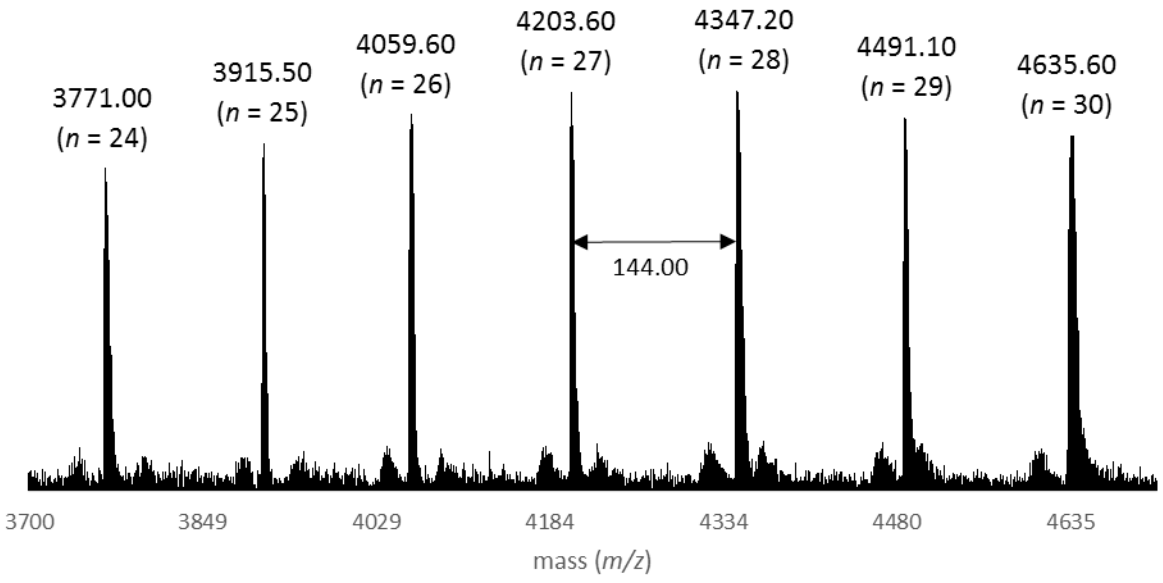

Figure E2. *Section of MALDI-ToF spectrum of poly(LA) with $[M]_0/[I]_0 = 25$.*

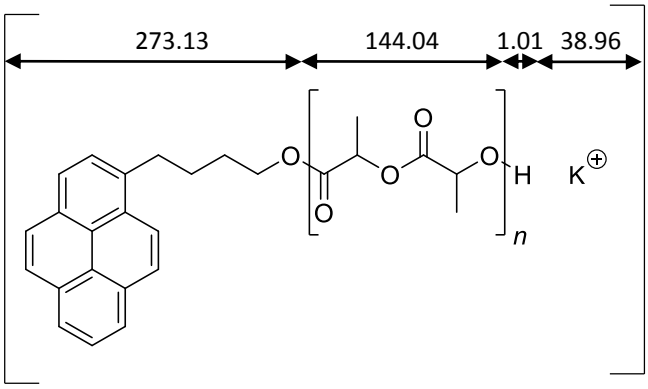

Figure E3. *Calculated molecular weights for 1-pyrenebutanol-initiated poly(LA).*

n	24	25	26	27	28	29	30
Theoretical MW	3770.06	3914.10	4058.14	4202.18	4346.22	4490.26	4634.30
Experimental MW	3771.00	3915.50	4059.60	4203.60	4347.20	4491.10	4635.60

Table E2. *Theoretical vs. experimental molecular weights for poly(LA).*

2.2 Poly(*δ*-valerolactone) representative procedure

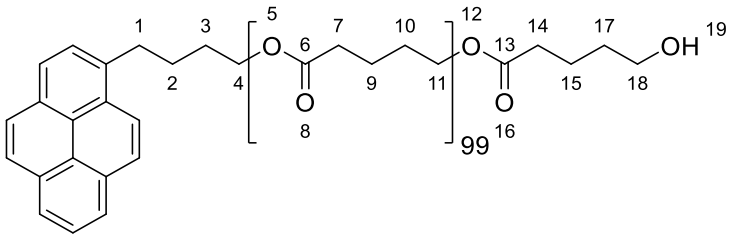

To a stirred solution of catalyst **148-*rac*** (75.8 mg, 0.100 mmol, 5.00 equiv.) and 1-pyrenebutanol (5.50 mg, 0.0200 mmol, 1.00 equiv.) in chlorobenzene (1 mL) under argon atmosphere was added *δ*-valerolactone (186 μL, 2.00 mmol, 100 equiv.) and the reaction mixture stirred for 9 h at room temperature, then quenched by the addition of acetic acid (0.1 mL, 1 M in CH_2Cl_2). The solvent was removed *in vacuo* and the crude reaction mixture analysed by ^{1}H-NMR to determine conversion and GPC to determine the molecular weight and polydispersity. **^{1}H NMR** (500 MHz, $CDCl_3$) *δ* (ppm): (selected peaks) 8.27 - 7.84 (9 H, ArH), 4.12 - 4.01 (170 H, m, CH_2-11), 2.39 - 2.25 (169 H, m, CH_2-7), 1.73 - 1.54 (347 H, m, CH_2-9,10); **^{13}C NMR** (125 MHz, $CDCl_3$) *δ* (ppm): (selected peaks) 173.4 (C-6), 64.0 (C-11), 33.8 (C-7), 28.2 (C-10), 21.5 (C-9); **GPC** (RI) M_n (PDI) = 10 100 g mol^{-1} (1.13). Spectroscopic data consistent with literature values.[26]

MALDI-ToF data for poly(VL)

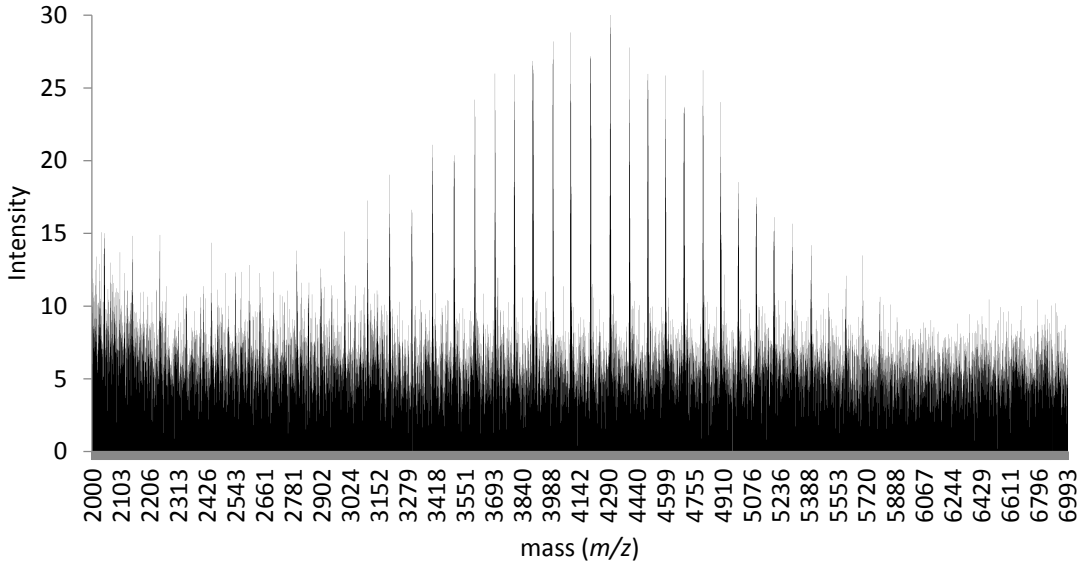

Figure E4. *MALDI-Tof spectrum of poly(VL) with $[M]_0/[I]_0 = 50$.*

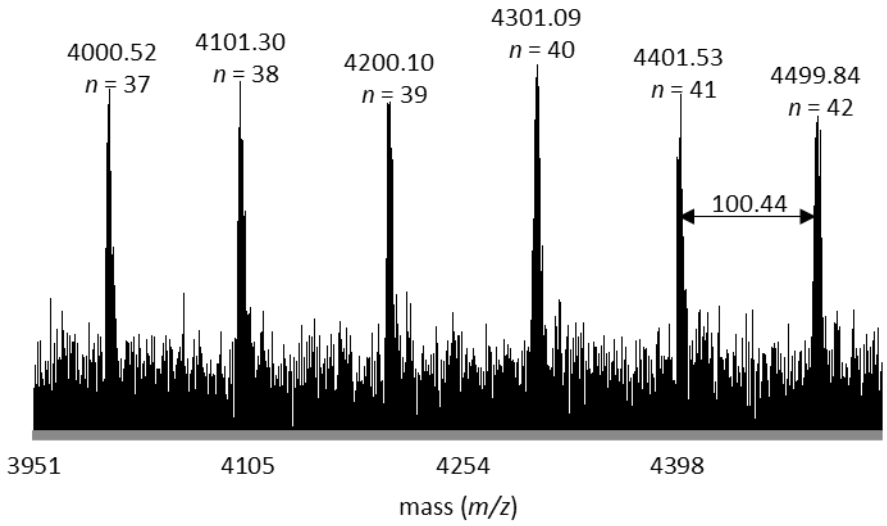

Figure E5. *Section of MALDI-ToF spectrum of poly(VL) with $[M]_0/[I]_0 = 50$.*

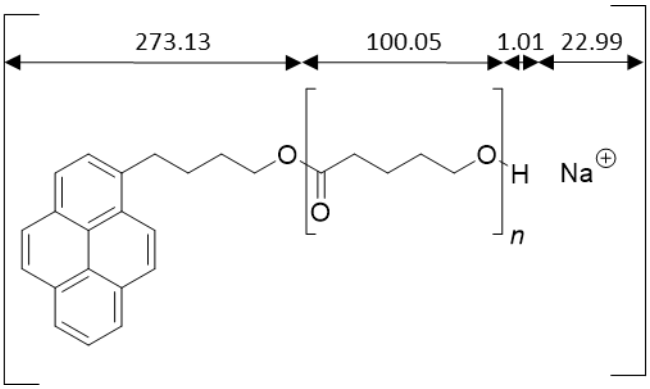

Figure E6. *Calculated molecular weights for 1-pyrenebutanol-initiated poly(VL).*

n	37	38	39	40	41	42
Theoretical MW	3998.98	4099.03	4199.08	4299.13	4399.18	4499.23
Experimental MW	4000.52	4101.30	4200.10	4301.09	4401.53	4499.84

Table E3. *Theoretical vs. experimental molecular weights for poly(VL).*

2.3 Poly(ε-caprolactone) representative procedure

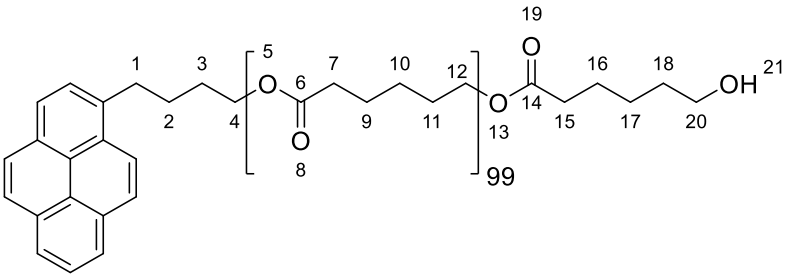

To a stirred solution of catalyst **148-*rac*** (75.8 mg, 0.100 mmol, 5.00 equiv.) and 1-pyrenebutanol (5.50 mg, 0.0200 mmol, 1.00 equiv.) in toluene (1 mL) under argon atmosphere was added ε-caprolactone (222 μL, 2.00 mmol, 100 equiv.) and the reaction mixture stirred for 100 h at room temperature, then quenched by the addition of acetic acid (0.1 mL, 1 M in CH_2Cl_2). The solvent was removed *in vacuo* and the crude reaction mixture analysed by ^{1}H-NMR to determine conversion and GPC to determine the molecular weight and polydispersity. **^{1}H NMR** (500 MHz, $CDCl_3$) δ (ppm): (selected peaks) 8.30 - 7.81 (9 H, m, ArH), 4.05 (162 H, t, J = 6.8 Hz, CH_2-12), 2.23 - 2.35 (177 H, m, CH_2-7), 1.56 - 1.70 (349 H, m, CH_2-9,11), 1.32 - 1.44 (175 H, m, CH_2-10); **^{13}C NMR** (125 MHz, $CDCl_3$) δ (ppm): (selected peaks) 173.7 (C-6), 64.3 (C-12), 34.2 (C-7), 28.5 (C-10), 25.6 (C-9 or 11),

24.7 (C-9 or 11); **GPC** (RI) M_n (PDI) = 4 900 g mol^{-1} (1.23). Spectroscopic data consistent with literature values.[26]

MALDI-ToF data for poly(CL)

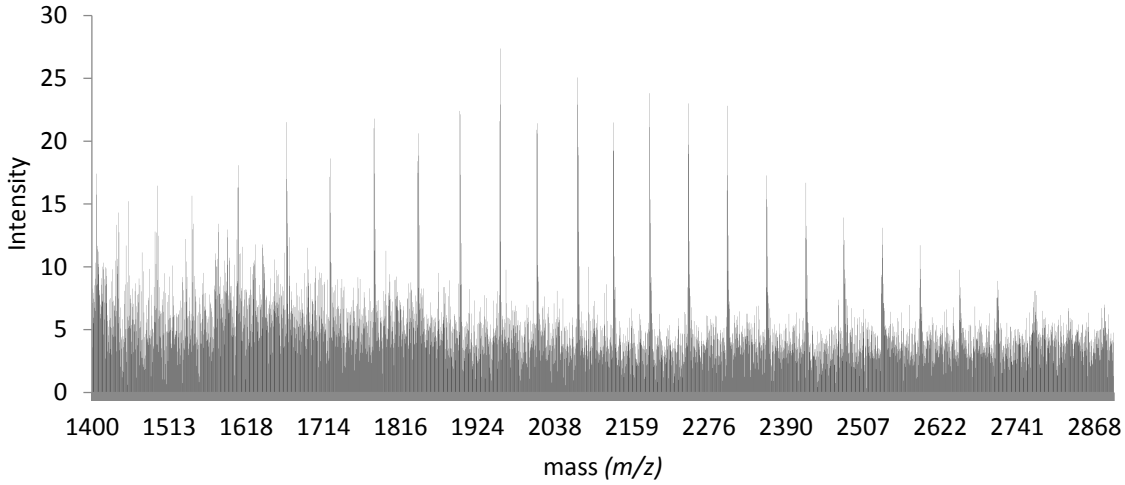

Figure E7. *MALDI-Tof spectrum of poly(CL) with $[M]_0/[I]_0$ = 50. Note that poly(CL) is doubly ionised.*

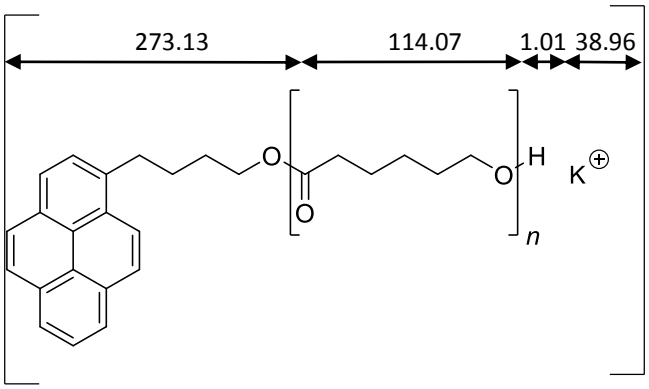

Figure E8. *Calculated molecular weights for 1-pyrenebutanol-initiated poly(CL). Total mass of end-group + K^+ ion = 313.46 g mol^{-1}.*

Due to the low quality of MALDI-ToF data for poly(CL), it is more reliably analysed using a linear regression of *(m/z)* × 2 (as the polymer chains are doubly ionised) vs. chain length.

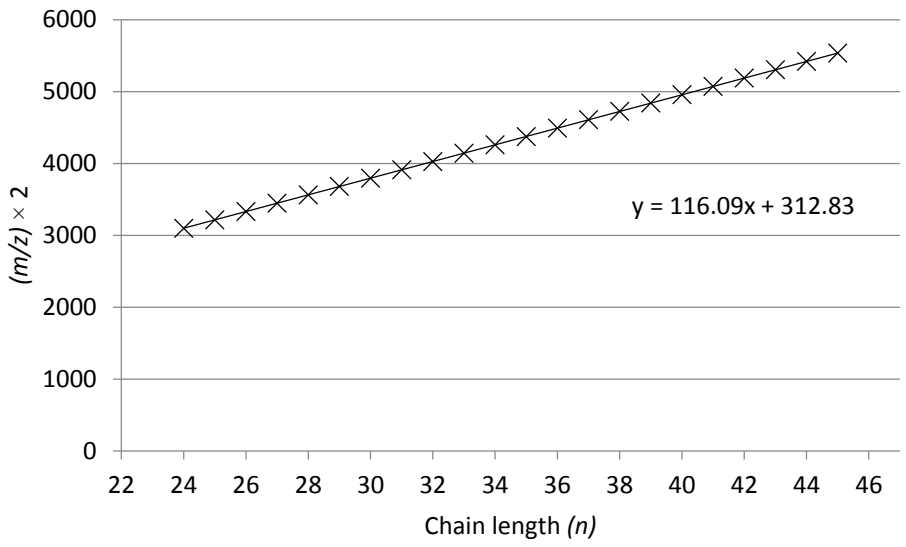

Figure E9. *Linear regression on MALDI-ToF data for poly(CL) from 3000 – 5500 m/z. The gradient represents the mass of the monomer, the intercept represents the mass of the end group. This corresponds to the calculated mass of pyrenebutanol + K^+.*

3. Block co-polymers by sequential monomer addition

3.1 Poly(VL)-*block*-poly(CL)

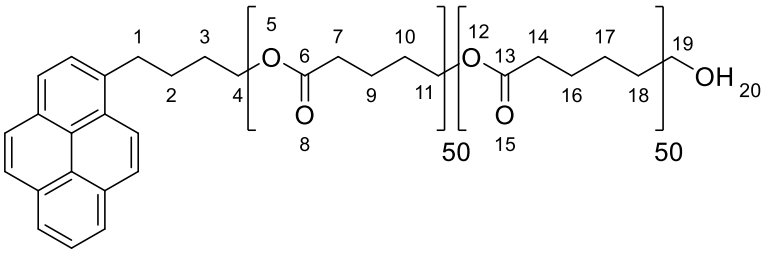

To a stirred solution of catalyst **148-*rac*** (26.3 mg, 0.0347 mmol, 5.00 equiv.) and 1-pyrenebutanol (1.9 mg, 0.0069 mmol, 1.0 equiv.) in chlorobenzene (0.34 mL) under argon atmosphere was added *δ*-valerolactone (32 μL, 0.35 mmol, 50 equiv.) and the reaction mixture stirred for 4 h at room temperature. After removal of a 50 μL aliquot of the reaction mixture for analysis of the conversion, molecular weight and polydispersity of the first polymerization, ε-caprolactone (38 μL, 0.35 mmol, 50 equiv.) was added and the reaction mixture stirred at room temperature for 48 h, then quenched by the addition of acetic acid (0.1 mL, 1 M in CH_2Cl_2). The solvent was removed *in vacuo* and the crude reaction mixture analysed by ^{1}H-NMR to determine conversion and GPC to determine the molecular weight and polydispersity. **^{1}H NMR** (500 MHz, $CDCl_3$) *δ* (ppm): (selected peaks) 8.27 - 7.85 (9 H, m, ArH), 4.09 - 4.03 (144 H, m, CH_2-11,18), 2.35 - 2.29 (157 H, m, CH_2-7,14), 1.73 - 1.61

(309 H, m, CH_2-9,10,16,18), 1.43 - 1.35 (67 H, m, CH_2-17); **^{13}C NMR** (100 MHz, $CDCl_3$) δ (ppm): (selected peaks) 173.8 (C-13), 173.3 (C-6), 64.2 (C-18), 64.0 (C-11), 34.2 (C-14), 33.7 (C-7), 28.4 (C-17), 28.1 (C-10), 25.6 (C-16 or 18), 24.6 (one of C-16 or 18), 21.5 (C-9); **GPC** (RI) M_n (PDI) VL sequence = 4 050 g mol^{-1} (1.10), final polymer = 5 920 g mol^{-1} (1.19).

3.2 Poly(VL)-*block*-poly(LA)

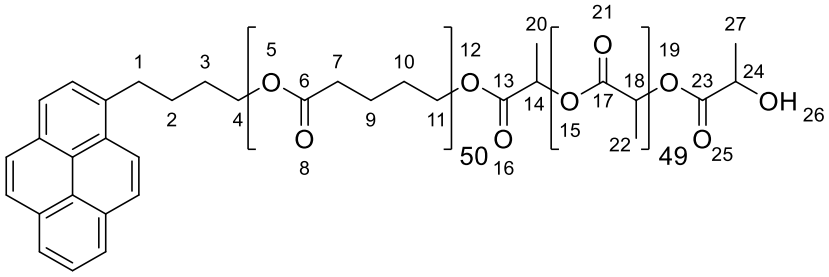

To a stirred solution of catalyst **148-*rac*** (26.3 mg, 0.0347 mmol, 5.00 equiv.) and 1-pyrenebutanol (1.9 mg, 0.0069 mmol, 1.0 equiv.) in chlorobenzene (0.34 mL) under argon atmosphere was added δ-valerolactone (32 μL, 0.35 mmol, 50 equiv.) and the reaction mixture stirred for 5 h at room temperature. After removal of a 50 μL aliquot of the reaction mixture for analysis of the conversion, molecular weight and polydispersity of the first polymerization, a solution of L-lactide (50.0 mg, 0.347 mmol, 50 equiv.) in CH_2Cl_2 (0.5 mL) was added in one portion and the reaction mixture stirred for 10 minutes, then quenched by the addition of acetic acid (0.1 mL, 1 M in CH_2Cl_2). The solvent was removed *in vacuo* and the crude reaction mixture analysed by ^{1}H-NMR to determine conversion and GPC to determine the molecular weight and polydispersity. **^{1}H NMR** (500 MHz, $CDCl_3$) δ (ppm): (selected peaks) 8.27 - 7.85 (9 H, ArH), 5.16 (88 H, q, J = 7.1 Hz, CH-18), 4.09 - 4.05 (89 H, m, CH_2-11), 2.36 - 2.29 (87 H, m, CH_2-7), 1.68 - 1.67 (180 H, m, CH_2-9,10), 1.58 (260 H, d, J = 7.2 Hz, CH_3-22); **^{13}C NMR** (125 MHz, $CDCl_3$) δ (ppm): (selected peaks) 173.3 (C-6), 169.6 (C-17), 69.0 (C-18), 64.0 (C-11), 33.7 (C-7), 28.1 (C-9 or 10), 21.5 (C-9 or 10), 16.7 (C-22); **GPC** (RI) M_n (PDI) VL sequence = 3 930 g mol^{-1} (1.12), final polymer = 7 530 g mol^{-1} (1.13).

3.3 Poly(CL)-*block*-poly(LA)

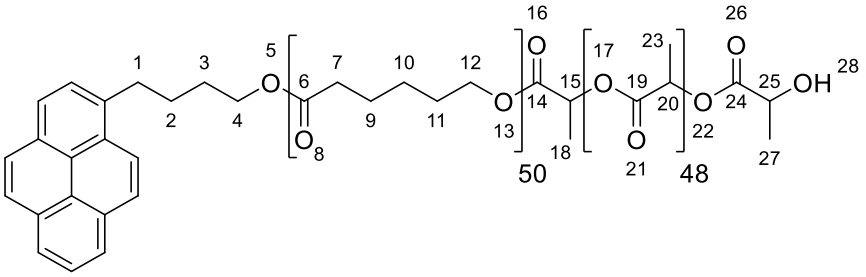

To a stirred solution of catalyst **148-*rac*** (26.3 mg, 0.0347 mmol, 5.00 equiv.) and 1-pyrenebutanol (1.9 mg, 0.0069 mmol, 1.0 equiv.) in chlorobenzene (0.34 mL) under argon atmosphere was added ε-caprolactone (38 μL, 0.35 mmol, 50 equiv.) and the reaction mixture stirred for 48 h at room temperature. After removal of a 50 μL aliquot of the reaction mixture for analysis of the conversion, molecular weight and polydispersity of the first polymerization, a solution of L-lactide (50.0 mg, 0.347 mmol, 50 equiv.) in CH_2Cl_2 (0.5 mL) was added in one portion and the reaction mixture stirred for 10 minutes, then quenched by the addition of acetic acid (0.1 mL, 1 M in CH_2Cl_2). The solvent was removed *in vacuo* and the crude reaction mixture analysed by ^{1}H-NMR to determine conversion and GPC to determine the molecular weight and polydispersity. **^{1}H NMR** (500 MHz, $CDCl_3$) δ (ppm): (selected peaks) 8.33 - 7.88 (9 H, ArH), 5.32 - 5.21 (124 H, m, CH-20), 4.11 (89 H, t, J = 6.7 Hz, CH_2-12), 2.37 - 2.35 (82 H, m, CH_2-7), 1.74 - 1.68 (171 H, m, CH_2-9,11), 1.66 - 1.61 (396 H, m, CH_3-23), 1.47 - 1.39 (92 H, m, CH_2-10); **^{13}C NMR** (100 MHz, $CDCl_3$) δ (ppm): (selected peaks) 173.4 (C-6), 169.8 (C-19), 69.1 (C-20), 64.3 (C-12), 34.3 (C-7), 28.5 (C-10), 25.7 (C-9 or 11), 24.7 (C-9 or 11), 16.8 (C-23); **GPC** (RI) M_n (PDI) CL sequence = 3 480 g mol^{-1} (1.12), final polymer = 5 670 g mol^{-1} (1.16).

4. Polymerisation from a macroinitiator

4.1 mPEG$_{50}$-*block*-poly(LA)

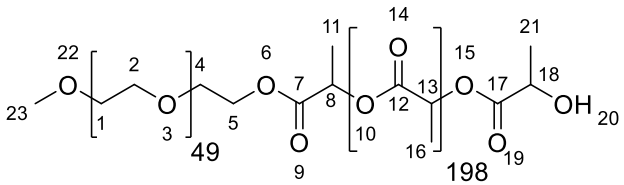

To a stirred solution of L-lactide (100 mg, 0.694 mmol, 100 equiv.) in CH_2Cl_2 (0.8 mL) under argon atmosphere was added a solution of catalyst **162** (23.6 mg, 0.0347 mmol, 5.00 equiv.) and mPEG$_{50}$

(13.9 mg, 0.00694 mmol, 1.00 equiv.) in CH_2Cl_2 (0.2 mL). The reaction mixture was stirred for 10 minutes at room temperature, then quenched by the addition of acetic acid (0.1 mL, 1 M in CH_2Cl_2). Solvent was removed *in vacuo* and the crude reaction mixture analysed by ^{1}H-NMR to determine conversion and GPC to determine the molecular weight and polydispersity. **^{1}H NMR** (400 MHz, $CDCl_3$) δ (ppm): (selected peaks) 5.16 (193 H, q, J = 7.1 Hz, CH-13), 3.64 (169 H, br. s, CH_2-1,2), 3.38 (3 H, s, CH_3-23), 1.58 (618 H, d, J = 7.1 Hz, CH_3-16); **^{13}C NMR** (100 MHz, $CDCl_3$) δ (ppm): (selected peaks) 169.7 (C-12), 70.7 (C-1,2), 69.1 (C-13), 55.8 (C-23), 16.7 (C-16); **GPC** (RI) M_n (PDI) = 16 800 g mol^{-1} (1.07).

4.2 mPEG$_{50}$-*block*-poly(VL)

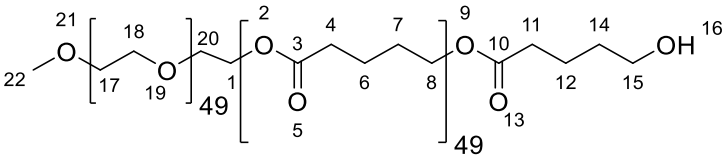

To a stirred solution of catalyst **148-*rac*** (13.1 mg, 0.0173 mmol, 5.00 equiv.) and mPEG$_{50}$ (13.9 mg, 0.00694 mmol, 1.00 equiv.) in chlorobenzene (0.34 mL) under argon atmosphere was added δ-valerolactone (32 µL, 0.35 mmol, 50 equiv.) and the reaction mixture stirred for 5 h at room temperature, then quenched by the addition of acetic acid (0.1 mL, 1 M in CH_2Cl_2). The solvent was removed *in vacuo* and the crude reaction mixture analysed by ^{1}H-NMR to determine conversion and GPC to determine the molecular weight and polydispersity. **^{1}H NMR** (500 MHz, $CDCl_3$) δ (ppm): (selected peaks) 4.06 - 4.03 (64 H, m, CH_2-8), 3.61 (127 H, CH_2-17,18), 3.35 (3 H, s, CH_3-22), 2.36 - 2.29 (67 H, m, CH_2-4), 1.67 - 1.64 (146 H, m, CH_2-6,7); **^{13}C NMR** (100 MHz, $CDCl_3$) δ (ppm): (selected peaks) 173.3 (C-3), 70.6 (C-17,18), 64.0 (C-8), 33.7 (C-4), 28.1 (C-7), 21.5 (C-6); **GPC** (RI) M_n (PDI) = 4 600 g mol-1 (1.04).

4.3 mPEG$_{50}$-*block*-poly(CL)

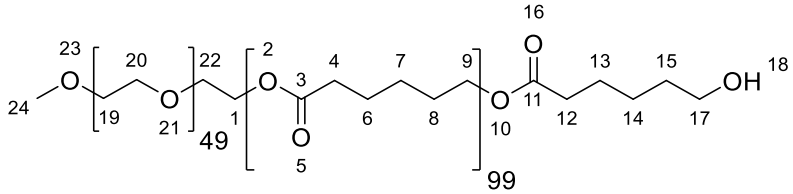

To a stirred solution of catalyst **148-*rac*** (13.1 mg, 0.0173 mmol, 5.00 equiv.) and mPEG$_{50}$ (13.9 mg, 0.00694 mmol, 1.00 equiv.) in toluene (0.34 mL) under argon atmosphere was added ε-caprolactone

(38 µL, 0.35 mmol, 50 equiv.) and the reaction mixture stirred for 72 h at room temperature, then quenched by the addition of acetic acid (0.1 mL, 1 M in CH_2Cl_2). The solvent was removed *in vacuo* and the crude reaction mixture analysed by ^{1}H-NMR to determine conversion and GPC to determine the molecular weight and polydispersity. **^{1}H NMR** (400 MHz, $CDCl_3$) δ (ppm): (selected peaks) 4.06 - 4.03 (64 H, t, J = 6.6 Hz, CH_2-9), 3.63 (186 H, CH_2-19,20), 3.37 (3 H, s, CH_3-24), 2.33 - 2.25 (67 H, m, CH_2-4), 1.68 - 1.54 (140 H, m, CH_2-6,8), 1.41 - 1.32 (74 H, m, CH_2-7); **^{13}C NMR** (100 MHz, $CDCl_3$) δ (ppm): (selected peaks) 173.6 (C-3), 70.5 (CH_2-19,20), 64.1 (C-9), 34.1 (C-4), 28.3 (C-7), 25.5 (C-6 or 8), 24.6 (C-6 or 8); **GPC** (RI) M_n (PDI) = 4 910 g mol^{-1} (1.18).

5. Control experiments

N-(3-cyclohexylpropyl)-5-hydroxypentanamide (**173**)

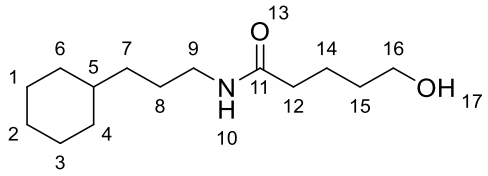

173

(3-azidopropyl)cyclohexane **172** (50.0 mg, 0.299 mmol, prepared by Dr. Marta Garcia Núñez) and tris(4-methoxy)phenylphosphine (105 mg, 0.299 mmol) were dissolved in anhydrous THF (1.5 mL) and stirred for 24 h at room temperature under argon atmosphere, followed by heating at 40 °C for 7 h. TLC indicated the consumption of the starting materials and mass spectrometry indicated the presence of the corresponding iminophosphorane.

To the reaction mixture containing the iminophosphorane was added ∂-valerolactone (28.0 µL, 0.299 mmol) and the reaction was stirred at room temperature for 24 h. Approximately one half of the reaction volume was then removed, water (50 µL) added and the resulting mixture stirred for 5 h at room temperature. Solvent was removed *in vacuo* and the residue purified by flash column chromatography over silica (5% methanol in ethyl acetate, then 10% methanol in CH_2Cl_2). This yielded compound **173** in a ~2:1 molar ratio with tris(4-methoxyphenyl)phosphine oxide (12.8 mg, ~9%). **^{1}H NMR** (500 MHz, $CDCl_3$) δ (ppm): (**122** peaks only) 5.79 (1 H, br. s., NH-10), 3.62 (2 H, t, J = 6.2 Hz, CH_2-16), 3.21 - 3.16 (2 H, m, CH_2-9), 2.21 (2 H, t, J = 7.2 Hz, CH_2-12), 2.15 (1 H, br. s., OH-17), 1.76 - 1.71 (2 H, m, CH_2-14), 1.69 - 1.65 (5 H, m, CH_{eq}-1,3 and 4,6 and 2), 1.61 - 1.54

(2 H, m, CH_2-15), 1.51 - 1.43 (2 H, m, CH_2-8), 1.27 - 1.07 (6 H, m, CH-5, CH_{ax}-1,3 and 2, CH_2-7), 0.88 - 0.81 (2 H, m, CH_{ax}-4,6); **^{13}C NMR** (125 MHz, $CDCl_3$) δ (ppm): 173.2 (C-11), 62.1 (C-16), 40.0 (C-9), 37.5 (C-5), 36.2 (C-12), 34.8 (C-7), 33.4 (C-6,4), 32.2 (C-15), 27.1 (C-8), 26.8 (C-2), 26.5 (C-1,3), 21.9 (C-14); **MS** (ES+) 242.3 $[M+H]^+$, 264.2 $[M+Na]^+$.

(2-azidoethyl)benzene (**175**)

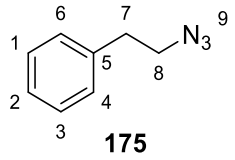

175

Phenethylamine (100 mg, 0.825 mmol), copper(II) sulfate pentahydrate (2.1 mg, 0.0083 mmol) and potassium carbonate (193 mg, 1.40 mmol) were taken up in methanol (4.1 mL) at room temperature. 1*H*-imidazole-1-sulfonyl azide hydrochloride (205 mg, 0.990 mmol) was added portionwise with stirring and the reaction was stirred for 24 h at room temperature. The solvent was removed under a flow of nitrogen and the residue was partitioned between water and diethyl ether. The organic layer was washed with brine, dried over anhydrous sodium sulfate and the solvent removed under a flow of nitrogen. The residue was purified by flash column chromatography over silica (petroleum ether, then 10% diethyl ether in petroleum ether) to give the product as a colourless oil (79 mg, 0.54 mmol, 65%). **^{1}H NMR** (250 MHz, $CDCl_3$) δ (ppm): 7.43 - 7.27 (5 H, m, ArH), 3.57 (2 H, t, J = 7.3 Hz, CH_2-7), 2.96 (2 H, t, J = 7.3 Hz, CH_2-8); **^{13}C NMR** (100 MHz, $CDCl_3$) δ (ppm): 138.2 (C-5), 128.9 (C-2), 128.8 (C-1,3), 126.9 (C-4,6), 52.6 (C-8), 35.5 (C-7). Spectroscopic data consistent with literature values.[8]

Polymerization catalysed by iminophosphorane **174**

Azide **175** (5.1 mg, 0.035 mmol) and tris(4-methoxy)phenylphosphine (12.2 mg, 0.0347 mmol) were dissolved in THF and stirred at room temperature under argon atmosphere for 24 h, after which TLC analysis indicated complete consumption of the starting materials and mass spectrometry indicated the presence of iminophosphorane **174**. Maintaining the flask under inert atmosphere, THF was removed under a flow of nitrogen and the residue was dissolved in CH_2Cl_2 (0.2 mL). The CH_2Cl_2 solution of **174** was then added to a solution of L-lactide (100 mg, 0.694 mmol) and 1-pyrenebutanol

(1.9 mg, 0.0069 mmol) in CH_2Cl_2 (0.8 mL) under argon atmosphere and the reaction stirred at room temperature for 1 h. The reaction was quenched by addition of acetic acid (0.1 mL, 1 M in CH_2Cl_2), the solvent removed *in vacuo* and the residue analyzed by ^{1}H-NMR to determine conversion and GPC to determine the molecular weight and polydispersity.

References

(1) Coudane, J.; Ustariz-Peyret, C.; Schwach, G.; Vert, M. *J. Polym. Sci. Part A Polym. Sci.* **1997**, *35*, 1651–1658.
(2) Braghiroli, D.; Di Bella, M. *Tetrahedron: Asymmetry* **1996**, *7*, 2145–2150.
(3) Liu, H.; Du, D.-M. *Adv. Synth. Catal.* **2010**, *352*, 1113–1118.
(4) Goddard-Borger, E. D.; Stick, R. V. *Org. Lett.* **2011**, *13*, 2514.
(5) Goddard-Borger, E. D.; Stick, R. V. *Org. Lett.* **2007**, *9*, 3797–3800.
(6) Núñez, M. G.; Farley, A. J. M.; Dixon, D. J. *J. Am. Chem. Soc.* **2013**, *135*, 16348–16351.
(7) Carriedo, G. A.; García Alonso, F. J.; González, P. A.; Díaz Valenzuela, C.; Yutronic Sáez, N. *Polyhedron* **2002**, *21*, 2579–2586.
(8) Suzuki, T.; Ota, Y.; Kasuya, Y.; Mutsuga, M.; Kawamura, Y.; Tsumoto, H.; Nakagawa, H.; Finn, M. G.; Miyata, N. *Angew. Chem., Int. Ed.* **2010**, *49*, 6817–6820.
(9) Lipshutz, B. H.; Shimizu, H. *Angew. Chem., Int. Ed.* **2004**, *43*, 2228–2230.
(10) Takuwa, T.; Minowa, T.; Fujisawa, H.; Mukaiyama, T. *Chem. Pharm. Bull.* **2005**, *53*, 476–480.
(11) Hegedus, L. S.; Williams, R. E.; McGuire, M. A.; Hayashi, T. *J. Am. Chem. Soc.* **1980**, *102*, 4973–4979.
(12) Terada, M.; Ube, H.; Yaguchi, Y. *J. Am. Chem. Soc.* **2006**, *128*, 1454–1455.
(13) Raimondi, W.; Lettieri, G.; Dulcere, J.-P.; Bonne, D.; Rodriguez, J. *Chem. Commun.* **2010**, *46*, 7247–7249.
(14) Nichols, P. J.; DeMattei, J. A.; Barnett, B. R.; LeFur, N. A.; Chuang, T.-H.; Piscopio, A. D.; Koch, K. *Org. Lett.* **2006**, *8*, 1495–1498.
(15) Chen, Y.; Sieburth, S. M. *Synthesis (Stuttg).* **2002**, *15*, 2191–2194.
(16) Corey, E. J.; Ruden, R. A. *Tetrahedron Lett.* **1973**, *14*, 1495–1499.
(17) Kantlehner, W.; Lehmann, H.-J.; Stieglitz, R. *Arkivoc* **2012**, *2012*, 442.
(18) Du, H.; Rodriguez, J.; Bugaut, X.; Constantieux, T. *Chem. – A Eur. J.* **2014**, *20*, 8458–8466.
(19) Jakubec, P.; Helliwell, M.; Dixon, D. J. *Org. Lett.* **2008**, *10*, 4267–4270.
(20) Jakubec, P.; Cockfield, D. M.; Hynes, P. S.; Cleator, E.; Dixon, D. J. *Tetrahedron: Asymmetry* **2011**, *22*, 1147–1155.
(21) Jakubec, P.; Cockfield, D. M.; Helliwell, M.; Raftery, J.; Dixon, D. J. *Beilstein J. Org. Chem.* **2012**, *8*, 567–578.
(22) Kyle, A. F.; Jakubec, P.; Cockfield, D. M.; Cleator, E.; Skidmore, J.; Dixon, D. J. *Chem. Commun.* **2011**, *47*, 10037–10039.
(23) Vakulya, B.; Varga, S.; Csámpai, A.; Soós, T. *Org. Lett.* **2005**, *7*, 1967–1969.
(24) Landi, F.; Johansson, C. M.; Campopiano, D. J.; Hulme, A. N. *Org. Biomol. Chem.* **2010**, *8*, 56–59.
(25) Tiecco, M.; Testaferri, L.; Bagnoli, L.; Scarponi, C.; Temperini, A.; Marini, F.; Santi, C. *Tetrahedron: Asymmetry* **2007**, *18*, 2758–2767.
(26) Lohmeijer, B. G. G.; Pratt, R. C.; Leibfarth, F.; Logan, J. W.; Long, D. a; Dove, A. P.; Nederberg, F.; Choi, J.; Wade, C.; Waymouth, R. M.; Hedrick, J. L. *Macromolecules* **2006**, *39*, 8574–8583.

Appendix

1. Calculated homogeneous catalyst structure

(Calculations performed by the group of Prof. Robert Paton, unpublished results)

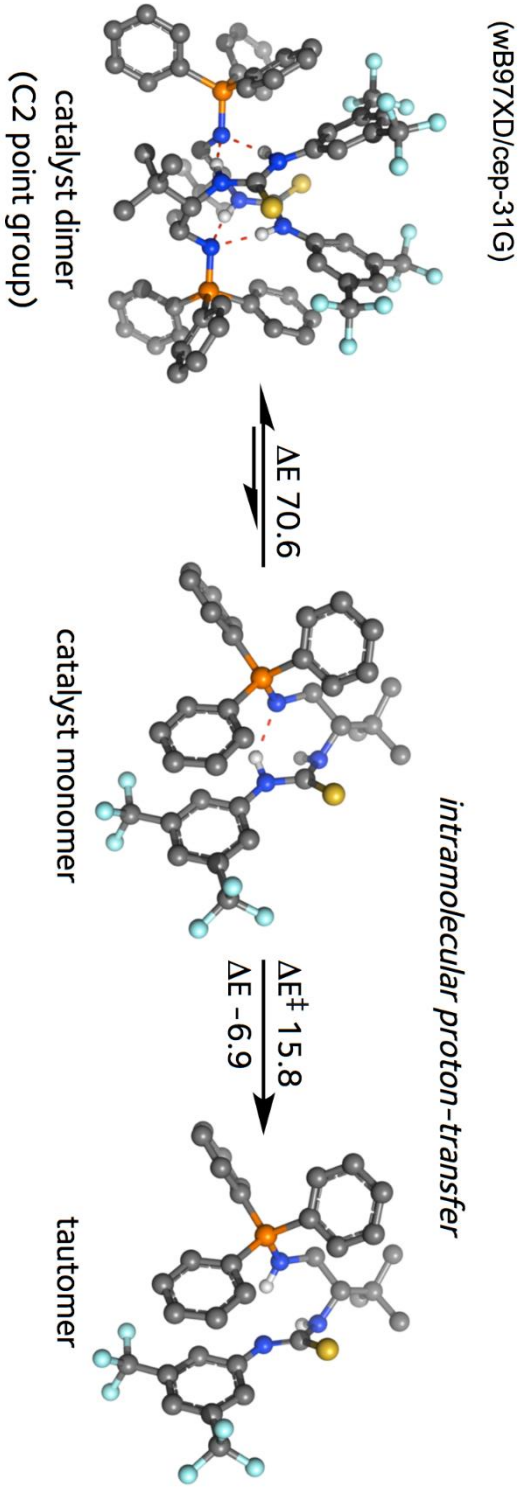

2. Immobilisation of bifunctional iminophosphoranes – Representative spectra

2.1 *N*-[(2*R*)-1-nitro-2-phenylpropan-2-yl]-*P*,*P*-diphenylphosphinic amide (**37a**)

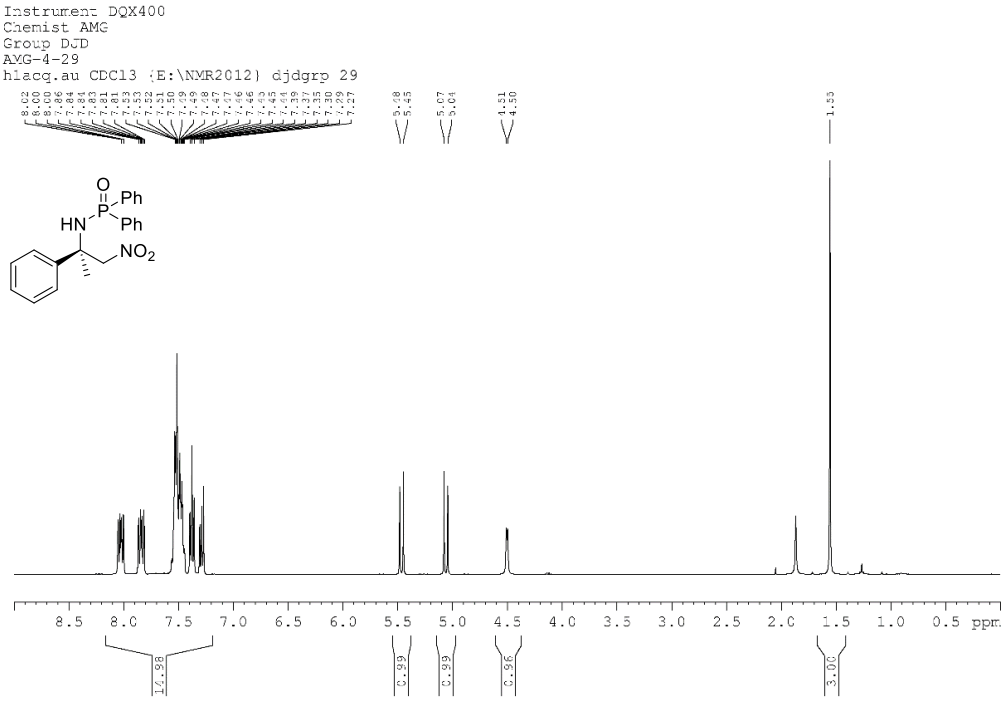

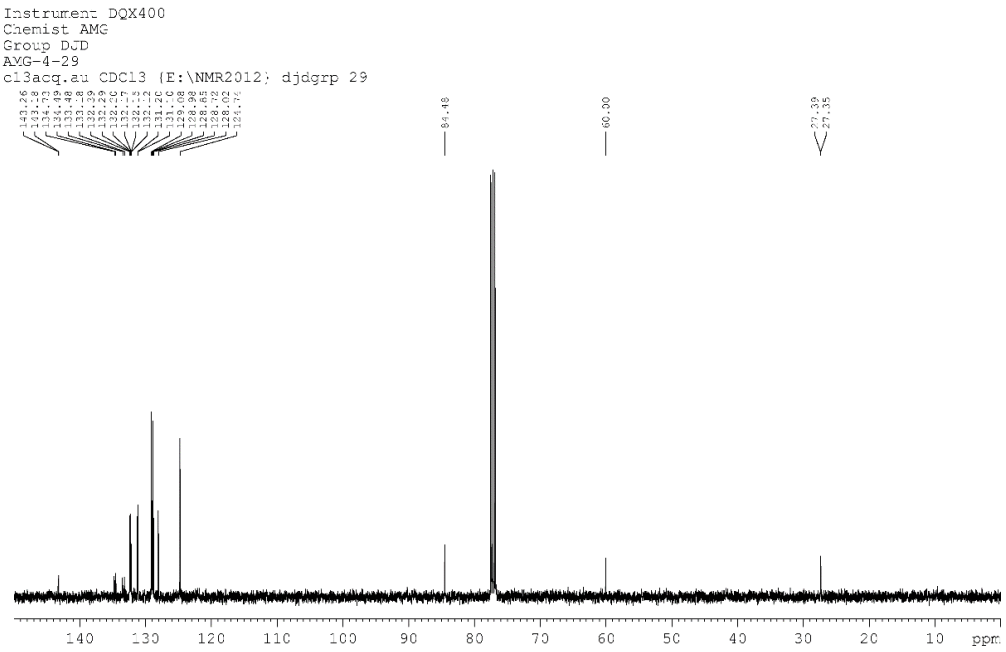

2.2 Dimethyl (*R*)-2-methyl-2-(2-nitro-1-phenylethyl)malonate (**123a**)

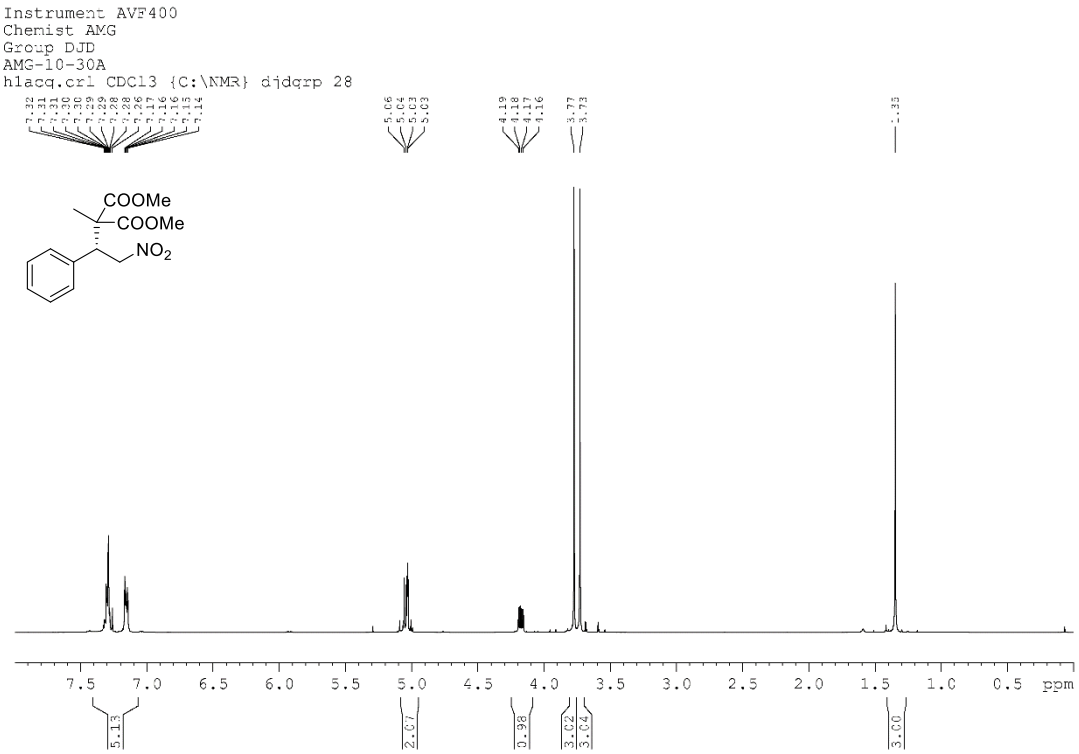

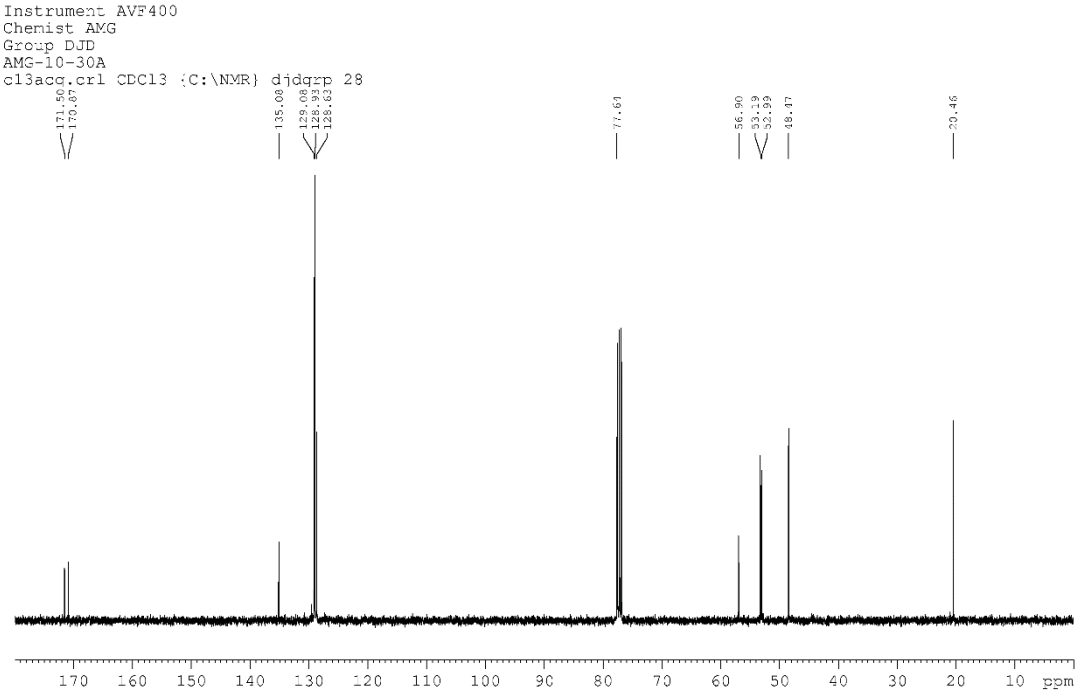

2.3 (2*R*, 3*S*)-2-Acetyl-*N*,*N*-dimethyl-4-nitro-3-phenylbutanamide (**131a**)

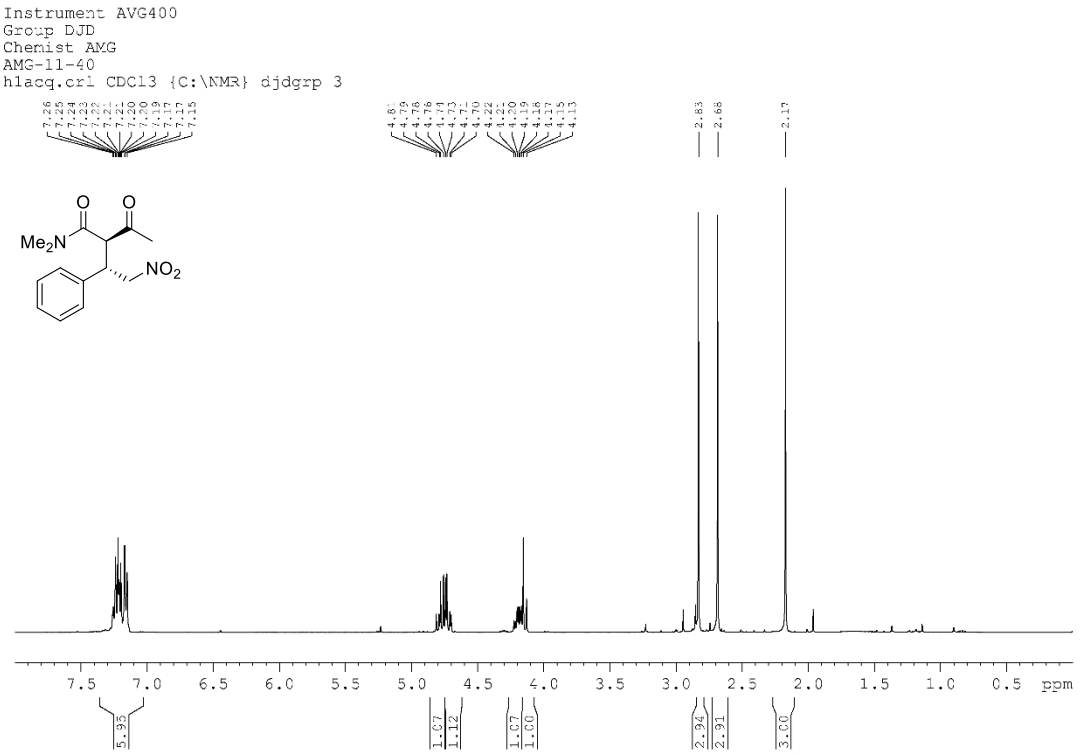

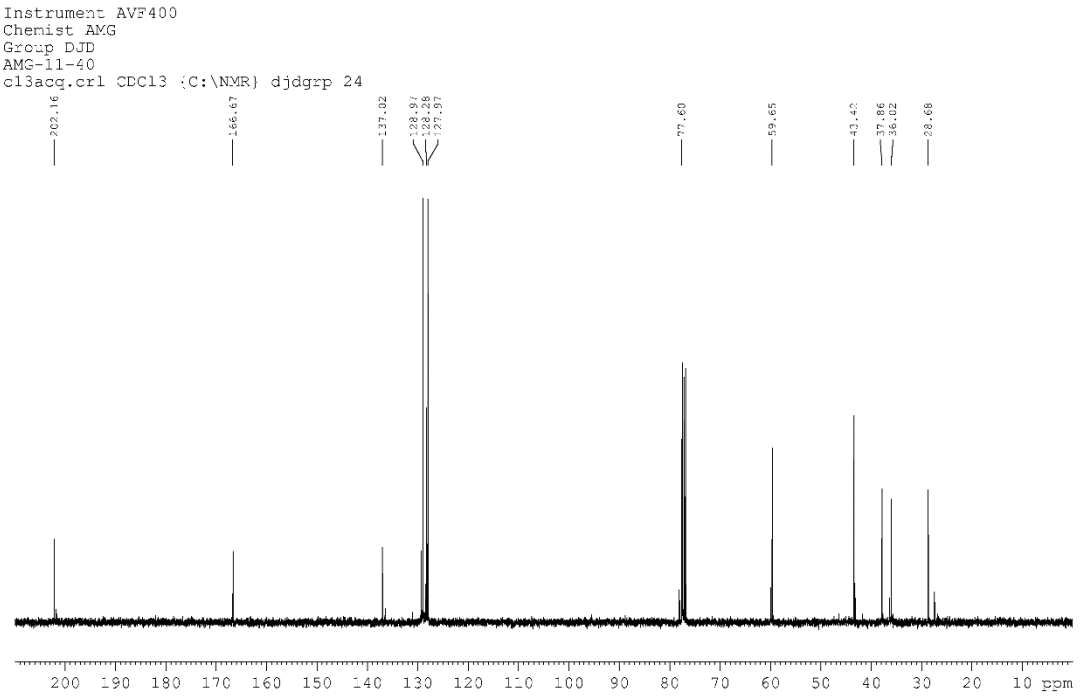

2.4 Methyl (3*S*)-1-methyl-3-[(1*S*)-2-nitro-1-phenylethyl]-2-oxopyrrolidine-3-carboxylate (**35**)

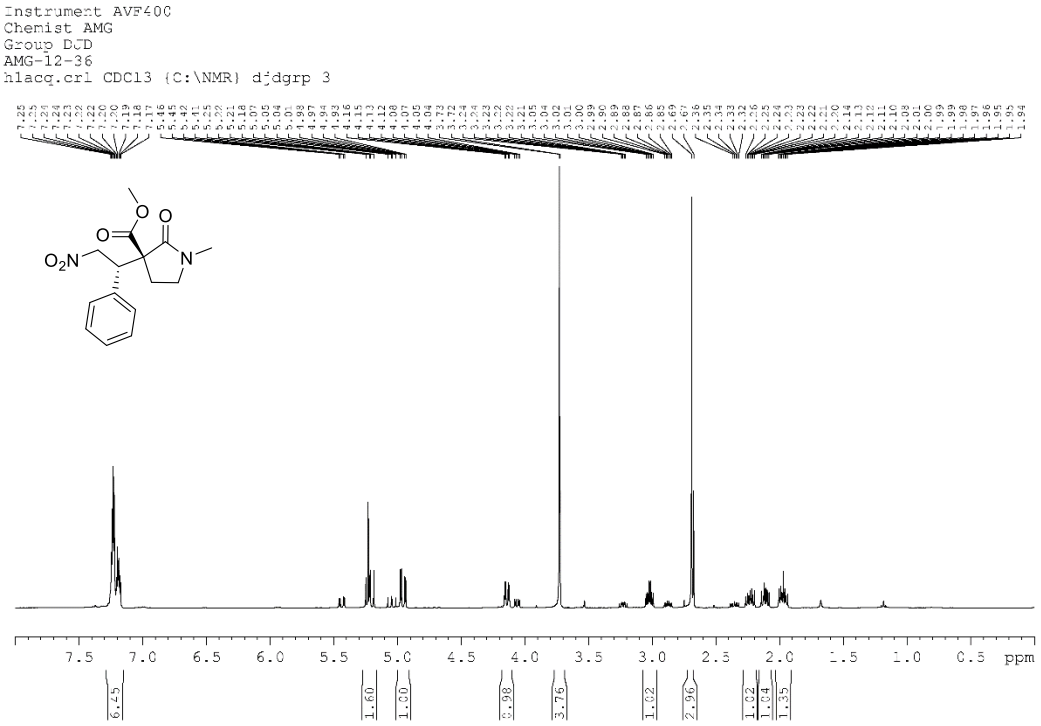

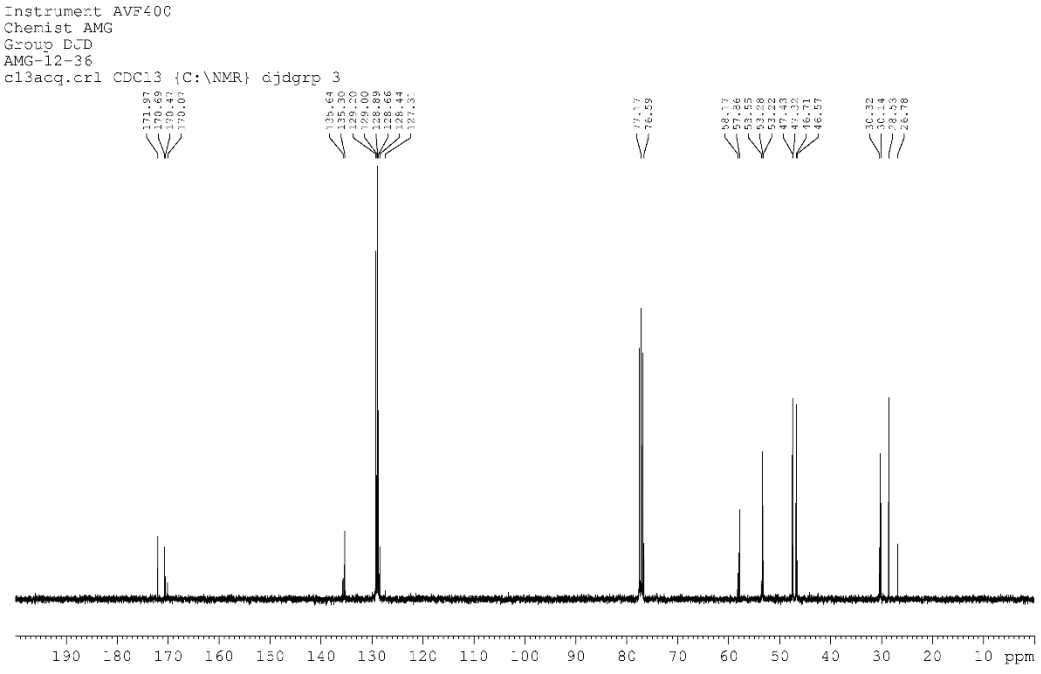

3. Polymerisation of cyclic esters – Representative spectra

3.1 Catalyst **162**

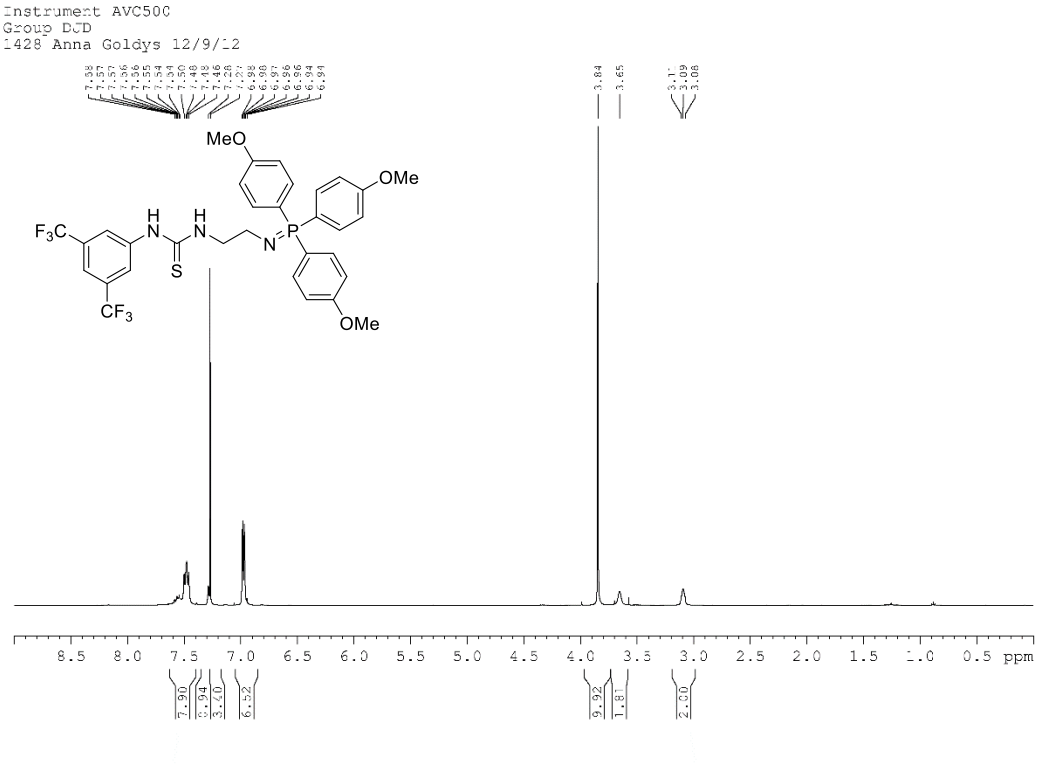

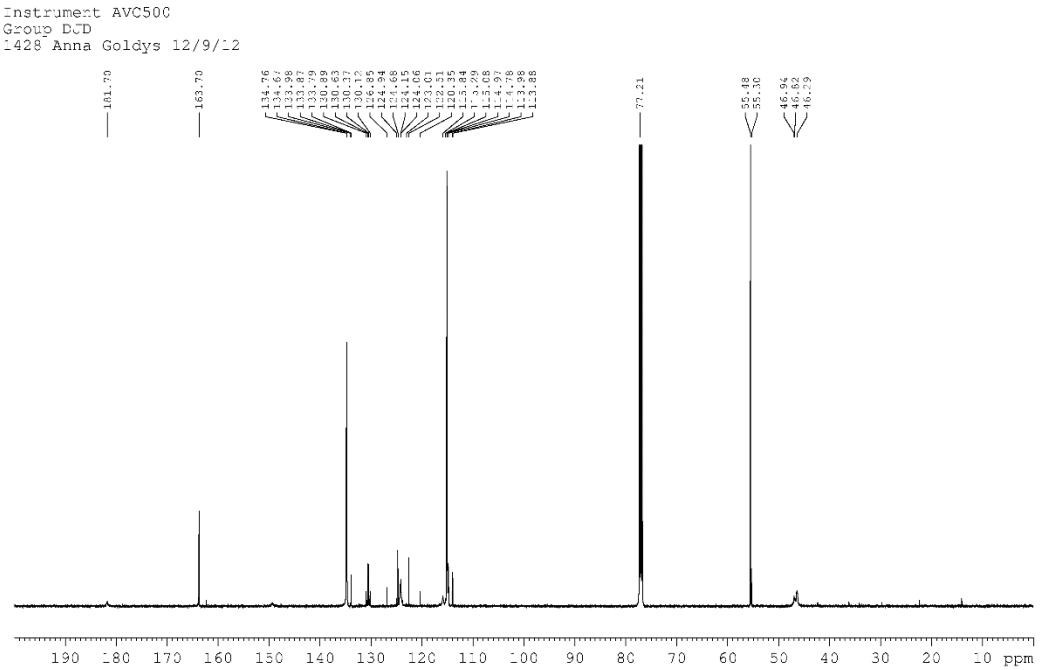

3.2 Poly(LA)

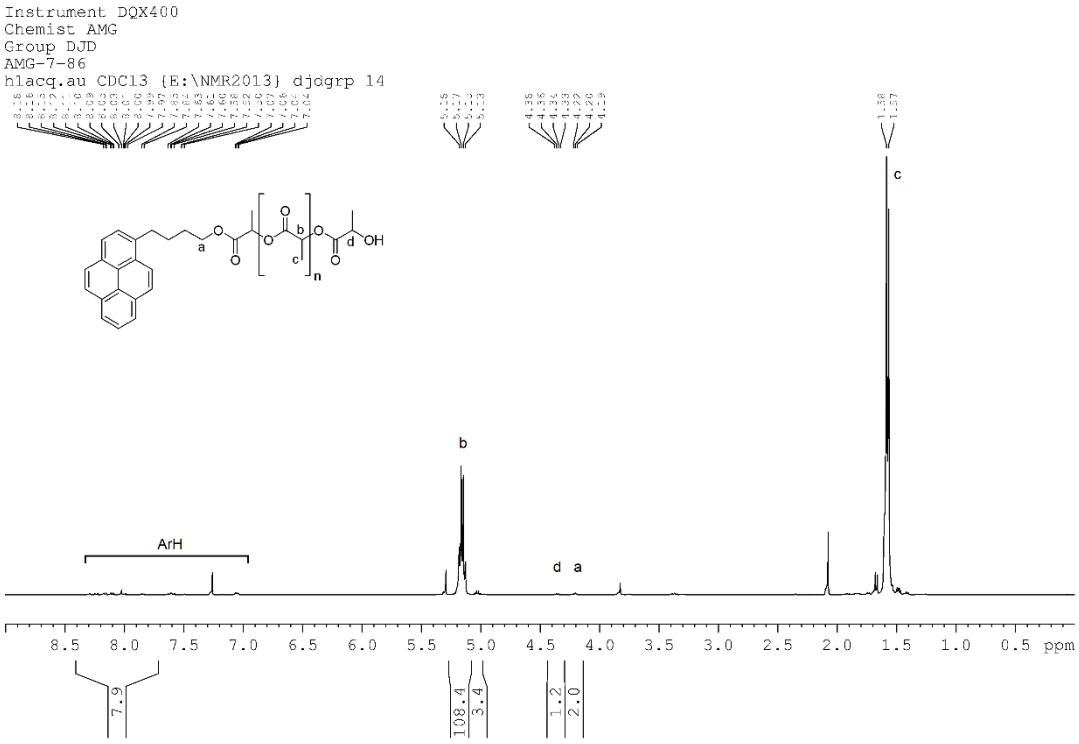
Instrument DQX400
Chemist AMG
Group DJD
AMG-7-86
hlacq.au CDCl3 {E:\NMR2013} djdgrp 14
ArH
b
c
d a
8.5 8.0 7.5 7.0 6.5 6.0 5.5 5.0 4.5 4.0 3.5 3.0 2.5 2.0 1.5 1.0 0.5 ppm
7.9
108.4
3.4
1.2
2.0

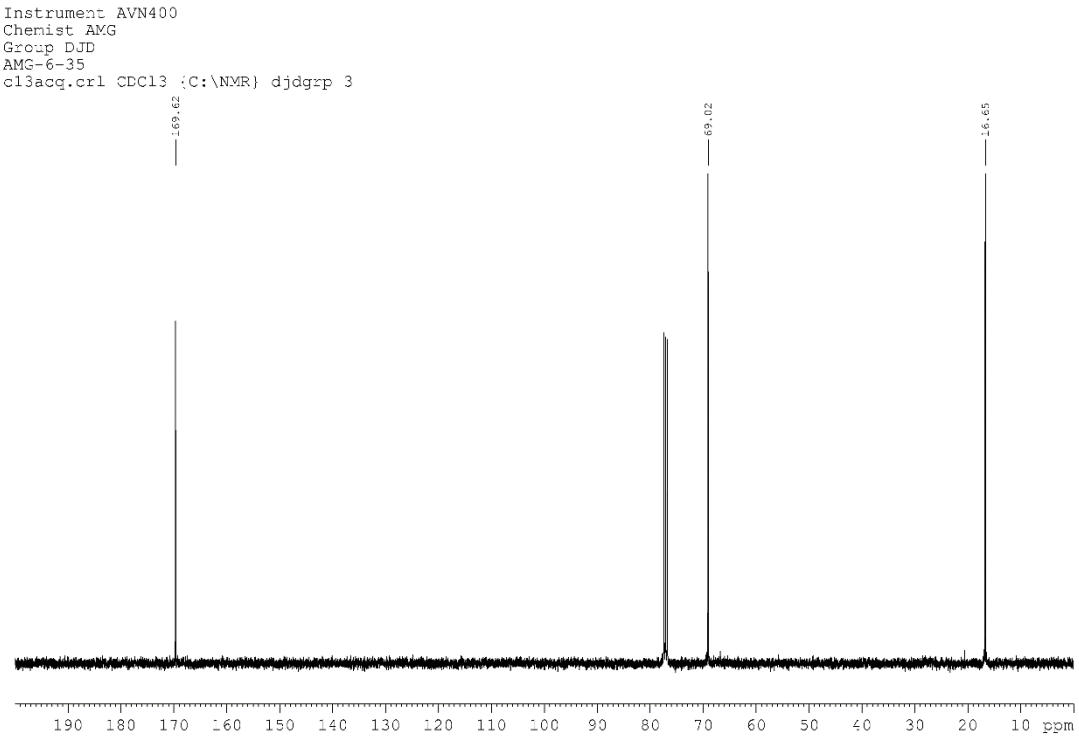
Instrument AVN400
Chemist AMG
Group DJD
AMG-6-35
c13acq.crl CDCl3 {C:\NMR} djdgrp 3
169.62
69.02
16.65
190 180 170 160 150 140 130 120 110 100 90 80 70 60 50 40 30 20 10 ppm

3.2.1 Homodecoupled ^{1}H-NMR

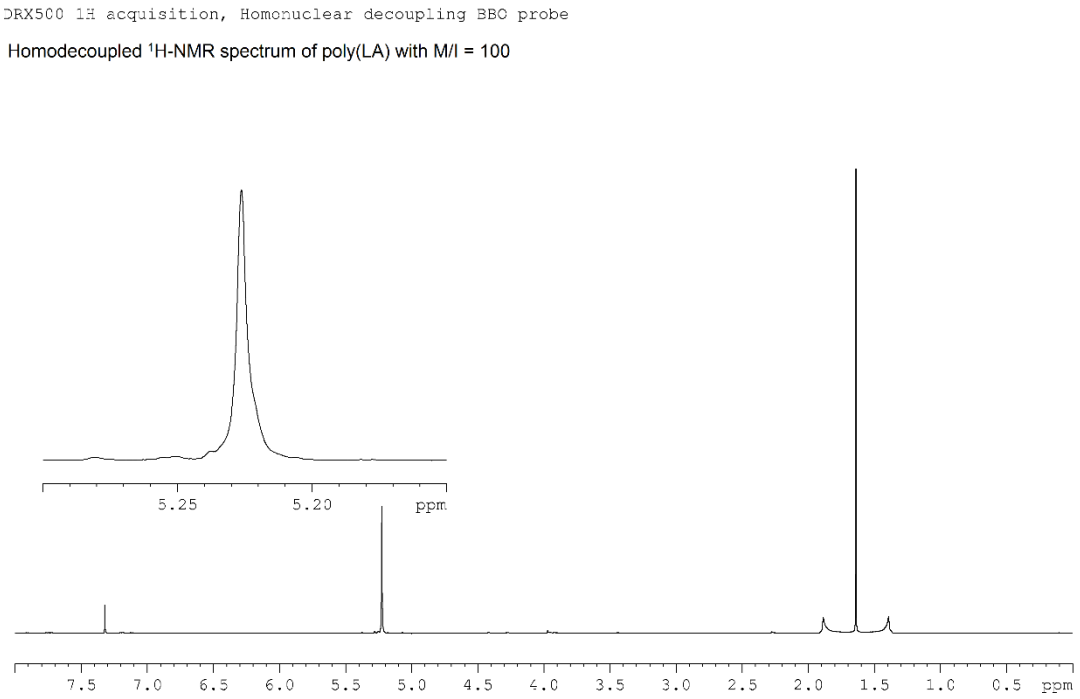

Homodecoupled ^{1}H-NMR spectrum of poly(LA) with M/I = 100

3.2.2 Homodecoupled ^{1}H-NMR of poly(rac-LA)

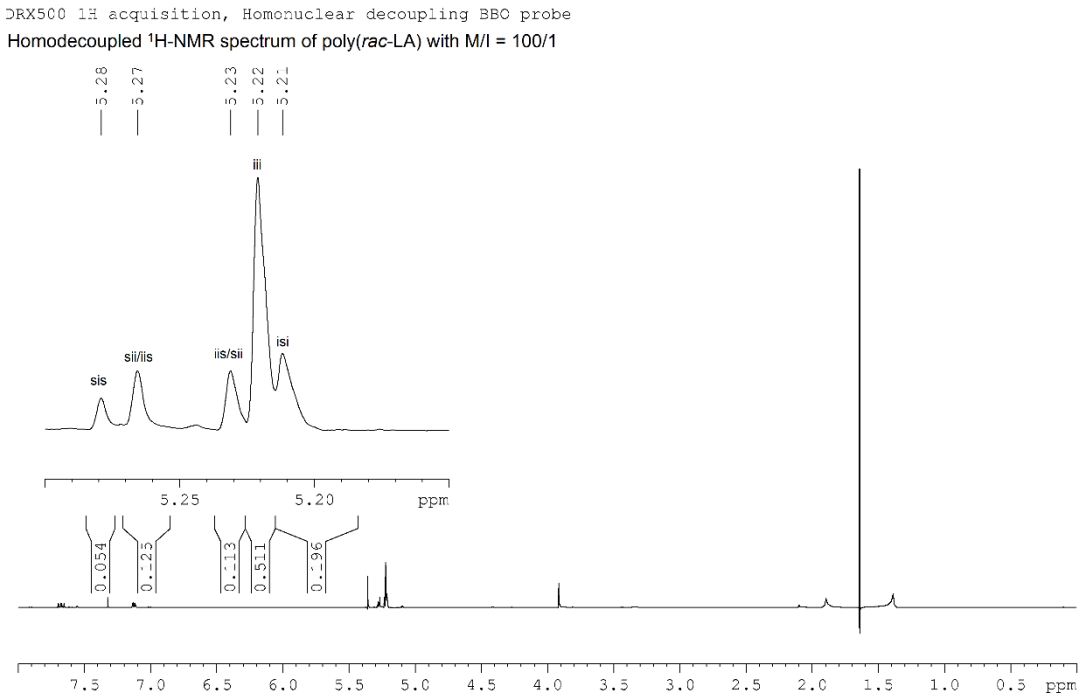

Tetrad[a]	Formula[b]	Normalised integral	P_i value
sis	$\frac{(1-P_i)^2}{2}$	0.054	0.67
sii/iis	$\frac{P_i(1-P_i)}{2}$	0.125	0.500[C]
iis/sii	$\frac{P_i(1-P_i)}{2}$	0.113	0.655
iii	$\frac{P_i(P_i+1)}{2}$	0.511	0.628
isi	$\frac{1-P_i}{2}$	0.196	0.608
		Average	0.64

Table AXX. *Example calculation of P_i for a sample of poly(rac-LA).[a] Tetrad assignments made following Chem.Soc.Rev. (39) p. 486. [b]Formulas for P_i calculations taken from J. Polym. Sci. Part A (35) p 1651.[c] This value was excluded from the average calculation as an outlier.*

3.3 Poly(VL)

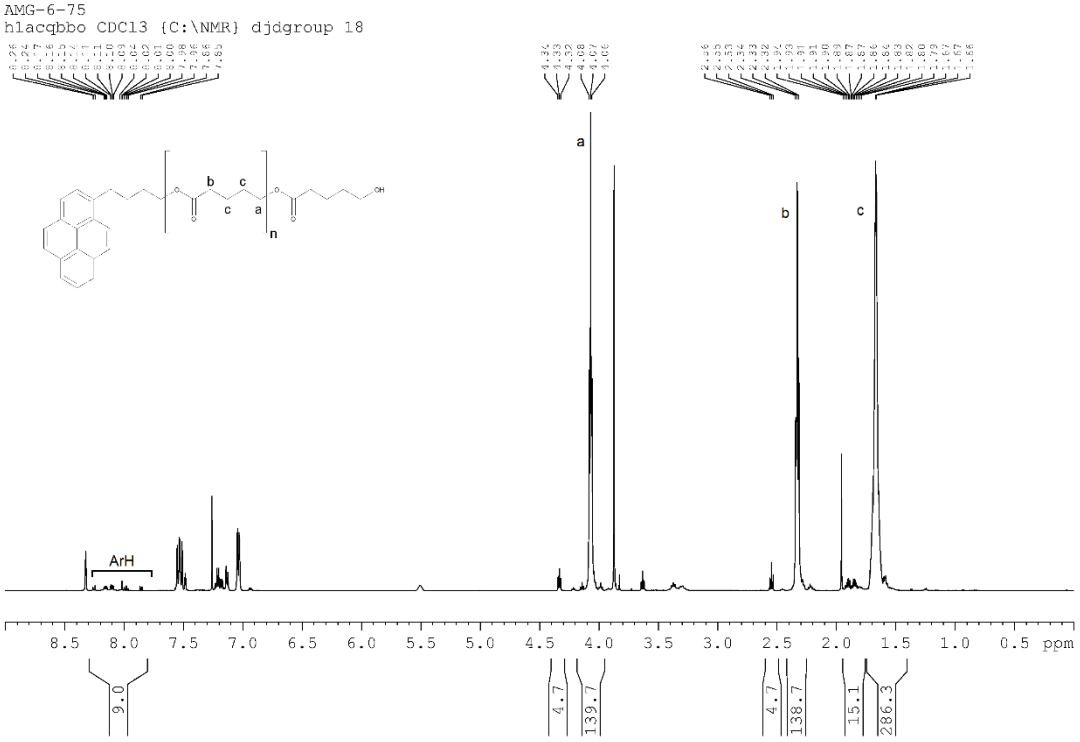
AMG-6-75
h1acqbbo CDCl3 {C:\NMR} djdgroup 18
a
b
c
ArH
8.5 8.0 7.5 7.0 6.5 6.0 5.5 5.0 4.5 4.0 3.5 3.0 2.5 2.0 1.5 1.0 0.5 ppm
9.0
4.7
139.7
4.7
138.7
15.1
286.3

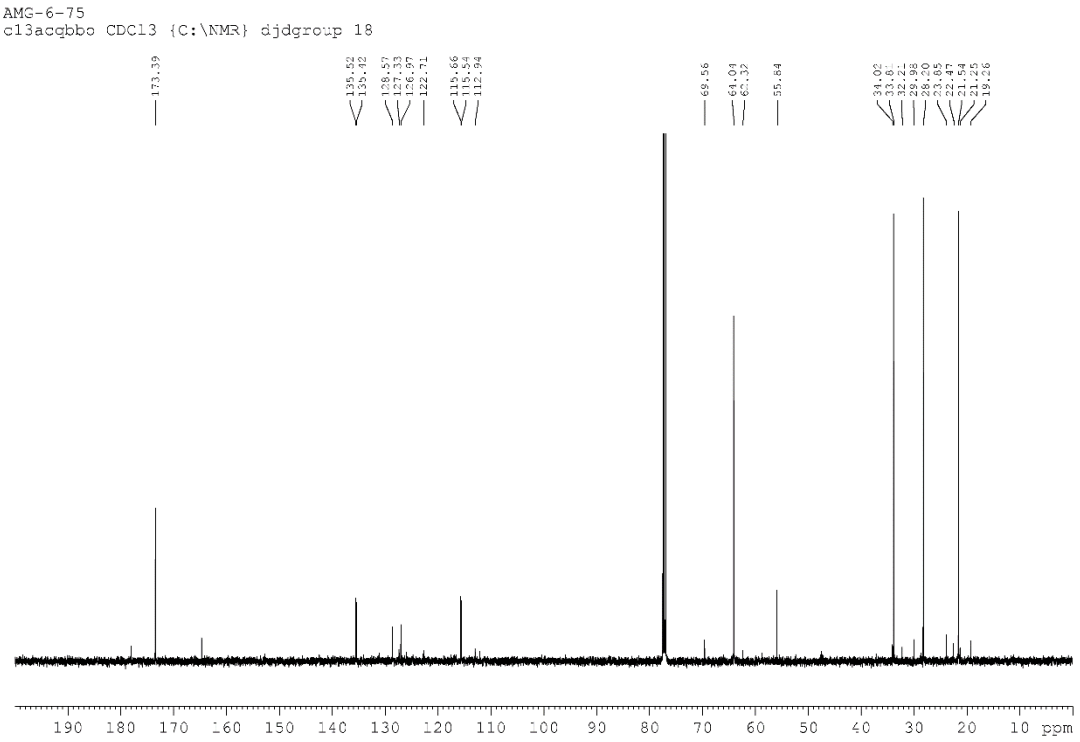
AMG-6-75
c13acqbbo CDCl3 {C:\NMR} djdgroup 18
173.39
135.52
130.42
128.57
127.33
126.97
122.71
115.66
115.54
112.94
69.56
64.04
62.32
55.84
34.02
33.61
32.22
29.98
28.60
25.45
22.47
21.54
21.25
19.26
190 180 170 160 150 140 130 120 110 100 90 80 70 60 50 40 30 20 10 ppm

3.4 Poly(CL)

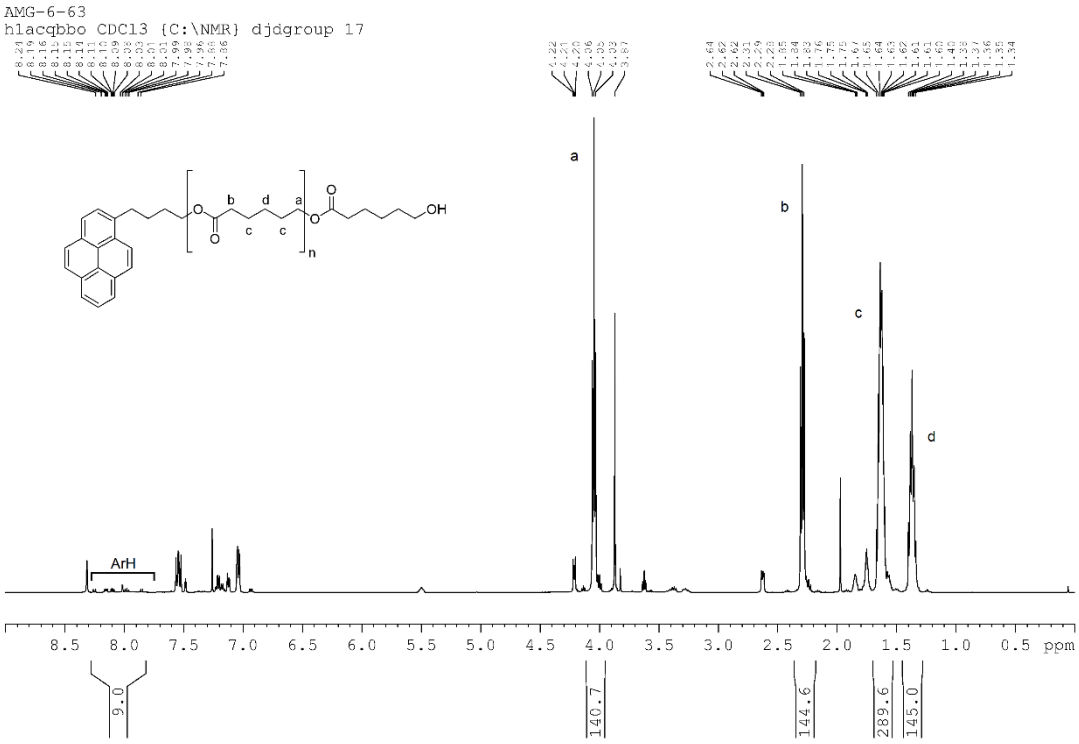
AMG-6-63
h1acqbbo CDCl3 {C:\NMR} djdgroup 17
a
b
c
d
ArH
9.0
140.7
144.6
289.6
145.0
ppm

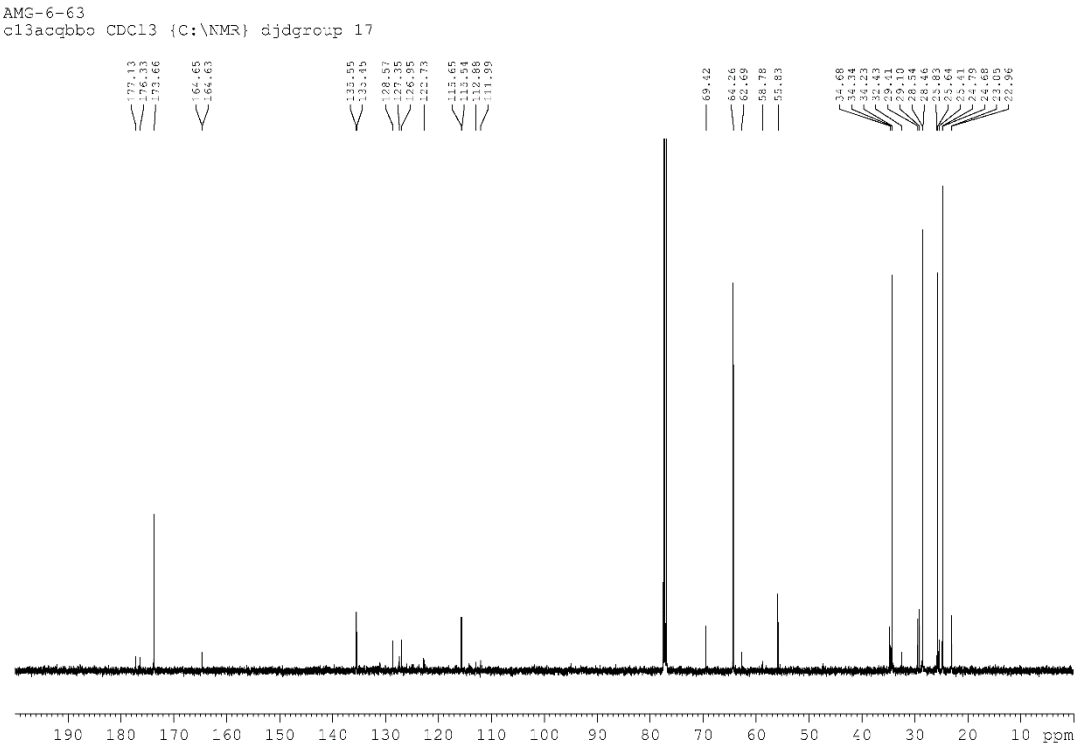
AMG-6-63
c13acqbbo CDCl3 {C:\NMR} djdgroup 17
ppm

3.5 Representative GPC trace of block co-polymer (mPEG-*block*-poly(LA))

mPEG: r.t. = 8.32 min

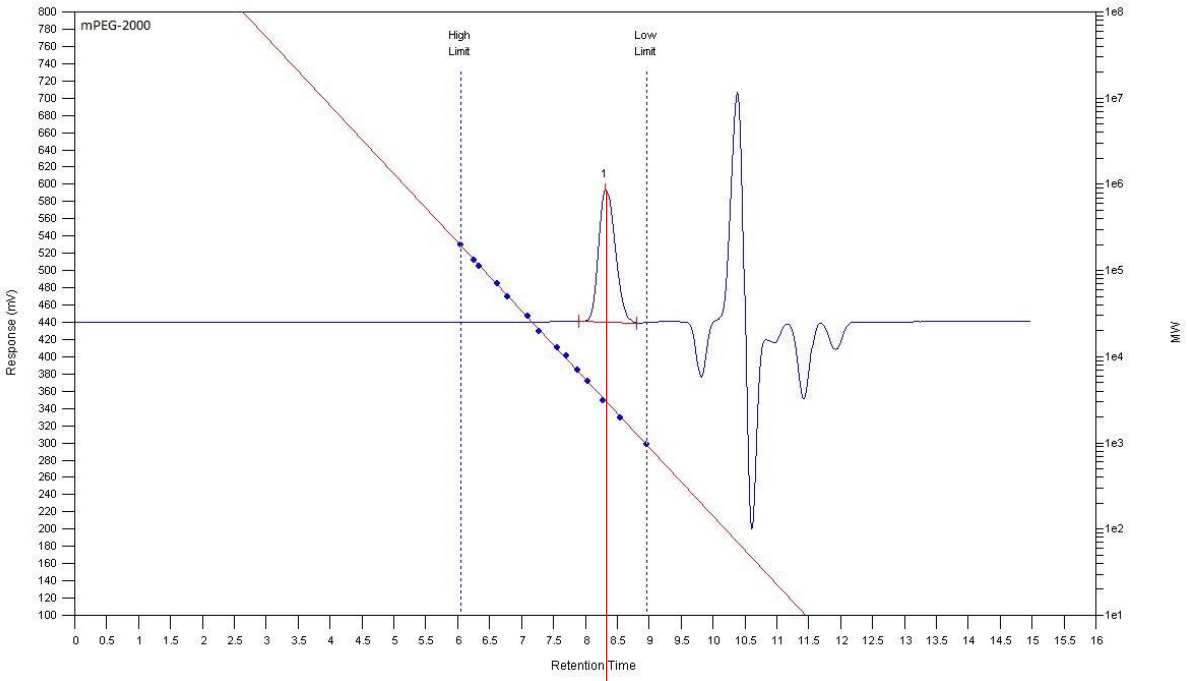

mPEG-*block*-poly(LA): r.t. = 7.37 min